FEASIBILITY STUDY, DESIGN, DYNAMIC MODELLING, SIMULATION, AND CONTROL OF A SOLAR-POWERED SUCKER ROD OIL PUMP

By

Charles Aimiuwu OSARETIN, B. Eng, M.Eng.

A thesis submitted to the School of Graduate Studies

In partial fulfillment of the requirements for the degree of

Doctor of Philosophy in Electrical Engineering.

Electrical and Computer Engineering Department

Faculty of Engineering and Applied Science

Memorial University of Newfoundland

St. John’s, NL, Canada

May 2025

ABSTRACT

As conventional oil and gas facilities continue to age, stripper wells and marginal field operations are increasingly suspended, orphaned, and abandoned at an alarming rate. In remote and isolated facilities, the deployment of onsite renewable energy and low-cost, open-source communications systems is an increasingly promising trend for sustainable and reliable management of onsite operations. Throughout this research, a 100% renewable energy-powered microgrid is proposed for driving a remote oil well located in the city of Medicine Hat, southeastern Alberta, Canada.

Two different oil and gas production system simulators: Quick Rod (QRod) and Production System Performance Analysis Software (PROSPER), are adopted to determine the optimal rating of the electric motor that can reliably drive the sucker rod pump. A parametric investigation is first performed in QRod, and the result is then integrated with the PROSPER workflow to minimize the iteration time and produce a more efficient electric motor sizing. The load applied by the pump on the rod string is determined in QRod by specifying the target production rate; and performing a parametric investigation to determine the impact of changing parameters (such as stroke rate, stroke length, and pump diameter), on the overall output torque on the polished rod and rod string loading, ultimately obtaining the minimum rating of squirrel cage electric motor required to serve as the prime mover for the remote oil well.

The research then extends to the novel application of off-grid renewable energy systems for powering artificial lift in remote oil facilities. Considering the load profile of the producing oil well and Utilizing HOMER Pro software, the study evaluates various renewable energy architectures of solar PV, wind turbine, and battery storage systems for both intermittent and continuous pumping scenarios. The feasibility study for the optimal sizing, technical, and economic feasibility of a renewable energy system for a remote oil well is performed. Two viable

alternatives are proposed, one based on cost minimization and the other based on minimization of unmet load. The most economical solution for repurposing idle wells at the selected remote location is identified as a system comprising solar PV and battery storage with intermittent pumping, offering a sustainable and cost-effective alternative to well abandonment and decommissioning.

To enhance remote monitoring and control capabilities, a low-cost, open-source, Supervisory Control and Data Acquisition (SCADA) system based on Node-RED and Arduino microcontrollers was developed. This Internet of Things (IoT) based system comprises a main terminal unit, a remote terminal unit, and a local server, which is integrated with various sensors and transducers for comprehensive data collection, including accelerometer, temperature, flow rate, water level, voltage, current, and distance measurements. A web-based graphical user interface (GUI) is developed in Node-RED for data collection, logging, and visualization. To facilitate communication between the server and the client, Nginx is adopted as the proxy server between the local server and the router, to implement Hypertext Transfer Protocol, ensuring load-balancing and basic access authentication.

To gain deeper insights into the behavior of the overall system and predict the response to various environmental and operating conditions, design, dynamic Modelling, simulation and control is perfomed in Simscape. The load Modelling of the sucker rod pump which entails hydraulic, and mechanical domains is first developed, followed by solar-powered microgrid modelling and simulation. The outcome of the research is an end-to-end virtual representation of the microgrid which can be efficiently deployed to scale the system configurations, test different power supply and load scenarios, and fine-tune system performance. This lays a solid foundation for physical prototypes, saving time and fostering optimal resource allocation during implementation.

ACKNOWLEDGEMENTS

I express my gratitude and profound acknowledgement to Jesus Christ, my personal Saviour and Lord, for His death on Calvary's cross and for the salvation of my soul. I am grateful for the grace to have come to know, love, and serve God, as a disciple and follower of Jesus Christ.

I extend my heartfelt appreciation to Professor Mohammad Tariq Iqbal, my esteemed thesis supervisor, whose unparalleled mentorship, and depth of knowledge have been instrumental in developing my research competence and elevating the quality and scope of this research. I am grateful for his encouragement, patient mentorship, and incisive feedback.

Professor Stephen Butt has been a conscientious co-supervisor. I immensely appreciate his insightful feedback, and constructive recommendations to improve the content and quality of the original manuscript.

I am grateful to Professor Weimin Huang for his feedback, insightful questions, and critical examination of my presented results to ensure attention to detail and establish novelty at various stages in executing this research.

I would like to share credit for this research with my wife Mrs. Osarugue Faith Aimiuwu. Thank you for holding me accountable, I am immensely grateful for your support, understanding, and patience. Without your encouragement, and sacrifice, this accomplishment would not have been possible. I appreciate my mentors from the Centre of Excellence in Geosciences and Petroleum Engineering, University of Benin: Dr. Kehinde Oluwatoyin Ladipo, Prof Joseph Ebeniro, Mr. Omagbemi George Kakayor and Dr. Steve E. Adewole, for laying my technical foundation in petroleum exploration, development and production; the basis for my interest and passion for this research study. I also like to thank my friends: Mr. Mohammad Zamanlou, Dr. Osezua Ibhadode, Mr. Chinedu Ifediorah, and many others too numerous to mention.

TABLE OF CONTENTS

Contents Page

CHAPTER 2

LITERATURE REVIEW

CHAPTER 3

SIZING, PARAMETRIC INVESTIGATION AND ANALYSIS OF AUTOMATED SUCKER ROD PUMP USING BEAM PUMP SIMULATORS

CHAPTER 5

OPEN-SOURCE IOT-BASED SCADA SYSTEM FOR REMOTE OIL FACILITIES USING NODE-RED AND ARDUINO MICROCONTROLLERS

CHAPTER 6

DESIGN, DYNAMIC MODELLING, SIMULATION, AND CONTROL OF A SOLAR-POWERED SUCKER ROD OIL PUMP

List of Figures

List of Tables

Acronyms

AOG	Abandoned Oil and Gas
AOFP	Absolute Open Flow Potential
API	American Petroleum Institute
BESS	Battery Energy Storage System
BPU	Beam Pumping Unit
CAD	Canadian Dollars or Computer Aided Design
CBM	CoalBed Methane
CBT	Counterbalance Torque
CBE	Counterbalance Effect
CCWconv	Counter Clockwise Conventional
CLF	Cyclic Load Factor
CLFCS	closed-loop frequency control scheme
CMC	Control and Monitoring Center
CWconv	Clockwise Conventional
CWEC	Canadian Weather Energy and Engineering Climate
DG	Diesel Generator
DOF	Digital Oil Field
EOR	Enhanced Oil Recovery
ESP	Electrical Submersible Pump
FFT	Fast Fourier Transform
FPGA	Field-Programmable Gate Array
FSPV	Floating Solar Photovoltaic Power

GHG	Green House Gas
GHI	Global Horizontal Irradiance
GSM	Global System for Mobile Communications
GUI	Graphical User Interface
GW	Gigawatt
HCGS	Hybrid Centralized Generation System
HMI	Human-Machine Interface
HOMER	Hybrid Optimization Model for Multiple Energy Resources
HTTP	Hypertext Transfer Protocol
HTTPS	Hypertext Transfer Protocol Secure
IDE	Integrated Development Environment
IDSRP	Interactive Digital Sucker Rod Pumping Unit
IIoT	ndustrial Internet of Things
IoT	Internet of Things
IPR	Inflow Performance Relationship
IWM	Intelligent Well Monitoring
LAN	Local Area Network
LCEF	Low carbon Emissions Fund
LCOE	Levelized Cost of Energy
LEAP	Long-range Energy Alternatives Planning system
LoRa	Long Range Radio
LPWAN	Low Power Wide Area Network

LSTM	Long Short-Term Memory
MATLAB	Matrix Laboratory
MEOWWS	Marginal Expense Oil Well Wireless Surveillance system
ML	Machine Learning
MPPT	Maximum Power Point Tracking
$MtCO_2e$	Metric Tons of Carbon Dioxide Equivalent
MTU	Master Terminal Unit
NASA	National Aeronautics and Space Administration
NAT	Network Address Translation
NEMA	National Electrical Manufacturers Association
NPC	Net Present Cost
OLFOS	open-loop frequency optimization scheme
OPC UA	Open Platform Communications Unified Architecture
PAS	Process Automation System
PDSRPS	Parallel Digital Sucker-Rod Pump System
PERC	Passivated Emitter and Rear Cell
PF	Pump Fillage
PID	Proportional-Integral-Derivative
PIP	Pump Intake Pressure
PLC	Programmable Logic Controller
PMS	Power Management System
PMT	Preventive Maintenance Terminal
PROSPER	Production and Systems Performance

P&O	Perturb and Observe
PV	Photovoltaic
PVT	Pressure-Volume-Temperature
PWM	Pulse-Width Modulation
QRod	QuickRod
RMS	Root-Mean-Square
RPOT	Rod Pump Optimization Tool
RTPO	Real-time Production Optimization
RTU	Remote Terminal Units
SAM	System Advisor Model
SCADA	Supervisory Control and Data Acquisition
SF	Safety Factor
SoC	State of Charge
SPM	Stroke Per Minute
SR	Solar Radiation
SRPU	Sucker Rod Pumping Unit
SSL	Secure Sockets Layer
STB/day	Stock Tank Barrel per Day
tCO2e/bbl	Tons of Carbon Dioxide Equivalent per Barrel
USB	Universal Serial Bus
USOSC	Upstream Oil Supply Chain
VBA	Visual Basic for Applications

VFD	Variable Frequency Drive
VLP	Vertical Lift Performance
WS	Wind Speed
WT	Wind Turbine
WRTU	Wireless Remote Terminal Unit

DEDICATION

This work is dedicated to Jesus Christ, my personal Saviour and Lord, for His death on Calvary's cross and for the salvation of my soul. I am grateful for the grace to have come to know, love, and serve God, as a disciple and follower of Jesus Christ.

I dedicate this to my dear wife Osarugue Faith Aimiuwu (my encourager, my cheerleader and my main support), I am immensely grateful for her strong, unwavering faith in me and for her unceasing travail in prayers, and encouragement to keep pressing forward through frustrations and discouragement. She never once lost faith, holding me accountable to tasks, deliverables and milestones all through this research work. To my children, Jarett Eloghosa Aimiuwu, Shiloh Oghosa Aimiuwu and Virtue Odosamamwen Aimiuwu, who endured the early mornings, long nights, working holidays and research weekends with me and for me, throughout this research; this could never have been possible without your support, understanding and sacrifice.

I sincerely appreciate my parents Mr. Chris Osaretin Uyimwen Itua and Mrs. Patience Eboigbe. I deeply honor the loving and blessed memory of my parents-in-law; the Late Pa Francis Igbinakenzua Ekhaguere and Late Mrs. Nosakhare Magareth Ekhaguere (Nee Asemota), I am immensely grateful for your vision, sacrifice, prayers, support and sterling legacy. Finally, to all my friends and research mentors, I am immensely for their guidance, advice and support all throughout this research.

Chapter 1

INTRODUCTION

1.1. Introduction

A significant portion of the world's oil production relies on artificial lift methods, making it crucial to minimize energy expenditure in extracting this essential resource. With numerous wells utilizing electrically powered beam pumping units, the proper sizing of prime movers and optimization of unit geometry and pumping modes have become paramount. These considerations reduce operational costs and maximize the conservation of primary energy sources.

The optimization of beam-pumped artificial lift systems represents a longstanding challenge which continues to captivate researchers and industry professionals. Addressing this complex issue effectively, demands a multifaceted and intergrated approach. Such a strategy necessitates the careful consideration of a wide array of variables, including the specific conditions of the well, the unique properties of the reservoir, and the intricate specifications of the equipment involved. The ultimate goal is to engineer an artificial lift solution that maximizes efficiency while minimizing costs [1].

Recent advancements in this field have been achieved through the combined use of diverse simulation tools and analytical methods. This integrated approach has yielded notable enhancements in critical performance metrics. Specifically, researchers have observed substantial reductions in both damped and polished rod horsepower requirements. Additionally, these innovations have led to a decrease in the minimum motor size needed for effective operation, further improving the overall system efficiency [2, 3].

The design of beam-pumped wells is indeed a complex process involving the careful selection of various components to ensure an optimal pumping mode. This mode is defined by the specific combination of pump size, pumping speed, stroke length, and sucker rod string design. When the pumping mode is strategically chosen, there can be an immediate and substantial reduction in power requirements and associated operational costs [4].

Well and fluid parameters significantly impact the design and optimal sizing of the sucker-rod pump system. This optimization process is crucial for the operation's economic viability. The ideal design of a sucker-rod pumped artificial lift system requires determination of precise system parameters and careful equipment selection to produce fluid economically and meet the well operator's technical and economic objectives [5].

It is essential to accurately estimate electrical demand and energy expenses for various combinations of prime movers, unit geometries, downhole equipment, and pumping modes. This enables the selection of the most efficient and economical configuration. The development of two key techniques underpins this approach: Optimal prime mover selection and precise prediction of electrical costs. This predictive capability forms the foundation for making informed decisions regarding equipment selection and operational parameters, ultimately leading to more energy-efficient and cost-effective oil production processes [6].

While continuous production is generally preferred in oil and gas extraction, certain circumstances necessitate intermittent production strategies. This approach is particularly beneficial for wells in specific situations, such as those approaching the end of their productive lifespan, wells prone to gas or water breakthroughs, or gas wells experiencing liquid loading issues. Intermittent production can help manage these challenges more effectively, potentially extending the well's operational life and optimizing resource extraction under less-than-ideal conditions. This method allows for better control of production dynamics, helping to mitigate problems associated with declining well performance or complex reservoir behaviors [7].

The petroleum industry is experiencing a shift towards less conventional and lower-quality reserves, which may lead to increased energy consumption and emissions in the coming years.

The rapidly growing number of aging wells exponentially amplifies the life cycle impact and administrative burden of these challenges compounded by the fiscal, environmental, and sustainability implications. The extraction and processing of oil and gas are inherently energy-intensive activities, often resulting in significant environmental consequences [8]. A promising solution to mitigate these challenges is the incorporation of renewable energy sources into oil and gas operations. This approach offers multiple benefits including reduced reliance on fossil fuels for energy production, potential decrease in operational expenses, lower emissions associated with extraction and processing, and conservation of petroleum resources for more valuable applications [9]. In certain scenarios, the integration of renewable energy has already proven to be a cost-effective and environmentally responsible method of meeting the energy demands of oil and gas operations [8].

The oil and gas industry is experiencing a growing trend towards marginal production of low-quality fluids characterized by deeper wells with a high water-to-oil ratio, resulting in energy-intensive production [10, 11]. This implies that the ratio of energy input to energy output continues to rise, providing an important opportunity to deploy renewable energy [10, 11]. This comes with the added advantage of curtailing direct emissions (tCO2e) and reducing the emissions intensity (emissions per barrel) in tCO2e/bbl associated with oil production [10, 11]. As the levelized cost of solar, wind, and battery storage continues to decline, investing in onsite electricity generation powered by renewable energy becomes an attractive alternative to deploy. Hence there is growing research interest for robust feasibility studies to determine where, when and how to sustainably and economically adopt these technologies in a way that ultimately reduces the environmental footprint and overhead cost of upstream production [10, 11].

An important determinant whether the system would be competitive or sustainable, is the appropriate design, sizing and implementation of onsite solar and/or wind powered distributed microgrids [10, 11]. When assessing the viability of energy systems, engineers should conduct a comprehensive comparison of various options. This evaluation should include estimating the opportunity costs associated with diesel engines, analyzing the efficiency and cost of natural gas internal combustion engines, and examining the cost and reliability of battery storage systems. By weighing these factors against each other, decision-makers can determine the most economically and technically viable solution for their specific energy needs, considering both financial implications and performance characteristics [10, 11]. Designing the system to the peak load demand also ensures the system's resilience to deliver the actual load demand under varying environmental conditions such as solar irradiance, wind speed, and ambient temperature [10, 11].

The Canadian oil and gas industry is the largest contributor to Canadian Greenhouse Gas (GHG) emissions, releasing an estimated 217 million metric tons of carbon dioxide equivalent ($MtCO_2e$) and accounting for about 31% of total emissions in 2022 [12,13]. In 2024, the province of Alberta had over 470,000 registered wells [14], and about one-third (over 155,000) are currently inactive (suspended, orphaned, or abandoned) [15].

Abandoned oil and gas wells in Canada contribute significantly to greenhouse gas emissions, particularly methane, which is a potent greenhouse gas [16, 17]. Recent studies have shed light on the extent of these emissions and their underestimation in national inventories [16, 17]. A study published in 2023 estimated that methane emissions from abandoned wells in Canada amount to 85-93 kilotonnes of methane per year. Of this total, surface casing vent emissions represent 75-82%, accounting for approximately 70 kilotonnes of methane annually [16]. Another study from 2021 suggests that methane emissions from abandoned oil and gas (AOG) wells in Canada have been underestimated by as much as 150%. This research indicates that AOG wells are the 11th largest source of anthropogenic methane emissions in Canada [17].

The Canadian Government is providing up to CAD 1.72 billion to the provinces of Alberta, Saskatchewan, and British Columbia, and to the Alberta Orphan Well Association, to decommission orphan and inactive oil and gas wells. The goal is to reduce methane emissions while supporting jobs. There are approximately 5,650 orphan wells and over 139,000 inactive wells in Canada. Alberta has by far the largest share of both—4,700 orphan wells and 91,000 inactive wells—and will receive the largest share of funding with up to CAD 1 billion to the Alberta government and a CAD 200 million loan to the Alberta Orphan Well Association. Saskatchewan has 600 orphan wells and 36,000 inactive wells and will receive up to CAD 400 million. British Columbia has 350 orphan wells and 12,000 inactive wells and will receive up to CAD 120 million [18].

In November 2024, the Government of Canada proposed the Oil and Gas Sector Greenhouse Gas Emissions Cap Regulations seeking to establish a national cap-and-trade system that applies to upstream oil and gas activities including onshore and offshore oil and gas production. This creates an incentive for operators to reduce their emissions and secures funds for investment in microgrid projects such as onsite renewable energy generation [19].

The Canadian government established the Low Carbon Emissions Fund (LCEF) to reduce GHG emissions by 40% by 2030 and to achieve net-zero emissions by 2050. LCEF aims to incentivize cost-effective decarbonisation, generate clean growth, build resilient communities, and help create jobs for Canadians [20]. This demonstrates that the capital and operating costs to invest in infrastructure, deploy renewable energy and decarbonize the upstream oil and gas sector is available and accessible to well operators, and inactive wells are strong candidates for these initiatives.

The paradigm recommended and adopted by the author in this research work is a technological approach which goes beyond indiscriminate and unsystematic plugging of idle wells, to adopting 100% renewable energy sources to curtail vented and leaked methane from idle, suspended and abandoned oil wells using existing technology [21]. This entails 100%

electrification of prime mover engines for pumping, producing, and transporting produced conventional oil and natural gas [22-24].

This research proposes an innovative approach to addressing key challenges in artificial lift sizing, system optimization, and remote monitoring of oil and gas facilities, particularly focusing on sucker-rod pumps, while incorporating low-cost, open source data collection, and visualization and monitoring capabilities. It examines novel and integrated approaches to modelling the adoption of renewable energy power supply system for artificial lift driven oil wells.

1.2. Research Problem

As conventional oil wells age, they plateau in production, and inevitably approach decline facing significant risk of being orphaned, suspended or abandoned. 100% renewable energy-powered artificial lift is proposed to sustain these aging wells. In doing this, the main research questions of concern are:

1. How can the energy requirement of a candidate idle well be estimated?
2. What are the parameters of a sucker rod pump artificial lift to consider when sizing?
3. What are the technical and economic considerations for well operators to choose between continuous and intermittent pumping?
4. How can artificial lift indices and production parameters be tracked using Internet of things SCADA and open source software?
5. Can remote wells be 100% powered by solar energy resource? If so, what is the impact of solar irradiance, temperature and other operational factors on the overall system performance?

This research provides an alternative framework and strategy to scrutinize the inventory of available wells and systematically select candidate wells that can be profitably restored to marginal production. This provides a clear framework to support reinvesting some of the abandonment budget in key long term energy infrastructure. This approach could significantly extend the lifecycle of brownfield operations while reducing the environmental footprint of the upstream oil and gas sector and developing renewable energy generation capacity for distributed energy generation and storage.

This research provides a 100% renewable energy approach for powering remote oil and gas operations while leveraging fully customizable, low-cost, open-source Internet-of-Things supervisory control and data acquisition systems for monitoring and managing production system operations.

1.3. Research Objectives

This study applies a multifaceted approach combining optimized sizing of sucker rod pump unit (SRPU) artificial lift system, advanced IoT-based monitoring and solar PV renewable energy integration.

This research aims to design , models, simulated and controls an off-grid Solar PV renewable energy system having a low-cost, open-source Internet-of-Things SCADA system with the following main objectives.

1. To develop an integrated methodology for the optimal sizing of beam-pumped artificial lift systems by combining parametric investigations and iterative sizing techniques using petroleum production system simulators.
2. To optimize the design and sizing of renewable energy systems for powering remote oil wells, particularly using a hybrid configuration of solar, wind, and battery storage systems.

3. To evaluate the technical and economic performance and feasibility of renewable energy systems for petroleum production, considering factors such as net present cost, levelized cost of energy, and operating cost.
4. To design and implement a cost-effective, open-source IoT-based SCADA system for remote monitoring and control of low-flowrate oil wells, with a focus on data accuracy, remote data logging, and visualization.
5. To design and develop a robust end-to-end dynamic model and simulation of the 100% renewable energy solar-powered microgrid and evaluate its stability and performance for remote flowrate oil well, under various environmental and operating conditions.

1.4 Research Contributions

The main contributions of this PhD thesis are:

a. **Sizing, Parametric Investigation and Analysis of Automated Sucker Rod Pump Using Beam Pump Simulators**: This parametric investigation develops a novel, systematic and integrated approach to optimal sizing and selection of the sucker rod pump artificial lift system parameters, combining and integrating two (2) artificial lift simulators and ensuring feasible design at the optimum energy requirement.

b. **Optimal Sizing and Techno-Economic Analysis of a Renewable Power System for a Remote Oil Well**: This technical and economic analysis presents a novel comparison of intermittent and continuous pumping configurations of sucker rod pump artificial lift systems using various architectures of 100% renewable energy sources. The results provide a framework for comparing primarily based on cost and unmet load criteria. The outcomes provides options for a well operator to choose depending on either the unmet load or cost criteria, based on the composition of the produced fluid.

c. **Open Source IoT-Based SCADA System for Remote Oil Facilities Using Node-RED and Arduino Microcontrollers**: This research presents an innovative approach to Supervisory Control and Data Acquisition (SCADA) systems for remote oil facilities, leveraging open-source technologies and Internet of Things (IoT) principles. The study develops a novel, cost-effective, open-source, web-based, data collection solution and communication system that enables real-time monitoring, visualization and control of oil production processes.
d. **Design, Dynamic Modelling, Simulation, and Control of a Solar-Powered Sucker Rod Oil Pump**: This study models the entire artificial lift system, simulating, and controlling the 100% solar-powered sucker rod pump and optimizing its performance at the component, load and system level. The study is novel in performing integrated load modelling, comparing the winter and summer performance of the microgrid, and demonstrating the sustainable operation of the system under varying environmental and operational conditions, using historical site-specific solar irradiance and temperature data.

1.5 Thesis Organization

As part of the preparation of this thesis, a manuscript format consisting of 3 published, peer reviewed, academic journal articles, and 1 published, peer previewed journal conference paper are adopted in the main body of this thesis. Chapters 3, 4 and 6 is wholly based on peer reviewed journal articles, while chapter 5 is based on the conference paper. The remainder of the thesis is arranged as follows:

Chapter 1 introduces the theme of this research, and presents the research problem, research objectives, research contributions and thesis organization. A comprehensive review of relevant literature is presented in chapter 2, laying a foundation for the available knowledge and identifying gaps in the available research, in chapter 3, this study presents an integrated simulation approach utilizing QRod™ and PROSPER™ platforms to optimize sucker rod pump artificial lift systems, focusing on energy efficiency and production maximization. Through a comprehensive parametric analysis of key design variables such as pump geometry, API rod number, pump diameter, and rod material, the research establishes optimal configurations for deep well applications exceeding 3500 feet. The study quantitatively assesses various rod string designs using performance indicators like damped horsepower, cyclic load factor, and prime mover rating to ensure reliable long-term operation. Additionally, it develops and validates an optimized sizing methodology that streamlines the design process, resulting in significant reductions in damped horsepower, polished rod horsepower, and minimum NEMA D motor size requirements.

In chapter 4, this study presents a comprehensive framework for developing renewable, off-grid solar PV and/or wind and battery storage systems to sustain oil production in remote wells. The chapter evaluates the technical and economic implications of adopting onsite renewable energy-based approaches, assessing their feasibility under varying technical and environmental conditions. It analyzes different renewable energy scenarios for both continuous and intermittent production in sucker rod pump artificially lifted wells, specifying criteria for selecting the optimal combination of energy source and pumping schedule. The research culminates in two recommendations for oil well operators, based strictly on either continuous or intermittent production, using key performance indicators such as Unmet Load, Capacity Storage, Net Present Cost, Levelized Cost of Energy, and Operating Cost.

In chapter 5, this study designs and implements a cost-effective, open-source IoT-based SCADA system for remote monitoring and control of oil facilities using Node-RED and Arduino microcontrollers. The study focuses on developing a web-based graphical user interface for real-time visualization, data logging, and remote access to sensor data and control functions. It integrates multiple sensors and actuators for comprehensive monitoring and control of oil production processes. The project implements a secure remote access solution using port forwarding, network address translation, and HTTP basic access authentication with Nginx. Finally, the research evaluates the performance and reliability of the proposed IoT-based SCADA system in monitoring critical operational parameters and enabling remote control of oil production equipment, providing a comprehensive solution for efficient and secure remote management of oil wells.

In chapter 6, this research presents a comprehensive model-based simulation of a solar-powered sucker rod pump system, optimizing the efficiency across all subsystems. The study decouples the microgrid into individual components, enabling targeted improvements from the solar PV source to the electric motor load. By incorporating load modelling from SolidWorks and Simscape into Simulink, the research provides a realistic representation of the system's behavior under various environmental and operating conditions. The approach combines mechanical and electrical models to design effective controls for the sucker rod pump. The study encompasses load modelling of the pump system, solar PV array design, energy storage system modelling, and control system implementation. Through extensive simulations and iterative design improvements, the research evaluates system behavior, stability, and overall performance, allowing for potential issues to be identified and addressed before real-world implementation. This robust methodology supports the development of an efficient and reliable solar-powered sucker rod pump system adaptable to diverse operating environments.

This thesis concludes in Chapter 7 with a discussion of its key conclusions from various aspects of the research and makes recommendations for future work that addresses the issues raised during the research.

1.6 References

[1] Gao, Z.W. and Jia, S., 2024. Modeling and Control for Beam Pumping Units: An Overview. Processes, 12(7).

[2] McCoy, J.N., Podio, A.L., Drake, B. and Rowlan, L., 2001, March. Modern total well management-sucker rod lift case study. In SPE Western Regional Meeting (pp. SPE-68864). SPE.

[3] Jennings, J.W., 1989, October. The design of sucker rod pump systems. In SPE Centennial Symposium at New Mexico Tech (pp. SPE-20152). SPE.

[4] Takacs, G., 2015. Sucker-rod pumping handbook: production engineering fundamentals and long-stroke rod pumping. Gulf Professional Publishing.

[5] Karhan, M.K., Nandi, S. and Jadhav, P.B., 2015. Design and optimization of sucker rod pump using prosper. Int. J. Interdiscip. Res. Innovations, 3(2), pp.108-122.

[6] Byrd, J.P. and Beasley, H.L., 1974, May. Predicting prime mover requirements, power costs, and electrical demand for beam pumping units. In PETSOC Annual Technical Meeting (pp. PETSOC-374035). PETSOC.

[7] Moncur, C.E., Jakeman, S., Berendschot, L., Cramer, R., Briers, J., Stroobant, F., Ahmad, R. and Goh, K.C., 2008, February. Extensions to and Roll Out of Data Driven Production Surveillance and Optimization. In SPE Intelligent Energy International Conference and Exhibition (pp. SPE-112037). SPE.

[8] Stolz, J., Bain, D. and Griffin, M. eds., 2022. Environmental Impacts from the Development of Unconventional Oil and Gas Reserves. Cambridge University Press.

[9] Temizel, C., Aydin, H., Hosgor, F.B., Yegin, C. and Kabir, C.S., 2023. Green Energy Sources Reduce Carbon Footprint of Oil & Gas Industry Processes: A Review. Journal of Energy and Power Technology, 5(1), pp.1-25.

[10] Ericson, S.J., Engel-Cox, J. and Arent, D.J., 2019. Approaches for integrating renewable energy technologies in oil and gas operations (No. NREL/TP-6A50-72842). National Renewable Energy Lab.(NREL), Golden, CO (United States).

[11] Krah, K., Ericson, S., Li, X., Olawale, W., Castillo, R., Newes, E. and Engel-Cox, J., 2020, August. Opportunities for clean energy in natural gas well operations. In 2020 IEEE International Systems Conference (SysCon) (pp. 1-7). IEEE.

[12] Environment and Climate Change Canada (2024) 'National Inventory Report 1990-2022: Greenhouse Gas Sources and Sinks in Canada'.

[13] Environment and Climate Change Canada (2024) 'Greenhouse gas emissions', Government of Canada, 7 December. Available at: https://www.canada.ca/en/environment-climate-change/services/environmental-indicators/greenhouse-gas-emissions.html#oil-gas (Accessed: 7 December 2024).

[14] Alberta Energy Regulator (AER) n.d., 'Well Status', viewed 27 November 2024, https://www.aer.ca/providing-information/data-and-reports/data-hub/well-status.

[15] Schiffner, D., Kecinski, M. and Mohapatra, S., 2021. An updated look at petroleum well leaks, ineffective policies and the social cost of methane in Canada’s largest oil-producing province. Climatic Change, 164(3), p.60.

[16] Bowman, L.V., El Hachem, K. and Kang, M., 2023. Methane Emissions from Abandoned Oil and Gas Wells in Alberta and Saskatchewan, Canada: The Role of Surface Casing Vent Flows. Environmental Science & Technology, 57(48), pp.19594-19601.

[17] Williams, J.P., Regehr, A. and Kang, M., 2020. Methane emissions from abandoned oil and gas wells in Canada and the United States. Environmental science & technology, 55(1), pp.563-570.

[18] International Energy Agency (n.d.) 'Funding to clean up orphan or inactive oil gas wells to create employment and reduce methane emissions', IEA. Available at: https://www.iea.org/policies/11482-funding-to-clean-up-orphan-or-inactive-oil-gas-wells-to-create-employment-and-reduce-methane-emissions (Accessed: 7 December 2024).

[19] Government of Canada (n.d.) 'Low Carbon Economy Challenge', Environment and Climate Change Canada. Available at: https://www.canada.ca/en/environment-climate-change/services/climate-change/low-carbon-economy-fund/challenge.html (Accessed: 7 December 2024).

[20] Government of Canada (n.d.) 'What is the Low Carbon Economy Fund?', Environment and Climate Change Canada. Available at: https://www.canada.ca/en/environment-climate-change/services/climate-change/low-carbon-economy-fund/what-is-lcef.html (Accessed: 7 December 2024).

[21] Canadian Energy Research Institute, Economic and Environmental Impacts of Methane Emissions Reduction in the Natural Gas Supply Chain (2019). https://ceri.ca/studies/economic-and-environmental-impacts-of-methane emissions-reduction-in-the-natural-gas-supply-chain

[22] Environment and Climate Change Canada, National Inventory Report 1990–2019: Greenhouse Gas Sources And Sinks In Canada (2021). https://publications.gc.ca/site/eng/9.506002/publication.html

[23] Government of B.C., "Industrial facility greenhouse gas emissions" (2020). https://www2.gov.bc.ca/gov/content/environment/climate-change/data/industrial-facility-ghg

Chapter 2

LITERATURE REVIEW

2.1 Literature Review

The oil and gas industry faces increasing pressure to improve efficiency, reduce costs, and minimize environmental impact. This is becoming increasingly important with the growing demand for the oil industry to reduce or completely eliminate the direct emissions associated with oil and gas production. This inevitably results in massive electrification of the upstream oil and gas industry and increased integration of large scale renewable energy, internet of things sensors and other intelligent well technologies. This literature review examines recent research on optimizing sucker-rod pump systems, integrating renewable energy sources, implementing low-cost SCADA systems, and dynamically modelling renewable-powered pumps.

The potential profitability of marginal wells in mature oil fields, particularly in Latin America, is presented in [1]. The study challenges the conventional wisdom that low-producing wells are not economically viable, arguing that with proper management and cost-effective technologies, these wells can become profitable assets. The authors analyze data from the United States, Mexico, and Argentina to demonstrate the significant presence of marginal wells in these markets. They emphasize the importance of efficient production management, rational cost control, and the application of suitable artificial lift systems to maximize returns from these wells. The study introduces several innovative technologies designed specifically for low-production wells. These technologies aim to reduce operational costs and extend well life without requiring extensive surface equipment or workover operations. The authors conclude by stressing the need for a specialized approach to managing marginal wells, including continuous cost analysis, enhanced production surveillance, and effective data management to ensure profitability in this niche sector of the oil industry.

2.2 Background of The Study

The background of this research is presented under four key aspects in the following sections: energy requirement estimation for oil well systems, renewable energy integration in oil well production, SCADA systems for oil and gas well operations, dynamic modelling of energy systems for oil well production.

2.3 Energy Requirement for Oil Well Production

Optimal production of oil from the sub-surface requires careful estimation of the amount of energy that the installed artificial lift system would require. The sucker rod pump artificial lift is the focus of this research with this section considering the attempt to optimally size and deploy it in oil production operations.

2.3.1 Sucker-Rod Pump Optimization

Sucker-rod pumps remain a common artificial lift method in the oil industry due to their reliability and effectiveness in various well conditions. Recent studies have focused on optimizing these systems to improve energy efficiency and performance. A comprehensive overview of sucker-rod pumping systems is presented in [2], emphasizing the importance of proper design and operation for maximizing efficiency.

The design and optimization of sucker rod pumping systems for oil production is presented in [3]. The authors present a comprehensive overview of the process, detailing the steps involved in designing an effective pumping installation. They discuss key factors such as fluid production rate, pump depth, and equipment selection, emphasizing the importance of considering various components like plunger size, rod string configuration, and surface unit specifications. The paper introduces PROSPER, a well performance software tool, and demonstrates its application in modelling sucker rod pumping systems. The authors provide a detailed case study, including fluid data, equipment specifications, and inflow performance relations. They analyze design results, examining parameters such as power requirements, rod loading, and production rates. The study also includes sensitivity analyses for different rod types and pumping speeds, highlighting the software's capability to optimize system performance. Overall, this research offers valuable insights into the complexities of sucker rod pump design and the use of modern computational tools to enhance oil production efficiency.

A comprehensive methodology for optimizing the design of sucker-rod pumping systems specifically tailored for coalbed methane (CBM) wells is presented in [4]. It emphasizes the importance of various design parameters, including pump setting depth, rod string taper, plunger size, stroke length, and pumping speed, which collectively influence the system's performance and efficiency. The authors introduce an iterative algorithm to determine these parameters based on desired production rates while addressing the complexities associated with traditional trial-and-error methods. Key findings indicate that both water production rates and pump setting depths are critical for optimization, with the production rate showing a consistent increase relative to adjustments in design variables. Furthermore, the study highlights the dynamic interplay between stroke length and load capacity, revealing that shorter strokes may lead to reduced load capacities and plunger diameters under specific conditions. Overall, this work aims to enhance the operational efficiency of sucker-rod pumps in CBM extraction through a systematic approach to design optimization.

An algorithm for the automated selection of the operating point of VLP and IPR curves intersection using the Petroleum Experts Prosper software is developed and presented in [5]. The automated selection process is implemented using the VBA script in MS Excel. This research highlights the potential for simulator integration with scripts in optimizing sucker rod performance and energy efficiency.

Innovative approaches to enhance the management and monitoring of sucker rod pumping units (SRPUs) in oil production are presented in [6]. The authors propose a novel technique utilizing robust normalized correlation functions derived from force sensor signals on the rod string hanger. By analyzing these functions, they identify a set of informative attributes that correspond to various SRPU technical conditions. The research demonstrates how these attributes can be effectively used for real-time identification and management of SRPUs using affordable controllers. The study outlines the mathematical foundations of their approach, addressing challenges such as noise reduction and signal normalization. The authors describe a practical implementation of their system, including a three-level management structure and real-time data processing methods. They present experimental results from field applications, showcasing the system's ability to accurately identify SRPU conditions without relying on traditional dynamometer card visual interpretation. The study concludes by highlighting the economic benefits of this approach, including significant energy savings and extended equipment lifespan, as observed in real-world deployments across multiple oil fields.

The challenges and potential improvements in electric drive systems for sucker rod pumps (SRPs) used in oil production are presented in [7]. The authors highlight the energy-intensive nature of downhole oil extraction and the inefficiencies often present in SRP operations. They analyze the cyclic load patterns of SRP electric motors, which lead to variations in efficiency and power factor throughout each oscillation cycle. The study reveals that many SRP units are underloaded and poorly balanced, resulting in suboptimal performance. To address these issues, the researchers propose several technical solutions, including proper counterweight balancing, installing lower-powered motors, utilizing permanent magnet motors, replacing balancer drives with chain drives, and implementing variable frequency drives. These modifications aim to enhance the energy efficiency, stability, and overall performance of SRP systems in oil production operations.

The optimization of energy consumption in oil fields through data analysis is presented in [8]. The study examines nearly 45,000 wells across six major Chinese oil fields, introducing a normalized consumption factor to evaluate energy efficiency. The authors investigate the impact of various factors on energy consumption, including lifting methods, daily production rates, pump depths, gas-oil ratios, and well angles. The analysis reveals that higher production rates generally lead to lower normalized consumption factors for beam pumps, progressive cavity pumps, and electric submersible pump systems. Additionally, the study finds that increased gas-oil ratios may result in lower normalized consumption for beam pump systems, while well angles have minimal impact. To optimize energy consumption in beam-pumped wells, several key recommendations are proposed. Firstly, selecting high-efficiency motors equipped with transducers is crucial for controlling power consumption as the load varies. Additionally, reducing the balance material and switching to lighter rods can significantly decrease energy usage. In some cases, replacing traditional beam pump systems with more energy-efficient alternatives like bending beam and digital pump units may be beneficial, as demonstrated in China's Changqing oil field. Furthermore, proper sizing and operation of the equipment are essential, including choosing appropriate pump diameters, lengths, and stroke frequencies to match production rates. Regular maintenance and prompt adjustment of operating parameters can also contribute to improved efficiency. Lastly, implementing data analysis and monitoring systems can help identify areas for optimization and guide decision-making in energy management for beam-pumped wells.

The methods to enhance the energy efficiency of electric drives in sucker rod pumps (SRPs) used for oil production are presented in [9]. The authors discuss the challenges associated with SRP operations, including cyclic loading, power reserve requirements, and efficiency losses due to multiple intermediary components. They propose analytical approaches to determine power characteristics, efficiency, and power factor under cyclic loading conditions. The study examines the impact of counterbalancing on power consumption and introduces a method to assess additional losses from imbalance. The researchers present a case study demonstrating potential energy savings through optimization measures such as motor replacement, improved counterweight balancing, and adjustments to well operating parameters.

The innovative approach to enhance the energy efficiency of sucker-rod pumps (SRPs) through optimal counterbalancing is presented in [10]. The authors propose a sensorless method that utilizes torque and speed calculations from the induction motor to determine the ideal counterweight settings. By employing adaptive observers and a Kalman filter-based speed estimation technique, the system can accurately assess the motor's electromagnetic torque and rotor speed without additional sensors. The research introduces a novel algorithm for computing the extra torque required to minimize active power consumption. Simulation results demonstrate the effectiveness of this method, showing a significant reduction in energy usage compared to conventional balancing practices. The proposed system's ability to optimize SRP performance using only motor variables makes it a promising solution for improving the efficiency of oil extraction operations.

The innovative approaches to enhance the energy efficiency of Sucker-Rod Pump (SRP) systems by reducing the electric motor ratings in the oil industry are presented in [11]. The authors propose two control schemes to optimize the performance of these widely used artificial lift mechanisms. The first is an open-loop frequency optimization scheme (OLFOS) that employs a genetic algorithm to minimize fluctuations in motor output power. While effective, this method is computationally intensive and lacks robustness to parameter variations. Building on these findings, the researchers developed a closed-loop frequency control scheme (CLFCS) that offers superior performance and adaptability. This novel approach utilizes the mean value of motor output power as a reference and the instantaneous power as feedback to generate the control signal. Simulation results demonstrate that the

CLFCS significantly reduces peak power requirements and power fluctuations, enabling the use of lower-rated motors and improving overall system efficiency. The proposed method shows resilience to changes in liquid levels and strokes per minute, making it a promising solution for real-world applications. The authors conclude that implementing this control strategy could lead to substantial energy savings and economic benefits for the oil industry.

Various energy-saving technologies for oil field pumping units, a critical component in petroleum extraction are presented in [12]. The authors discuss several approaches to improve efficiency, including structural modifications to conventional beam pumping units, the development of non-beam pumping units, and the use of energy-efficient motors. They also examine advanced control technologies, such as artificial intelligence and expert systems, to optimize pumping unit operations. The study highlights the potential of renewable energy sources, particularly wind and solar power, in reducing energy consumption in oil fields. The authors propose an innovative direct-drive wind turbine system for pumping units, utilizing hydraulic transmission technology to increase wind energy utilization without electric energy conversion. The study concludes by suggesting future research directions, including enhanced utilization of renewable energy, implementation of intelligent control systems, and the adoption of digital oil production technologies to further improve energy efficiency.

Innovative approaches to analyze and optimize sucker rod pumping systems in oil production is discussed in [13]. The author combines electrical and petroleum engineering concepts to develop new methods for rod pump analysis and supervision. The research focuses on modelling induction motors used in sucker rod pumping, with particular attention to high-slip motors. The author introduces novel techniques for estimating motor parameters and efficiency, including an empirical correlation for high-slip motor efficiency and a parameter estimation method using a modified Particle Swarm Optimization algorithm. The thesis also presents a new approach to infer dynamometer diagrams based solely on electrical measurements, potentially offering a cost-effective alternative to traditional dynamometry. Throughout the work, the author emphasizes the importance of accurate motor modelling and efficiency calculations in improving the overall performance and energy efficiency of sucker rod pumping systems, particularly in mature oil fields.

The design and simulation of a novel hydraulic pump jack system aimed at improving the efficiency of sucker rod pumping, which is a widely used artificial lift method in oil and gas extraction is presented in [14]. Traditional beam pumping units face challenges such as high energy consumption, large physical footprint, limited stroke length, and inefficiencies in speed control. The study introduces hydraulic pumping units as a viable alternative, offering advantages like precise control of motion, reduced energy requirements, and adaptability to various operational conditions. Using Simulink/MATLAB software, the research compares the performance of hydraulic units with conventional systems under identical wellbore conditions. The proposed hydraulic unit demonstrates superior energy efficiency, enhanced productivity, and better control over stroke length and speed. Additionally, it supports both conventional sucker rod strings and continuous wire rope systems, showing improved operational flexibility and reduced mechanical failures compared to traditional setups. This innovative system addresses key limitations of conventional beam pumps, making it a promising solution for modern oilfield applications.

An innovative approach to enhance the efficiency and longevity of sucker rod pumping systems in oil production is presented in [15]. The authors introduce a frequency elastic drive system that dynamically adjusts the motor frequency during the pumping cycle to optimize performance. By modulating the rotational speed of the electrical engine, this method aims to reduce peak loads, minimize mechanical stress, and improve energy efficiency. The researchers conducted field tests to validate their concept, comparing standard operations with two variations of the new frequency-adjusted approach. Results showed significant reductions in peak torque and energy consumption, with one variation achieving a 15% decrease in energy usage. The study also delves into the advantages of using different types of induction machines, comparing the high starting torque of NEMA D with the higher efficiency of IEFF2 and explores additional benefits of variable speed drives, such as soft start capabilities and power-balanced operation for multiple pumps.

The innovative approach to optimizing sucker-rod oil pumping units (SRPU) for marginal wells is presented in [16]. The authors propose an electromechanical control system that utilizes a Hamming neural network to analyze load curves and determine pump filling factors. This adaptive system adjusts the motor speed based on real-time data, ensuring optimal operation and energy efficiency. The research includes a comprehensive mathematical model of the SRPU, incorporating elements such as the jack pump, induction motor, and frequency converter. The authors developed a computer simulation in MATLAB to validate their approach, demonstrating the system's ability to respond quickly to changes in well conditions and detect emergency situations.

The dynamic analysis of beam pumping units, which are crucial components in sucker rod pumping systems for oil production is presented in [17]. The authors present a comprehensive examination of the unit's kinematics and dynamics, focusing on the four-bar linkage mechanism. They derive equations for the polished rod's motion, including displacement, velocity, and acceleration, based on geometric relationships. The study then delves into the dynamic aspects, analyzing various loads acting on the polished rod and establishing equations for stress analysis of the beam, linkage, and crank. By combining these equations, the researchers develop a method to calculate the output torque of the crankshaft, which is essential for system balance and condition monitoring. The study's innovative approach to stress analysis and dynamic modelling provides a foundation for further research into sucker rod string vibration characteristics, potentially improving the efficiency and reliability of oil extraction processes.

The energy consumption optimization in sucker rod pump (SRP) units for oil production is presented in [18]. The authors present a novel methodology and mathematical model to calculate and analyze the electric energy consumption of SRP units. Their research investigates the impact of various factors on energy efficiency, including oil properties, well operation modes, and SRP balancing. The study reveals that maximum energy efficiency is achieved with longer stroke lengths and lower oscillation frequencies of the walking beam. The authors emphasize the importance of optimizing motor and pump efficiency, maintaining high depression, and ensuring complete fluid extraction. Their model allows for finding optimal operation modes for individual wells, potentially enabling adaptive strategies based on electricity tariffs.

The integration of Process and Asset Performance/Maintenance digital twins to create autonomous production platforms in the offshore oil and gas industry is presented in [19]. The author presents a vision for normally unmanned platforms with minimal maintenance interventions, achievable through advanced digital technologies. The Process Twin, which has been successfully deployed in real-world applications, enables closed-loop production optimization by considering multiple constraints and key performance indicators. Complementing this, the Asset Performance Twin continuously monitors equipment health, predicting remaining useful life and suggesting operational adjustments to extend equipment longevity. The study highlights the benefits of combining these twins, allowing for real-time optimization that balances production goals with equipment maintenance needs. Various optimization scenarios are explored, demonstrating the flexibility and power of this integrated approach. The author argues that this holistic strategy, leveraging synchronous equation-based modelling and virtual flowmeters, represents a significant step towards autonomous offshore operations, addressing challenges such as limited real-time data and complex multi-variant optimization problems.

An innovative approach to enhance the energy efficiency of sucker-rod pump electric drives in oil production is presented in [20]. The authors propose a method that utilizes the kinetic energy of the pump's unbalanced mechanical parts to reduce electrical energy consumption. By implementing a variable speed control system, the drive's motor speed is adjusted cyclically, decreasing during the upward stroke and increasing during the downward stroke. This technique aims to balance the load torque on the motor shaft, potentially lowering peak power demands and overall energy usage. The proposed system incorporates a programmable logic controller (PLC) and a position sensor on the pump's crankshaft to regulate the motor's speed reference signal. The authors suggest that this method could lead to a reduction in the required rated capacity of the electric drive components and improved overall system efficiency. While developed for sucker-rod pumps, the authors note that this approach could be adapted for other reciprocating machinery with similar motion characteristics.

An innovative approach to measuring oil production in sucker rod pump (SRP) wells using electrical parameters and big data analytics is presented in [21]. The authors propose a method that utilizes easily obtainable continuous electrical data, such as power, current, and voltage, along with real-time well production information as training parameters for a deep learning model. By converting the electric power curve into a dynamometer card and calculating pump efficiency, the model can estimate well production based on stroke, frequency, and pump diameter. The study involved over 300 SRP wells in an experimental area, employing techniques like Fast Fourier Transform (FFT) for data processing and Long Short-Term Memory (LSTM) networks for production forecasting. The results demonstrate the model's ability to accurately predict production across various well types, including stable, intermittent, and erratic producers. This method offers potential benefits in terms of cost reduction, improved efficiency, and real-time production monitoring, particularly valuable in low oil price environments.

2.4 Renewable Energy Integration in Oil and Gas Industry

There has been a growing adoption and deployment of various types of renewable energy systems in the upstream, mid-stream, and downstream oil and gas sectors, and with deployment cutting across different stages in the oil production lifecycle. While onsite renewable energy is sometimes deployed in small-scale, low power applications in mobile and DC-powered use cases, there is a growing push for its adoption in high voltage, high power, and large scale microgrid applications in oil wells . We will be reviewing various levels, stages, and kinds of renewable energy adoption in upstream oil production.

2.4.1 Renewable Energy Integration in Oil Well Production

The integration of renewable energy technologies in upstream oil and gas production, examining several promising opportunities, is presented in [22]. As conventional reserves deplete and production shifts to more energy-intensive sources, renewable solutions offer pathways to reduce costs and emissions. Key areas for integration include electrification of drilling operations and primary recovery, where solar and wind power can supplement or replace diesel generators. In secondary recovery, offshore wind shows potential for powering water injection pumps. Tertiary recovery, or enhanced oil recovery (EOR), offers significant opportunities for renewable integration, particularly through concentrated solar power for steam generation. Geothermal cogeneration from produced water also shows promise in some fields. These technologies can help address the industry's growing energy needs while mitigating environmental impacts. However, challenges such as variability of renewable generation and the need for high reliability must be overcome. As renewable costs continue to decline and environmental concerns grow, the economic and operational benefits of integrating these technologies in upstream operations are likely to increase significantly [22].

The potential for solar energy utilization in the global petroleum sector, encompassing both upstream (extraction and transport) and downstream (refining) operations is presented in [23]. The study employs open-source models to analyze 83 representative oil fields and 75 refinery crude streams, representing approximately 25% of global production. By estimating energy intensities and applying various solar resource quality criteria, the researchers assess the feasibility of solar deployment in different regions. The findings suggest significant potential for both solar thermal and photovoltaic (PV) applications in the oil and gas industry. Upstream operations could potentially accommodate 19-44 GW of solar thermal capacity and 6-11 GW of PV capacity, while downstream operations show potential for 21-95 GW of solar thermal and 17-91 GW of PV capacity. However, the study acknowledges limitations due to factors such as offshore production, geographical constraints, and varying energy intensities across different crude types. The authors conclude that the oil and gas sector could become a substantial consumer of solar energy, although further research incorporating detailed economic analysis and location-specific data would be beneficial for more precise estimates.

The application of renewable energy sources to power artificial lift systems represents a promising avenue for improving sustainability in oil and gas operations. The feasibility of using a floating photovoltaic power (FSPV) system and offshore wind for artificial lifts to meet the demand for 10 pumps in remote oil fields is explored in [24]. The study examines the potential of integrating hybrid energy systems, specifically floating solar photovoltaic (FSPV) technology, to power artificial lift pumps on offshore oil platforms in the Brazilian equatorial margin. The study conducts a comprehensive technical evaluation, focusing on a 10 MW FSPV system designed to meet the energy demands of 10 pumps. Through detailed simulations using the System Advisor Model (SAM), the researchers assess the viability and performance of the

FSPV system in the region's unique environmental conditions. The analysis reveals that the proposed FSPV system can generate approximately 17 GWh of electricity annually, exceeding the energy requirements of the artificial lift pumps. The study finds that it could be both technically viable and economically attractive in certain scenarios. The research also examines the environmental impacts and compares FSPV with offshore wind energy, ultimately concluding that FSPV presents a more suitable and promising solution for powering offshore platforms in the Brazilian equatorial region due to its abundant solar resources, modularity, and minimal visual interference. This research contributes valuable insights to the ongoing efforts in transitioning towards cleaner energy sources in offshore oil and gas operations.

The feasibility of implementing solar-powered artificial lift systems in remote oil wells in Sudan's Heglig oil field is presented in [25]. The study examines three wells currently using diesel generators for power, analyzing the technical, economic, and environmental aspects of transitioning to photovoltaic (PV) systems. The authors utilize PVsyst software to design and simulate standalone PV setups for each well, comparing their performance and costs to the existing diesel generators and a potential hybrid system. The research highlights the challenges of powering remote oil sites, including high operational costs, greenhouse gas emissions, and maintenance issues associated with diesel generators. By proposing solar energy as an alternative, the study aims to reduce production costs, minimize environmental impact, and improve overall operational efficiency. The study provides a comprehensive analysis of the solar potential in the region, system design considerations, and economic feasibility, offering valuable insights for the oil industry's transition towards more sustainable energy solutions in remote locations.

The implementation of renewable energy sources in the oil and gas industry, focusing on a case study in Egypt, is presented in [26]. The researchers conducted a techno-economic analysis comparing four different power supply configurations for an oil production well in a remote area. These configurations included a standalone diesel generator system and three hybrid systems incorporating photovoltaic panels, wind turbines, and battery storage. Using HOMER software for optimization, the study evaluated the economic and environmental impacts of each configuration. The results demonstrated significant benefits in adopting renewable energy systems, including substantial reductions in fuel consumption, carbon emissions, and levelized cost of energy (LCOE). The study also examined the effects of carbon pricing policies, such as emissions trading systems and carbon taxes, on the economic viability of renewable energy integration. Overall, the study highlights the potential for renewable energy to enhance sustainability and cost-effectiveness in the oil and gas sector, particularly in remote locations.

The energy efficiency potential of the Solar Jack Energy Management System, an innovative technology designed for rod beam pumps in oil production is evaluated in [27]. The assessment, conducted by Lincus Inc. for Pacific Gas and Electric Company's Emerging Technologies Program, examined the system's performance at two test sites. Solar Jack combines three components: a variable frequency drive (VFD), a regenerative capacitor bank, and a solar photovoltaic system. The study found that energy savings ranged from 16.7% to 51.7% of baseline consumption, with varying contributions from each component. However, the wide variation in results highlights the impact of site-specific factors such as well characteristics and operational parameters. While the technology shows promise, the report recommends further evaluation across a larger sample of wells before considering it for deemed energy efficiency offerings. The study also identified challenges in data monitoring and suggested areas for future research, including comparisons with other control technologies and financial analysis.

The potential applications of solar energy in the oil and gas industry are examined in [28]. It explores how solar technologies can meet energy demands across the upstream and downstream sectors, potentially reducing fossil fuel consumption and environmental impacts. The study discusses various solar applications, including photovoltaic systems for powering remote operations, solar thermal technologies for enhanced oil recovery and process heat, and solar desalination for treating produced water. It also highlights emerging research in solar-powered high-temperature processes relevant to refining, such as steam reforming and hydrogen production. While solar adoption faces some challenges in the industry, the authors argue it presents significant opportunities to improve energy efficiency, reduce costs, and lower carbon footprints. The review concludes that integrating solar energy into oil and gas operations could benefit both the petroleum and renewable energy sectors as the global energy landscape evolves.

An innovative approach to oil production that combines intelligent intermittent pumping with a photovoltaic-storage microgrid system is presented in [29]. The authors propose a novel technology that integrates solar power, energy storage, and DC motor-driven pumping units to optimize energy efficiency and reduce carbon emissions in oil fields. The research outlines the development of a specialized microgrid controller and software platform to manage this hybrid system effectively. By utilizing machine learning algorithms and real-time data analysis, the technology adapts to changing conditions and optimizes production parameters. Field experiments demonstrated significant improvements in system efficiency, electricity savings, and oil production increases. The integration of renewable energy sources not only enhances the sustainability of oil extraction operations but also reshapes the work environment for oil field personnel. This cutting-edge solution addresses the challenges of low-producing wells while promoting “greener” and low-carbon development strategies in the petroleum industry.

The RenuWell project in Alberta, Canada, which demonstrates an innovative approach to repurposing inactive oil and gas well sites for small-scale solar energy generation is presented in [30]. The RenuWell initiative has established a pair of demonstration locations featuring small-scale photovoltaic installations. These pilot projects collectively generate 1.5 megawatts of electricity, showcasing the potential for community-oriented solar energy development in the region. This initiative addresses multiple challenges simultaneously: the environmental liabilities of abandoned fossil fuel infrastructure, the need for renewable energy development, and the economic struggles of rural communities affected by the decline of the oil and gas industry. RenuWell's approach is characterized by its emphasis on community engagement, partnerships with diverse stakeholders, and a focus on distributed energy generation. The project not only transforms degraded land into productive solar sites but also provides economic benefits to local communities through job creation, training programs, and cooperative ownership models.

The implementation of a pioneering solar-fossil hybrid power plant in Egypt's Western Desert, designed to enhance oil production efficiency is presented in [31]. The project carried out between 2012 and 2013, integrated a 110 kWp photovoltaic system with a 200 kW diesel generator to power sucker rod pumps in a remote location. A key innovation was the development of a patented Power Management System (PMS) that optimized energy flow between solar panels, diesel generators, and electric engines. The hybrid system operated successfully for over 8,000 hours in harsh environmental conditions, demonstrating reliability and achieving up to 12% reduction in diesel fuel consumption and CO2 emissions. This pilot project not only validated the feasibility of hybridization in oil and gas operations but also paved the way for future optimizations, including the potential integration of energy storage solutions like supercapacitors for improved peak shaving and system stability.

The integration of a hybrid photovoltaic (PV) and diesel generator (DG) system for powering sucker rod pumps in an oil field located in Egypt's Western Desert is presented in [32]. The study aims to optimize energy production and reduce costs in remote areas where grid access is limited. The authors propose a novel approach that combines a metaheuristic optimizer with PV sizing models for sucker rod pumping systems. They compare distributed and centralized generation topologies, evaluating their technical and economic feasibility. The research utilizes real-world data from ten wells to calculate power requirements and system configurations. Through their analysis, the authors determine that a hybrid system with 54% PV contribution offers the best performance. They conclude that a hybrid centralized generation system (HCGS) can potentially reduce the levelized cost of energy (LCOE) by 62.8% compared to the existing diesel-only setup, making it the recommended configuration for implementation in similar oil field environments.

A pilot project implementing a photovoltaic (PV) and diesel generator hybrid system in the Aghar oil field, located in Egypt's Western Desert is presented in [33]. The project aimed to reduce fossil fuel consumption and CO2 emissions by incorporating solar energy into the power supply for sucker rod pumps. The system faced several challenges, including load stability issues with the variable load of the sucker rod pumps and problems with load sharing between the PV system and diesel generator. The researchers conducted various trials to optimize the system, including replacing the variable load with a constant load, upgrading the generator capacity, and addressing harmonics issues. They found that the generator's power capacity should be at least 1.6 times that of the PV system for stable operation. The study also highlighted the importance of considering factors such as power factor correction and harmonic distortion when designing hybrid systems for variable loads in oil fields. Despite initial setbacks, the system ultimately achieved stable operation, demonstrating the potential for solar energy integration in remote oil field operations.

A case study of solar energy utilization in oil extraction by PetroFarah, an Egyptian petroleum company, is presented in [34]. The study focuses on a pilot project at the Farah-8 well, where a 72.9 kW photovoltaic solar unit was installed to power a sucker rod pump, replacing a diesel generator. The initiative aimed to reduce greenhouse gas emissions and align with global climate change mitigation efforts. The results were impressive, showing a 44% reduction in diesel consumption and corresponding GHG emissions. The project demonstrated a net reduction of 0.5 kg CO2 equivalent per barrel of oil produced, with an estimated CO2 avoidance cost of $0.05 per kg. Beyond environmental benefits, the project proved economically viable with a payback period of less than two years. This innovative approach not only supports Egypt's Vision 2030 and international climate agreements, but also sets a precedent for sustainable practices in the oil and gas industry, potentially paving the way for wider adoption of renewable energy solutions in fossil fuel extraction.

An innovative approach to powering sucker rod pump units in oil production using renewable energy sources is presented in [35]. The authors propose integrating wind turbines and solar panels to supplement the traditional electrical grid supply for these pumps. This hybrid system aims to reduce electricity consumption from the grid, lower production costs, and enhance power supply reliability. The study discusses the cyclical nature of sucker rod pump power consumption and how renewable sources can help smooth out these fluctuations. It presents technical calculations for sizing wind turbines and solar panels to meet the pumps' power requirements. The authors also suggest a novel configuration where renewable energy sources connect directly to the DC link of a variable frequency drive, potentially improving system efficiency. Overall, this research highlights the potential for renewable energy integration in oil production to address both economic and environmental concerns in the industry.

The potential integration of solar energy into hydrocarbon extraction and enhanced oil recovery (EOR) operations, particularly in high-latitude regions, is presented in [36]. The authors argue that despite challenges such as reduced sunlight intensity and shorter daylight hours, recent technological advancements make solar power viable in these areas. They discuss various applications, including powering drilling rigs, artificial lift pumps, and microbial EOR processes. The study highlights the environmental benefits of reducing greenhouse gas emissions and the potential economic advantages of replacing costly fuel sources with solar energy. The authors present data on global horizontal irradiance (GHI) for different regions and propose innovative solutions like using solar thermal energy to maintain optimal conditions for microbial cultures in EOR projects. While acknowledging the need for further feasibility studies, the article suggests that implementing solar technologies in high-latitude oil fields could improve the industry's public perception and contribute to sustainable energy practices in petroleum.

An innovative method for extracting bitumen from oil sands using solar energy instead of natural gas is proposed in [37]. The concept involves utilizing concentrated solar radiation to generate mid-temperature steam, which is then injected into oil sand formations to stimulate bitumen recovery. The thermal mass of the formation allows for continuous extraction despite intermittent solar availability. The study examines the thermodynamic and economic feasibility of this approach in Alberta, Canada. By eliminating natural gas consumption, the method could significantly reduce greenhouse gas emissions and operating costs. The authors present calculations for energy requirements, solar collector area, and potential savings. While the initial capital investment is substantial, the projected return on investment is promising, especially considering potential carbon taxation and depreciation benefits. This solar-assisted bitumen recovery technique offers a more sustainable and environmentally friendly alternative to conventional extraction methods, addressing challenges related to natural gas supply and environmental regulations in the oil sands industry.

The potential for reducing greenhouse gas (GHG) emissions in Canada’s oil sands industry by integrating renewable and low-carbon energy technologies is evaluated in [38]. It develops a novel framework combining market penetration modelling and bottom-up energy accounting using the LEAP system to assess 27 scenarios across extraction, upgrading, and electricity generation. Key findings reveal that nuclear energy offers the highest GHG mitigation potential at the lowest cost, while geothermal, bioenergy, and hydropower show cost-effectiveness in specific cases but limited emission reductions. Wind and solar technologies demonstrate minimal feasibility due to high costs and technical constraints. Carbon pricing significantly enhances technology adoption, with higher incentives (e.g., \$50/t CO_2e) leading to greater emission reductions and cost savings. The study concludes that while renewable technologies alone cannot meet emissions caps, nuclear options could contribute substantially to long-term GHG reduction goals in the oil sands sector.

The integration of renewable energy, particularly solar power, into the upstream oil supply chain (USOSC) to mitigate environmental impacts such as greenhouse gas (GHG) emissions is evaluated in [39]. It highlights the energy-intensive nature of oil production and its reliance on fossil fuels, which contribute significantly to CO2 emissions and hazardous waste. The study evaluates solar energy as a viable alternative to partially replace conventional energy sources in non-critical operations and enhance oil recovery processes. It examines various solar technologies, their economic feasibility, and their compatibility with oil industry requirements while considering challenges like irradiation levels, weather conditions, and regulatory policies. Through case studies and scenario analyses, the research identifies optimal solar energy applications and strategies for reducing GHG emissions while maintaining production targets. This work underscores the potential of renewable energy to make oil operations more sustainable and environmentally friendly.

The potential for decarbonizing remote microgrids in Canada, addressing a significant gap in the country's renewable energy landscape, is presented in [40]. While most of Canada's electricity is produced using renewables, many remote communities still rely on fossil fuels for power generation. The study employs a cost-based binary integer optimization model to determine the most economical renewable energy solutions for 148 off-grid settlements across Canada. By analyzing factors such as wind speed, solar irradiance, and projected technology costs, the research identifies whether solar or wind power is more suitable for each location and when implementation would be most cost-effective. The findings suggest that transitioning to renewable microgrids is financially feasible, with total costs aligning with previous decarbonization estimates. The study reveals that communities currently using diesel or heavy fuel oil should prioritize immediate decarbonization, while those using natural gas may benefit from waiting for technology costs to decrease. Additionally, the research highlights the importance of considering fossil fuel savings when planning transition timelines. This comprehensive analysis provides valuable insights for policymakers and stakeholders in developing strategies to decarbonize Canada's remote communities and improve their energy independence.

2.5 SCADA Systems for Industrial Operations

The advent of Industry 4.0 has ushered in a new era of industrial innovation, characterized by the integration of cyber-physical systems, and the Internet of Things (IoT). This technological revolution has significant implications for various sectors, including the field of Supervisory Control and Data Acquisition (SCADA) systems.

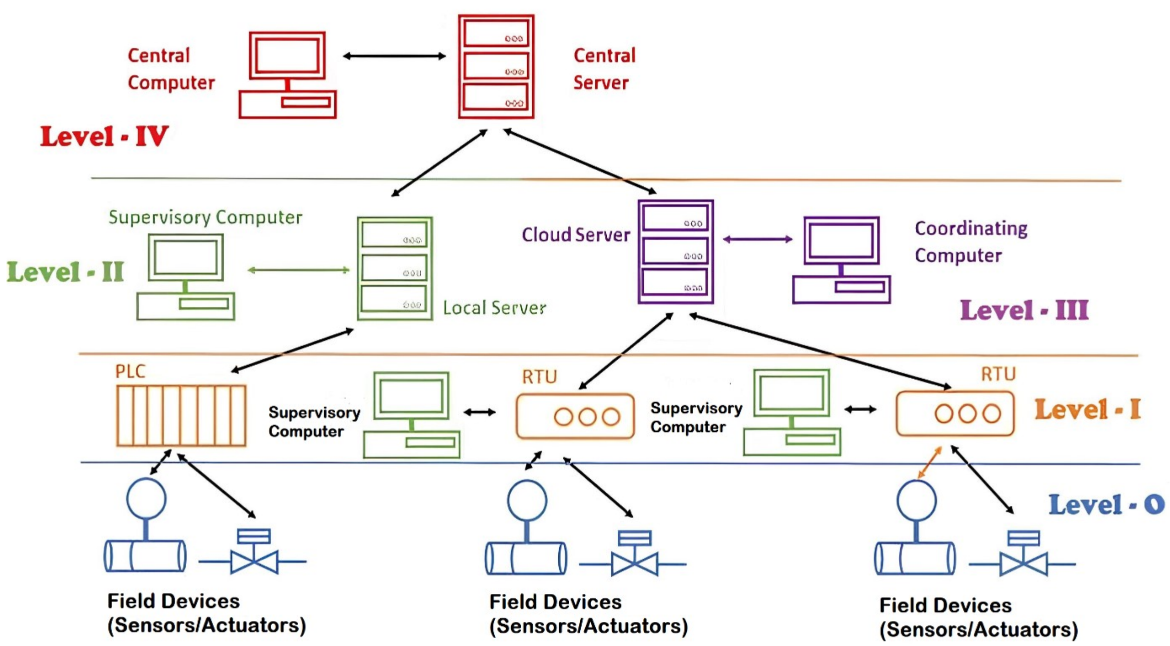

Figure 2.1 Architecture of SCADA System [41]

Key features of SCADA Systems are shown in Figure 2.1 . SCADA comprises of sensors which collect real-time data from physical processes and serve as the data acquisition system. Actuators in SCADA systems effect control by executing commands based on processed data. Supervisory systems support monitoring by visualizing process status for operators, while hierarchical communication systems between levels ensures seamless operation by integrating data from multiple sources for analysis by centralized servers.

The provided diagram illustrates the hierarchical structure of a typical SCADA (Supervisory Control and Data Acquisition) system, showcasing its various operational levels and components. The Hierarchy of a SCADA system from the architecture is presented in levels as follows:

1. **Level 0, Field Devices** : This level includes sensors and actuators that interact directly with the physical processes (e.g., temperature sensors, flow meters, valves). These devices collect raw data and execute control commands [42, 43].

2. **Level I, PLCs and RTUs** : Programmable Logic Controllers (PLCs) and Remote Terminal Units (RTUs) are responsible for processing data from field devices. RTUs as responsible for real-time data collection and communication with Master Terminal Units (MTUs). They act as intermediaries between field devices and supervisory computers, collecting sensor data from field devices which is then processed for supervisory control, and executing local control logic [44]. PLCs are industrial-grade controllers designed for specific tasks in critical infrastructure [45].

3. **Level II, Supervisory Computers** : Supervisory computers monitor and control processes by communicating with PLCs and RTUs. Supervisory computers aggregate data from Level I devices, manage HMIs, and generate actionable insights [46]. Local servers may also be

present at this level to store data temporarily. The control center in SCADA architecture includes servers, HMIs, and databases for real-time monitoring [42].

4. **Level III, Coordination Systems** : This level includes coordinating computers and cloud servers that aggregate data from multiple supervisory systems. Cloud servers and coordination systems enable centralized monitoring across distributed SCADA networks. Modern architectures integrate cloud computing for scalability. Cloud servers enable remote access to SCADA data for centralized monitoring [46]. This layer supports IoT integration for advanced automation and remote access [45].

5. **Level IV, Central Servers** : Central servers store all collected data for long-term analysis, and decision-making. They provide high-level oversight of the entire SCADA system [43]. These servers integrate multi-source data for decision-making in critical infrastructure sectors like energy and transportation [42].

In the context of well-production monitoring and control, SCADA technology offers the potential to transform operations from manual, human-dependent processes to automated, real-time data-driven systems. This shift has demonstrated enhanced efficiency, reliability and safety in production management. However, the widespread adoption of SCADA technology faces a substantial hurdle in the form of high implementation costs, which may limit its accessibility and application across industries. Low cost SCADA system deployments for oil field operations will be reviewed in this section.

2.5.1 SCADA Implementation for Oil and Gas Production

The evolution and application of Supervisory Control and Data Acquisition (SCADA) systems in oilfields is presented in [47]. The authors outline three major stages in the development of oilfield automation: computerized, digital, and smart oilfields. The importance of real-time data collection and analysis in improving oil production efficiency and reducing operational costs is emphasized. It highlights the challenges faced in implementing SCADA systems in oilfields, particularly in terms of data communication and multiphase flow rate measurement. The study also explores recent trends in oilfield data communication, including the use of satellite technology, portable SCADA systems, and wireless communication. The authors stress the potential for further advancements in SCADA technology to meet the unique requirements of the oil and gas industry, especially as global energy demand continues to rise.

The adoption of Internet of Things (IoT) technology in the oil and gas (O&G) industry, highlighting its potential to transform operations across upstream, midstream, and downstream sectors is presented in [48]. While Supervisory Control and Data Acquisition (SCADA) systems have long been used for asset monitoring in the O&G industry, they face limitations such as interoperability issues, high costs, and inflexibility. IoT emerges as a solution to overcome these SCADA-related challenges, offering seamless real-time data collection, processing, and analysis capabilities. The review identifies key applications of IoT in O&G, including remote monitoring, predictive maintenance, automation, safety compliance, and supply chain management. However, the industry faces several hurdles in IoT adoption, such as cybersecurity risks, technological readiness for hazardous environments, interoperability concerns, and data management challenges. The study emphasizes the need for collaborative research efforts and greater engagement from O&G operators to drive innovation and address these challenges effectively.

The transformative potential of edge computing and Industrial Internet of Things (IIoT) technologies in oilfield management is presented in [49]. It highlights how these innovations enable real-time data analysis, proactive maintenance, and autonomous operations, leading to significant improvements in operational efficiency and cost reduction. The authors present several case studies demonstrating the practical applications of edge computing in various scenarios, such as remote asset monitoring, automated gas handling in ESP operations, and intelligent rod pump diagnostics. These implementations resulted in reduced manual interventions, improved safety, and increased production. The study emphasizes the importance of an open, secure, and scalable edge computing platform that can integrate with existing infrastructure and leverage domain expertise. By adopting these technologies, oil and gas operators can achieve a step change in performance, enhancing operational efficiency and productivity while minimizing safety risks and environmental impact. The authors conclude that as the digitalization of field assets matures, more operators will recognize and capitalize on the benefits of IIoT solutions for comprehensive field optimization

Table 2.1 A comparison of different SCADA system technologies.

SCADA System Type	Description	Key Features	Advantages	Disadvantages
Standalone SCADA	Operates independently without network connections. Ideal for small installations.	Simple, low cost, stable in environments with connectivity issues.	Easy to install and maintain, low cost.	Limited scalability, not suitable for complex processes. [50]
Distributed SCADA	Connects multiple workstations and control units via a centralized network. Used in large industrial installations.	Scalable, integrates multiple processes, real-time monitoring.	Offers flexibility and scalability, suitable for large businesses.	More expensive, requires robust infrastructure. [51]
Cloud-Based SCADA	Stores and processes data on remote servers, enabling remote access and reducing local infrastructure needs.	Remote monitoring, cost-effective, integrates with digital platforms.	Reduces operational costs, enhances remote access and integration capabilities.	Data security concerns, requires reliable providers. [52]
Web SCADA	Combines distributed and cloud-based features, offering multi-platform access via a browser-based interface.	Flexible, accessible, supports OPC UA protocol.	Highly adaptable, supports Industry 4.0 demands, reduces costs.	May require advanced infrastructure for full functionality. [50]
Monolithic SCADA	Basic architecture with a single system communicating with RTUs. No network connectivity.	Simple, independent operation.	Easy to implement in isolated environments.	Limited functionality, no scalability. [53]
Networked SCADA	Uses WANs and Ethernet to connect systems, enabling data access from multiple locations.	Scalable, interconnected systems.	Enhances data sharing and system integration.	Requires advanced networking infrastructure. [51]
IoT-Integrated SCADA	Incorporates IoT technology for real-time data collection and analysis across interconnected systems.	Advanced data analysis, reduced infrastructure costs.	Offers enhanced automation and data insights.	May require significant investment in IoT infrastructure. [51]

A comparison of different SCADA system technologies is shown in Table 2.1 presenting the types, description, key features, advantages and disadvantages.

The implementation of advanced technologies to optimize sucker rod pumping operations in a challenging oil field is presented in [54]. The authors describe how they leveraged Internet of Things (IoT) devices, edge computing, and machine learning algorithms to transform their approach from reactive to proactive well management. By installing edge gateway devices on multiple wells, they were able to collect and analyze real-time data, including dynamometer cards, which provide crucial insights into downhole pump behavior. The system utilizes cloud-based dashboards and sophisticated analytics modules to visualize data, detect anomalies, and generate smart alarms. This digitalization effort has resulted in significant improvements, including reduced well downtime, prevention of equipment failures, and more efficient resource utilization. The authors emphasize how this technology-driven approach enables remote management of numerous wells, optimizes production, and enhances decision-making processes, ultimately leading to improved operational efficiency and cost savings in economically challenged remote fields.

An innovative Supervisory Control and Data Acquisition (SCADA) system designed for CO2 Enhanced Oil Recovery (EOR) is presented in [55]. The system incorporates cutting-edge technologies to create an efficient, flexible, and cost-effective solution for oilfield operations. At its core, the design utilizes Arduino Yun single-board computers as Remote Terminal Units (RTUs), which enable local data processing and control. The system employs wireless Ethernet/IP communication via Ubiquiti NanoStation radios, forming a robust mesh network. A central server acts as the Master Terminal Unit (MTU), hosting a MySQL database and providing web-based access through Apache and PHP. The design includes an optimized sucker-rod pump control algorithm based on the Everitt-Jennings method. Notable features include over-the-air programmability, low cost (approximately $1,000 per wellhead post-installation), compatibility with various sensors and actuators, and a user-friendly web interface accessible from any device. While prototype testing in North Dakota showed promising results, the authors suggest further investigation into wireless communication stability and potential component upgrades before commercialization.

The design and implementation of a microcomputer-based Remote Terminal Unit (RTU) for a Supervisory Control and Data Acquisition (SCADA) system is presented in [56]. The RTU, developed for an oil and gas company in the Middle East, showcases the evolving role of SCADA in modern industrial applications. By incorporating a microcomputer into its core, the RTU offers enhanced functionality, including real-time data acquisition, report-by-exception communication, and even complex gas flow calculations. The system's modular hardware design and structured software architecture contribute to its versatility and maintainability. Notable features include a Preventive Maintenance Terminal (PMT) for on-site diagnostics and a select-before-operate mechanism for secure control operations. This RTU exemplifies how SCADA systems are becoming more distributed and intelligent, offloading tasks from central stations to field devices, thereby improving overall system efficiency and responsiveness in various industries beyond oil and gas.

The implementation and testing of an optimized Remote Terminal Unit (RTU) design for wireless Supervisory Control and Data Acquisition (SCADA) systems is presented in [57]. The researchers developed an FPGA-based RTU, which offers enhanced reliability and reconfigurability compared to traditional solutions. SCADA systems play a crucial role in various industries, including energy management, oil and gas, and water distribution. The study focuses on creating a cost-effective and efficient RTU that can operate in wide-area networks. The authors detail the design process, hardware implementation, and prototype testing of their FPGA-based RTU. They highlight the advantages of their approach, such as improved performance, flexibility, and reduced costs compared to commercially available options. The research demonstrates the potential for FPGA technology to revolutionize SCADA systems, offering a more powerful and adaptable solution for remote monitoring and control applications across various industrial sectors.

The implementation of telemetry SCADA (Supervisory Control and Data Acquisition) and Machine Learning (ML) technologies to optimize pumpjack wellhead production facilities is presented in [58]. The authors present a comprehensive system architecture that integrates field sensors, Remote Telemetry Units (RTUs), telecommunication systems, SCADA, and analytics gateways. By leveraging these technologies, operators can monitor and analyze dynamometer card data in real-time, enabling more efficient well operations. The integration of ML models allows for automated dynamometer card pattern recognition and predictive analytics, leading to reduced pump failures, lower maintenance costs, and optimized production. The study also highlights the benefits of edge computing and cloud-based solutions in managing remote pump jacks. The authors report that implementing this system on four remote pump jacks over 12 months resulted in significant improvements, including reduced pump failures, increased production uptime, and lower carbon emissions due to fewer site visits. Overall, the study demonstrates how advanced technologies can enhance operational efficiency and sustainability in oil and gas production.

An innovative approach to Supervisory Control and Data Acquisition (SCADA) systems, focusing on the development of a Wireless Remote Terminal Unit (WRTU) and a comprehensive cybersecurity framework is presented in [59]. The WRTU, designed for versatility and cost-effectiveness, incorporates multiple communication modes, including GSM, satellite, and Wi-Fi, allowing for flexible deployment in various environments. The system's architecture comprises the WRTU, a Control and Monitoring Center (CMC), and a multi-tiered cybersecurity framework. The CMC serves as the central hub for real-time monitoring, control, and cyber-incident management, while the cybersecurity framework addresses the growing concerns of cyber threats to critical infrastructure. By integrating advanced technologies and security measures, this SCADA system aims to enhance operational efficiency, reduce costs, and provide robust protection against cyber attacks. The authors emphasize the importance of a holistic approach to cybersecurity, encompassing technology, policy, and human factors, to safeguard critical SCADA infrastructure in an increasingly interconnected world.

The innovative deployment of a private Industrial Internet of Things (IIoT) network integrated with SCADA systems in ADNOC Onshore's oil and gas facilities is presented in [60]. The project aimed to enhance remote monitoring and control capabilities while addressing data security concerns associated with traditional IoT solutions. By leveraging existing SCADA infrastructure as a backbone, the team implemented a Low Power Wide Area Network (LPWAN) using LoRa technology. This approach allowed for the integration of legacy instrumentation and enabled bidirectional communication for remote well shutdown. The SCADA system played a crucial role in this implementation, serving as the central control and data acquisition platform. It facilitated the seamless integration of LoRa devices with existing field equipment and provided a secure means of transmitting data to the control room. The pilot deployment demonstrated improved operational efficiency, enhanced safety measures, and cost-effectiveness compared to traditional wired solutions. This novel approach to combining IIoT with SCADA showcases a promising direction for modernizing brownfield oil and gas facilities while maintaining robust security and leveraging existing infrastructure.

The implementation of an Internet of Things (IoT) surveillance and optimization system in Block X, a mature oil field in South Sumatra, Indonesia is presented in [61]. The project aimed to enhance operational efficiency, reduce costs, and maximize production in a field with over 100 wells. By integrating existing controllers with IoT devices, the system enabled real-time monitoring and control of Electric Submersible Pump (ESP) and Sucker Rod Pump (SRP) wells. The Supervisory Control and Data Acquisition (SCADA) system played a crucial role in this transformation, serving as the central hub for data collection, analysis, and decision-making. SCADA facilitated quick identification of problematic wells, enabled efficient optimization strategies, and supported the implementation of intelligent alarm notifications. The results were significant, including a 25% reduction in loss oil potential, substantial cost savings, and increased production revenue. The success of this project demonstrates the potential of IoT and SCADA technologies in revolutionizing oil field operations, particularly in mature fields seeking to improve efficiency and productivity

The challenges and requirements for establishing an effective digital oil field (DOF) data architecture are presented in [62]. It emphasizes the need for a more integrated and standardized approach to handle the increasing volumes of data from various sources in upstream oil and gas operations. The authors highlight the importance of developing intelligent instrumentation, streamlined data acquisition processes, and unified production automation systems (PAS). A key focus is placed on the role of Supervisory Control and Data Acquisition (SCADA) systems in this context. The study suggests that SCADA, along with other PAS components, should evolve to handle complex data types, support real-time applications, and facilitate seamless integration with enterprise systems. The authors propose adopting open standards like OPC UA for improved interoperability and discuss the potential benefits of this approach, including enhanced production optimization, reduced IT costs, and improved operational efficiency. The study concludes by outlining the evolving requirements for sensors, PAS systems, and integration strategies to sustain and maximize the benefits of digital oil field initiatives.

An innovative approach to monitoring renewable energy systems using an Internet of Things (IoT)-aided Supervisory Control and Data Acquisition (SCADA) system is presented in [63]. The researchers developed a hybrid power system comprising photovoltaic panels, wind turbines, and battery storage, which is monitored and controlled remotely through a SCADA interface. By leveraging IoT technology, the system enables real-time data collection and analysis, allowing for efficient management of renewable energy sources, particularly those installed in remote or offshore locations. The study demonstrates the integration of simulation software, hardware prototypes, and online platforms to create a comprehensive monitoring solution. The SCADA system's role is pivotal, as it facilitates the supervision and control of multiple energy sources, data visualization, and remote operation of system components. This approach offers advantages in terms of cost-effectiveness, reliability, and real-time monitoring capabilities, potentially revolutionizing the management of renewable energy assets and contributing to the optimization of hybrid power systems.

The implementation of ZigBee wireless technology in SCADA systems for oil and gas pipeline monitoring and control is presented in [64]. The authors propose replacing traditional fiber optic cables with ZigBee devices, citing advantages such as lower costs, reduced maintenance requirements, and suitability for desert environments. The study outlines the current use of fiber optic cables in oil and gas fields, discussing their limitations in certain environments. It then delves into the structure of SCADA systems, explaining their components and functions in industrial settings. The authors highlight ZigBee's capabilities, including its long-range communication, data transfer rates, and ability to support numerous nodes simultaneously. The integration of ZigBee with SCADA systems is presented as a solution for remote pipeline management, offering real-time data acquisition and control without the need for extensive cabling. This approach is suggested to enhance operational efficiency, reduce manpower requirements, and optimize transmission processes in oil and gas operations

The application of Industrial Internet of Things (IIoT) technology to optimize crude oil production through enhanced pump efficiency control is presented in [65]. The researchers developed an innovative IIoT platform that integrates real-time data collection, analysis, and control mechanisms for sucker rod pumps. By implementing wireless communication, remote monitoring, and intelligent control algorithms, the system addresses common challenges like gas lock and maintains optimal pump fillage. The study demonstrates significant improvements in production rates, with a 90% increase observed in the test well. Key components of the solution include a SCADAPack 535E controller, 5G wireless connectivity, and custom software for data visualization and decision support. The authors emphasize the potential of IIoT to revolutionize upstream and downstream operations in the oil and gas industry, leading to reduced maintenance costs, improved production efficiency, and increased reliability. The developed SCADA system monitors and controls the sucker-rod pumps leading to improved efficiency and reduced downtime compared to traditional manual monitoring methods [65]. This research highlights the transformative impact of digitalization and data-centric approaches in modernizing traditional oil field operations. This study also highlights the potential of using IoT-based SCADA solutions for collecting, storing, and analyzing required parameters to improve pump fillage, and enhance operational efficiency in intelligent oil and gas production. The Marginal Expense Oil Well Wireless Surveillance system (MEOWWS) represents a significant advancement in monitoring and optimizing marginal oil wells and is presented in [66]. Developed through a collaborative effort between Petrolects and Vaquero Energy, this innovative technology addresses the challenges of maintaining profitability in low-producing wells. The system utilizes a proprietary flow-detection method, incorporating wireless sensors and microcontrollers to measure well health and pumping efficiency. By transmitting daily data to a central base station, MEOWWS enables operators to identify issues promptly, leading to increased production and reduced energy consumption. The system's low power requirements and battery-operated design make it cost-effective and easy to implement. Field tests have shown promising results, with potential improvements in oil and gas production, as well as significant cost savings in personnel time and electricity usage. Future developments may include automated pump-off controllers and applications in various monitoring scenarios, potentially revitalizing inactive wells and enhancing overall field management.

The implementation of SCADA optimization software for monitoring and analyzing the performance of sucker rod pump units, focusing on unit balance and gearbox torque is presented in [67]. Traditional Counterbalance Effect (CBE) measurements, used to calculate Counterbalance Torque (CBT), are limited to balanced wells. For unbalanced wells, the study introduces a modified CBE method that incorporates a correction factor derived from crank movement timing. This corrected CBT value is integrated into SCADA software, enabling real-time monitoring and accurate analysis of gearbox torque and pumping unit balance. The SCADA system also generates alarms for anomalies, helping operators perform preventive maintenance to extend the lifespan of critical components like gearboxes. Validation of the modified method through electrical measurements confirms its accuracy, making it a practical tool for improving operational efficiency and reliability in oil production.

The optimization of sucker rod pump operations in the Wafra oil field, located in the neutral zone between Kuwait and Saudi Arabia, through advanced real-time surveillance and data analysis is presented in [68]. By instrumenting 450 wells with SCADA systems, the study identified wells with high load issues or suboptimal performance. A classification system grouped wells into categories such as those requiring equipment upgrades or parameter adjustments. Optimization strategies included swapping surface pumping units between wells based on load conditions and modifying downhole equipment to maximize efficiency. This approach minimized costs, reduced deferred production, and enhanced oil output by an estimated 1,500 barrels per day across 57 targeted wells. Additionally, continuous monitoring and adjustments using real-time data allowed for safe and efficient operations while addressing structural and gearbox loading challenges. Case studies demonstrated successful implementation of these strategies, highlighting significant production gains and improved resource utilization.

The implementation of an innovative real-time field surveillance and well services management system in a mature onshore oil field in California is presented in [69]. The project aimed to improve efficiency and reduce operating costs across a large number of wells. A key component of the system was the integration of existing Supervisory Control and Data Acquisition (SCADA) technologies with new software interfaces. This allowed for comprehensive monitoring of well performance, automated data collection, and streamlined decision-making processes. The SCADA infrastructure provided real-time data from various field devices, including pump-off controllers, tank level sensors, and flow line temperature sensors. This data was then consolidated and made accessible through a user-friendly web-based interface, enabling more effective well surveillance, downtime reporting, and maintenance planning. The implementation of this system, combined with other initiatives, resulted in significant reductions in well failure rates and associated costs. The success of the project led to its expansion across multiple business units, demonstrating the scalability and potential of integrated SCADA and software solutions in improving operational efficiency in mature oil fields

The implementation of a smart field optimization system in the Wafra oil field, located in the neutral zone between Kuwait and Saudi Arabia is presented in [70]. The project, initiated in 2011, involved instrumenting over 900 artificially lifted wells with SCADA (Supervisory Control and Data Acquisition) technology. This advanced system enabled real-time monitoring, control, and analysis of well performance, significantly enhancing production management. The SCADA implementation faced several challenges, including server availability, field scanning, data integration, and validation. However, these were overcome through collaborative efforts. The system's capabilities include real-time data collection, historical data analysis, and intelligent alarm configurations. This allowed engineers to identify issues such as chemical injection candidates, unbalanced rod pumps, gas interference, and motor overloads more efficiently. The SCADA-based smart field approach has revolutionized well management, reducing response times, minimizing failures, and optimizing power consumption, ultimately leading to improved production outcomes and operational efficiency

An innovative method for estimating downhole pressure and temperature conditions in the Schoonebeek steamflood development using readily available SCADA (Supervisory Control and Data Acquisition) data is presented in [71]. The author introduces two novel approaches: one for determining flowing bottomhole pressure (fBHP) based on rod load measurements, and another for estimating flowing bottomhole temperature (fBHT) using wellhead temperature trends. These methods leverage the wealth of continuous SCADA data collected at the wellhead, which is typically used for rod pump operation optimization. By applying simplified models and statistical analysis to this data, the author demonstrates how to obtain robust estimates of downhole pressure and temperature regimes without the need for additional equipment or well interventions. The study highlights the potential of SCADA data to complement or even substitute expensive downhole surveillance techniques, thereby reducing operational costs while maintaining data availability for effective well and reservoir management. This approach not only provides near-continuous monitoring capabilities but also enables the recovery of historical downhole conditions, ultimately improving well and reservoir management practices in thermal EOR projects, even for periods when direct measurements were unavailable or inconsistent.

An innovative approach to rod pump monitoring and failure detection using Industrial Internet of Things (IIoT) Edge Analytics is presented in [72]. The solution employs machine learning models deployed at the wellhead to analyze dynagraph cards in real-time, enabling automated identification of pump abnormalities. While traditional methods relied on centralized data repositories and expert analysis, this system pushes intelligence to remote assets, allowing for immediate corrective actions. The architecture integrates with existing Supervisory Control and Data Acquisition (SCADA) systems, enhancing their capabilities by providing localized, real-time insights. SCADA plays a crucial role in this setup by facilitating communication between the Remote Terminal Unit (RTU) and the supervision site, allowing operators to monitor multiple pumps simultaneously. The Edge Analytics solution complements SCADA by performing on-site analysis and generating alarms, which can be incorporated into the broader SCADA-based monitoring and control framework. This synergy between Edge Analytics and SCADA creates a more responsive and efficient system for managing rod pump operations, potentially reducing downtime and optimizing maintenance schedules.

An innovative approach to optimizing rod pump systems in oil production using big data analytics and visualization tools is presented in [73]. The authors describe the development of a Rod Pump Optimization Tool (RPOT) that integrates data from multiple sources, including SCADA systems, to provide real-time insights and recommendations for pump adjustments. By leveraging SCADA data, the tool enables automated workflows that analyze well performance, equipment constraints, and production targets to generate specific optimization actions. The RPOT's interactive visualizations allow engineers to quickly identify underperforming wells and make data-driven decisions to improve efficiency. This approach has led to enhanced communication between field and office teams, significant time savings in well surveillance, and the potential for increased production and reduced operating costs. The study highlights how integrating SCADA systems with advanced analytics can transform traditional rod pump management, paving the way for more proactive and efficient oilfield operations.

The transformative impact of edge computing and Industrial Internet of Things (IIoT) solutions on oil and gas production operations is presented in [74]. While traditional SCADA systems have been instrumental in monitoring and controlling field operations, they face limitations in device integration, scalability, and data contextualization. The authors present a novel approach that complements SCADA with edge computing, enabling real-time data analysis and decision-making at the well site. This combination addresses challenges such as remote well management, equipment diagnostics, and proactive maintenance. The study illustrates the benefits through case studies involving electrical submersible pumps, sucker rod pumps, and multiphase flowmeters. By leveraging edge gateways and intelligent algorithms, operators can achieve improved operational efficiency, reduced field visits, and enhanced collaboration between field and office personnel. The integration of edge computing with existing SCADA infrastructure emerges as a powerful strategy for oil and gas companies to optimize production, minimize downtime, and reduce operational costs in an increasingly competitive industry landscape.

An innovative approach to optimizing oil and gas production through the implementation of autonomous well control systems is presented in [75]. The solution leverages cutting-edge technologies such as edge computing, artificial intelligence, and advanced analytics to enhance the efficiency and sustainability of sucker rod pump (SRP) operations. By integrating smart alarming, pump-off control, and speed optimization, the system enables real-time monitoring and autonomous decision-making at the well site. While SCADA systems are not the primary focus, they play a crucial role in the overall architecture by facilitating data exchange between the autonomous well controllers and centralized monitoring systems. The solution's ability to connect with enterprise-level SCADA platforms allows for comprehensive fleet management and enterprise-wide visibility, enabling operators to make informed decisions based on real-time data from multiple wells. This integration of autonomous well control with SCADA systems represents a significant step towards achieving fully autonomous and sustainable upstream production operations.

The implementation of a comprehensive digital oil field solution across multiple areas in Kuwait, integrating real-time data from artificially lifted wells into a single, secure platform is presented in [76]. The project's cornerstone was the deployment of a sophisticated SCADA (Supervisory Control and Data Acquisition) system, which revolutionized well monitoring and control practices. By leveraging SCADA technology, engineers gained the ability to remotely access, analyze, and modify well parameters in real-time, significantly enhancing production optimization efforts. The integration faced numerous challenges, including network security concerns and the need to harmonize data from diverse fields. However, the successful implementation resulted in improved well performance, reduced downtime, and more efficient asset management. The SCADA-based solution enabled "management by exception," allowing teams to focus on wells requiring immediate attention while automating routine monitoring tasks. This digital transformation not only boosted productivity but also enhanced safety by minimizing the need for physical site visits, particularly in adverse conditions.

The implementation of automated control solutions to enhance beam pump performance and increase well productivity in Block-5, Oman is presented in [77]. By transitioning from conventional manual controllers to advanced automated systems, Daleel Petroleum achieved significant improvements in operational efficiency and production rates. The automated controllers, utilizing Pump Fillage (PF) and Pump Intake Pressure (PIP) modes, optimized the balance between inflow and outflow performance. This led to reduced failure rates, extended equipment lifespan, decreased environmental impact, and lower power consumption. SCADA (Supervisory Control and Data Acquisition) systems played a crucial role in this transformation by enabling remote monitoring and control of well operations. The integration of SCADA with the automated controllers facilitated real-time data collection, analysis, and adjustment of pump parameters, contributing to the overall success of the optimization efforts. The study demonstrates the value of embracing advanced technologies in mature oil fields to overcome production challenges and maximize resource recovery.

The evolving landscape of Industrial Internet of Things (IIoT) adoption in the oil and gas industry, emphasizing the transition from traditional SCADA systems to more advanced IoT solutions is presented in [78]. While SCADA has long been the backbone of industrial control and data acquisition, the authors argue that IIoT represents a significant leap forward in capabilities and potential benefits. Unlike SCADA's often isolated and proprietary nature, IIoT architectures integrate multiple sensors, enterprise systems, and advanced analytics to enable more comprehensive operational insights and decision-making. The study highlights various use cases where IIoT has been implemented, such as artificial lift optimization, equipment maintenance, asset life extension, and safety improvements. However, it also acknowledges the challenges in this transition, including the need to bridge legacy SCADA systems with new IoT technologies, address connectivity issues in remote locations, and enhance cybersecurity measures. The authors suggest that while SCADA remains relevant, the industry is gradually moving towards a more interconnected, data-driven approach that combines edge computing, cloud analytics, and machine learning to unlock new levels of efficiency and value creation in oil and gas operations.

A novel approach to hydrocarbon production optimization using a digital twin model that encompasses the entire value chain is presented in [79]. The authors present a solution called Real-time Production Optimization (RTPO), which utilizes an equation-based optimization engine to address challenges in traditional simulation methods. RTPO integrates data from various sources, including SCADA systems, to create a comprehensive digital twin of the oilfield. By leveraging SCADA data for real-time insights into well performance, pressure, flow rates, and equipment status, RTPO enables more accurate and timely optimization. This integration allows for strategic optimization, rapid response to field upsets, and exploration of "what-if" scenarios. The study emphasizes how SCADA integration is crucial for generating up-to-date well curves and virtual flow meter data, which are essential for reliable optimization runs. By combining SCADA data with advanced modelling techniques, RTPO aims to bring the industry closer to autonomous well operations and closed-loop production optimization

The critical role of Supervisory Control and Data Acquisition (SCADA) systems in the oil and gas industry, particularly for pipeline monitoring and control is presented in [80]. It emphasizes the importance of selecting appropriate communication media and protocols for SCADA implementation. The authors advocate for the use of advanced seven-layer protocols, which offer benefits such as network redundancy, remote diagnostics, and efficient data transmission. The study explores various aspects of SCADA communications, including protocol features, integration of multiple devices, wide area network connections, and direct IP connectivity. It also highlights innovative functions enabled by modern SCADA systems, such as video image transmission and instant pager notifications. The authors argue that investing in advanced communication protocols for SCADA systems can lead to significant operational benefits and cost savings in the long run, making it a crucial consideration for oil and gas companies seeking to optimize their pipeline operations

The challenges and advancements in real-time data architecture for upstream oil and gas operations, particularly focusing on the implementation of the digital oilfield concept is presented in [81]. Supervisory Control and Data Acquisition (SCADA) systems play a pivotal role in this ecosystem by enabling efficient communication between field devices through simple, power-efficient protocols like Modbus. SCADA facilitates both one-way and limited two-way communication, allowing remote monitoring and basic control of operations, such as opening or closing valves. These systems are crucial for managing data from sensors operating in harsh, remote environments and integrating it into centralized networks. Despite their long-standing utility since the 1960s, SCADA systems face limitations in handling the massive and diverse data generated by modern oilfield operations. However, advancements in sensor technology, wireless transmission, and data integration standards are making SCADA systems more robust and adaptable. These developments, combined with big data technologies, enhance decision-making, operational efficiency, and safety in the oil and gas industry.

An innovative approach to real-time well monitoring in marginal oil fields using a custom-built Intelligent Well Monitoring (IWM) system is presented in [82]. The authors describe the development and implementation of a cost-effective solution that utilizes smart microcontrollers and sensors to monitor key well parameters such as pressure, temperature, and load current. Unlike traditional SCADA (Supervisory Control and Data Acquisition) systems, which are often expensive and limited to high-priority wells, the IWM offers a more affordable alternative suitable for widespread deployment across marginal fields. While SCADA systems typically provide more comprehensive data, including features like dynagraphs, the IWM's lower cost allows for broader implementation, potentially covering a larger number of wells. The system significantly improves crew response time from hours to minutes by sending real-time notifications to smartphones, enhancing production efficiency and safety. The authors report that the IWM demonstrated high accuracy compared to calibrated manual tools and proved to be 82% more economical than traditional SCADA-based monitoring systems in their field trials, making it a promising solution for marginal field operators seeking to optimize production while managing costs.

The implementation of an innovative approach to well optimization in Bakken horizontal wells using Internet of Things (IoT) devices and machine learning is presented in [83]. The authors highlight the limitations of traditional rod pump control systems, particularly in modern, deviated wellbores. By employing a more sophisticated wave equation that accounts for additional friction factors and utilizing high-resolution data from IoT devices, the system can more accurately model downhole conditions. The study emphasizes the shortcomings of conventional SCADA-based systems, which are limited in their ability to transmit large volumes of data and react to dynamic well conditions. The new approach overcomes these limitations by deploying IoT-enabled edge devices that provide real-time, high-quality data directly to improved physics models. This allows for more accurate well classification and autonomous setpoint management. The pilot study, conducted on 50 wells, demonstrated significant improvements in well optimization, including increased production in under-pumping wells and improved efficiency in over-pumping wells. The results underscore the potential of this data-driven, autonomous optimization technique to enhance operational efficiency and production in unconventional oil fields, while highlighting the limitations of traditional SCADA systems in achieving similar results.

The integration of Supervisory Control and Data Acquisition (SCADA) systems with Machine Learning (ML) techniques to optimize pumpjack wellhead production facilities is presented in [84]. The SCADA system plays a crucial role in this setup by collecting real-time data from various sensors, including proximity sensors and load cells, which are used to generate dynamometer card. These dynamometer card provide valuable insights into well performance and potential issues. The SCADA infrastructure enables remote monitoring and control of the pumpjacks, allowing operators to make informed decisions from a central control room. By incorporating ML algorithms, the system can automatically analyze dynamometer card, predict potential problems, and optimize production parameters. This combination of SCADA and ML not only enhances operational efficiency but also reduces maintenance costs, minimizes downtime, and contributes to sustainability efforts by reducing the need for frequent site visits. The study demonstrates how this integrated approach can lead to significant improvements in pump jack performance, energy consumption, and overall production optimization.

The implementation of a Supervisory Control and Data Acquisition (SCADA) system to transform three offshore oil platforms in Egypt's Red Sea from manned to unmanned operations is presented in [85]. The project involved several key components, including the installation of new instrumentation networks, modification of control circuits, implementation of high-speed communication links, and the integration of solar power systems. The SCADA system played a crucial role in modernizing the control infrastructure, replacing outdated relay-based and pneumatic systems with a more efficient, reliable, and remotely operable solution. By integrating real-time monitoring, automated control, and advanced communication technologies, SCADA enabled comprehensive oversight of well operations, production processes, and safety protocols from an onshore control center. The project also incorporated PID (Proportional-Integral-Derivative) algorithms to optimize control processes and utilized renewable energy sources to power certain platform systems, to enhance sustainability and reduce operational costs. The transition to unmanned platforms, facilitated by SCADA, resulted in significant economic benefits, improved safety measures, and increased operational efficiency. This case study demonstrates the transformative potential of SCADA technology in offshore oil and gas operations, showcasing its ability to streamline processes, minimize human intervention, and optimize resource utilization in challenging marine environments.

The implementation of Internet of Things (IoT) technology in the KS brownfield in South Sumatra, Indonesia, to enhance the monitoring and control of Electrical Submersible Pump (ESP) systems is presented in [86]. The authors highlight how Supervisory Control and Data Acquisition (SCADA) technology, integrated with IoT, revolutionized the field's operations. By utilizing existing GSM cellular networks and implementing a dynamic IP architecture, the project achieved cost-effective real-time monitoring of ESP parameters. The SCADA system, equipped with intelligent alarms and automatic notifications, significantly improved operator response times and reduced production losses. The implementation faced challenges such as varied ESP controller types and communication issues, which were addressed through programmable modems and tailored communication modes. The study emphasizes the importance of a robust SCADA platform in enabling data-driven decision-making and paving the way for future advancements in big data analysis and machine learning within the oil and gas industry.

The application of low-cost data loggers and controllers to optimize oil production using progressive cavity pumps are presented in [87]. While traditional methods rely on limited daily observations, this innovative approach enables continuous monitoring and data collection. The system primarily measures rod torque, which reflects various well conditions such as sand influx, gas presence, and pump-off situations. By analyzing this data, operators can make informed decisions to prevent problems and enhance production efficiency. The technology allows for real-time monitoring at the well site and remote data access through wireless connectivity. Additionally, the system can implement automated controls to respond to adverse conditions, potentially reducing equipment damage and downtime. While SCADA systems are mentioned as helpful for well monitoring, they are described as costly and limited in data handling capabilities. In contrast, this low-cost solution offers a more accessible and comprehensive alternative for optimizing oil production, particularly for smaller operations or those seeking a more cost-effective approach to well management and data analysis.

The implementation of an integrated SCADA (Supervisory Control and Data Acquisition) system in a west Texas oil field is presented in [88], showcasing the benefits of combining RTU (Remote Terminal Unit) functionality with programmable controller-based control systems. The project aimed to evaluate the cost-effectiveness of new technologies in oil production applications. The SCADA system incorporated various functions, including automatic well testing, water injection control, and remote monitoring of production facilities. Key design criteria included the use of existing communication infrastructure, expandability, and remote diagnostic capabilities. The system architecture utilized Local Area Networks (LANs) at both the master location and the lease, allowing for significant expansion potential. The implementation process involved extensive software development, testing, and integration of various components. The resulting SCADA system demonstrated several benefits, including reduced production downtime, increased operational efficiency, and improved remote control capabilities. Overall, the project highlighted the viability and reliability of programmable controller LANs in accessing field data and alarms, leading to the initiation of similar installations in other fields.

A novel Internet of Things (IoT) based architecture for the oil and gas industry, aiming to address limitations of existing monitoring systems are proposed in [89]. While Supervisory Control and Data Acquisition (SCADA) systems have been widely used, they face challenges such as high costs, inflexibility, and delayed data transmission. The authors present a modular IoT architecture comprising smart objects, gateways, and a control center to enable efficient, secure, and real-time monitoring across upstream, midstream, and downstream operations. This approach leverages IoT devices and cloud technologies to simplify configurations and reduce complexity. The architecture supports various scenarios, including pipeline monitoring, wellhead management, and storage tank oversight. By facilitating predictive maintenance, enhancing security, and optimizing operations, the proposed system aims to improve productivity and reduce costs in the oil and gas sector. The authors emphasize the potential for this IoT-based solution to overcome SCADA's limitations and provide more responsive, scalable, and cost-effective monitoring capabilities.

The challenges and potential improvements for future Supervisory Control and Data Acquisition (SCADA) systems are presented in [90], focusing on enhancing their interoperability and extensibility. The authors argue that current SCADA systems are often inflexible, static, and centralized, which limits their ability to integrate with other technologies and adapt to new applications. To address these issues, they propose three key areas for research and development: implementing a flexible communication architecture, developing open and interoperable protocols, and creating smarter remote terminal units (RTUs). The study suggests adopting Internet technologies for networking, establishing a two-tiered architecture that incorporates wireless sensor networks, and designing RTUs capable of preliminary data processing and real-time event detection. By addressing these areas, future SCADA systems could significantly improve their functionality and adaptability, particularly in applications such as oil and gas field monitoring, where enhanced interoperability and extensibility could lead to increased productivity at minimal cost.

2.6 Dynamic Modelling of Energy Systems for Oil Well Production

Significant amount of energy is required to drive the artificial lift systems that produce oil from aging reservoirs. Depending on the prime mover and the type of artificial lift system, the energy could be sourced from diesel, natural gas or associated gas produced on-site. The growing demand to reduce the carbon footprint of these aging wells is driving the wave of electrification of the upstream oil and gas industry and hence increasing the adoption and integration of large scale, high power onsite renewable energy sources such as solar (PV, thermal and concentrated solar power), wind turbines (electric, hydraulic), storage (battery, flywheel), and geothermal (steam generation and steam injection for enhanced oil recovery). This section will review literature featuring approaches adopted to integration of renewable energy in powering oil wells.

2.6.1 Dynamic Modelling of Renewable-Powered Pumps

As the integration of renewable energy resources with artificial lift systems becomes more prevalent, there is a growing need for accurate modelling and simulation tools and frameworks. A methodology for Power Supply of Sucker Rod Pumping Units using Renewable Energy Sources is presented in [35]. The study presents innovative approaches to powering sucker rod pump units in the oil industry using renewable energy sources, specifically wind and solar generators. Recognizing that electricity consumption significantly impacts oil production costs, the study proposes a hybrid power supply strategy that reduces strain on the electrical grid and enhances power reliability. By integrating wind turbines and solar panels into the existing electrical infrastructure, the researchers demonstrate a method to supplement traditional grid power with renewable energy, particularly focusing on smoothing the cyclic power consumption characteristic of sucker rod pump electric motors. The proposed system allows for dynamic power management, where constant power is drawn from the electrical grid while variable power components are supplied by renewable sources, ultimately improving energy efficiency and potentially reducing operational expenses in oil extraction processes. Their approach ensured that the frequency-controlled electric drive has a direct current link. The wind generator and solar panel are then directly connected to the sucker rod pump through a DC link without an inverter [35].

The evolution of wind power technology and its application in the oil industry is presented in [91]. As wind turbines have become more advanced and powerful, they have found new uses in oil field operations. Larger turbines can now supply energy to multiple pumping units, while smaller ones can be employed to operate individual beam pump units (BPUs). The integration of hydraulic transmission systems allows for direct power transfer from the wind turbines to the oil field equipment. This innovative approach demonstrates the growing synergy between renewable energy and traditional fossil fuel extraction, potentially reducing the carbon footprint of oil production operations. [91] Identified the low efficiency of wind to electrical energy for beam pumps and proposed an improved hydraulic system for using off-grid wind energy for driving the load of the sucker rod pump.

A novel wind-motor hybrid power pumping unit for oil fields is presented in [92], aiming to improve energy efficiency and reduce costs. The system directly utilizes wind energy through a mechanical-hydraulic transmission, eliminating the need for intermediate electricity conversion. It can operate in both hybrid and wind-only modes, adapting to varying wind conditions. The authors develop mathematical models, conduct simulations, and perform experiments to validate the system's performance. They propose optimization methods for key parameters like rated wind speed, system pressure, and transmission ratios. A dual-pump configuration is suggested to enhance efficiency at low wind speeds. The study demonstrates that this new approach can achieve higher wind energy utilization rates (over 60%) compared to traditional wind power generation methods (around 43%). The system's ability to match loads dynamically and recycle energy contributes to its improved efficiency. Overall, this innovative design shows promise for reducing energy consumption in oil field operations, particularly in remote areas with limited access to electricity.

An innovative approach to utilizing wind energy in oil fields through a novel wind-motor hybrid pumping unit is proposed in [93]. The proposed system combines a small wind turbine with a mechanical-hydraulic transmission to directly drive oil pumping units, eliminating the need for wind power generation equipment. This design aims to improve energy efficiency, reduce costs, and optimize power distribution compared to traditional large-scale wind turbine setups. The study presents a comprehensive mathematical model of the hybrid system and conducts extensive experiments and simulations to validate its effectiveness. Key findings include the system's ability to achieve power mixing, energy regulation, and recycling of gravitational potential energy. The researchers also analyze various parameters affecting system efficiency, such as wind speed, pressure, coupling rotation speed, and displacement ratios. Overall, this new method shows promise for enhancing wind energy utilization in oil fields, particularly in remote areas with abundant wind resources but limited access to electricity.

A parallel digital sucker-rod pump system (PDSRPS) was developed by [94]. The research integrates real oil pump systems with their customized digital twins to establish cyber-physical systems. The adaptive optimization in pumping processes is developed with the interaction between physical pump units and their digital versions. The research presents the concept of Parallel Digital Sucker Rod Pump Systems (PDSRPS) as an innovative approach to optimize oil pumping operations. The authors propose a framework that integrates physical sucker rod pump (SRP) units with their digital twins, creating a cyber-physical system for adaptive optimization. By leveraging technologies such as 5G, IoT, cloud computing, and artificial intelligence, the PDSRPS aims to enhance the efficiency and intelligence of oilfield management. The framework facilitates real-time monitoring, continuous modelling, and virtual-real collaborative computing, moving away from traditional offline or manual management approaches. The feasibility of the proposed framework is demonstrated through computational experiments on conventional beam-pumping units, showcasing improvements in structural dimensions and dynamic performance. While the study primarily focuses on optimization, it also presents the potential for parallel diagnosis and control within the PDSRPS framework, suggesting avenues for future research in intelligent oilfield operations [94].

The development of a digital sucker rod pumping (SRP) unit for research and educational purposes at the University of Oklahoma is presented in [95]. The project aims to create a versatile laboratory setup that can simulate various pumping unit geometries and operational conditions using a single linear actuator. The system incorporates modern technology, including sensors, data acquisition systems, and LabVIEW software for control and data analysis. Key objectives include mimicking different pumping units, bridging the technology gap in academia, establishing a research platform, and providing an educational tool for students. The setup allows for the study of various SRP-related phenomena, such as friction in deviated wells and gas interference. By generating and analyzing dynamometer cards, the system enables students and researchers to gain hands-on experience with digital oilfield technologies and explore solutions to common SRP challenges. This innovative approach seeks to prepare future engineers for the increasingly digitalized oil and gas industry while advancing research in artificial lift systems.

A data-driven approach for monitoring and diagnosing sucker rod pump systems is presented in [96]. The author developed an experimental setup called the Interactive Digital Sucker Rod Pumping Unit (IDSRP) at the University of Oklahoma to simulate field-scale operations. The facility includes a 50-foot vertical structure with sensors to collect data on pressure, load, and displacement. Using this data, the author applied machine learning techniques to predict pump performance and detect anomalies. Key contributions include transforming surface dynamometer cards to downhole cards, developing a predictive model to classify normal and abnormal pump operations, and using explainable AI methods to identify important features driving pump behavior. The research demonstrates the potential for automated, real-time monitoring and optimization of sucker rod pump systems using data analytics and machine learning. Overall, this work aims to advance the digitalization and automation of artificial lift systems in the oil and gas industry.

A comprehensive model for analyzing the operating modes of sucker-rod pumping units (SRPUs) using the SimMechanics library in MATLAB Simulink is presented in [97]. The authors detail the process of developing a digital representation of a rear-mounted sucker-rod pumping unit SRPD8-3-5500, focusing on its mechanical components and their interactions. The model aims to optimize pump productivity, enable sensorless diagnostics, and improve energy efficiency. Key aspects of the simulation include the frame structure, reducer and transmission systems, horse head mechanics, and the behavior of the sucker rod and plunger pump. The researchers emphasize the importance of dynamometer and wattmeter cards in diagnostics and showcases how the model can generate these crucial operational indicators. By simulating various fault conditions, the study lays the groundwork for developing advanced sensorless diagnostic tools and automated control systems for SRPUs, potentially revolutionizing oil extraction monitoring and maintenance practices.

A novel approach to modelling sucker rod pumps using MATLAB Simscape, a physical modelling toolbox is presented in [98]. The authors developed a comprehensive simulation model that accurately represents the complex dynamics of sucker rod pumping systems, including the prime mover, pumping unit, rod string, and pump system. By utilizing Simscape's library of physical components, the researchers created a detailed representation of the pump's mechanical and hydraulic elements. The model successfully simulates various operating conditions, including normal operation and common fault scenarios such as valve leakages and insufficient liquid supply. The study demonstrates the model's capability to generate dynamometer cards, motor power curves, and wattmetrograms, which are crucial for analyzing pump performance and diagnosing issues. This Simscape-based approach offers advantages over traditional mathematical modelling techniques, providing a more intuitive and efficient method for studying the nonlinear behavior of sucker rod pumps. The developed model has potential applications in training diagnostic systems and optimizing pump operations in the oil industry.

2.7 Justification for Renewable Energy Powered Oil Well

Technology advancement and growing energy demand are fostering improvements in the efficiency, and reduction in the cost of renewable energy systems. Climate change and the impact of greenhouse gases on global warming is accelerating the advancement in energy transition, and the Oil and gas industry continues to play a key role, increasingly adopting onsite renewable energy to mitigate the direct emissions associated with oil and gas production. As conventional oil wells age, they plateau in production, and decline, facing significant risk of being orphaned, suspended or abandoned. The rapidly growing number of aging wells exponentially amplifies the life cycle impact and administrative burden of these challenges, compounded by the fiscal, environmental, and sustainability implications. This research provides a framework than can be adopted to scrutinize the inventory of available wells, and systematically select candidate wells that can be profitably restored to marginal production. This provides an alternative option for reinvesting some of the abandonment budget. This approach potentially extends the lifecycle of brownfield operations while reducing the environmental footprint of the upstream oil and gas sector and developing renewable energy generation capacity for distributed energy generation and storage. This research provides a renewable energy approach for powering remote oil operations while leveraging fully customizable, low-cost, open-source, Internet-of-Things, supervisory control and data acquisition systems for monitoring and managing production system operations.

2.8 Assumptions and Limitations

Assumption made for the research outcomes to be valid and viable are as follows:

- The site chosen is significantly remote, with electric grid power supply sufficiently distant to justify investment in stand-alone off-grid renewable supply.
- The hydrocarbon composition of the fluid produced from the sub-surface is of significant value, such that revenue accruable from its sale covers the capital and operating cost for onsite renewable energy, after adjusting for the time value of money.
- Regulatory environment in terms of cost per MtCO2e is favourable, stable and sustained throughout the lifecycle of the project ensuring the project maintains long-term feasibility.
- The environmental impact of the project is limited to scope 1 (direct emissions) curtailed from upstream oil and gas production and does not extend to scope 2 (indirect emissions) or full life cycle assessment.

- There is no interruption to production, during the prescribed pumping hours for either intermittent or continuous production profiles.
- The open-source, IoT SCADA system does not include a load cell for strain measurement and the system is not mounted on a sucker rod pump model. Future studies could include these, so SRPU metrics can be determined and sensor outputs calibrated for the pump.

2.9 References

[1] Bertomeu, F., Hirschfeldt, M., Delgado, P. and Lobato-Barradas, G., 2015, May. Marginal Wells Inside Brownfields a High Profitability Business. In SPE Artificial Lift Conference-Latin America and Caribbean (pp. SPE-173941). SPE.

[2] Takacs, G., 2015. Sucker-rod pumping handbook: production engineering fundamentals and long-stroke rod pumping. Gulf Professional Publishing.

[3] Karhan, M.K., Nandi, S. and Jadhav, P.B., 2015. Design and optimization of sucker rod pump using prosper. Int. J. Interdiscip. Res. Innovations, 3(2), pp.108-122.

[4] Liu, X., Qi, Y., Wu, J., Yang, L. and Chen, F., 2010, August. An approach to the optimum design of sucker-rod pumping system. In 2010 WASE International Conference on Information Engineering (Vol. 3, pp. 140-143). IEEE.

[5] Muryskina, K.I. and Muryskin, A.S., 2021, March. Automation of Process of The Setting Up Well Model in Updating of The Integrated Asset Model for Wells Operated by Sucker Rod Pumps. In Tyumen 2021 (Vol. 2021, No. 1, pp. 1-6). European Association of Geoscientists & Engineers.

[6] Aliev, T.A., Rzayev, A.H., Guluyev, G.A., Alizada, T.A. and Rzayeva, N.E., 2018. Robust technology and system for management of sucker rod pumping units in oil wells. Mechanical Systems and Signal Processing, 99, pp.47-56

[7] Gizatullin, F.A., Khakimyanov, M.I. and Khusainov, F.F., 2018. Features of electric drive sucker rod pumps for oil production. In Journal of physics: conference series (Vol. 944, No. 1, p. 012039). IOP Publishing.

[8] Liang, X., Xing, Z., Yue, Z., Ma, H., Shu, J. and Han, G., 2024. Optimization of Energy Consumption in Oil Fields Using Data Analysis. Processes, 12(6), p.1090.

[9] Khakimyanov, M. and Khusainov, F., 2018, October. Ways of increase energy efficiency of electric drives sucker rod pump for oil production. In 2018 X International Conference on Electrical Power Drive Systems (ICEPDS) (pp. 1-5). IEEE.

[10] Solodkiy, E.M., Kazantsev, V.P. and Dadenkov, D.A., 2019, September. Improving the energy efficiency of the sucker-rod pump via its optimal counterbalancing. In 2019 International Russian Automation Conference (RusAutoCon) (pp. 1-5). IEEE.

[11] Li, W., Vaziri, V., Aphale, S.S., Dong, S. and Wiercigroch, M., 2021. Energy saving by reducing motor rating of sucker-rod pump systems. Energy, 228, p.120618.

[12] Wang, L. and Zhang, C., 2018, August. Analysis on energy-saving technology of oil field pumping unit. In 2018 IEEE International Conference on Mechatronics and Automation (ICMA) (pp. 1739-1743). IEEE.

[13] Koncz, Á., 2018. Sucker rod pumping analysis based on measured electrical parameters. University of Miskolc.

[14] Hilali, M.H.A., 2018. Design of a New Pump Jack for Continuous Sucker Rod Pumping Systems.

[15] Vishnyakov, D., Solodkiy, E. and Salnikov, S., 2021, January. Improving Sucker-rod pump energy efficiency through electric drive movement control. In 2021 28th International Workshop on Electric Drives: Improving Reliability of Electric Drives (IWED) (pp. 1-3). IEEE.

[16] Malyar, A. and Holovach, I., 2021, September. Simulation of Sucker-Rod Oil Pumping Unit Operation for Marginal Wells. In 2021 IEEE International Conference on Modern Electrical and Energy Systems (MEES) (pp. 1-4). IEEE.

[17] Zhu, Q., Zeng, S., Li, Y. and Sun, Q., 2017, May. Dynamic analysis of beam pumping unit. In 2017 7th International Conference on Applied Science, Engineering and Technology (ICASET 2017) (pp. 260-265). Atlantis Press.

[18] Khakimyanov, M.I., Shafikov, I.N. and Khusainov, F.F., 2015, May. Control of sucker rod pumps energy consumption. In 2015 International Siberian Conference on Control and Communications (SIBCON) (pp. 1-4). IEEE.

[19] Okhuijsen, B., 2022, April. Combining the Process and Maintenance Digital Twin to Create an Autonomous Production Platform. In Offshore Technology Conference (p. D011S003R005). OTC.

[20] Ladygin, A.N., Bogachenko, D.D., Kholin, V.V. and Ladygin, N.A., 2020, January. Method of efficient control of the sucker-rod pump electric drive. In 2020 27th

International Workshop on Electric Drives: MPEI Department of Electric Drives 90th Anniversary (IWED) (pp. 1-4). IEEE.

[21] Chen, S., Zhao, R., Deng, F., Zhang, D., Chen, G., Hao, H., Shi, J. and Zhang, X., 2023. Research of Big Data Production Measurement Method for SRP Wells Based on Electrical Parameters. Processes, 11(7), p.2158.

[22] Ericson, S.J., Engel-Cox, J. and Arent, D.J., 2019. Approaches for integrating renewable energy technologies in oil and gas operations (No. NREL/TP-6A50-72842). National Renewable Energy Lab.(NREL), Golden, CO (United States).

[23] Wang, J., O'Donnell, J. and Brandt, A.R., 2017. Potential solar energy use in the global petroleum sector. Energy, 118, pp.884-892.

[24] Silva, W.K., Cunha, A.L., Alves, A.C., Gomes, V.J.C., Freitas, P.P., Restrepo, D.F., Salinas-Silva, R., Camacho-Galindo, S., Guerrero-Martin, L.E. and Guerrero-Martin, C.A., 2023, October. Technical Evaluation of the Use of Hybrid Energy (Solar and Offshore Wind) to Supply Artificial Lift Pumps on an Oil Platform on the Equatorial Margin. In Offshore Technology Conference Brasil (p.D011S011R003). OTC

[25] Mahgoub, I.K.I., 2020. Solar Powered Artificial Lift, Heglig oil field (Doctoral dissertation, University of Khartoum).

[26] Kashef, M., Attia, M.A., Kamh, M.Z. and Abdel-Rahman, M., 2022, December. Techno-Economic Analysis of Renewable Energy Application in Oil and Gas Industry: A Case Study. In 2022 23rd International Middle East Power Systems Conference (MEPCON) (pp. 1-6). IEEE.

[27] Endurthy, A.R., Kialashaki, A. and Gupta, Y., 2016. Solar Jack Emerging Technologies Technical Assessment.

[28] Halabi, M.A., Al-Qattan, A. and Al-Otaibi, A., 2015. Application of solar energy in the oil industry—Current status and future prospects. Renewable and Sustainable Energy Reviews, 43, pp.296-314.

[29] Zhang, X., Wang, C., Sun, Y., Zhao, R., Shi, J., Yu, Y., Ma, G., Li, M., Li, S., Shen, Z. and Xu, J., 2024, February. An Intelligent Intermittent Pumping Production Technology Based on Fusion of Photovoltaic Unit and Storage Battery. In International Petroleum Technology Conference (p. D031S112R009). IPTC.

[30] Egler, M. and Barbieri, L., 2024. Prefiguring energy futures: Hybrid energy initiatives and just transitions in fossil fuel regions. Energy Research & Social Science, 118, p.103830

[31] Cimino, R., Brocco, V., Castaldo, F., De Ghetto, G., Favaretto, M. and Akmal, T., 2015. Deploying a Solar Hybrid Technology in a Remote Oil and Gas Production Site. Journal of the Japan Institute of Energy, 94(10), pp.1163-1168.

[32] El-Yamany, M.M., Abdullatif, S.O. and Ghali, H.A., 2021. Investigating the Techno-economic Utility of Integrating an Optimized PV/diesel Hybrid System in an Entire Oil Field in the Western-dessert in Egypt. WSEAS Transactions on Power Systems, 16, pp.104-120.

[33] Elhousieny, M. and Khalil, A., 2017, March. Photovoltaic/Gen-set hybrid system at Egyptian western desert. In Offshore Mediterranean Conference and Exhibition (pp. OMC-2017). OMC.

[34] El Bosaty, A. and Khafagy, S., 2024, October. Reducing Greenhouse Gas Emissions in Oil Extraction: A Case Study of Solar Energy Utilization in PetroFarah. In Mediterranean Offshore Conference (p. D021S022R002). SPE.

[35] Yashin, A., Konev, A. and Khakimyanov, M., 2021, November. Power Supply of The Sucker Rod Pump Unit Electric Drive Using Renewable Energy Sources. In 2021 International Conference on Electrotechnical Complexes and Systems (ICOECS) (pp. 43-46). IEEE.

[36] Mangushev, R., Ibrahimova, F. and Gaffarov, M., 2024. Possible application of solar energy to power hydrocarbon extraction and enhanced oil recovery operations in high latitudes. Nafta-Gaz, 80.

[37] Kraemer, D., Bajpayee, A., Muto, A., Berube, V. and Chiesa, M., 2009. Solar assisted method for recovery of bitumen from oil sand. Applied Energy, 86(9), pp.1437-1441.

[38] Janzen, Ryan, Matthew Davis, and Amit Kumar. "Greenhouse gas emission abatement potential and associated costs of integrating renewable and low carbon energy technologies into the Canadian oil sands." Journal of Cleaner Production 272 (2020): 122820.

[39] Abureden, S., 2014. Techno-Economic Study of Renewable Energy Integration in the Upstream Oil Supply Chain (USOSC) (Master's thesis, University of Waterloo).

[40] Stringer, T. and Joanis, M., 2023. Decarbonizing Canada's remote microgrids. Energy, 264, p.126287.

[41] AutomationForum (no date) Different Types of SCADA System Architecture. Available at: https://automationforum.co/different-types-of-scada-system-architecture/ (Accessed: 12 March 2025).

[42] Ogunmesa, O., 2021. Strategies Security Managers Used to Prevent Security Breaches in SCADA Systems' Networks (Doctoral dissertation, Walden University).

[43] Shahzad, A., Musa, S., Aborujilah, A. and Irfan, M., 2014. The SCADA review: system components, architecture, protocols and future security trends. American Journal of Applied Sciences, 11(8), p.1418.

[44] Yadav, G. and Paul, K., 2021. Architecture and security of SCADA systems: A review. International Journal of Critical Infrastructure Protection, 34, p.100433.

[45] Danylenko, M.M. and Sotnik, S.V., 2025, January. Comparative analysis of modern SCADA packages for production automation. International Journal of Academic Engineering Research (IJAER), 9(2), pp 26-34

[46] Wali, A. and Alshehry, F., 2024. A Survey of Security Challenges in Cloud-Based SCADA Systems. Computers, 13(4), p.97.

[47] Sun, Z.H. and Tian, X., 2010. SCADA in Oilfields. Measurement and Control, 43(6), pp.176-178.

[48] Wanasinghe, T.R., Gosine, R.G., James, L.A., Mann, G.K., De Silva, O. and Warrian, P.J., 2020. The internet of things in the oil and gas industry: a systematic review. IEEE Internet of Things Journal, 7(9), pp.8654-8673.

[49] Sharma, A., Samuel, P., Gupta, D., Whatley, C., Agarwal, S. and Gey, G.M., 2020, November. Edge Computing: A Powerful and Agile Platform for Digital Transformation in Oilfield Management. In SPE Asia Pacific Oil and Gas Conference and Exhibition (p. D013S104R004). SPE.

[50] atvise® (no date) Types of SCADA Systems. Available at: https://atvise.vesterbusiness.com/en/news/types-of-scada-systems/ (Accessed: 12 March 2025).

[51] IndMALL (no date) How Many Types Of SCADA Are There? | Key System Variations. Available at: https://www.indmall.in/faq/how-many-types-of-scada-are-there/ (Accessed: 12 March 2025)

[52] High Tide Technologies (2024) The Role of Cloud-Based SCADA in Industry 4.0 and IoT. Available at: https://www.htt.io/learning-center/the-role-of-cloud-based-scada-in-industry-4-0-and-iot (Accessed: 12 March 2025).

[53] Instrumentation Tools (n.d.) SCADA System Architecture. Available at: https://instrumentationtools.com/scada-system-architecture/ (Accessed: 12 March 2025).

[54] Kumar, M., Varma, N., Rao, M., Chandak, R., Jadhav, S., Sharma, H., Singhal, J., Ranjan, A., Chauhan, S., Bohra, A. and Patni, A., 2023, October. Enabling Autonomous Well Optimization by Applications of Edge Gateway Devices & Advanced Analytics. In Abu Dhabi International Petroleum Exhibition and Conference (p. D021S074R002). SPE.

[55] Lu, X., 2014. Supervisory control and data acquisition system design for CO2 enhanced oil recovery. Master of Engineering Thesis, Technical Report No. UCB/EECS-2014-123. EECS Department, University of California at Berkeley.

[56] Heng, G.T., 1996. Microcomputer-based remote terminal unit for a SCADA system. Microprocessors and Microsystems, 20(1), pp.39-45.

[57] Aamir, M., Uqaili, M.A., Poncela, J., Khan, N.A. and Chowdhry, B.S., 2014, May. Implementation and testing of optimal design of RTU hardware for Wireless SCADA. In 2014 4th International Conference on Wireless Communications, Vehicular Technology, Information Theory and Aerospace & Electronic Systems (VITAE) (pp. 1-5). IEEE.

[58] Susanto, T., 2022, October. Leverage Telemetry SCADA and Machine Learning on Pumpjack Wellhead Production Facilities. In Abu Dhabi International Petroleum Exhibition and Conference (p. D042S199R002). SPE.

[59] Durrani, S., Jattala, I., Farooqi, J., Shakeel, N. and Murad, M., 2013, December. Design and development of wireless RTU and cybersecurity framework for SCADA system. In 2013 5th International Conference on Information and Communication Technologies (pp. 1-6). IEEE.

[60] Ahmed, M.S., Al Bloushi, M.A., Ali, A., Yousef, A.A., Mistry, K.J., Henson, H.H. and Shar, A.A., 2023, October. Pilot Deployment of IIoT-SCADA by Leveraging Low Power Communication Technologies, Sensors, and Legacy SCADA Controllers. In Abu Dhabi International Petroleum Exhibition and Conference (p. D021S074R003). SPE.

[61] Hidayat, A., Isnanto, S., Lazuardi, H., Kurniawan, C., Kusuma, H., Ramadhan, G.B., Santoso, H.B., Hesti, K. and Handarianto, H., 2023, October. Next Gen of Field Operation Era for Artificial Lift Real-Time Monitoring: A Method to Significantly Optimize Oil Production of Mature Field. In Abu Dhabi International Petroleum Exhibition and Conference (p. D031S117R004). SPE.

[62] Cramer, R., Krebbers, J., van Oort, E., Lanson, T., Palermo, B., Murthy, A., Duncan, P. and Sowell, T., 2012, March. Establishing a Digital Oil Field data architecture suitable for current and foreseeable business requirements. In SPE Intelligent Energy International Conference and Exhibition (pp. SPE-149959). SPE.

[63] Qays, M.O., Ahmed, M.M., Parvez Mahmud, M.A., Abu-Siada, A., Muyeen, S.M., Hossain, M.L., Yasmin, F. and Rahman, M.M., 2022. Monitoring of renewable energy systems by IoT-aided SCADA system. Energy Science & Engineering, 10(6), pp.1874-1885

[64] Machap, K. and Garadan, A.M.A., 2018. SCADA system for oil and gas using ZigBee devices. International Journal of Pure and Applied Mathematics, 119(10), pp.1805-1809.

[65] Allahloh, A.S., Sarfraz, M., Alqahtani, M., Ahmad, S. and Huda, S., 2022. Application of industrial Internet of things (IIOT) in crude oil production optimization using pump Efficiency control. Wireless Communications and Mobile Computing, 2022(1), p.1005813.

[66] JPT staff, _., 2005. Daily Monitoring Reduces Cost of Production in Marginal Wells. Journal of Petroleum Technology, 57(11), pp.18-22.

[67] Aryadi, Y., Hidayat, A., Lazuardi, H., Isnanto, S., Ariwibowo, B., Muklas, A.N., Fathurachman, A., Gema Ramadhan, G.B. and Kamil, M.I., 2021, October. Novel Approach of Sucker Rod Pump Unit Balance Determination and Monitoring. In SPE Asia Pacific Oil and Gas Conference and Exhibition (p. D012S032R017). SPE.

[68] Bahbahani, B., Attia, A., Jagannathan, R., Heshmat, K. and Mohamed, A., 2016, November. Sucker rod pump production optimization via intelligent real time surveillance in joint operations–wafra Field illustrated through case examples. In Abu Dhabi International Petroleum Exhibition and Conference (p. D031S086R001). SPE.

[69] Ormerod, L., Sardoff, H., Wilkinson, J., Erlendson, B., Cox, B. and Stephenson, G., 2007. Real-time field surveillance and well services management in a large mature onshore field: case study. SPE Production & Operations, 22(04), pp.392-402.

[70] Babahani, B., Spain, J., Bhat, M.S., Heshmat, K., Assem, A. and Mohammed, Z., 2015, October. Exceptional Management and Optimization for Intelligently Controlled Wells using Smart Surveillance and Diagnostics in Joint Operations-Wafra Field. In SPE Kuwait Oil and Gas Show and Conference (pp. SPE-175249). SPE.

[71] Zakharov, A., 2016, March. A New Approach to Obtain Producer FBHP and FBHT from SCADA Data in the Schoonebeek Steamflood. In SPE EOR Conference at Oil and Gas West Asia (p. D021S012R003). SPE.

[72] Boguslawski, B., Boujonnier, M., Bissuel-Beauvais, L., Saghir, F. and Sharma, R.D., 2018, November. IIoT edge analytics: Deploying machine learning at the wellhead to

identify rod pump failure. In SPE Middle East Artificial Lift Conference and Exhibition (p. D021S004R001). SPE.

[73] Palmer, T. and Turland, M., 2016, October. Proactive rod pump optimization: Leveraging big data to accelerate and improve operations. In SPE Artificial Lift Conference and Exhibition-Americas? (p. D011S001R003). SPE.

[73] Sharma, A., Samuel, P., Gey, G.M. and Kumar, S., 2020, October. Edge Computing: Continuous Surveillance and Management of Production Operations in a Cost Effective Manner. In SPE Annual Technical Conference and Exhibition? (p. D031S022R003). SPE.

[75] Schnabl, H. and Wimmer, H., 2022, October. Digitalization Deployed–Enabling Sustainable Operations with Autonomous Well Control. In Abu Dhabi International Petroleum Exhibition and Conference (p. D031S093R003). SPE.

[76] Al-Rakyan, S., Marie, O.A., Ledesma, F., Heshmat, K., Mohamed, A. and Zahourdin, M., 2017, November. Integrated Deployment of Digital Oil Field in Multiple Kuwait Areas in One Platform and Benefits Realized. In Abu Dhabi International Petroleum Exhibition and Conference (p. D031S089R001). SPE.

[77] Al Badi, S.S., Al Abri, A.T., Al Hinai, N., Al Abri, A.N. and AL Busaidi, K., 2024, October. Automated Control Solutions to Enhance Beam Pump Performance and Increase Well Productivity: Block-5 Oman. In SPE Middle East Artificial Lift Conference and Exhibition (p. D021S004R001). SPE.

[78] Flichy, P. and Baudoin, C., 2018, September. The industrial IoT in oil & gas: Use cases. In SPE Annual Technical Conference and Exhibition? (p. D031S032R002). SPE.

[79] Okhuijsen, B., 2021, December. Real-Time, Data-Driven Hydrocarbon Production Optimization: Digital Twin Model Addressing the Entire Value Chain. In World Petroleum Congress (p. D041S004R001). WPC.

[80] Ehrenreich, D. and May, D., 2001, March. Operating benefits achieved by use of advanced data communications for oil and gas SCADA systems. In SPE Latin America and Caribbean Petroleum Engineering Conference (pp. SPE-69464). SPE.

[81] Sletcha, B., Vivas, C., K. Saleh, F., Ghalambor, A. and Salehi, S., 2020, February. Digital Oilfield: Review of Real-time Data-flow Architecture for Upstream Oil and Gas Rigs. In SPE International Conference and Exhibition on Formation Damage Control (p. D021S013R005). SPE.

[82] Massewa, D.A., Rifaat, M., Akbar, F.I., Fadri, R., Akbar, D.M., Rachmadani, A., Uswitra, I., Nugraha, F., Purnama, F.E., Zaelani, B. and Widijanto, R., 2021, October. Innovative Method for Efficient Real Time Online Well Monitoring to Enhance Crew Respond Time in Marginal Field. In SPE Asia Pacific Oil and Gas Conference and Exhibition (p. D011S005R006). SPE.

[83] Freeman, J., Kulkarni, P., Benoit, R., Filipi, J. and Arnst, B., 2018, August. Enabling autonomous well optimization via using IoT-enabled devices and machine learning in Bakken horizontal wells. In SPE Artificial Lift Conference and Exhibition-Americas? (p. D021S006R003). SPE.

[84] Susanto, T., 2022, October. Leverage Telemetry SCADA and Machine Learning on Pumpjack Wellhead Production Facilities. In Abu Dhabi International Petroleum Exhibition and Conference (p. D042S199R002). SPE.

[85] Naieem, M. and Salvatore, M., 2019, March. Long-Term Improvement by Implementation of SCADA System for Three Off-Shore Platforms (Egypt-Red Sea) and Converting Platforms to Be Unmanned. In Offshore Mediterranean Conference and Exhibition (pp. OMC-2019). OMC.

[86] Hidayat, A., Sujai, A., Aryadi, Y. and Fathurachman, A., 2020, October. IoT Implementation on Artificial Lift System in the KS Brownfield in South Sumatra Indonesia. In SPE Asia Pacific Oil and Gas Conference and Exhibition (p. D032S009R011). SPE.

[87] Feluch, P.J. and Hiney, R.J., 2002, June. The application of using low cost data logger and controller in optimizing oil production using progressive cavity pumps. In PETSOC Canadian International Petroleum Conference (pp. PETSOC-2002). PETSOC.

[88] Neeley, C.H., Abshire, P.W. and Hoge, D.J., 1990, September. Programmable controllers integrate oil field SCADA and automation. In 37th Annual Conference on Petroleum and Chemical Industry (pp. 235-241). IEEE.

[89] Khan, W.Z., Aalsalem, M.Y., Khan, M.K., Hossain, M.S. and Atiquzzaman, M., 2017, February. A reliable Internet of Things based architecture for oil and gas industry. In 2017 19th International conference on advanced communication Technology (ICACT) (pp. 705-710). IEEE.

[90] Ye, W. and Heidemann, J., 2006. Enabling interoperability and extensibility of future SCADA systems. University Southern California, USC/ISI Technical Report, ISITR-625.

[91] Gao, Z.W. and Jia, S., 2024. Modeling and Control for Beam Pumping Units: An Overview. Processes, 12(7).

[92] Zhang, C., Wang, L., Wu, X. and Gao, X., 2022. Performance analysis and design of a new-type wind-motor hybrid power pumping unit. Electric Power Systems Research, 208, p.107931.

[93] Zhang, C., Wang, L. and Li, H., 2020. Experiments and simulation on a late-model wind-motor hybrid pumping unit. Energies, 13(4), p.994.

[94] Cheng, X., Wang, X., Liu, S., Lu, J., Zhang, Z., Liu, Z. and Wang, F.Y., 2022. Optimization of sucker rod pump operations using parallel systems. IEEE Journal of Radio Frequency Identification, 6, pp.977-981.

[95] Pienknagura Dolberg, E., 2019. Implementation of a Digital Sucker Rod Pumping Unit for Research and Educational Purposes.

[96] Tran, N., 2022. A Data-Driven Approach For Monitoring And Predictive Diagnosis Of Sucker Rod Pump System.

[97] Zyuzev, A.M. and Bubnov, M.V., 2018. Model for sucker-rod pumping unit operating modes analysis based on SimMechanics library. In Journal of Physics: Conference Series (Vol. 944, No. 1, p. 012130). IOP Publishing.

[98] Semenov, A.V., Tecle, S.I. and Ziuzev, A., 2020, September. Modeling induction motor driven sucker rod pump in MATLAB simscape. In 2020 Russian Workshop on Power Engineering and Automation of Metallurgy Industry: Research & Practice (PEAMI) (pp. 67-71). IEEE.

Chapter 3

SIZING, PARAMETRIC INVESTIGATION, AND ANALYSIS OF AUTOMATED SUCKER ROD PUMP USING BEAM PUMP SIMULATORS

Co-authorship statement

This chapter achieves research objective 1 of this thesis as stated in Section 1.3. It presents the Sizing, Parametric Investigation, and Analysis of Automated Sucker Rod Pump using Beam Pump Simulators with a focus on developing an integrated simulation methodology combining QRod™ and PROSPER™ platforms for optimizing the sizing of sucker rod pump artificial lift systems, with emphasis on minimizing energy requirements and maximizing production efficiency. This study conducts a comprehensive parametric investigation of key design variables affecting sucker rod pump performance, including pump geometry, API rod number, pump diameter, and rod material, to establish optimal configurations for deep well applications. This study quantitatively evaluates and compares the performance of different rod string designs using key indicators such as damped horsepower, cyclic load factor, and prime mover rating, with focus on wells deeper than 3500 feet, to ensure reliable long-term operation. This study develops and validates an optimized sizing methodology that reduces iteration requirements and optimizes artificial lift system design, achieving significant reductions in damped horsepower, polished rod horsepower, and minimum NEMA D motor size requirements.

I (Charles Aimiuwu Osaretin) am the principal author and contributed to Conceptualization, Methodology, Software Investigation, Writing of Original Draft and Editing of the research manuscript. The research in this chapter was supervised by Dr. M. Tariq Iqbal, and Dr. Stephen Butt. The supervisors contributed to the conceptualization and methodology. They also supervised the entire chapter, reviewed and corrected the research manuscript. The work in this Chapter has been published in the Journal of Chemical and Petroleum Engineering (JChPE), Volume 54, Issue 2, December 2020, Pages 235-251, Article ID 226313435, 17 pages, https://doi.org/10.22059/jchpe.2020.295689.1303.

Abstract

Reciprocating piston artificial lift systems are widely adopted especially, for onshore wells. Matching the pump mode to well and reservoir conditions reduces the pumping cost and increases production efficiency. Parameters influencing the energy requirement of sucker-rod lifted oil wells are investigated in this study, and new insights are provided for the parametric investigation of design variables required for sizing beam-pumped wells. Two (2) artificial lift simulators are integrated for automated sizing of beam-pumped systems. A sucker-rod artificial lift system is optimally sized for a case study oil well, to obtain the minimum API rating of the pumping unit, sustain the target production rate, and determine the corresponding minimum prime mover required to drive the pump sustainably. Compared to using a single simulator for the case study, the integrated approach reduces the damped and polished rod horsepower by 54.9% and 26.5% respectively, for a corresponding decrease in minimum NEMA D motor size by 38.6%. These key performance indicators demonstrate the benefits of simulator integration in automated sizing of beam pumps.

3.1 Introduction

Globally, conventional hydrocarbon resources are being steadily depleted, with a growing need for an artificial lift for production management [1]. Oil price is projected to settle between \$(40- 60)/barrel in the next two decades [2]. Hence at every phase during the life of a well, the need to minimize the cost of production, increase energy return on investment, improve pump volumetric efficiency, prolong pump life and improve overall production efficiency, cannot be overemphasized [3-6].

Deployment of artificial lift (gas or beam pumping) to extend the life of a producing well [7, 8] is vital to maintain production at the desired level, particularly where the natural drive of the well is sufficiently depleted, and reservoir pressure becomes insufficient to produce at the desired flow rate. Artificially lifted wells consist of about 87% of all oil-producing wells worldwide, and roughly 71% of these wells are of the beam-pumped system [9]. The popularity of the sucker-rod pumping system is primarily due to its durable, simple, flexible, and familiar operation to most operators [3, 10, and 11].

The design of optimum beam-pumped artificial lift systems is a classic problem that has attracted a lot of research effort, and a proactive attempt to solve the problem entails adopting a holistic and integrated approach [12, 4]. Due to the relative ease of installation and maintenance of electric motors compared to gas engines, the former is increasingly adopted as the prime mover to drive beam-pumped wells [13]. Electricity cost is one of the most significant, if not the highest operating expense, especially for old oil wells [14], and accounts for about 33.38% of the total power consumption. Electric power bills typically range from 20-35% of the direct cost of petroleum production [13]. Well and reservoir conditions introduce certain constraints to fluid production, and optimal artificial lift design aims to produce fluids economically while working around the imposed constraints [15]. This work presents a simplified approach to obtaining the energy requirement of the electric motor required to drive the downhole pumps.

A typical sucker-rod pumping system consists of a surface transmission system and a subsurface (or downhole) system. The surface components include the prime mover (motor), gearbox, reciprocating pump unit, polished rod, and wellhead. The metal rod string, tubing, and downhole pumps are components of the subsurface equipment [16, 17]. The prime mover could be a fuel-powered internal combustion engine or an electric motor, whose rotational motion is converted by the surface unit into the reciprocating linear motion of the rod string within the tubing [18]. The downhole pump consists of a barrel or cylinder and a plunger or piston. The direction of energy transfer is such that the oscillating motion of the rod string causes the plunger to be displaced within the barrel. The subsurface pump has two (2) check valves: a travelling valve and a stationary valve, which systematically work together to transfer well fluids into the tubing, and cumulatively displace fluid to the surface [16, 11].

In the design, installation, and operation of beam-pumped wells; the pumping mode is specified by the unique selection of pump size, pumping speed, stroke length, and sucker rod string design [15]. The satisfactory performance and favorable interaction of the reservoir, wellbore, subsurface, and surface equipment, demands that the pumping system is sized to optimize production (increase production/minimize cost) [4]. The optimal design of a sucker- rod pumped artificial lift system implies that the parameters of the pumping system are correctly determined, and the equipment is carefully selected to produce the fluid economically and also attain other goals set by the well operator [15]. The dynamic nature of the reservoir, fluid, well, and pump conditions places a demand for continuous parametric investigation (in addition to production tests) throughout the life of a producing well, to ensure that production is both sustainable and profitable, [15] alluded to the fact that the power requirements and cost could be significantly small when the pumping mode is appropriately selected.

Optimal design and accurate selection of the appropriate pumping mode could include lifting a target rate from the well under optimum conditions and matching the pump behaviour to the inflow rate of the well. When the pump behaviour is specified, the aim is to size the beam pump to the inflow or target rate of the well. An operating point could also be obtained for the well such that the deliverability of the reservoir (inflow performance relationship) is matched with the vertical lift performance of the well [19].

The inflow performance relationship or reservoir deliverability is deduced from the productivity index of the well. In contrast, the vertical lift performance or pump deliverability is determined from the pump characteristic curve. Given specific operational conditions, an intersection point between the inflow and outflow performance can be obtained to indicate the operating point/production rate of the well and the corresponding flowing bottom hole pressure [20]. The pumping unit must be sized to match the well conditions, and the pumping modes dynamically adjusted to suit the reservoir conditions [1].

3.2 Methodology

It is economically imperative to perform feasibility studies on stripper wells and marginal oil fields requiring an artificial lift. This work aims to estimate the energy requirement of a case study well by integrating two simulators: QRod™ (Quick Rod) and PROSPER™ (Production and System Performance Analysis Software). The number of trials or iterations required to attain the minimum API pump rating is reduced. QRod™ will initially be used to ascertain a provisional minimum API rating of the beam pumping unit and the size of the NEMA D motor (high slip electric motor). The tentative size is then combined with other design input parameters in PROSPER™ to obtain a more robustly sized unit. The case study is an onshore well "X" that requires an artificial lift to sustain production. The goal is to perform preliminary studies that will help in accurately selecting an optimal pumping mode and hence properly size the sucker rod system, to keep the well producing sufficient volumes profitably at a reduced cost.

3.2.1 Automated Sizing Methodologies of Sucker Rod Pump Artificial Lift System

One significant challenge in analyzing the operation of a sucker rod pump arises from the elastic behavior of the rod strings. The polished rod stroke length (at the surface) is significantly different from the stroke length at the downhole pump and surface parameters cannot be directly used to estimate pump displacement [15]. Modelling of viscous and mechanical friction in addition to rod elasticity, results in a one-dimensional wave equation, with pumping action denoted by stress waves or elastic forces travelling at the speed of sound along the string length [21].

Automated sizing of a sucker rod pumped system uses Fourier analysis (harmonic analysis) to determine the position of the rod string, the amount of load, and the type of load that the rod string is subjected to downhole. The plot of rod load versus rod position is presented as a measured or predicted dynamometer card, which is useful for monitoring, predicting, and diagnosing production problems [22, 23]. Modelling the rod string as ideal slender bars (with the pumping action represented by stress waves travelling along the rod length) results in a 1-dimensional damped wave equation, which takes rod elasticity and friction into account in predicting the useful work done downhole, the position and load on the rod string in the subsurface. The elastic behavior of the sucker-rod is defined by the wave equation [21].

3.2.2 Parametric Investigation

Some of the design input parameters have significant impacts on the sizing of the beam-pumped artificial lift system. A parametric investigation is performed in QRod™ to determine these specific parameters, quantify their influence on overall system objectives, and ensure that the parameters chosen are neither impractical nor uneconomical [15].

3.2.2.1 Effect of Pump Geometry on Energy Requirement

Figure 3.1 shows API gravity versus energy requirement for different geometries. As shown in Figure 3.1., it is observed that Mark II has a significantly lower energy requirement than the conventional units: clockwise (CWconv) and counterclockwise (CCWconv) [15]. This is irrespective of the API gravity of the produced fluid considered. Air-balanced geometry has the least energy rating of the four geometries considered; followed by mark II, counterclockwise conventional, and clockwise conventional units respectively, in order of increasing energy requirements. Air-balanced units are typically deployed for portability and well testing [15], and they have an advantage over crank-balanced units where space and weight requirements are crucial. Air-balanced units are usually preferred for wells that require larger unit sizes or longer pump strokes.

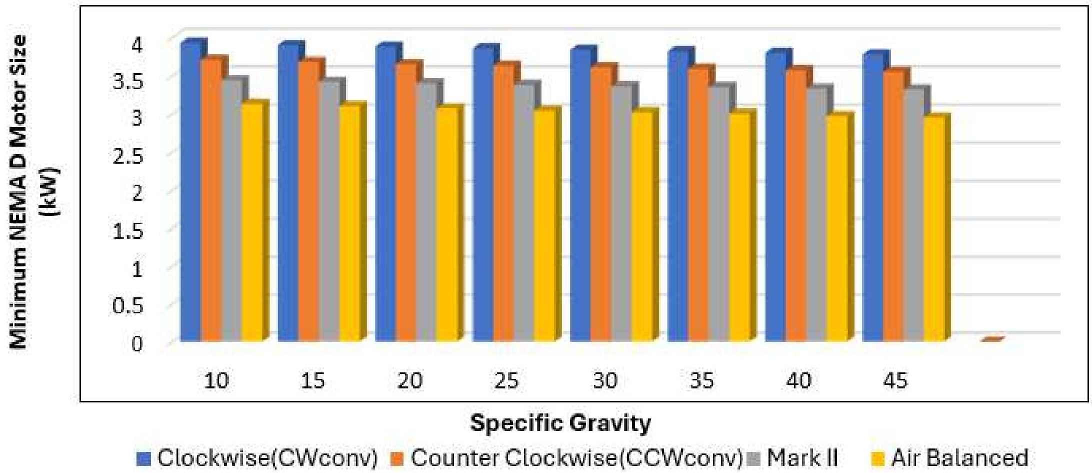

Figure 3.1. API gravity versus Energy requirement for different geometries

Hence in pump selection and sizing for minimum energy requirement, the mark II pump is preferred to decrease the power requirement. The geometry of the pumping unit is demonstrated to have a profound impact on the energy requirement and the corresponding size of prime mover required. There is a significant reduction in the energy requirement as one transitions from heavy oil (10^0) to lighter oil (45^0).

3.2.2.2 Effect of API Rod Number on Energy Requirement of Pumping Unit

Figure 3.2 shows API rod number as a function of minimum polished rod size, stroke rate, and prime mover rating. It can be deduced from Figure 3.2., that with an increase in the tapering from 65 to 97, there is a corresponding increase in the energy requirement and a decrease in the stroke rate required to sustain a target level of production. This is understandable as the mass per unit length of the rod string is expected to increase from a tapering of 65 to 97.

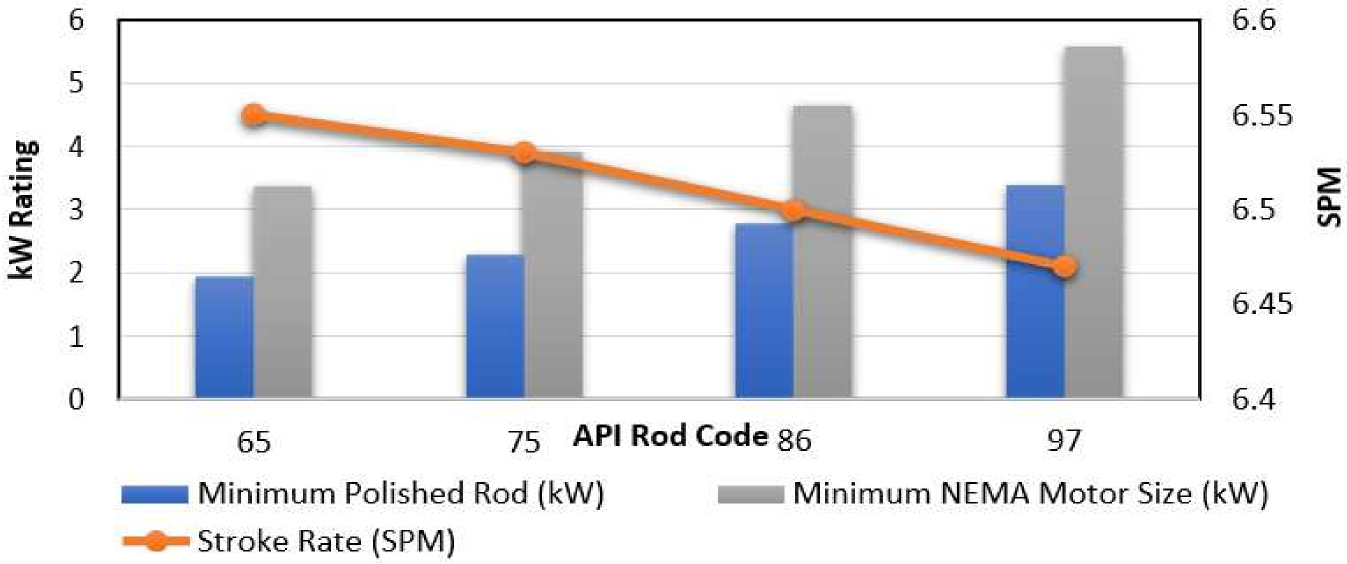

Figure 3.2. API rod number as a function of minimum polished rod size, stroke rate,.

Figure 3.3 shows the prime mover rating as a function of pump diameter. It is observed from Figure 3.3 that irrespective of the pump diameter chosen, the energy requirement consistently increases with tapering for API rod numbers 65, 75, 86 to 97. Such that the rating of the electric motor (prime mover) decreases with increases in the diameter of the pumps from 1.06, 1.25 to 1.5 inches. The minimum electric motor prime mover rating, generally decreases with an increase in pump diameter, as shown in Figure 3.3.

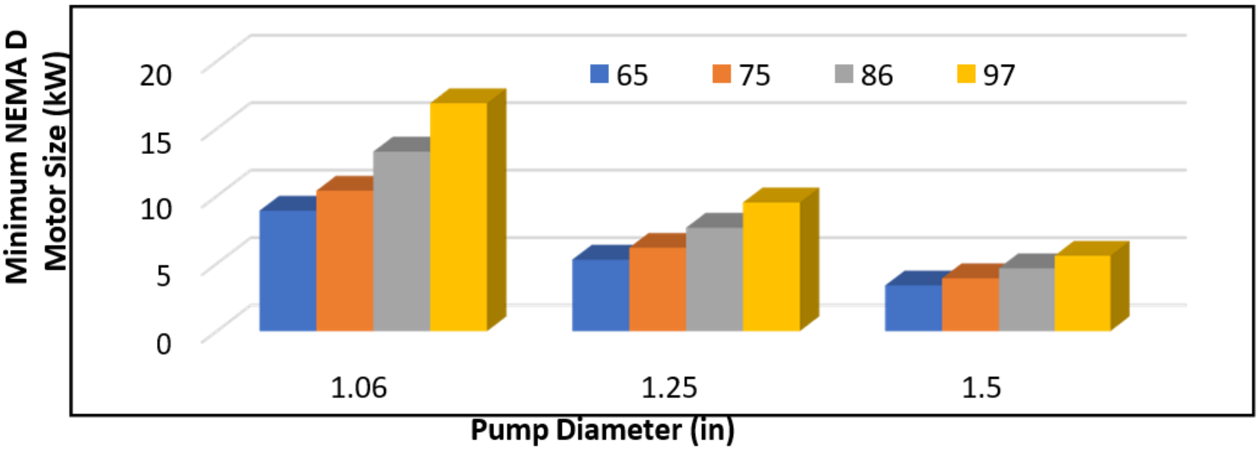

Figure 3.3. Prime mover rating as a function of pump diameter (at respective API rod numbers)

The tapering criterion for the design of the sucker rod string greater than or equal to 3500 feet is satisfied by implementing significant tapering in the rod string; so that any potential rod failure will concentrate at the point of maximum stress. Given the desired production level, It can be deduced from Figures 3.2 & 3.3 that the equivalent stroke rate generally decreases with an increase in the API rod number. Hence for our design at a well depth of 3,500ft, the tapering criterion is adopted, and an API rod number of 65 is chosen to result in the least pump and prime mover rating, with a correspondingly maximum stroke rate (strokes per minute). The motor sizes also increase from API rod number 65, 75, 86 to 97.

3.2.2.3 Effect of Pump diameter and API Gravity on Minimum Rating of Prime Mover

Figure 3.4. shows the effect of pump diameter on minimum NEMA motor size in QRod™. It can be observed from Figure 3.4. that the energy requirement (minimum prime mover size in kW) generally decreases with an increase in the API gravity, from 10^0 to 45^0. API gravity of 25 is adopted in sizing the artificial lift system. In general, for a specific API gravity, the horsepower needed for a given rod type decreases with an increase in pump diameter (from 1.06 to 1.5 inches), being higher for lower API (heavier fluids) and lower for higher API gravity

(lighter fluids). Based on the mentioned figures, the pump size of 1.50 inches is chosen for the design as it is the widest rod pump that can practically run in a 2.375 or ($2\frac{3}{8}$) inches anchored tubing.

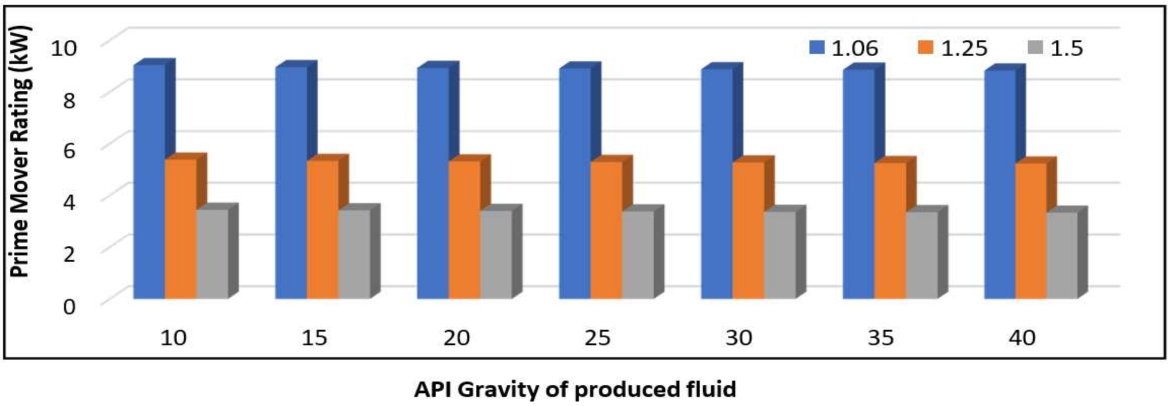

Figure 3.4. Effect of pump diameter on minimum NEMA motor size in QRod™

3.2.2.4 Effect of The Rod Material on The Stretch of The Rod String

Excessive rod stretch is undesirable as it reduces the effective stroke length; hence sinker bars are adopted to increase the overtravel between the pump and the plunger and therefore compensate for excessive rod stretch [26] as can be seen in Figures 3.5a and 3.5b. The proportion of the plunger stroke that is effective in lifting fluids is the effective plunger stroke (inches) given by [15]:

$$\text{Effective plunger stroke (inch)} = \text{polished rod stroke} + \text{plunger over} - \text{travel} - (\text{rod stretch} + \text{tubing stretch}) \quad (1)$$

PPRL	6,187.7 lb	MPRL	3,429.0 lb	Fo	470.6 lb
Pump Stroke Length	72.76 in	Static Stretch	1.83 in	Overtravel	0.59 in
Fo/Skr	0.025	Kr	257 lb/in	Kt	1277 lb/in

(a)

PPRL	7,216.3 lb	MPRL	3,741.0 lb	Fo	470.6 lb
Pump Stroke Length	73.27 in	Static Stretch	2.03 in	Overtravel	1.30 in
Fo/Skr	0.027	Kr	232 lb/in	Kt	1277 lb/in

(b)

Figure 3.5. Static stretch and overtravel in rod string, a) steel and b) fiberglass

When combination rods containing fiberglass sucker-rods are used, the regular operation is significantly dependent on rod diameter. If the fiberglass diameter is too small, it can result in too much rod stretch, and from Eq. 1, this reduces the pump displacement and minimizes the stroke length available to do useful work at the pump [27]. For deep wells, fiberglass rods are generally considered more economical for fluid production than steel rods [18].

When the sucker-rod length is significantly longer or its diameter is sufficiently small, excessive stretch becomes inevitable, plunger stroke is limited, and crude oil production minimized, hence compensation for production loss may require increased pumping speed [31].

The behavior of the sucker rod pump is such that pumping (resulting from the lifting of the fluid) and stretching of the elastic rod, only occurs for the upstroke [24]. During the downstroke, rod compression occurs, and the fluid mass is not considered [25]. Solid steel or fiberglass could be used as material for the rod. From Figures 3.6a and 3.6b, the use of fiberglass sucker rods can lead to a significant reduction in rod loading (from 42.3% to 31.5%). It even practically eliminates corrosion [18, 26]. Aside from the fact that fiberglass material is not considered where pump friction is significant, another drawback is that fiberglass often results in excessive stretch which limits the productive capacity of the pump or even completely negates pump displacement [27].

3.2.3 Quick Rod (QRod™)

QRod™ (Quick Rod) is a tool that mathematically simulates or imitates the motion of the pumping unit. A damped wave equation describes the movement of the rod string, and the solution to the partial differential equation (expressing the action of the rod string) is obtained. The load applied by the pump on the rod string is determined using the pump intake pressure. It uses surface boundary conditions as an approximation for the motion of the surface unit. The propagating stress waves influence the resultant loading of the rod string, the torque required, power demands, and dynamometer card plots obtained. QRod™ uses a wave equation to synthesize the surface and pump dynamometer loads, determine in-balance gearbox torque, counterbalance, and determines the plunger velocity for a stroke. Given the pump setting depth and target production rate; the effect of changing parameters (such as tubing anchor, stroke length, stroke rate, and pump diameter) on pump displacement, rod string loading, surface unit and motor size requirements can be readily ascertained and the artificial lift system designed, as shown in Figure 3.7. Some distinctive features of QRod™ are as follows:

- the option for tapered steel rod strings and fiberglass/steel combination strings is provided,
- sinker bars can be adjusted to increase the overtravel and compensate for the negation of pump displacement due to excessive rod stretch,
- the effect of pump diameter and clearance on pump slippage can be considered in the simulation of pump operation.

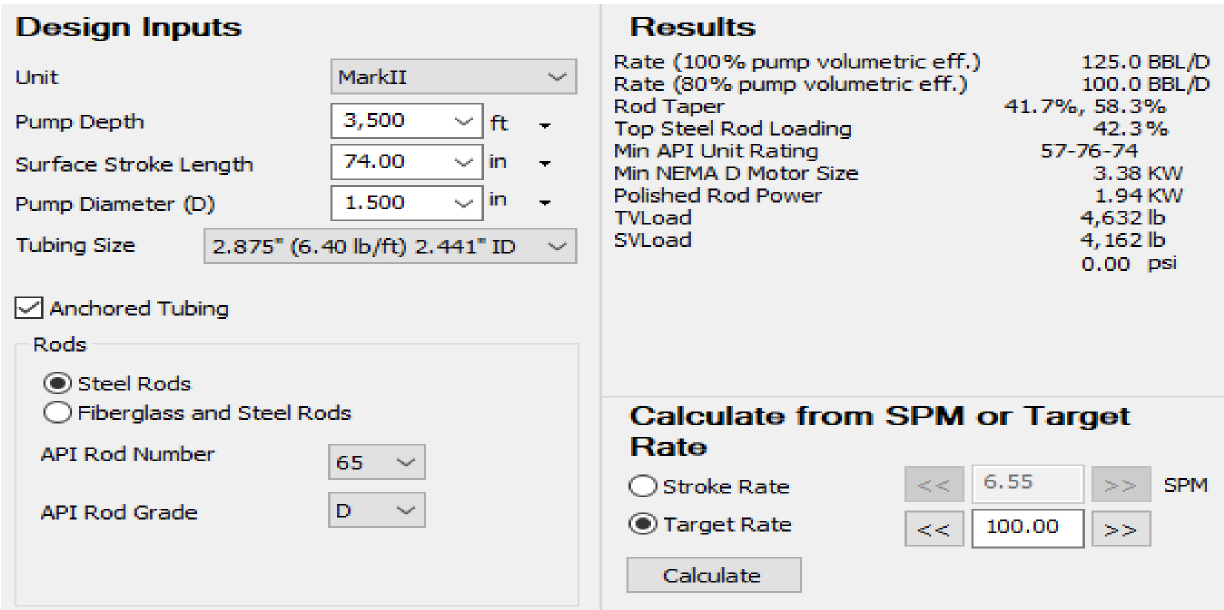

(a)

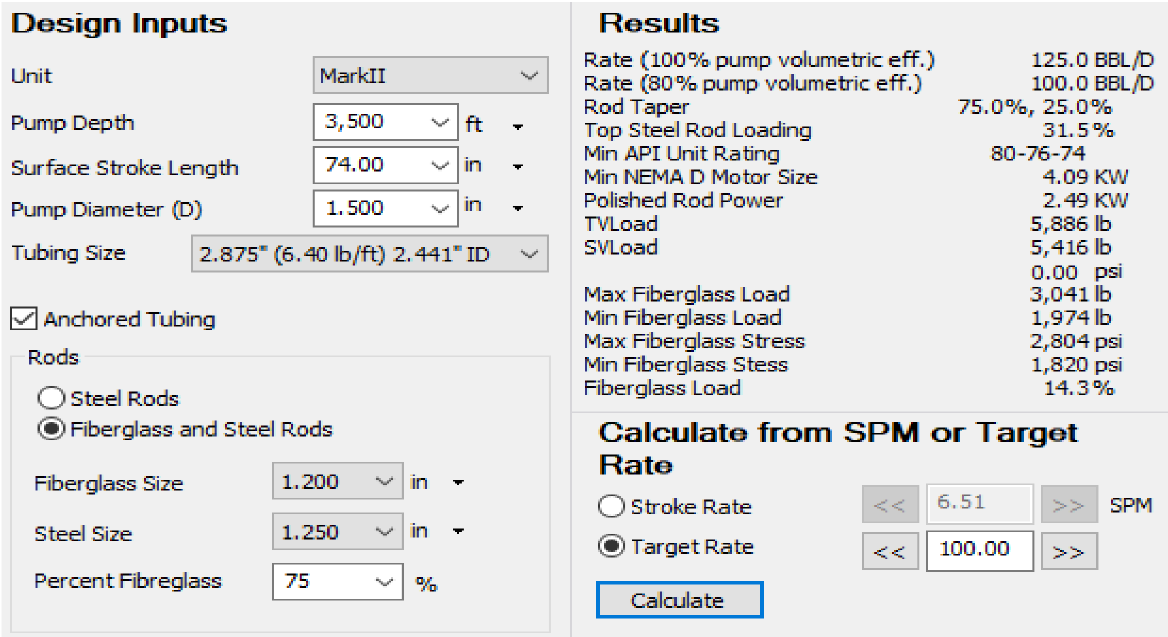

(b)

Figure 3.6. Design inputs and results using a) steel and b) fiberglass

After conducting the parametric investigation in QRod™, for the minimum production level of 100bbl/day, the input and default parameters are selected that will optimize the energy requirement of the sucker-rod pumped artificial lift system and also minimize the corresponding prime mover rating (minimum NEMA D motor size), as shown in Figure 3.7.

3.2.4 Production and System Performance Analysis Software (PROSPER™)

PROSPER™ is a production and system performance analysis software, useful for optimizing already existing system designs and assessing the effect of variation in system parameters. It finds application in modelling existing wells (diagnostic) and for the optimal design of new wells (prediction). It is used to model inflow performance (IPR) for the reservoir(s) of various configurations with completions that are usually complex and deviated. It is a very robust software that can be used to design, optimize, and troubleshoot many artificial lift options including the sucker-rod or beam pumps. The approach to sizing the artificial lift system is shown in Figure 3.8.

The workflow in Figure 3.8. is briefly summarized as follows:

- the properties of the produced fluid are matched with standard fluid correlations,
- the well and downhole equipment are modelled,
- the appropriate model for the IPR is selected to determine the producing bottom hole pressure,
- the initial design conditions for the sucker rod pump are provided,
- the simulation is executed, and results obtained are considered,

the process is repeated continuously (iteratively) until the design expectations are satisfied [34].

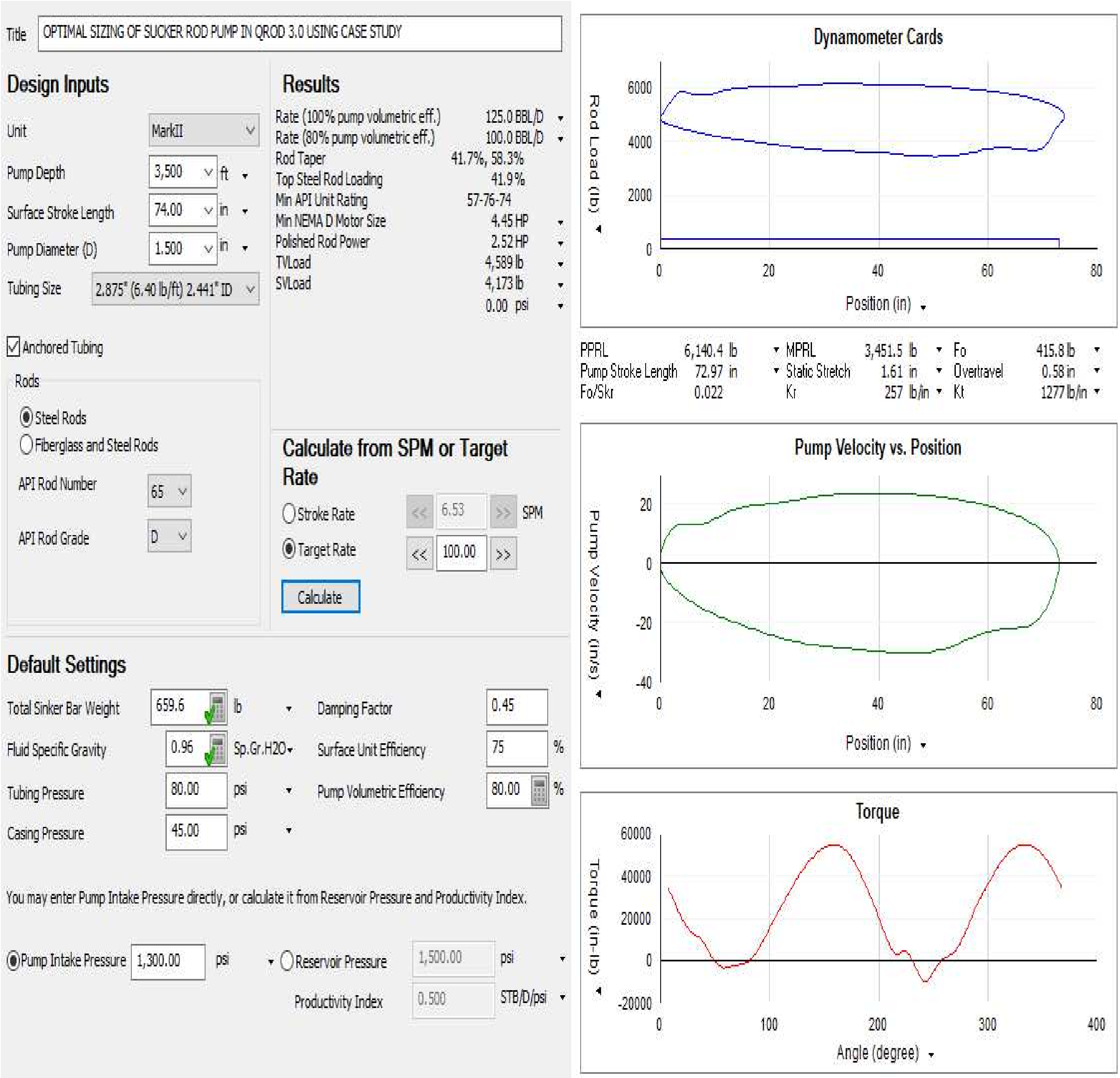

Figure 3.7. Sucker-rod pump artificial lift design in QRod™

3.2.5 Integrated Sizing Procedure (PROSPER™ Integrated with QRod™)

The challenge with designing artificial lift systems using PROSPER™ simulator alone is that the design is highly iterative, as it requires several unsuccessful attempts of trial and error before a practical solution can be found and even many more iterations before an optimal design can be attained. An alternative simulator (QRod™) helps to reduce iteration time, by first performing a parametric investigation after which the parameters selected are applied in PROSPER™ software to obtain a more efficient sizing, as shown in Figure 3.9.

The workflow from Figure 3.8 (based on sizing using PROSPER™ alone) is integrated with the results obtained from Figure 3.7 to obtain a modified workflow, shown in Figure 3.9. The process of achieving this integration is further explained in detail below.

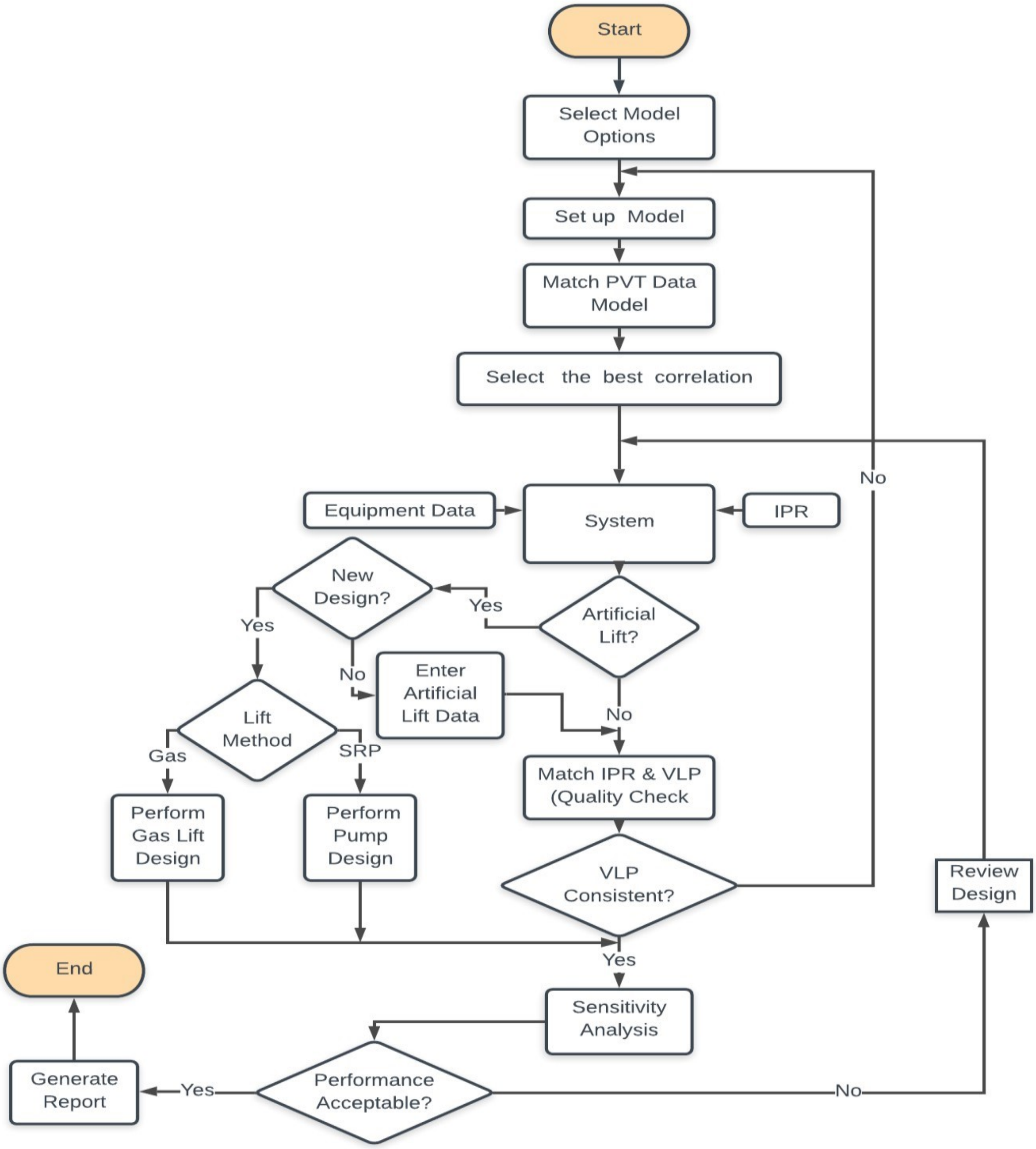

Figure 3.8. Iterative Sucker-rod pump (SRP) artificial lift design workflow in

PROSPER™

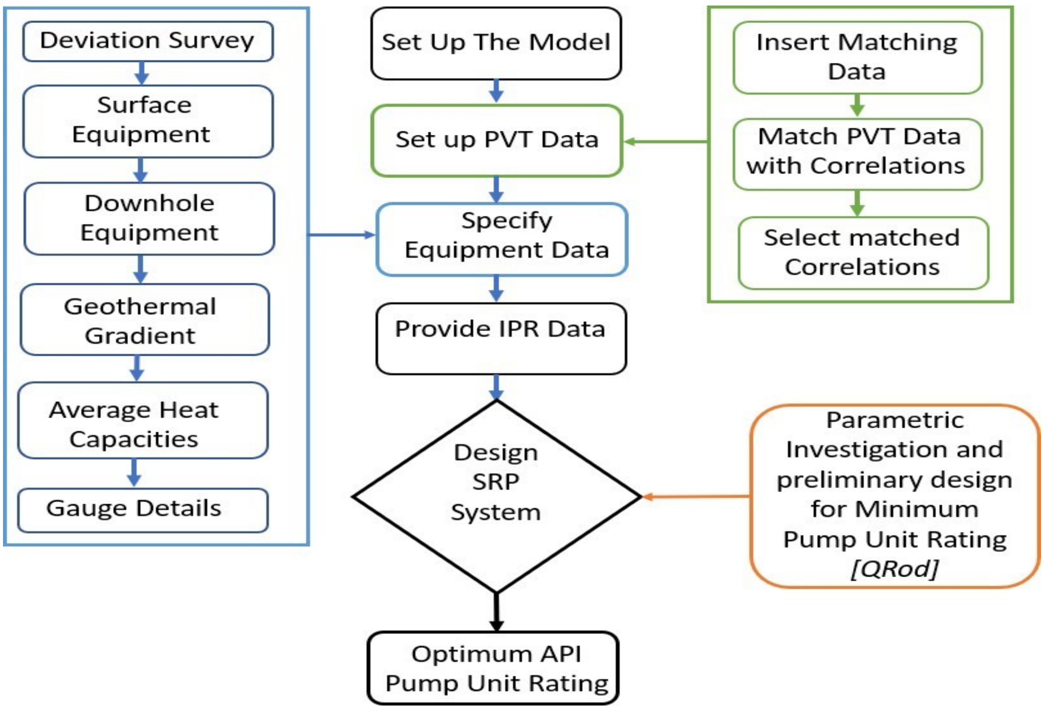

Figure 3.9. Modified PROSPER™ Workflow (With QRod™ Integrated)

The fluid type for the petroleum system is oil and water, modelled as black oil, a single-stage separator is adopted, and the fluid viscosity is modelled as Newtonian. The design procedure begins by inserting the PVT properties, shown in Figure 3.10., followed by the selection of the correlation or regression that most closely matches the field data in terms of bubble point, gas-oil ratio, oil formation volume factor, and oil viscosity.

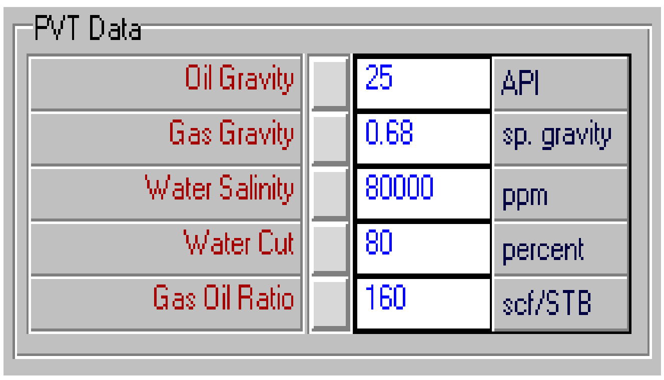

Figure 3.10. PVT data inputs in PROSPER™

Before the artificial lift system is designed, the well path and downhole equipment are thoroughly described. Details such as the deviation survey, the surface equipment, the downhole equipment, geothermal gradient, average heat capacity, and gauge details arerequired. For the deviation survey, a vertical well is chosen; the model in this sizing does not account for surface equipment.

Modelling the fluid as black oil implies that the fluid is considered undersaturated hence productivity index (PI) reservoir model is user-defined, after which the IPR curve is estimated.Any change in the properties will require that the IPR is recalculated and the absolute open flow potential (AOFP) used as the maximum possible (theoretical flow rate).

There are two calculation models provided in artificial lift simulators QRod™ and PROSPER™ concerning production rate, as shown in Figure 3.11., PROSPER™ software can be used for both the diagnostic and predictive models.

- In the diagnostic model, the stroke rate is provided, while we calculate/predict production rate (measure surface loads and predict pump performance) as shown in Figure 3.11a.
- In the predictive model, the production rate is provided, while the stroke rate is predicted (assume pump performance and predict surface loads), as shown in Figure 3.11b.

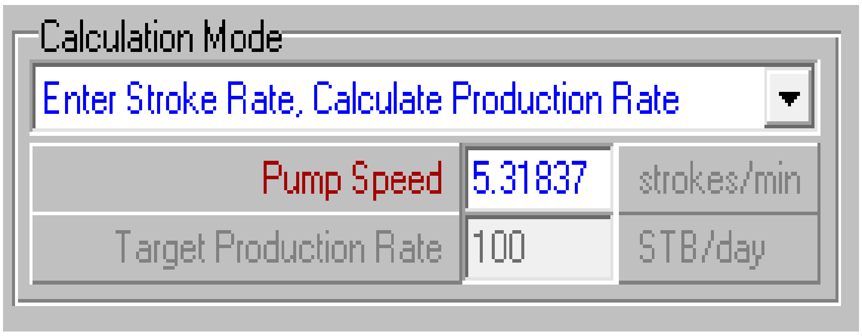

(a)

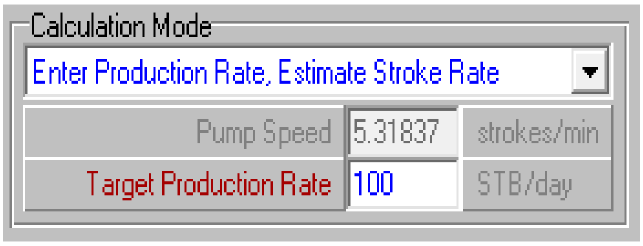

(b)

Figure 3.11. Predictive Model in PROSPER™, a) diagnostic and b) predictive

In the diagnostic model, a realistic stroke rate is provided, and the resulting production rate is computed, but in the predictive model, a target production rate is used in the design of the artificial lift system. The target or desired production rate is chosen, and the software is used to determine the stroke rate required and the corresponding size of the artificial lift to sustain production. In this work, we will be using the simulators in the predictive model.

Non-corrosive (grade D) tapered rod (6/5) is chosen (as determined from the parametric investigation). The diameter of the plunger and the thickness of the rod are provided when the rod type is specified. The plunger diameter must be less than the pump diameter, with enough tolerance or pump clearance for oil slippage. The percentages of each rod string section deduced from QRod™, and PROSPER™ are practically identical (41.7%, 58.3% in QRod™, and 42%, 58% in PROSPER™), with PROSPER™ providing more details in terms of the diameter of each rod section, as shown in Figure 3.12.

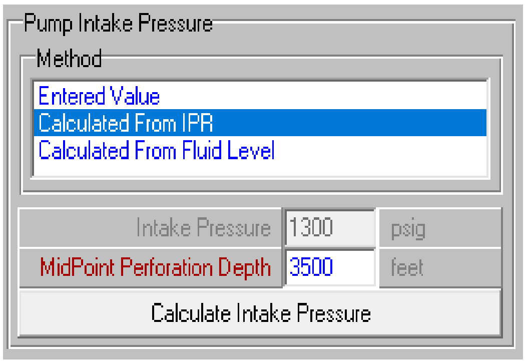

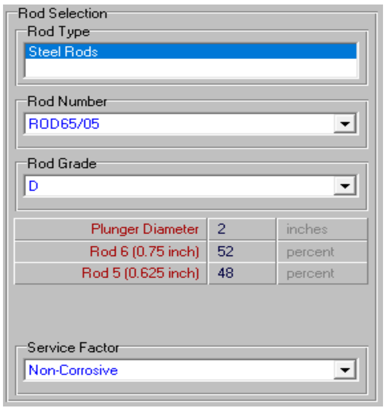

Figure 3.12. Rod selection in PROSPER™

Figure 3.13. Pump intake PROSPER™

In specifying the pump intake pressure, the value can be:

- entered directly into the simulator,
- calculated from the IPR curve, or
- derived from the fluid gradient.

IPR curve and the design rate specified are used to estimate the pressure which will be required to produce the design rate from the producing interval. This decision assumes that the mid-perforation depth is the same as the pump intake depth, as shown in Figure 3.13.

The design is executed, and the actual liquid production rate is 140.08 STB/day. The obtained design outcomes do not flag any cautions or indicate any parameters to be out of range. Therefore, the design is acceptable considering the constraints and input requirements.

The pressures and temperatures are then provided for the system, as well as the surface stroke length and pump diameter, as shown in Figure 3.14. The tubing is specified as anchored to maximize the pump displacement and minimize loading on the rod string.

Design Input

Unit Type	Type II	
Anchored Tubing	Yes	
MidPoint Perforation Depth	3500	feet
Pump Depth	3500	feet
Pump Volumetric Efficiency	80	percent
Unit Efficiency	75	percent
Pump Diameter	2''	
Surface Stroke Length	74 (inches)	
Bottom Hole Temperature	130	deg F
Well Head Temperature	90	deg F
Well Head Pressure	45	psig

Figure 3.14. Pump input parameters in PROSPER™

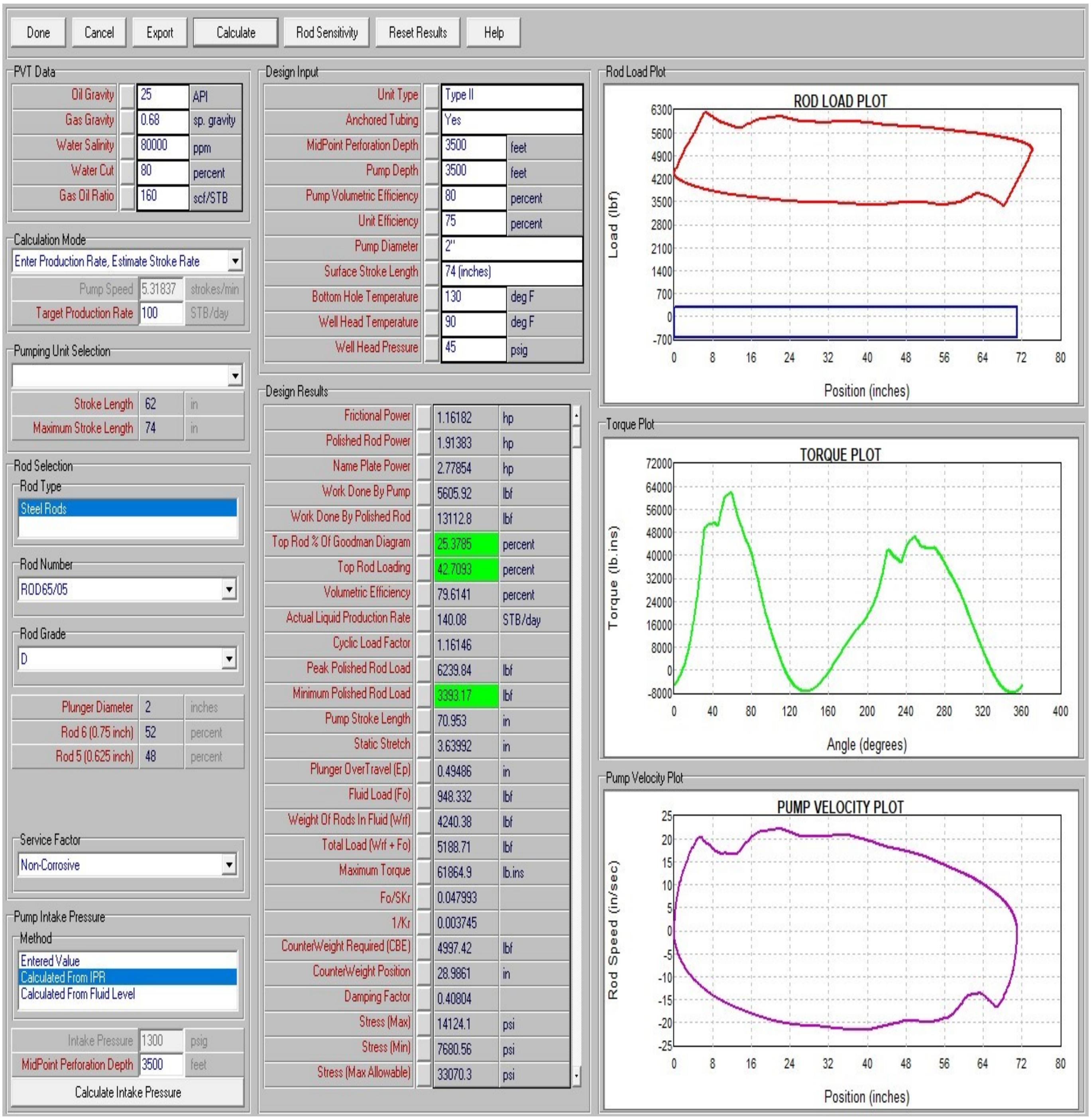

Figure 3.15. Sucker-rod pump artificial lift design in PROSPER™

The pressures and temperatures are then provided for the system, as well as the surface stroke length and pump diameter, as shown in Figure 3.14. The tubing is specified as anchored to maximize the pump displacement and minimize loading on the rod string.

3.3 Discussion of Results

Three sets of plots are typically obtained from artificial lift simulators, namely:

- rod displacement versus load/tension (pump dynamometer card),
- angular displacement versus mechanical torque (torque plot), and
- pump position versus pump velocity (velocity plot).

By identifying the indices without integration and comparing it with the integrated performance obtained with simulators, conclusions can be drawn (shown in Figure 3.15). The comprehensive design from the integrated workflow is given in Figure 3.15. showing the design results. As shown in Figure 3.16., three indices will be used in comparing the performance of the pump size obtained from the two design stages.

- Damped horsepower
- Cyclic load factor
- Prime mover rating

Table 3.1 Showing key indices, comparing a single simulator with an integrated approach

Simulator	**Minimum NEMA D Motor Size (HP)**	**Polished Rod Power**	**Damped Horse power**	**Cyclic Load Factor**	**Theoretical efficiency (%)**
QRod™	4.53	2.60	1.93	1.31	57.40
QRod™ + PROSPER™	2.78	1.91	0.87	1.09	68.71

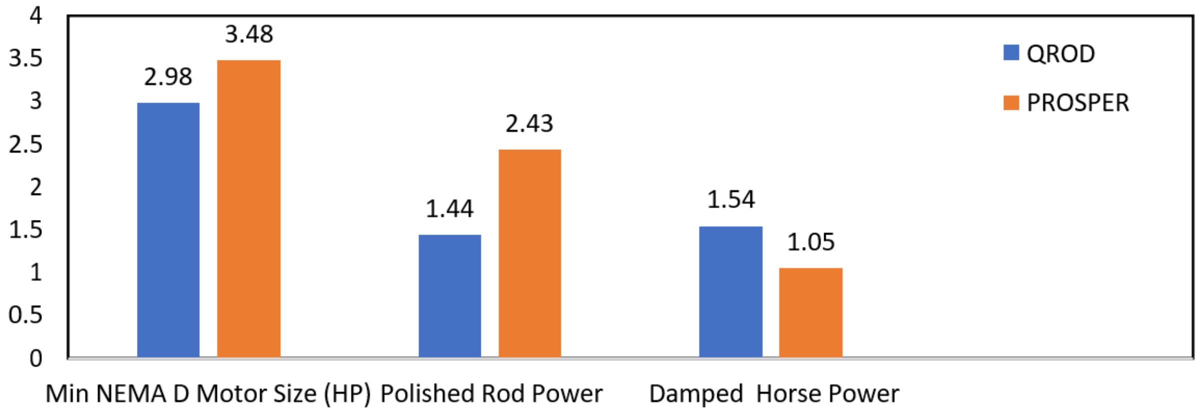

Figure 3.16. Key indices and performance indicators

From Table 3.1, the damped horsepower is higher in the motor sized with QRod™ alone, than with the integrated approach (QRod™ + PROSPER™). Electric motor prime movers subjected to constant load have an equal root-mean-square and average current. In contrast, the RMS current is always higher than the average current for cyclic or fluctuating loads as experienced in a rod pump. The damage due to overheating is minimized by oversizing (derating) the chosen electric motor, hence an electric motor with a higher capacity than is required is selected to drive the cyclic load [29], this implies that a prime mover with sufficient starting torque, is chosen over one with high efficiency [5]. The measure of the evenness or variation of the current drawn by the motor or torsional load on the gear reducer is the cyclic load factor (CLF) [29]. The cyclic load factor is always greater than 1. For one pumping cycle, CLF provides a parameter to estimate the net torque on a gear reducer. It is defined as the ratio of the root-mean-square torque to the average net torque [15, 30]:

$$Cyclic\ Load\ Factor\ (CLF) = \frac{Motor\ Hp\ \times Unit\ Efficiency}{Polished\ Rod\ HorsePower}$$

$$= \frac{Root\ Mean\ Square\ Current}{Average\ Current} = \frac{Root\ Mean\ Square\ Power}{Average\ Power}$$

Considering the effect of the cyclic load factor in derating the electric motor prime mover and considering a safety factor of 1.15 [31], the electric motor is rated, as shown in Table 3.2.

Table 3.2 Derating of High slip electric motor

HP	$1\ \mathbf{kW} = \mathbf{0.746HP}$	CLF	SF	Motor = (kW x CLF x SF)
2.78	2.07	1.09	1.15	2.59

The CLF is also significantly higher in the motor sized with QRod™ alone than with the integrated approach. With smaller CLF values, the pumping utilizes available power more efficiently [32]. Hence, the overall theoretical efficiency in the motor sized with the integrated approach is significantly higher than that sized with QRod™ alone.

3.4 Rod Sensitivity Analysis

By rod sensitivity analysis as shown in Table 3.3, the various API rod numbers are evaluated for both uniform rod strings and tapered rod strings. The production rates which are obtainable from the strings and the energy requirements for each corresponding rod type are considered.

Table 3.3 Sucker rod pump design - Rod Sensitivity

Rod Index	Rod Name	Production (BBL/D)	Horsepower (Hp)	BBL/Hp/D
4	44/05	190.74	1.85	103.24
15	54/05	185.39	2.13	87.11
22	55/05	138.87	1.69	82.51
37	65/05	140.09	1.91	73.19
46	66/05	121.89	1.84	66.28
57	75/05	123.31	2.43	50.66
63	76/05	122.40	2.03	60.42
73	77/05	113.39	2.11	53.77
88	86/05	122.97	2.30	53.39
96	87/05	113.63	2.27	50.15
107	88/05	109.24	2.47	44.17
124	97/05	113.92	2.51	45.42
133	98/05	109.38	2.62	41.82
144	99/05	106.46	2.90	36.72
163	108/05	109.53	2.84	38.62
173	109/05	106.54	3.03	35.15

Figure 3.17 shows the production rate of different rod types. As can be seen from Table 3.3 and Figure 3.17., comparing rod indices 4, 15, 22, and 37 correspond to rod names 44/05, 54/05, 55/05, and 65/05. Although 44/05 and 55/05 have very high production rates, uniform diameter rod strings (from the top of the well to the bottom) are usually deployed for well depths less than 2000ft [33]. With well depth greater than or equal to 3500ft, the design of rod string imposes the criterion for tapering; hence 54/05 would be the next best option, but since it is not available in both sucker-rod pump simulators (QRod™ and PROSPER™), 65/05 is chosen for implementing the optimal design.

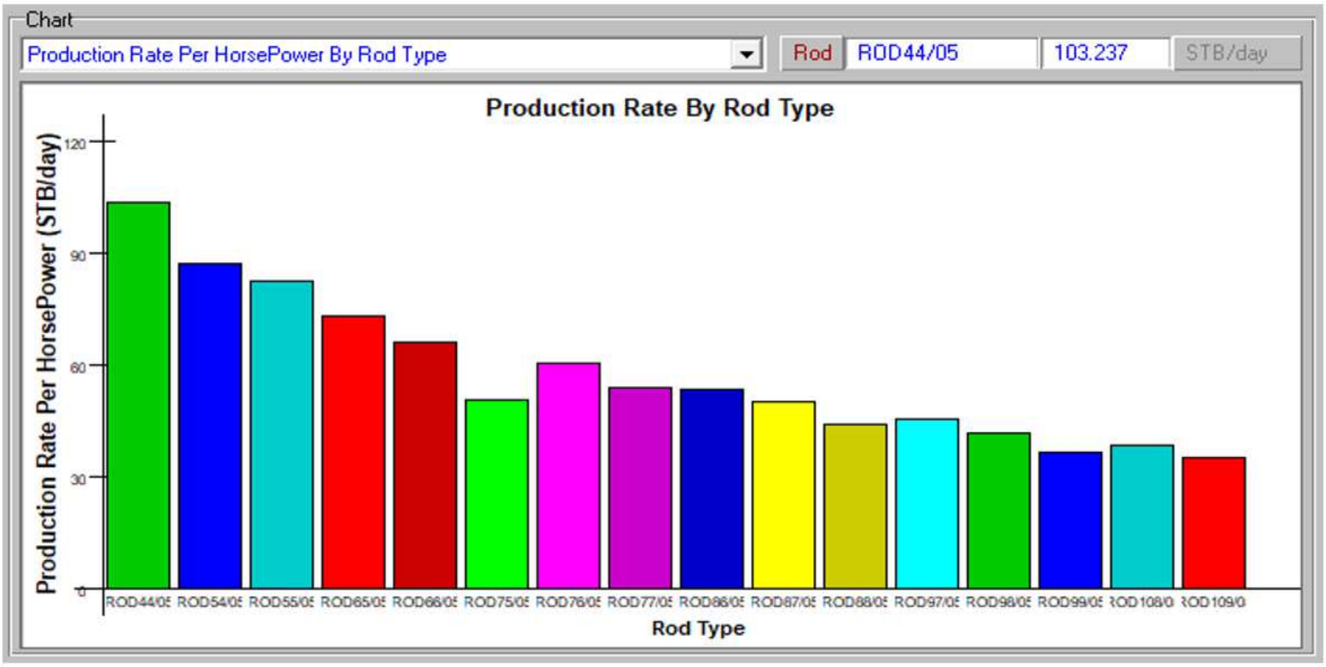

Figure 3.17. Production rate per horsepower required by rod type

3.5 Conclusion

This study presents new insights into parameters affecting the sizing of beam-pumped units. It also deploys an integrated methodology that minimizes the need for iteration in one simulator alone, making it possible to perform a feasibility study at low cost and come to a single optimal motor design size, in limited trials. PROSPER™ has very robust PVT (fluid correlation) and deliverability options but adopts an iterative process in the sizing of artificial lift systems. Hence if a parametric investigation is performed in QRod™ and integrated with the workflow in PROSPER™, it becomes relatively easier to size the unit in PROSPER™ and complete the design with fewer iterations. Each simulation platform has its unique advantages, merits, and strengths in sizing applications. By integrating both simulators, the authors do not imply that one simulation platform is superior to the other. The findings presented for the case study well show that the integrated approach reduces the damped horsepower and the polished rod horsepower by 54.9% and 26.5% respectively for a corresponding decrease in minimum NEMA D motor size by 38.6%. These key performance indicators are used to demonstrate the benefits of simulator integration in the sizing of beam-pumped oil wells.

3.6 Acknowledgments

The authors would like to appreciate the Tertiary Education Trust Fund (TETFUND) of the Federal Government of Nigeria for funding this research. We also acknowledge the support of the Memorial University of Newfoundland for the enabling environment to carry out this research.

3.7 References

[1] Shedid, S.A., 2009, April. Effects of Subsurface Pump Size and Setting Depth on Performance of Sucker-Rod Artificial Lift—A Simulation Approach. In SPE Oklahoma City Oil and Gas Symposium/Production and Operations Symposium (pp. SPE-120681). SPE.

[2] Aguilera, R.F., 2019. The Exceptional Price Performance of Oil–Explanations and Prospects. Natural gas, 25, p.25.

[3] Dave, M.K. and Ghareeb Mustafa, M., 2017, November. Performance evaluations of the different sucker rod artificial lift systems. In SPE Symposium: Production Enhancement and Cost Optimisation (p. D011S002R004). SPE.

[4] McCoy, J.N., Podio, A.L., Drake, B. and Rowlan, L., 2001, March. Modern total well management-sucker rod lift case study. In SPE Western Regional Meeting (pp. SPE-68864). SPE.

[5] Podio, A.L., McCoy, J.N. and Becker, D., 1995, March. Total well management-A methodology for minimizing production cost of beam pumped wells. In SPE Western Regional Meeting (pp. SPE-29637). SPE.

[6] Hein Jr, N.W. and Loudermilk, M.D., 1992, October. Review of New API Pump Setting Depth Recommendations. In SPE Annual Technical Conference and Exhibition? (pp. SPE-24836). SPE.

[7] Agarwal, A.K., Purwar, S. and Bravo, C.E., 2014, April. Real-time Diagnostic Analysis of Artificially Lifted Wells: A Smart Workflow Approach. In SPE Intelligent Energy International Conference and Exhibition (pp. SPE-167822). SPE.

[8] Dave, M.K. and Ghareeb Mustafa, M., 2017, November. Performance evaluations of the different sucker rod artificial lift systems. In SPE Symposium: Production Enhancement and Cost Optimisation (p. D011S002R004). SPE.

[9] Xing, M. and Dong, S., 2015. A new simulation model for a beam-pumping system applied in energy saving and resource-consumption reduction. SPE Production & Operations, 30(02), pp.130-140.

[10] Feng, Z.M., Tan, J.J., Li, Q. and Fang, X., 2018. A review of beam pumping energy-saving technologies. Journal of Petroleum Exploration and Production Technology, 8, pp.299-311.

[11] Di Tullio, M.T. and Marfella, F., 2018, November. Enhanced sucker rod pumping model: a powerful tool for optimizing production, efficiency and reliability. In SPE Middle East Artificial Lift Conference and Exhibition (p. D022S020R002). SPE.

[12] Jennings, J.W., 1989, October. The design of sucker rod pump systems. In SPE Centennial Symposium at New Mexico Tech (pp. SPE-20152). SPE.

[13] Durham, M.O. and Lockerd, C.R., 1988, October. Beam pump motors: The effect of cyclical loading on optimal sizing. In SPE Annual Technical Conference and Exhibition? (pp. SPE-18186). SPE.

[14] Paik, M.E., 1996, April. Reducing electric power costs in old oil fields. In SPE Improved Oil Recovery Conference? (pp. SPE-35408). SPE.

[15] Takacs, G., 2015. Sucker-rod pumping handbook: production engineering fundamentals and long-stroke rod pumping. Gulf Professional Publishing.

[16] Liu, X., Guo, B. and Tan, X., 2017. Petroleum production engineering. Gulf Professional Publishing.

[17] Rowlan, O.L., Mccoy, J.N. and Podio, A.L., 2005. Best method to balance torque loadings on a pumping unit gearbox. Journal of Canadian Petroleum Technology, 44(07).

[18] Hicks, A.W., 1986, April. Using fiberglass sucker rods in deep wells. In SPE Deep Drilling and Production Symposium (pp. SPE-14974). SPE.

[19] Osaretin, C.A., Iqbal, T., and Butt, S., 2020. Optimal sizing and techno-economic analysis of a renewable power system for a remote oil well. AIMS Electronics and Electrical Engineering, 4(2), pp.132-153.

[20] Agrawal, N., Baid, R., Mishra, L., Ghosh, P. and Kushwaha, M., 2015, November. Quick look methodology for progressive cavity pump sizing and performance monitoring. In SPE Oil and Gas India Conference and Exhibition? (pp. SPE-178097). SPE.

[21] Gibbs, S.G., 2012. Rod pumping: modern methods of design, diagnosis and surveillance. Sam Gavin Gibbs.

[22] Gibbs, S.G., 1982. A review of methods for design and analysis of rod pumping installations. Journal of Petroleum Technology, 34(12), pp.2931-2940.

[23] Palka, K. and Czyz, J.A., 2009. Optimizing downhole fluid production of sucker-rod pumps with variable motor speed. SPE Production & Operations, 24(02), pp.346-352.

[24] Bellarby, J., 2009. Well completion design. Elsevier.

[25] Tripp, H.A., 1988. Mechanical performance of fiberglass sucker-rod strings. SPE production engineering, 3(03), pp.346-350.

[26] Watkins, D.L. and Haarsma, J., 1978. Fiberglass sucker rods in beam-pumped oil wells. Journal of Petroleum Technology, 30(05), pp.731-736.

[27] Gibbs, S.G., 1991. Application of fiberglass sucker rods. SPE Production Engineering, 6(02), pp.147-154.

[28] Tripp, H.A., 1988. Mechanical performance of fiberglass sucker-rod strings. SPE production engineering, 3(03), pp.346-350.

[29] Takács, G., 2003. Sucker-rod pumping manual. PennWell Books.

[30] Rowlan L.,2006. International Sucker Rod Pumping Workshop, South-Western Petroleum Short Course. Artificial Lift Research and Development Council (ALRDC).

[31] National Electrical Manufacturers Association (NEMA) Standards, 2018. ANSI/NEMA Motors and Generators MG1.

[32] Lekia, S.D. and Evans, R.D., 1995. A Coupled Rod and Fluid Dynamic Model for Predicting the Behavior of Sucker-Rod Pumping Systems—Part 2: Parametric Study and Demonstration of Model Capabilities. SPE Production & Facilities, 10(01), pp.34-40.

[33] Lyons, W.C. and Plisga, G.J., 2011. Standard handbook of petroleum and natural gas engineering. Elsevier.

[34] IPM PROSPER User Manual, Version 13, 2015. Petroleum Experts Limited (PETEX).

Chapter 4

OPTIMAL SIZING AND TECHNO-ECONOMIC ANALYSIS OF A RENEWABLE POWER SYSTEM FOR A REMOTE OIL WELL

Co-authorship statement

This chapter achieves research objectives 2 and 3 of this thesis as stated in Section 1.3. It presents the Optimal sizing, and techno-economic analysis of a renewable power system for a remote oil well, with a focus on developing and reporting a detailed and systematic approach to selecting and sizing the optimum renewable energy system to adopt for remote wells based on defined technical and economic criteria. This research provides a framework for developing a renewable, off-grid solar PV power system to sustain oil production from remote wells. This study evaluates the technical and economic implications of adopting onsite renewable energy-based approaches and assesses their feasibility, especially under varying weather and battery storage conditions. This study analyzes the feasibility of different renewable energy scenarios for continuous and intermittent production for an artificially lifted well. This study specifies the technical and economic criteria required in choosing the best solution for the optimum combination of energy source and pumping schedule. It Proffers two recommendations to the oil well operator based strictly on either the continuous or intermittent production using the following criteria: Unmet Load (kWh/yr), Capacity Storage (kWh/yr), the Net Present Cost ($), Levelized Cost of Energy ($/kWh) and Operating Cost ($/yr).

I (Charles Aimiuwu Osaretin) am the principal author and contributed to Conceptualization, Methodology, Technical and Economic analysis, Writing of Original Draft and Editing of the research manuscript. The research in this chapter was supervised by Dr. M. Tariq Iqbal, and Dr Stephen Butt. The supervisors contributed to the conceptualization and methodology. They also supervised the entire chapter, and reviewed, and corrected the research manuscript. The work in this Chapter has been published in the American Institute of Mathematical Sciences (AIMS) Electronics and Electrical Engineering, Volume 4, Issue 2, March 2020, Pages 132–153, Article ID 216223132, 17 pages, https://doi.org/10.3934/ElectrEng.2020.2.132.

Abstract

There is a growing interest in the deployment of off-grid renewable energy, especially for remote oil and gas facilities. This work is a novel attempt to optimally size a renewable energy system to power an artificial lift for an oil well. It proposes a low-cost alternative to the abandonment and decommissioning of old wells. Sucker-rod pump artificial lift simulators (QRod™ and PROSPER™) are deployed to estimate the energy requirement of a well, with both intermittent and continuous pumping considerations. Simulation and optimization are performed using HOMER optimizer™, which produces different system configurations and presents the possible configurations in order of increasing system costs. Based on economic and technical merits, continuous pumping using a hybrid renewable energy system consisting of a solar, wind and battery storage is chosen as the most feasible solution with 0 kWh/yr of unmet load, a capacity storage of 0.56 kWh/yr, net present cost of $145,150.50, levelized cost of energy of $0.51/kWh and an operating cost of $3,056.04/yr. The optimal configuration is finally examined to determine its sensitivity to variation in daily solar radiation and average wind speed. It is demonstrated to be the most preferred system design, even at the least daily average solar radiation.

4.1 Introduction

Petroleum production currently faces the reality of low prices, and hence low budget operations are required [1, 2]. The reality is that more fields are required to be developed in remote locations and such developments are also more energy intensive [3]. The need for a simple, economical and environmentally sustainable alternative to keep the oil and gas wells onstream and minimize the impact of the depressive market cannot be overemphasized [4]. There is also a pandemic of the indefinite suspension of producing oil wells due to the economics of production, as wells previously considered economical, have suddenly become sub-economical at best and uneconomical at worst. The petroleum production engineer and facility engineer continue to face the challenge of keeping presently producing wells onstream and providing innovative solutions to restore idle facilities to production [5]. Considering the safety and environmental impact of suspending producing oil wells, economic losses due to inactivity and the prohibitive cost of abandonment; it becomes imperative and favorable for operators, jobs, the economy and the environment to minimize losses, defer costs, maintain production and provide innovative alternatives for producing wells classified as marginal/stripper wells [6]. Since wells are subjected to various production schedules, the cost implication of innovative renewable energy-based approaches also needs to be evaluated for feasibility, especially under varying weather and battery storage conditions. This work analyzes the feasibility of different renewable energy scenarios for continuous and intermittent production for an artificially lifted well; taking technical and economic factors into consideration in choosing the best solution in terms of the most suitable combination of energy source and pumping schedule.

4.2 Literature Review

The increasing deployment of renewable energy for oil and gas production reflects a shift in paradigm, as the role of renewable energy evolves from competing to a complementary energy source [7]. Deployment of 100% renewable energy for hydrocarbon production has received some attention in literature: Van Heel et at. [8] examined the effect of using concentrated solar power for cyclic production of high-pressure steam required for steam injection, Poythress et al. [9] implemented a solar energy-based system for de-watering an onshore gas well using a low power DC electric motor. A gap still exists in the literature that consider the technical and economic feasibility of deploying 100% renewable energy to produce oil in remote facilities. Finding the least cost and most suitable combination of renewable sources and storage, that satisfies the energy demand for production in different scenarios is the task of this study.

There comes a time in the life of an oil well, when the need arises to provide external energy to sustain or attain a target production. For onshore wells, about 85% of the wells requiring artificial lift deploy sucker rod or beam pumps, as they are simple, durable and familiar to most operators [10–12]. Given that the average oil production for a well is taken daily over a period of 12 consecutive months with peak value less than or equal to 15 barrels or when the average gas production considered daily over a period of 12 consecutive months has a peak value of at most 90,000 cubic feet per day, then for taxation purpose, such a well is considered a stripper well. On land, if a well becomes marginal primarily due to low production, it is usually classified as a stripper well. It should be noted that each oil field or producing well has a unique price that determines its critical profit point (benchmark price for profitable operation), below which a field or well will become unprofitable [13]. The producing well being examined in this work no longer produces adequate oil volumes to generate enough revenue from oil sale and hence is considered for suspension, plugging or abandonment due to either the high cost of operation or low volume of production or both [14]. Continuous operation of such wells requires a higher price [per barrel of oil produced or thousand cubic feet (Mcf) of natural gas] or a reduced cost of operation/production. The system cost component is composite and influenced by the conditions of operation such as access to the site (remoteness), fluid viscosity, depth of the well and energy requirement (artificial lift required), the composition of produced fluids, and need for separation, processing, and disposal [13].

For various production conditions and at different phases in the life of an oil well, it is often desirable to determine and predict the power requirement for an artificially lifted petroleum production system. It becomes necessary to determine the rating of the prime mover required to drive and sustain production at the desired rate or level [14]. During artificial lift design, after estimating the appropriate fluid load for the well, it is normally difficult to get a standard motor (prime mover) to match the estimated cyclic load. It is a regular practice to settle for the lowest-sized motor that satisfies the load requirement. Oversizing the motors inevitably leads to over-pumping the wells, reducing pump efficiency and ultimately pump life. It is also typical at the design stage to adjust the pumping mode (stroke length, pump displacement, strokes per minute) [15]. This adjustment changes the speed and torque requirements and results in a pumping system that could over time eventually also over-pump the wells [16]. Due to the dynamics of the well and fluid conditions, it may be necessary to adopt a form of pump scheduling using a pump cycle controller (fixed-interval time clocks, percentage timers, and pump-off controllers/pump control system) to dynamically match the pump action to the available production rate [17]. A timer is a simple solution, but a pump-off controller may be preferable to respond to fluid-pound, allow accumulation of reservoir fluids in the wellbore, minimize damage to the pump, and ensure high volumetric efficiency [10, 14, and 17]. In this study, the electrical energy from renewable energy generators will be used to power a high-slip

AC electric motor, which serves as the prime mover for the sucker-rod-pumped artificial lift system as shown in Figure 4.1.

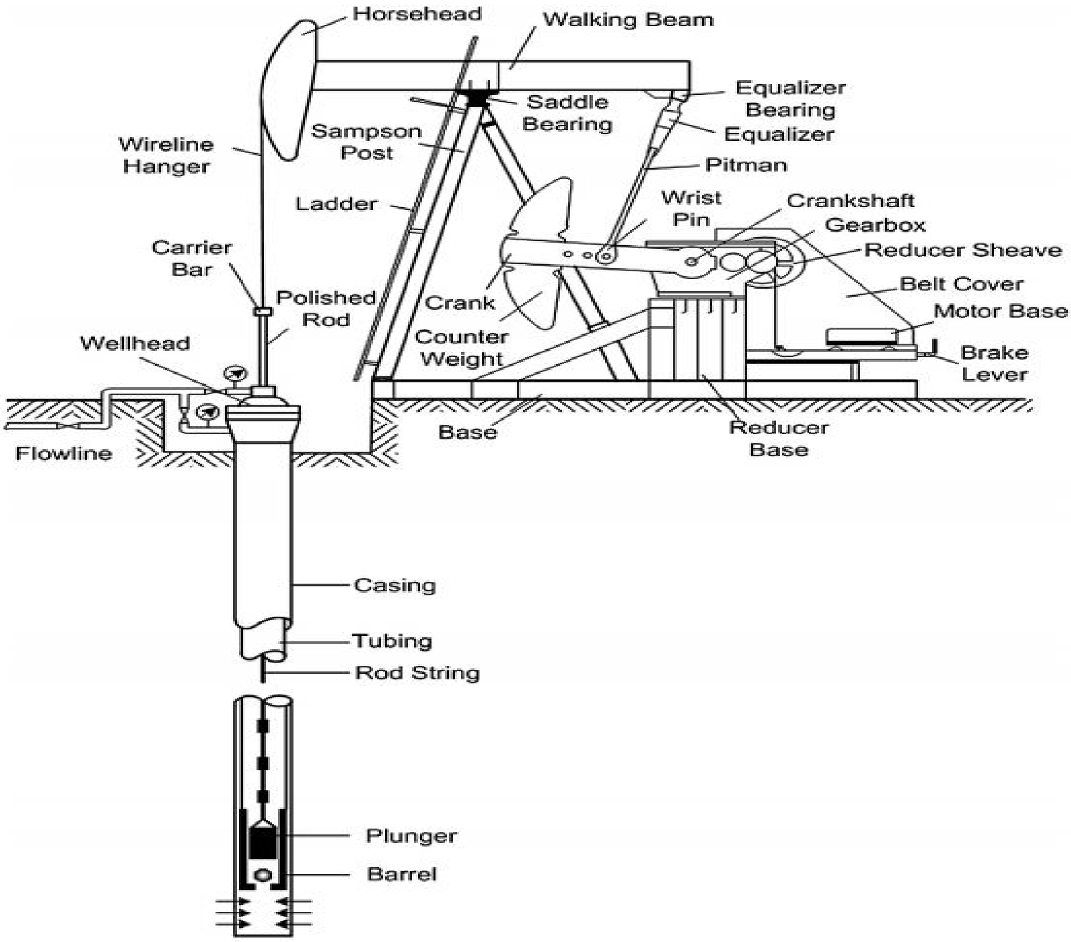

Figure 4.1. Sucker-rod pumping unit [15].

4.3 System Description

The renewable microgrid evaluated for simulation exhibits hybrid generation and redundancy. It tentatively consists of two (2) primary power sources: solar PV and wind, one (1) backup source (battery storage), and the prime mover or high slip AC electric motor (NEMA D) as shown in Figure 4.2. The proposed system matches the requirement of the producing well and is to be 100% renewable to ensure minimal interruption of hydrocarbon production, reduce noise, and eliminate exhaust gas pollution.

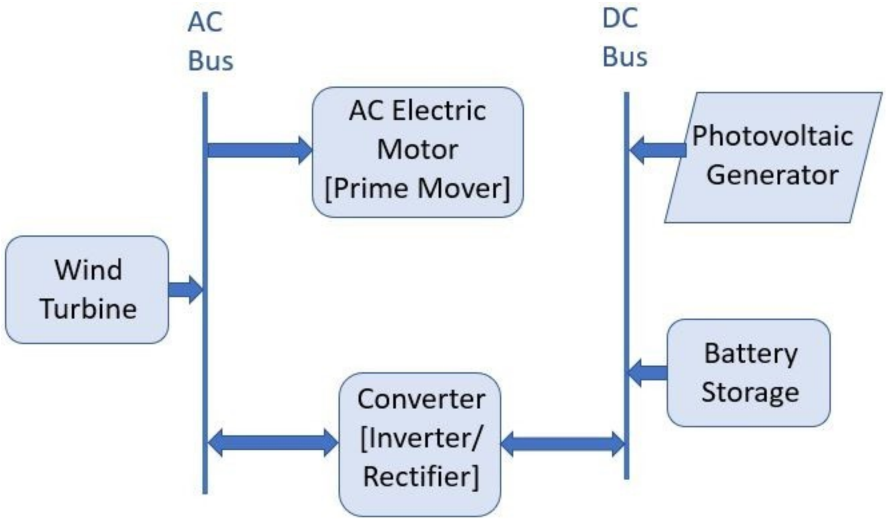

Figure 4.2. Hybrid renewable microgrid system with integrated components.

4.4 Renewable Energy Potential of The Selected Location

Medicine Hat is a city in southeast Alberta, latitude 50^{0}2'32" N and longitude 110^{0}48'49" W. It is one of the sunniest parts of Canada with an average of 2,544 sunshine hours and 330 days of sunshine per year [18]. In recent times a crisis has been looming in the oil and gas sector in Alberta, with the City of Medicine Hat been one of the worse hit due to the low prices. About 2,000 producing wells in Medicine Hat (75%) are to be shut down, and only the least cost wells are to be left producing [19]. With the oil and gas market going through a depression, massive job losses are anticipated. The approach considers an idealized well, combined with the weather data of Medicine Hat to propose a system design.

4.4.1 Solar Potential

The monthly average solar radiation data (global horizontal irradiance GHI in kWh/m^2/day) and dimensionless clearness index were obtained from NASA surface meteorology and solar energy database [20] and plotted in Figure 4.3. As shown in Table 4.1, Medicine Hat has the highest values for solar radiation and peak clearness index in the summer months, with a scaled annual average solar radiation of 3.61 kWh/m^2/day.

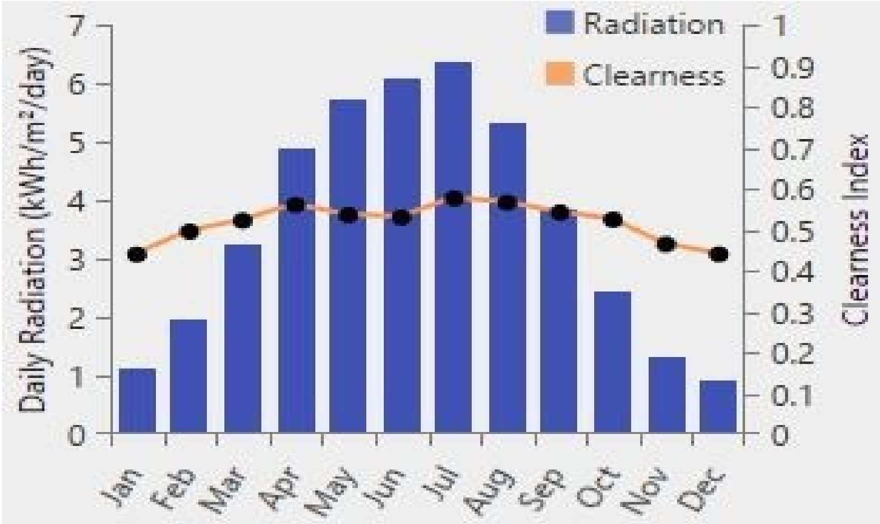

Figure 4.3. Monthly average solar radiation (global horizontal Irradiance GHI) data in HOMER.

Table 4.1. Monthly solar radiation and clearness index

Month	Clearness index	Daily Radiation ($kWh/m^2/day$)
January	0.438	1.110
February	0.494	1.970
March	0.520	3.250
April	0.559	4.890
May	0.534	5.710
June	0.529	6.100
July	0.575	6.380
August	0.565	5.340
September	0.540	3.830
October	0.523	2.430
November	0.463	1.320
December	0.439	0.930

4.4.2 Wind Energy Potential

Data available from surface meteorology and solar energy database [20] is given in Table 4.2. The scaled annual average wind speed at 50 m above the earth's surface for flat terrain in Medicine Hat is given as 5.70 m/s. The average monthly wind speed is obtained from NASA with minimal variation and plotted for one year in Figure 4.4.

Table 4.2. Monthly average wind speed data for Medicine Hat.

Month	Average Wind Speed (m/s)
January	5.670
February	5.620
March	5.640
April	6.180
May	6.320
June	5.830
July	5.260
August	5.100
September	5.480
October	5.910
November	5.590
December	5.770

Figure 4.4. Monthly average wind speed plot for Medicine Hat.

From the data in Table 4.2 and Figure 4.4., it can be inferred that at a hub height of 50 m, the average wind speed of Medicine Hat is high enough for wind power generation. Hence it is justifiable to consider wind power as one of the primary sources of power for driving production of the artificially lifted well. It should be noted that apart from generating electricity from a wind turbine to power the AC electric motor, drive sucker-rod pump and produce at the desired flow rate, hydraulic wind pumps can also be tested directly for lifting fluids from the producing well, but such application is beyond the scope of this work.

4.5 Description of Load Profile for The Case Study Well

Several possibilities could be considered as case studies, and different scenarios can thus arise as follows:

Only artificial lift required: Telecommunication, remote monitoring, electronic metering and control, not required. The facility could be:

- a remote gas well that requires de-watering only,
- a remote gas well that requires chemical injection only,
- a remote oil well that requires artificial lift only.

Remote oil wells (in digital oilfields): oil wells powered by artificial lift requiring telecommunications, process automation, remote sensing, instrumentation and advanced process control (SCADA, PLC, etc.). Such facilities are usually powered by the electric grid and/or diesel/gas power only, as the energy requirement may result in very high system cost, except in shallow oil wells, gas wells requiring dewatering and/or chemical injection.

Remote well requiring artificial lift only (will be considered in this work): This well for technical and/or economic reasons cannot be connected to the grid but is proposed to be powered by a small stand-alone hybrid renewable power system. It should be noted that in practice, between pumping cycles, several combinations of a timer on/off schedules could be used, depending on the downhole conditions, the pumps could be turned off for 5, 10 or as much as 15 minutes before restarting [16]. In this study, two (2) pumping schedules (pump duty cycle) are considered:

- Scenario A: Intermittent production (diurnal, during the day, 12 hours on, 12 hours off).
- Scenario B: Continuous production (uninterrupted).

For intermittent production, the daily and monthly load profile are shown in Figures 4.5. and 3.6., respectively. The pump is turned on for 12 hours of daylight from 7 am to 7 pm and off otherwise.

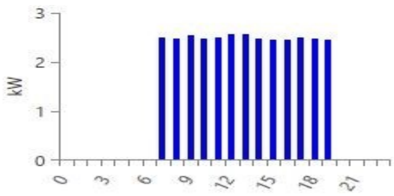

Figure 4.5. Daily load profile for scenario A: Intermittent production (diurnal, during the day).

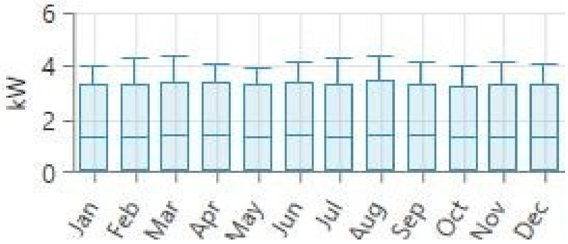

Figure 4.6. Monthly (seasonal) load profile for scenario A: (diurnal, during the day).

For continuous production, the load is run continuously. It is expected that the cost contribution of the required storage system will be justified by the extra production made possible by continuous operation. The daily and monthly load profile are shown in Figures 4.7. and 4.8., respectively.

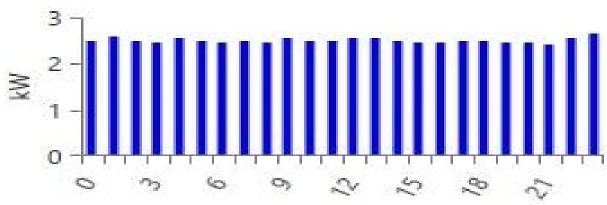

Figure 4.7. Daily load profile for scenario B: continuous pumping.

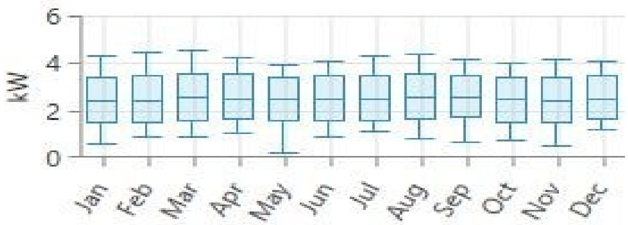

Figure 4.8. Monthly load profile for scenario B: continuous pumping.

4.6 Methodology

Estimation of the load requirement begins with the design of a sucker-rod pumped artificial lift system. The sizing begins with selection of a suitable pumping mode (stroke length, stroke per minute, plunger diameter and rod string design) as shown in Figure 4.9(a)., after which a parametric investigation is carried out to determine the effect of API rod number, pump diameter and pump geometry on the energy requirement of the prime mover in an artificial lift simulator QRod (Quick Rod). The parameters chosen from the investigation are subsequently deployed in another simulator PROSPER as shown in Figure 4.9(b). The well, fluid and pump characteristics are defined, and the design repeated in PROSPER to obtain a more robust rating of sucker-rod pump and appropriately size a high slip AC electric motor, the prime mover rating is shown in Figure 4.9(c).

HOMER (Hybrid Optimization of Multiple Energy Resources) is the tool that is adopted for simulation, optimization and sensitivity analysis. Based on the selected geographical location (longitude and latitude), the solar, wind and temperature data are updated in HOMER. The energy flow between components is calculated and considering variability in weather conditions and the load profile, the cost of installing and operating the system over the project lifetime is estimated. Simulation entails that given specified conditions, the flow of energy between the components of the system is calculated for each time interval, to find a balance that ensures continuous and consistent operation, hence reliably and optimally balancing the electrical energy demand with supply. Optimization (deploying HOMER Optimizer ™) implies identifying the configuration with the best mix of renewable resources that meets the load requirements all year round at the least cost [21]. Since storage is adopted and the sources are 100% renewable, cycle charging is adopted as the power dispatch strategy, such that a producing generator runs at or close to its rated maximum capacity, without producing any excess electricity; but any excess electricity generated is stored in the battery bank to supply the primary load when needed [22]. The battery bank serves as a backup to deliver power to the load below the cut in or rated speed, at night or on cloudy days. In Homer, feasible solutions are ranked in order of increasing net present cost, but technically any system with the least unmet load is considered the most reliable [23] and hence the most feasible solution among the available alternatives [24].

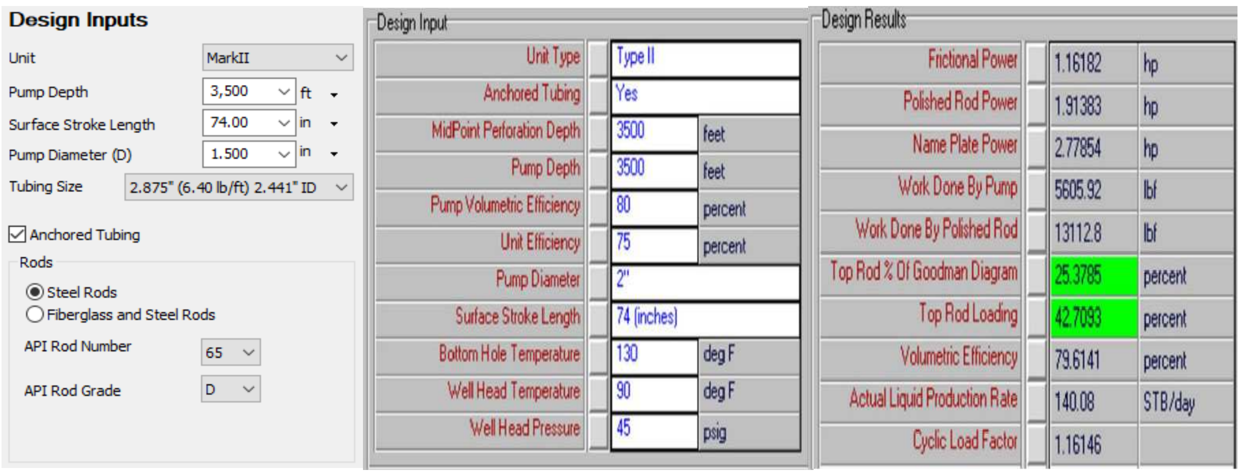

(a) (b) (c)

Figure 4.9. (a) Design inputs for beam pumped well in QRod, (b) Design inputs for beam pumped well in PROSPER, (c) Design results showing size and power rating of pump required.

4.7 Description of Proposed Renewable Power System

From a continuous pumping load perspective, the energy consumption of the prime mover (AC electric motor) is 60.11 kWh/d, with a peak load of 4.55 kW. The system is designed with a discount rate of 8%, for 25 years and consists of solar panels (Jinko Eagle PERC60, 300W) with an efficiency of 18.33%, deep cycle batteries [SAGM 12 205 (12V, 219Ah)] with four (4) units per string to obtain a string voltage of 48 V. A 5.5 kW system converter (battery dedicated inverter: Schneider Conext XW +5548) was deployed with 93% efficiency. A wind turbine with a 4.5 m rotor and a hub height of 12 m (AWS HC, 3.3 kW) was also selected as a secondary energy source, as shown in the schematic of the system in Figure 4.10.

The system types are presented in order of decreasing system cost. The case study is considered sufficiently remote to justify the exclusion of the diesel generator. This approach ensures a 100% renewable power system mix and eliminates the need for refueling, routine maintenance, and servicing operations normally required for operating a diesel generator. The proposed design should economically exploit the solar energy, wind energy or both, with battery storage to sustain hydrocarbon production.

HOMER calculates the energy flow to and from each system component, determines how to run the generators to consistently supply the AC electric loads and charge batteries when possible. It should be noted that solutions obtained from the simulations are considered infeasible either due to capacity shortage constraint, minimum renewable energy fraction or unmet load. The optimized results from HOMER are arranged by default in order of increasing cost [net present cost (NPC), levelized cost of energy (LCOE) and operating cost], with the least cost configuration ranking higher.

Renewable energy fraction is adopted as a constraint criterion in sifting the simulation results considered as feasible options. Additionally, some system types may return “a feasible option with caution”. These will also not be considered, as such system types may experience stability problems due to sufficiently high renewable penetration. Addition of more storage (battery bank or flywheel) may be helpful, but more detailed modelling is required, which is beyond the scope of this study. The system structure for diurnal pumping is shown in Figure 4.10., with a daily energy consumption of 32.43 kWh/d and a peak load of 4.44 kW.

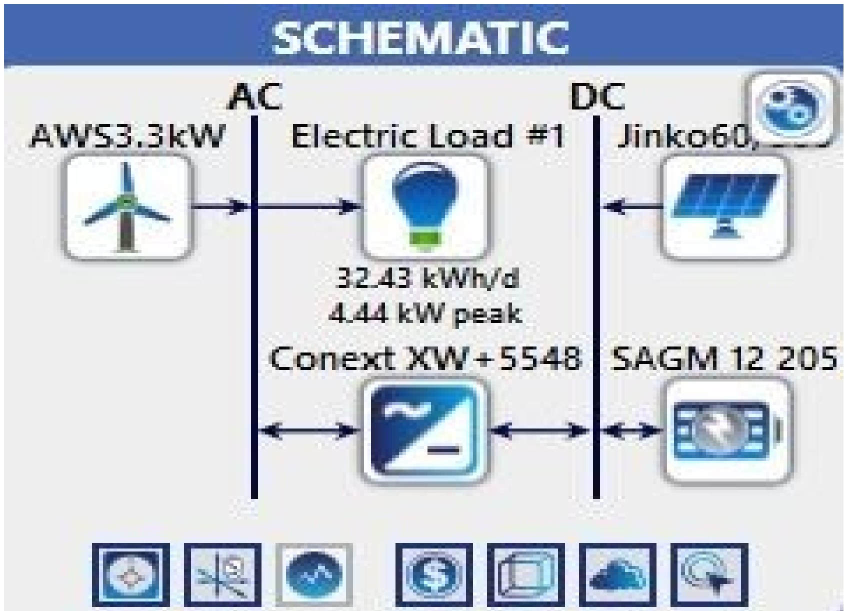

Figure 4.10. System structure optimized in HOMER with components integrated (For intermittent pumping).

4.7.1 Scenario A: Intermittent Production (diurnal, during the day)

A total of 1,204 solutions were simulated, 578 were feasible, and 626 were infeasible due to the capacity shortage constraint. Of the 292 omitted solutions, 123 lack a converter, 37 have an unnecessary converter and, 126 have no power generation source. The simulation results for candidate configurations for diurnal production is shown in Table 4.3(a) and 4.3(b), ranked in order of increasing system cost.

Table 4.3(a) Simulation results by system types or categories for intermittent production (diurnal, during the day), (b) Cost of system types for intermittent production.

Architecture				
Jinko60/300 (kW)	AWS3.3kW	SAGM 12 205	Conext XW+5548 (kW)	Dispatch
27.3		64	4.49	CC
26.4	1	60	4.12	CC
	4	80	3.80	CC

Cost				System	
NPC ($)	COE ($)	Operating cost ($/yr)	Initial capital ($)	Ren Frac (%)	Total Fuel (L/yr)
$64,969	$0.425	$1,318	$47,932	100	0
$89,512	$0.585	$1,466	$70,563	100	0
$157,555	$1.03	$1,863	$133,474	100	0

4.7.1.1 System type 1A

Solar PV and battery storage.

A solar PV generator rated 27.3 kW, 16.0 strings of battery storage and a system converter of 4.49 kW make up this system type. The battery storage is the dominant cost component in this system type, accounting for 46.7% of the total system cost. The NPC, LCOE, and operating cost are $64,969.30, $0.4247/kWh and $1,317.93/yr. On a monthly basis, the produced electricity for this configuration is plotted in Figure 4.11.

Figure 4.11. Monthly electricity production for system type 1A.

This system generates 39.009 MWh/yr of electricity of which 11.832 MWh/yr is consumed by the AC electric motor, and 65.9% of total generation (25.721 MWhr/yr) is excess electricity. The capacity factor of the solar PV generator is 16.3%. The renewable energy fraction is 100% with 4.55 kWh/yr of unmet electric load. The system storage has a usable nominal capacity 118 kWh and 87.1 hours of autonomy, which is equivalent to almost four (4) days of backup time. In this system type, the solar PV generator is the sole energy source, with the battery serving as the backup at night, on cloudy days or both, as required.

4.7.1.2 System type 2A

Solar PV, wind and battery storage.

A solar PV generator rated 26.4 kW, 1 unit of 3.3 kW of the wind turbine generator, 15 strings of battery storage and 4.12 kW of system converter make up this system type. The wind generator is the dominant cost component accounting for about 32.1% of the total system cost. The NPC, LCOE, and operating cost of the system are $89,512.41, $0.5850/kWh, and $1,465.86/yr respectively. The electricity produced by this system type is shown in Figure 4.12(a), as described by the cost summary plot in Figure 4.12(b)., it is worthy of note that although the wind turbine generator accounts for the highest cost percentage for the system, it contributes only 5,862 kWh/yr (19.5%) to the total electricity in a year. Hence from a cost-benefit perspective, the electricity output of the wind generator does not justify the cost incurred.

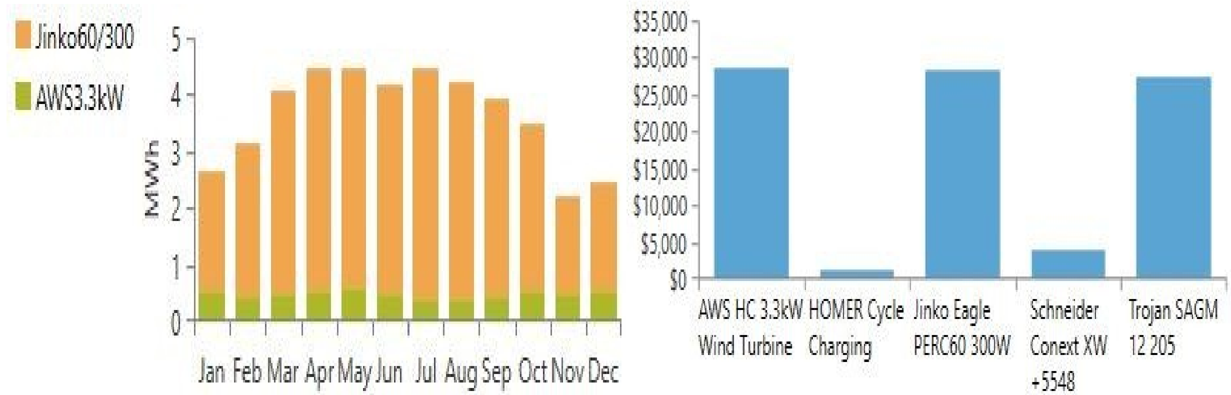

(a) (b)

Figure 4.12. (a) Monthly electricity production for system type 2A, (b) Cost summary for system type 2A showing cost contribution of system components.

This system generates 37.756 MWh/yr of electricity of which 11.837 MWh/yr is consumed by the AC electric motor and, 70.4% of total generation (30.707 MWhr/yr) is excess electricity, available for charging the battery. The capacity factor of the wind generator is 20.3%. The renewable energy fraction is 100% with 0.0759 kWh/yr of unmet electric load. The battery storage system has a usable nominal capacity of 110 kWh and 81.6 hours of autonomy, which is equivalent to over 3 days of backup time. Hybrid renewable generation is adopted in this system type as solar PV, and wind turbines are deployed as dual sources of energy. When the wind speed is below the cut in or rated speed, at night or on cloudy days, the excess generated electrical energy retained in the battery storage system is made available (after inversion) to drive the AC electric motor.

4.7.1.3 System type 3A

Wind generator and battery storage.

Four (4) units of 3.3 kW of the wind turbine generator, 20 strings of battery storage and a 3.80 kW of system converter, make up this system type. In this system type, the wind is the sole power resource, as shown in Figure 4.13., with the wind generators alone accounting for about 72.96% of the total system cost. The net present cost (NPC), levelized cost of energy (LCOE) and annual operating cost are $157,555.10, $1.03/kWh and $1,862.76/yr respectively.

Figure 4.13. Monthly electricity production for system type 3A.

This system generates 23. 446 MWhr/yr of electricity of which 11.836 MWh/yr is consumed by the AC electric motor and 43.6% of total generation (10.227 MWhr/yr) is excess electricity, which is available to charge the battery. The capacity factor of the wind generator is 20.3%. The renewable energy fraction is 100% with 0.669 kWh/yr of unmet electric load. The system has a usable nominal capacity 147 kWh and 109 hours of autonomy, which is equivalent to almost 5 days of backup time. The wind turbine is the sole source of energy in this configuration. When the wind speed is below the rated speed, the battery storage system discharges, delivering its stored energy for artificial lift.

4.7.2 Scenario B: Continuous/Uninterrupted Pumping

A total of 1,538 solutions were simulated, 739 were feasible, and 799 were infeasible due to the capacity shortage constraint. Of the 358 omitted, 135 lack a converter, 37 have an unnecessary converter, and 180 have no source of power generation. The simulation results for candidate configurations of continuous production is shown in Table 4.4(a) and 4.4(b), ranked from the lowest to the highest system cost. The system structure for continuous pumping is shown in Figure 4.14 with a daily energy consumption of 60.11 kWh/d and a peak load of 4.55 kW.

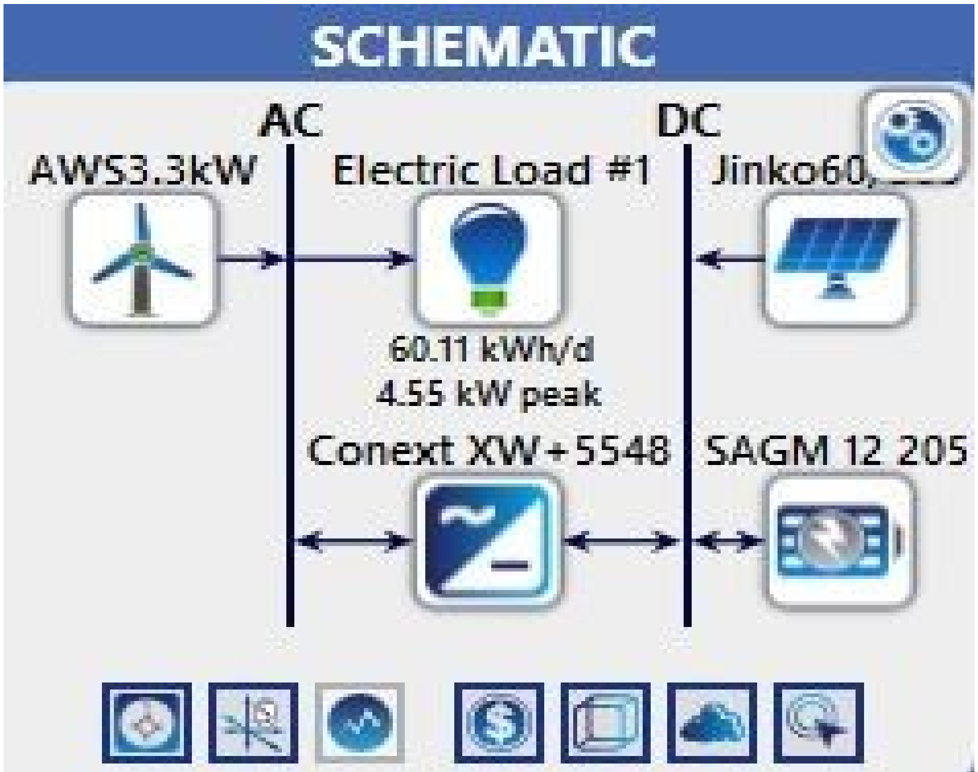

Figure 4.14. System structure showing integrated components in HOMER

(For continuous pumping).

Table 4.4. (a) Simulation results by system types or categories for continuous production,

(b) Cost of system types for continuous production.

Architecture				
Jinko60/300 (kW)	AWS3.3kW	SAGM 12 205	Conext XW+5548 (kW)	Dispatch
50.8		128	4.89	CC
50.8	1	104	4.67	CC
	6	160	6.54	CC

Cost				System	
NPC ($)	COE ($)	Operating cost ($/yr)	Initial capital ($)	Ren Frac (%)	Total Fuel (L/yr)
$130,774	$0.461	$3,163	$89,883	100	0
$145,151	$0.512	$3,056	$105,644	100	0
$255,377	$0.901	$3,095	$215,369	100	0

4.7.2.1 System type 1B

Solar PV and battery storage

A solar PV generator rated 50.8 kW, 32 strings of battery storage and a system converter of 4.89 kW make up this system type. As in system type 1A, the battery storage is the dominant cost component in this system type, accounting for 54.1% of the total system cost. The NPC, LCOE and operating cost are $130,773.60, $0.4614/kWh, $3,163.08/yr respectively. The plot of monthly electricity distribution is shown in Figure 4.15.

Figure 4.15. Monthly electricity production for system type 1B.

This system generates 72.70 MWh/yr of electricity of which 21.926 MWh/yr is consumed by the AC electric motor, 64.5% of total generation (46.862 MWhr/yr) is excess electricity. The capacity factor of the solar PV generator is 16.3%. The renewable energy fraction is 100% with 14.0 kWh/yr of unmet electric load. The battery storage system has a usable nominal capacity of 235 kWh and 94.0 hours of autonomy, which is equivalent to about 4 days of backup time. In this system type, the solar PV generator is the sole energy source, with the battery serving as the backup at night or on cloudy days as required.

4.7.2.2 System type 2B

Solar PV, wind and battery storage

A PV generator rated 50.8 kW, 1 unit of 3.3 kW wind turbine generator, 26 strings of battery storage and 4.67 kW of system converter, make up this system type. Unlike in system type 2A, here the battery is the dominant cost component accounting for about 39.0% of the total system cost. The NPC, LCOE, and operating cost of the system are $145,150.50, $0.5118/kWh, $3,056.04/yr respectively. The plot of monthly electricity production is shown in Figure 4.16.

Figure 4.16. Monthly electricity production for system type 2B.

This system generates 78.562 MWh/yr of electricity of which 21.940 MWh/yr is consumed by the AC electric motor, and 68.2% of total generation (53.598 MWhr/yr) is excess electricity, available for charging the battery storage. The capacity factor of the wind generator is 20.3%. The renewable energy fraction is 100% with 0 kWh/yr of unmet electric load (no unmet load). The battery storage system has a usable nominal capacity of 191 kWh and 76.3 hours of autonomy, which is equivalent to over 3 days of backup time. The effect of variability in weather conditions is reduced as the presence of two power generation sources ensures that the unmet load and capacity storage are both minimized compared to system type 1B.

4.7.2.3 System type 3B

Wind generator and battery storage

Six (6) units of the wind turbine generator, 40 strings of battery storage and a 6.54 kW of system converter make up this system type. The wind generators alone account for about 67.5% of the total system cost with net present cost (NPC), levelized cost of energy (LCOE) and annual operating cost of $255,376.90 $0.9011/kWh and $3,094.82/yr respectively. The plot of monthly electricity distribution is shown in Figure 4.17.

Figure 4.17. Monthly electricity production for system type 3B.

This system generates 35.17 MWhr/yr of electricity of which 21.922 Mwh/yr is consumed by the AC electric motor, and 39.4% of total generation (10.474 MWhr/yr) is excess electricity, which is available to charge the battery. The capacity factor of the wind generator is 20.3%. The renewable energy fraction is 100% with 17.9 kWh/yr of unmet electric load. The battery storage system has a usable nominal capacity 420 kWh and 117 hours of autonomy, which is equivalent to almost 5 days of backup time. For this system type, the wind turbine is the primary source of energy, while the battery storage system stores energy for petroleum production, when the wind speed is either below the cut in or rated speed.

4.8 Discussion of Results

There are several conditions that could affect the decision on the system type to be chosen as optimal. Several factors could play a significant role in determining the ideal system type. The considerations could include the peculiarities of the petroleum production environment (rural, urban, sub-urban), level of remoteness, the presence of additional loads (apart from the ones imposed on the pump due to produced hydrocarbon) and availability of cheap diesel, natural gas or associated gas to power an internal combustion engine. It is also important to note that in this design, the unmet load is the ultimate criterion in choosing between two equally feasible architectures and not the cost of the system alone.

The least-cost configuration for intermittent and continuous pumping are shown in Table 4.5.

Considering 100% renewable energy fractions with three (3) system configurations, and six (6) scenarios as shown in Figure 4.18. :

- Type 1 (solar photovoltaic + battery storage),
- Type 2 (solar photovoltaic + wind turbine + battery) storage) and
- Type 3 (wind turbine + battery storage).

Type 3 will be ignored in the analysis as it has the highest overall cost of the feasible system configurations. Considering: Intermittent pumping: (1A, 2A) and Continuous pumping: (1B and 2B).

(a) Net present Cost for each architecture
(e) Power Consumption for each architecture
(b) LCOE for each architecture
(f) Excess generated electricity for each architecture
(c) Operating cost for each architecture
(g) Unmet load for each architecture

Figure 4.18. (a) to (e) Compares key indices for continuous and intermittent pumping for the six (6) 100% renewable architectures.

Table 4.5 Comparing least cost alternatives for Intermittent (type A) and Continuous (type B) pumping: system type 1 (solar photovoltaic + battery storage).

Solar PV	**Type 1A**	**Type 1B**	**Unit**
Rated capacity	27.3	50.8	kW
Mean output	4.45	8.30	kW
Mean daily Output	107	199	kWh/d
Capacity factor	16.3	16.3	%
Hours of operation	4,377	4,377	hrs/yr
PV penetration	330	331	%
Battery			
Number	64	128	(4bt/string)
String in parallel	16	32	Strings
Bus voltage	48	48	V
Nominal capacity	168	336	kWh
Usable nominal capacity	118	235	kWh
Energy in	3,860	15,244	kWh/yr
Energy out	3,294	12,982	kWh/yr

The following can be inferred from Figure 4.18. :

(a) Scheduling the load (changing the load cycle time or the number of hours the electric motor prime mover is run), has no effect on which configuration type is considered optimal as system type 1 (solar photovoltaic + battery storage) has proven to be the least cost consideration, irrespective of load scheduling as shown in Figure 4.18(a).

(b) For the least cost option, if the pumping transitions from intermittent to continuous (type 1A to type 1B), the change in the levelized cost of energy is negligible [Figure 4.18(b)], but the net present cost and operating cost of the well are increased by 101% and 140% respectively (by over 100%) as shown in Figure 4.18(a) and 4.18(c).

(c) Using the electrical energy and system cost criteria to compare the performance of system type 1 and 2, the total production, consumption, excess electricity, unmet electricity and capacity storage are all observed to increase with increase in daily pumping hours for both architectures 1 and 2, except for 2B (continuous pumping with solar photovoltaic, wind turbine and battery storage) where the levelized cost, unmet load and capacity storage reduce with increase in pumping hours.

(d) It can be observed from Figures 4.18(f)., 4.18(g). and 4.18(h). respectively that (due to hybrid power generation), system type 2 results in a higher level of excess electricity, a lower amount of unmet load and lower capacity storage compared to system 1. All these advantages come at a premium of higher net present cost and higher levelized cost of energy).

(e) It is important to note that continuous production with hybrid renewable power generation (2B) is seen to have the least amount of unmet load (0 kWh/yr) for all the system types and pumping configurations. Transitioning from type 1B to 2B also leads to a cut in operating cost of the system.

In general, for both intermittent and continuous pumping schedules. Comparing system 1 and 2: system type 1, **minimizes** [net present cost, levelized cost of energy, total production, consumption and excess electricity], while system type 2, **minimizes** [unmet load, capacity storage].

Generally, the system cost of type 2 is significantly higher than those of type 1, but instead of merely considering the system cost alone, the total unmet load and unmet load fraction are jointly used as the ultimate criteria for selection. The hybrid generator option: type 2, will be most reliable and hence most preferred (type 2A for intermittent pumping and type 2B for continuous pumping). This makes technical and economic sense, especially in wells where the production due to the extra pumping hours can justify the higher system cost incurred over the life of the well.

Key technical indices are used to compare continuous pumping with intermittent pumping for the proposed system configuration, as shown in Table 4.6.

Table 4.6 Proposed feasible solutions for intermittent and continuous pumping.

Solar PV	**Type 2A**	**Type 2B**	**Unit**
Rated capacity	27.3	50.8	kW
Mean output	4.45	8.30	kW
Mean daily output	107	199	kWh/d
Capacity factor	16.3	16.3	%
Hours of operation	4,377	4,377	hrs/yr
PV penetration	330	331	%
Wind			
Total rated capacity	3.30	3.30	kW
Mean output	0.669	0.669	kW
Total production	5,862	5,862	kWh/yr
Capacity factor	20.3	20.3	%
Hours of operation	7,329	7,329	hrs/yr
Wind penetration	49.5	26.7	%
Battery			
Number	64	128	(4bt/string)
String in parallel	16	32	Strings
Bus voltage	48	48	V
Nominal capacity	168	336	kWh
Usable nominal capacity	118	235	kWh
Energy in	3,860	15,244	kWh/yr
Energy out	3,294	12,982	kWh/yr

4.9 Sensitivity analysis

The architectures obtained are all 100% renewable; hence daily solar radiation and average wind speed will be used as sensitivity variables to examine the response of the key indices (system cost parameters and unmet load) to maximum and minimum variations from the average value. The optimization process is repeated for the system architectures. The daily solar radiation varies sharply from 0.93 kWh/m^2/day to 6.38 kWh/m^2/day, while the average wind speed varies from 5.10 m/s to 6.32 m/s. The results are shown in Table 4.7.

Table 4.7 Showing variation in NPC, COE and unmet load (%) due to variation in daily solar radiation and average wind speed. (The italicized section is the hybrid RES: type 2B).

Solar Radiation (SR)	**Wind Speed (WS)**	**Photovoltaic Power (PV)**	**Wind Turbine Power (WT)**	**Battery Strings (BS)**	**Net Present Cost (NPC)**	**Cost of Energy (COE)**	**Unmet Load Percentage (Unmet)**
(kWh/m^2/day)	(m/s)	(kW)	(kW)	(St)	($1,000)	($)	(%)
0.93	*5.1*	*8.09*	*8*	*30*	*304*	*1.07*	*0.0494*
0.93	*5.7*	*20.5*	*5*	*29*	*229*	*0.81*	*0.0546*
0.93	*6.32*	*4.87*	*5*	*30*	*213*	*0.75*	*0.0583*
3.61	5.1	50.8	-	32	131	0.46	0.0636
3.61	5.7	50.8	-	32	131	0.46	0.0636
3.61	6.32	50.8	-	32	131	0.46	0.0636
6.38	5.1	25.2	-	27	98	0.35	0.0797
6.38	5.7	25.2	-	27	98	0.35	0.0797
6.38	6.32	25.2	-	27	98	0.35	0.0797

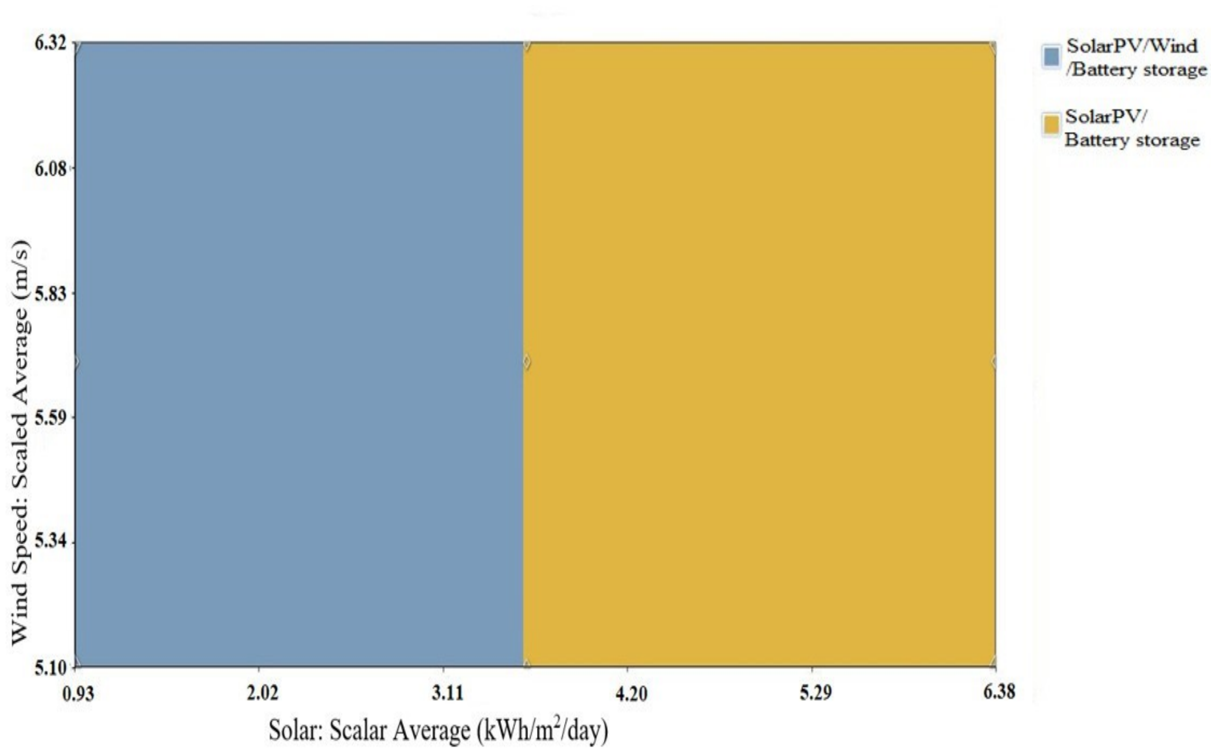

Figure 4.19. Optimization system type plot showing type 1 and type 2 architectures for respective average wind speed and daily solar radiation.

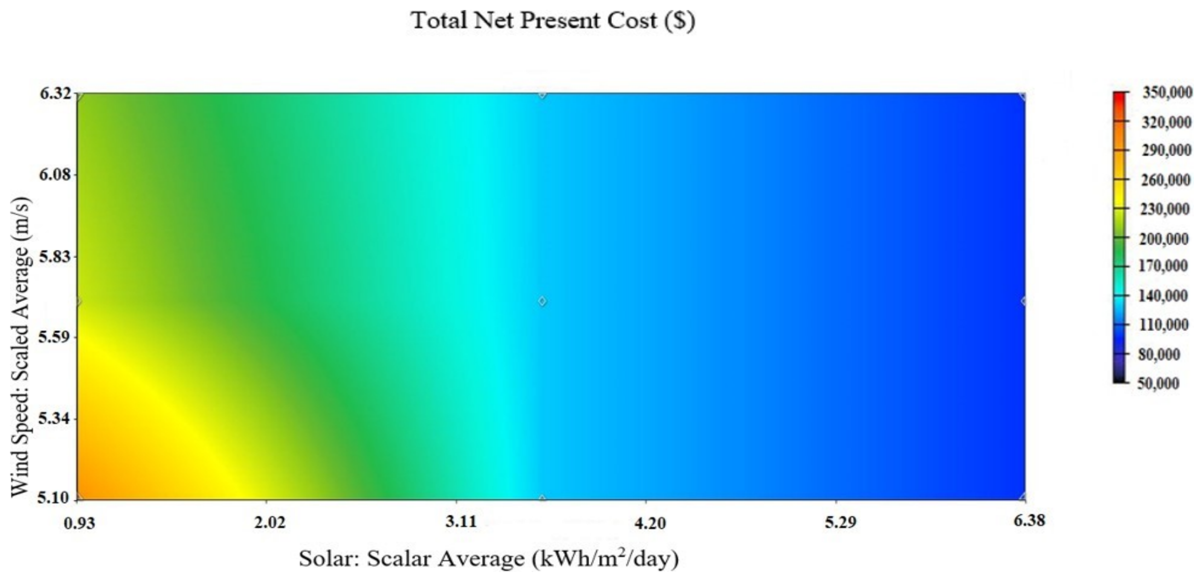

Figure 4.20. Surface plot showing the sensitivity of total net present cost to variations in average wind speed and average daily solar radiation.

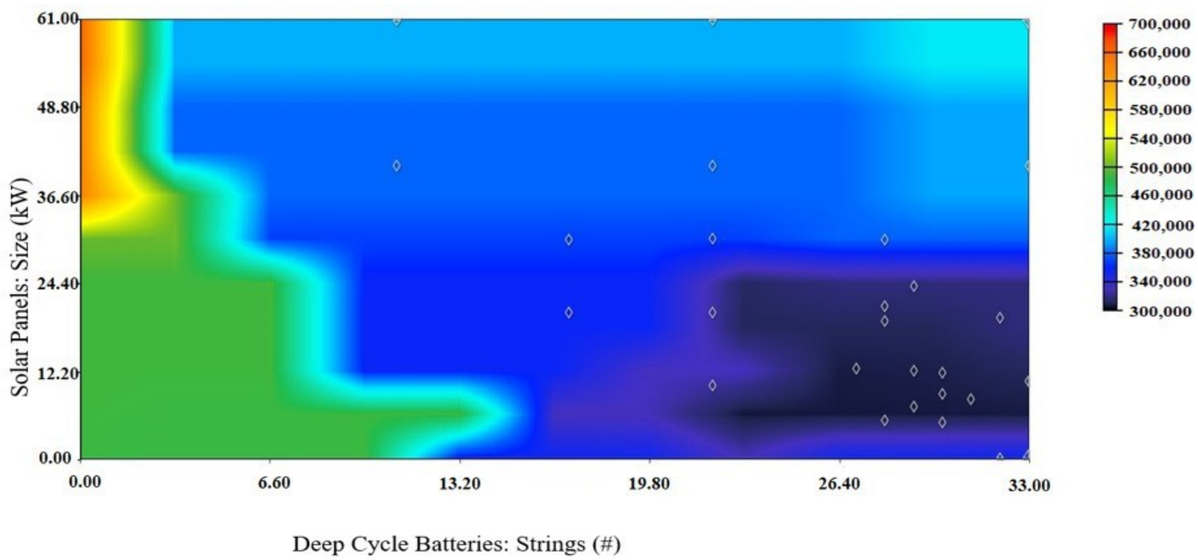

Figure 4.21. Optimization surface plot showing least cost combinations of solar PV generators (kW) and battery storage (number of strings) for the cheapest/ least cost configuration (type 1A).

The results from the sensitivity analysis is shown in Table 4.7 and in the optimization system type plot in Figure 4.19. It can clearly be inferred that for the italicized section, below the average daily solar radiation (3.61 kWh/m2/day), the hybrid renewable energy system (solar photovoltaic, wind turbine, and battery storage: type 2) is the most preferred architecture with the least unmet load percentage and highest system NPC and LCOE. Above the mean daily solar radiation (3.61 kWh/m2/day), type 1 (solar photovoltaic and battery storage) is the preferred architecture with the least system cost and relatively higher unmet load than type 2.

The sensitivity analysis from Table 4.7 and the surface plot in Figure 4.20 jointly demonstrate that the lowest system costs are incurred at the highest mean daily solar radiation and average wind speeds. But as can be inferred from Table 4.7, the unmet load percentage is also the highest. This can be explained by the fact that type 1 is the most feasible architecture under such conditions and is independent of the wind speed.

From Table 4.7 and Figure 4.21., it can be inferred from the sensitivity analysis and the optimization surface plot, that the cost of the least-cost system (type 1), is minimized for photovoltaic systems rated at most 25.2 kW, with battery sizes of at most 27 strings.

$$Least\ cost\ [type\ 1]\ =\ at\ most\ [25.2kW\ of\ PV, 27\ strings]$$

Such a system is seen to settle at an estimated net present cost of $98,189.05 and a levelized cost of energy of $0.3465.

4.10 Conclusions

Analysis of the six (6) scenarios considered in Figure 4.18. leads to the conclusion that irrespective of the system architecture deployed, intermittent pumping is seen to be cheaper than continuous pumping for all the indices considered, and for all configurations observed except for continuous pumping with solar photovoltaic, wind turbine and battery storage (type 2B) for which the LCOE is lower than that of type 1, and which is proposed as the most feasible configuration. Type 2B is chosen as the most feasible solution for continuous pumping with 0 kWh/yr of unmet load, capacity storage of 0.56 kWh/yr, the net present cost of $145,150.50, levelized cost of energy of $0.51/kWh and an operating cost of $3,056.04/yr. In this case study well and for the location chosen, although the hybrid renewable system (type 2) has a higher net present and higher levelized cost of energy than type 1, continuous pumping with solar PV, wind and battery system has been demonstrated to have the least unmet load and capacity storage. Hybrid generation (type 2: solar PV, wind and battery storage) has a very clear advantage over other configurations, as demonstrated by the sensitivity analysis in Table 4.7, and plots in Figure 4.18(g). and 4.18(h). This is because the available intermittent energy sources are harnessed economically (for both intermittent and continuous pumping) and are thus optimal for reliably driving the artificially lifted well. In this way, the battery storage system provides extra energy for petroleum production when it is cloudy or nighttime.

4.11 Acknowledgements

The authors would like to appreciate the Tertiary Education Trust Fund (TETFUND) of the Federal Government of Nigeria, for funding this research. We acknowledge the support of Memorial University of Newfoundland for the enabling environment to carry out this research.

4.12 Conflicts of Interest

The authors declare that there are no conflicts of interests in the execution and publication of this work.

4.13 References

[1] Aguilera, R.F. and Radetzki, M., 2015. The price of oil. Cambridge University Press.

[2] Armacanqui, J.S., Eyzaguirre, L., Lujan, C. and Rodríguez, J., 2016, October. Managing Oil Fields in a Low Oil Price Environment. In SPE Latin America and Caribbean Heavy and Extra Heavy Oil Conference (p. D021S011R001). SPE.

[3] Saadawi, H., 2019, March. Application of renewable energy in the oil and gas industry. In SPE Middle East Oil and Gas Show and Conference (p. D022S060R002). SPE.

[4] Shedid, S.A., 2009, April. Effects of Subsurface Pump Size and Setting Depth on Performance of Sucker-Rod Artificial Lift—A Simulation Approach. In SPE Oklahoma City Oil and Gas Symposium/Production and Operations Symposium (pp. SPE-120681). SPE.

[5] Guillory, R., Wan Razali, W.A.A., Masoudi, R., Singh, R. and Ahmad, N.A., 2019, March. Total Well Management: Maximising Well Lifecycle Value–A Regulator Perspective. In International Petroleum Technology Conference (p. D011S015R007). IPTC.

[6] Muehlenbachs, L., 2017. 80,000 inactive oil wells: A blessing or a curse? SPP Research Paper No, 10(3).

[7] Temizel, C., Irani, M., Canbaz, C.H., Palabiyik, Y., Moreno, R., Balikcioglu, A., Diaz, J.M., Zhang, G., Wang, J. and Alkouh, A., 2018, December. Technical and economical aspects of use of solar energy in oil & gas industry in the Middle East. In SPE International Heavy Oil Conference and Exhibition (p. D022S028R001). SPE.

[8] van Heel, A.P., Van Wunnik, J.N., Bentouati, S. and Terres, R., 2010, April. The impact of daily and seasonal cycles in solar-generated steam on oil recovery. In SPE EOR Conference at Oil and Gas West Asia (pp. SPE-129225). SPE.

[9] Poythress, M. and Rowlan, L., 2008, June. Low-Volume Pumping Systems: Moving Gallons to Produce Thousands. In SPE Unconventional Resources Conference/Gas Technology Symposium (pp. SPE-115077). SPE.

[10] Dave, M.K. and Ghareeb Mustafa, M., 2017, November. Performance evaluations of the different sucker rod artificial lift systems. In SPE Symposium: Production Enhancement and Cost Optimisation (p. D011S002R004). SPE.

[11] Feng, Z.M., Tan, J.J., Li, Q. and Fang, X., 2018. A review of beam pumping energy-saving technologies. Journal of Petroleum Exploration and Production Technology, 8, pp.299-311.

[12] Di Tullio, M.T. and Marfella, F., 2018, November. Enhanced sucker rod pumping model: a powerful tool for optimizing production, efficiency and reliability. In SPE Middle East Artificial Lift Conference and Exhibition (p. D022S020R002). SPE.

[13] National Stripper Well Association (2019) Stripper Well Facts. Available at: http://nswa.us/custom/showpage.php?id=25 (Accessed: 02 October 2019).

[14] Hicks, A.W., 1986, April. Using fiberglass sucker rods in deep wells. In SPE Deep Drilling and Production Symposium (pp. SPE-14974). SPE.

[15] Takacs, G., 2015. Sucker-rod pumping handbook: production engineering fundamentals and long-stroke rod pumping. Gulf Professional Publishing.

[16] Skinner DR (1984) Efficient Use of Electric Power in Production Operations. Society of Petroleum Engineers.

[17] Johnson, J.E., 1988. Electrical savings in oil production. SPE production engineering, 3(04), pp.625-628.

[18] Normals, C.C., 2016. Normals 1981-2010 Station Data. Electronic Document [online]

[19] CBC News (2019) Alberta's 'Gas City' to shut down 2,000 wells, laying off up to 100 people. Available at: https://www.cbc.ca/news/canada/calgary/medicine-hat-natural-gas-wells-close-1.5286693 (Accessed: 04 October 2024).

[20] Surface meteorology and Solar Energy (SSE) Data Archive (2019) POWER projects Data Sets. Available at: https://power.larc.nasa.gov (Accessed: 03 October 2019).

[21] Lambert, T., Gilman, P. and Lilienthal, P., 2006. Micropower system modeling with HOMER. Integration of alternative sources of energy, 1(1), pp.379-385.

[22] Aziz, A.S., Tajuddin, M.F.N., Adzman, M.R., Ramli, M.A. and Mekhilef, S., 2019. Energy management and optimization of a PV/diesel/battery hybrid energy system using a combined dispatch strategy. Sustainability, 11(3), p.683.

[23] Aziz, A.S., Tajuddin, M.F.N., Adzman, M.R., Azmi, A. and Ramli, M.A., 2019. Optimization and sensitivity analysis of standalone hybrid energy systems for rural electrification: A case study of Iraq. Renewable energy, 138, pp.775-792.

[24] Baniasad Askari, I., Baniasad Askari, L., Kaykhah, M.M. and Baniasad Askari, H., 2014. Optimisation and techno-economic feasibility analysis of hybrid (photovoltaic/wind/fuel cell) energy systems in Kerman, Iran; considering the effects of electrical load and energy storage technology. International Journal of Sustainable Energy, 33(3), pp.635-649.

Chapter 5

OPEN SOURCE IOT-BASED SCADA SYSTEM FOR REMOTE OIL FACILITIES USING NODE-RED AND ARDUINO MICROCONTROLLERS

Co-authorship statement

This chapter achieves research objectives 4 of this thesis as stated in Section 1.3. It presents the open-source IoT-based SCADA system for remote oil facilities using node-red and Arduino microcontrollers with a focus on designing and implementing a low-cost, open-source IoT-based SCADA system for remote monitoring and control of oil and gas facilities using Node-RED and Arduino microcontrollers. This research develops a web-based graphical user interface (GUI) using Node-RED for real-time visualization, data logging, and remote access to sensor data and control functions. This study integrates multiple sensors (temperature, flow rate, water level, voltage, current, position, accelerometer, distance) and actuators (motors) into the SCADA system for comprehensive monitoring and control of oil production processes. This study implement a secure remote access solution for the SCADA system using port forwarding, network address translation (NAT), and HTTP basic access authentication with Nginx . It evaluates the performance and reliability of the proposed IoT-based SCADA system in monitoring critical operational parameters and enabling remote control of oil production equipment.

I (Charles Aimiuwu Osaretin) am the principal author and contributed to Conceptualization, Methodology, Technical and Economic analysis, Writing of Original Draft and Editing of the research manuscript. The research in this chapter was supervised by Dr. M. Tariq Iqbal, and Dr. Stephen Butt. The supervisors contributed to the conceptualization and methodology. They also supervised the entire chapter, and reviewed and corrected the research manuscript. The work in

this Chapter has been published in the 2020 11th IEEE Annual Information Technology, Electronics and Mobile Communication Conference (IEMCON), Vancouver, BC, Canada, December 2020, ISBN:978-1-7281-8416-6, ISSN: 2644-3163, Article ID 229373697, 5 pages, https://doi.org/10.1109/IEMCON51383.2020.9284826.

Abstract

An open-source and low-cost Supervisory Control and Data Acquisition System based on Node-RED and Arduino microcontrollers is presented in this study. The system is designed for monitoring, supervision, and remotely controlling motors and sensors deployed for oil and gas facilities. The Internet of Things (IoT) based SCADA system consists of a host computer on which a server is deployed using the Node-RED programming tool and two terminal units connected to it: Arduino Uno and Arduino Mega. The Arduino Uno collects and communicates the data acquired from the temperature, flow rate, and water level sensors to the Node-Red on the computer through the serial port. It also uses a local liquid crystal display (LCD) to display the temperature. Node-RED on the computer retrieves the data from the voltage, current, rotary, accelerometer, and distance sensors through the Arduino Mega. Also, a web-based graphical user interface (GUI) is created using Node-RED and hosted on the local server for parsing the collected data. Finally, an HTTP basic access authentication is implemented using Nginx to control the clients' access from the Internet to the local server and to enhance its security and reliability.

5.1 Introduction

SCADA stands for Supervisory Control and Data Acquisition. It is a general term used to refer to groups of hardware and associated software devices that enable the supervision and control of operational processes, typically in manufacturing plants and industrial settings. The collection and aggregation of data are followed by processing, logging, and visualization of the collected data. The instrumentation and control of critical operational parameters in most oil and gas production processes are made possible by deploying field instrumentation devices such as transmitters, receivers, sensors, actuators, pumps, and valves. The collection of data and communication of corrective action to field instrumentation devices is made possible by the deployment of microprocessors/microcontrollers in the SCADA system. Programmable logic controllers (PLC) and terminal units (TUs) help to route the collected data through communication channels to the central SCADA computers called master terminal units (MTUs). The software on MTUs provides a suitable human-machine interface (HMI) for analysis, interpretation, and visualization of process variables. Indicators and alerts also help operators to identify and react to trigger events [1-4]. Traditional SCADA deployed in oil field operations is generally limited in terms of upgrading, programmability, and efficiency of network administration. Regular SCADA systems are also relatively expensive, preventing their adoption in low-flow rate wells. The SCADA architecture employed in this work is a fourth-generation SCADA based on the Internet of Things framework. By deploying software and electronics to sensors embedded in critical processes, distributed computing resources in the IoT-based SCADA can aggregate, log, process, and visualize the data collected either on-site or remotely using internet connectivity. The core of the IoT-based SCADA server proposed in this study is the Node-RED server deployed on a local computer [5-7].

5.2 Literature Review

Production from oil wells driven by artificial lift is complicated and requires instrumentation, metering, supervision, and control. The level of fluid produced requires close monitoring to optimize fluid level in the tank between the upper and lower limit and hence minimize or prevent leakages, spills, and environmental pollution [8]. Flowrate monitoring also helps to estimate the gross volume of produced fluids and to compare with flowrates recorded downhole for early detection of wax formation. Measurement and control of temperature at different nodes in the production process directly impacts the phase behavior and flow assurance of the produced fluids. Critical interventions, such as chemical injection, dewaxing, heating, and production adjustment, require temperature monitoring for flow assurance and asset integrity [9]. Industrial automation and IoT technology provide a sustainable, secure, and scalable alternative for low-cost monitoring, supervision, and control of several operational parameters in remote oil and gas operations [10-12]. Data acquisition, data logging, aggregation, and visualization are generally required for making important decisions, hence the adoption of SCADA systems.

In terms of licensing, there are two classes of SCADA, proprietary and open source system. In open source, the system is entirely built from scratch using modularized and often freely licensed applications. It is beneficial because adding and replacement of components is cheaper and more manageable without the need for special expertise and training. By using open standards, interoperability is enhanced, and the system lifecycle cost can be reduced. On the contrary, a proprietary or “closed” system is developed and managed by a vendor, with upgrade and modifications dependent on the availability of the specific vendor and the license stipulating the terms and conditions of service [13].

Although cloud server architecture is increasingly deployed for hosting, logging, aggregation, storage, supervision, and control of data received by embedded sensors, cybersecurity is a major concern, as leveraging of cloud architecture exposes the system to cyberattacks with a significant risk of data loss, data corruption or disruption of service [12]. This work adopts a local on-premises server running Node-RED for collection, aggregation, logging, monitoring, and control of data.

Remote access to the local server is controlled by setting up an authentication request for username and password. The internet protocol (IP) address of the server is also concealed from the client by using a reverse proxy server called Nginx. It enhances the security and reliability of the local server; hence by running the application on an on-premise machine, the user can take advantage of most of the required features of cloud-based architecture without long term subscription costs and reduced risk of cyberattacks [14-16].

5.3 Experimental Design of Proposed IoT-Based SCADA System

The case study is a low flowrate oil well driven by an electric motor and powered by solar energy. Figure 5.1 shows the schematic of the project in the case study. The scenario consists of a single well artificially lifted with a jack pump. In this scenario, the produced fluid is collected and accumulated into a single tank. The essential nature of oil production requires continuous site monitoring to acquire, log, and process the data so that timely intervention can ensure continuous and optimal operation.

Accurate tracking of the flowrate from the tubing and monitoring of the tank level is also needed for logging daily, monthly, and annual production from the well of interest. Logging and appropriately tracking the fluid flowrate could lead to early detection of sand and wax in the tubing. The temperature of the produced fluid at the wellhead and the storage tank will also need to be closely monitored to avoid wax formation and deposition. Maintenance planning and early fault detection are also considerations that justify this research for remote low flowrate oil wells.

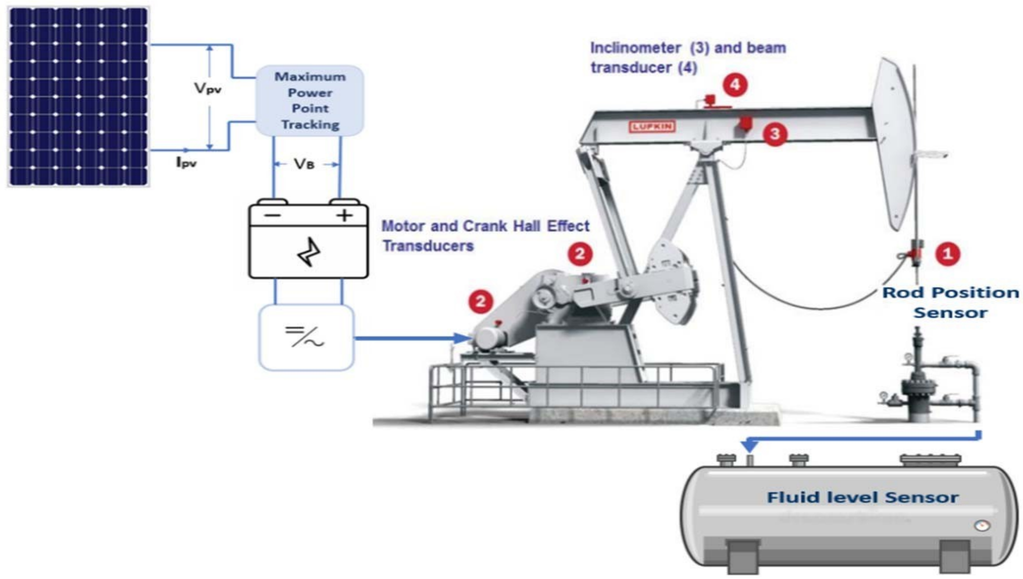

Figure 5.1. Schematic diagram of a case study showing elements of the proposed system.

The IoT-based open source SCADA system consists of three subsystems, a master terminal unit and two terminal units, as shown in Figure 5.2.

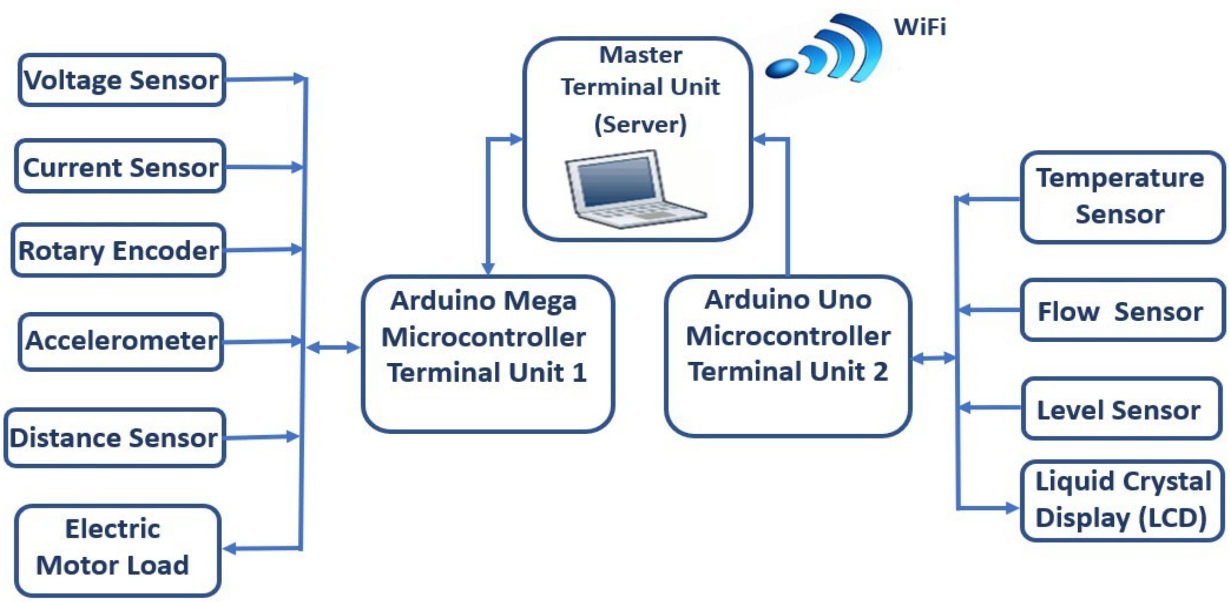

Figure 5.2. Schematic diagram of the proposed IoT-based SCADA System

The design and implementation of the SCADA system entail hardware and software selection. At the subsystem level, the sensor hardware is connected to the Arduino microcontrollers through base shields and breadboards; each sensor is then programmed in the Arduino integrated development environment (IDE). The decision to adopt two terminal units stems from the need for redundancy and the limitation of available input and output Arduino nodes in Node-RED.

In terms of read/write capability of the Arduino pins, Node-RED can manage digital and analog input and outputs, PWM, and servo over the Arduino pins via the use of both Firmata protocol and serial communication. The design methodology is to develop a web application that serves as both a dashboard and a graphical user interface (GUI), enabling an operator to remotely read, log, and monitor field sensor conditions on the web.

5.4 Implementation Methodology

The proposed SCADA system consists of a master terminal unit (MTU) and two other terminal units (TUs). Each instrumentation device is connected to the terminal units (Arduino microcontrollers) through base shields and breadboards. The Arduino microcontrollers collects the data and messages; acting as clients to the master terminal unit, which aggregates and processes the received data as a host. The USB connection is adopted as the communication channel between MTU and TUs. Serial communication is used in the Arduino Uno, while the Arduino Mega microcontroller implements the Firmata protocol in its firmware. Standard Firmata is used on the Arduino Mega for the connected accelerometer, distance, position, voltage, and current sensors. Therefore, using the Firmata protocol, the Node- RED application on the host server is able to interact with the Arduino Mega and hence directly access the respective pins of the Arduino Mega, altering the state, mode, and reading the desired signals from the connected sensors. The design methodology is to develop a web- based application that serves as a human-machine interface

(HMI) for visualization and enables an operator to remotely read, log, and monitor field sensor conditions over the Internet.

5.4.1 Master Terminal Unit (MTU)

The MTU is a local server that hosts the Node-RED application. It also logs and aggregates the sensor data. In addition to the dashboard, a graphic user interface is also hosted on the MTU for real-time visualization. The MTU controls and influences the operation of the terminal units, which are directly connected to the field instrumented devices (sensors, actuators, and on-site display). It logs, aggregates, and publishes sensor data from the IoT devices onto a web interface for visualization and interpretation.

5.4.2 Terminal Units (TUs)

The Arduino microcontrollers used in this work are both connected to the host server on the computer via a USB port. The Arduino microcontrollers model or represent the field-deployed terminal units. Arduino Mega is used as the first terminal unit (TU1). In this subsystem, the voltage, current, rotary, accelerometer, and distance sensors are all connected to the Arduino mega and read on the local server through Node-RED using Firmata. Also, the motors are controlled through Node-RED using Arduino nodes and Firmata. Arduino Uno is used as the second terminal unit (TU2). In this subsystem, an Arduino sketch is uploaded to read the fluid level, flowrate, and temperature sensors' values connected to the Arduino Uno, display them on the on-site LCD, and send them to the Node- RED local server via the serial port connection.

5.4.3 Voltage Sensor Module

The sensor uses the principle of a voltage divider to measure an input source voltage. Due to its simple design, the voltage sensor is low-cost, an output voltage (V_{out}) from 0 to 5V is produced and supported by the Arduino. In this work, the signal pin (S) of the voltage sensor is connected to the analog pin A9; the plus and minus sign pins are connected to the 5V and GND pins, respectively on the Arduino. GND and the input pins of the sensor are connected in parallel across the output of the solar panel to measure the PV output voltage.

5.4.4 ACS 723 Hall-Effect current sensor

ACS 723 is a high precision current sensor that is economical and fully integrated. The principle of "Hall-Effect" is employed. Such that when a single supply voltage V_{CC} of (4.5 to 5.5V) is applied across the inputs: IP+ and IP- (copper conduction path), a resulting current flow is produced, which generates a magnetic field. The magnetic is sensed by the Hall-effect IC to produce a proportional current.

Hence there is electrical isolation between the sensed circuit and the sensing circuit. A high-power sensed circuit arrangement with either DC or AC sources is thus compatibly sensed by a low power sensing circuit. The two input pins: V_{CC} and GND of this sensor are connected in series to the solar panel, while the output signal is read from the analog pin A_{10} on the Arduino Mega.

5.4.5 Rotary Position Sensor

The rotary sensor turns continuously and hence behaves like a potentiometer. It is also called the shaft encoder, enabling the precise measurement of motors' rotation, with less temperature drift and higher precision. The rotary sensor used in this work produces an analog signal value based on the angular displacement or motion of the shaft with an output voltage range from 0 to 5V DC. It is used as a position monitoring device in this work. The V_{CC} and the GND pins of this sensor go to the supply and ground of the Arduino Mega respectively, and the output signal is read by the analog pin A_8 of the Mega.

5.4.6 ADXL335 Accelerometer

The accelerometer works on the principle of the piezoelectric effect. The ADXL335 is a low cost, low power, and highly integrated 3-axis accelerometer that measures both static and dynamic acceleration. Static acceleration is the acceleration due to gravity, which enables the device to be used as a tilt sensor, hence enabling the device to detect free fall and measure tilt. In contrast, dynamic acceleration results from motion, vibration, or shock. In this work, the output signals are analog voltages from three pins X, Y, and Z, which are proportional to the acceleration and directly integrated with the analog pins A_{13}, A_{12}, and A_{11}, respectively.

5.4.7 SharpIR GP2Y0A21YK0F Distance Sensor

The Sharp infrared sensor is a low-cost distance measuring sensor unit of the analog output type. It is an integrated unit that combines an infrared emitting diode with a position-sensitive detector and signal processing unit. The detectable distance for this sensor ranges from 10 - 80cm. This device can also be used as a proximity sensor and outputs a voltage corresponding to the detection distance. The VCC and GND pin of this sensor is connected to the supply and ground of the Arduino Mega, respectively, while the V_{out} signal is read by the analog pin A_7 of the Mega.

5.4.8 DC Motor

The prime movers on the Arduino Mega (controller 1) are two DC gear motors. They are connected to the Arduino Mega via the Arduino motor shield, which models the variable frequency drive as implemented. The Arduino motor shield REV3 is based on the L298P motor controller chip and contains a dual full-bridge driver. The base shield has an operating voltage range of 0.5-12V and is powered by a 9V regulated power supply from the DC solar panel. The shield provides a suitable hardware interface between the Arduino mega and the DC motors for independent direction control, speed control, and braking. The pins D_3, D_9, and D_{12} of the Arduino Mega are used for driving Motor A, and the pins D_8, D_{11}, and D_{13} of the Arduino Mega are used for driving Motor B.

5.4.9 Fluid Level Sensor

The Grove fluid level sensor is a low power sensor that adopts the principle of capacitance and 2, 8-bit microcontroller units: ATTINY1616 MCUs. It consists of capacitive pads embedded on a printed circuit board and sealed to be completely waterproof. It measures the water level up to 10 cm. The analog input from the capacitors is converted into a digital signal by three (3) comparators It communicates over the I2C bus of the Arduino and is typically deployed in water level sensing applications. V_{CC} and the GND pins of this sensor go to the supply and ground of the Arduino Uno, respectively, and I2C serial communication is used.

5.4.10 Flowrate Sensor

The YF-S401 is a low-cost fluid flow sensor with a flow range of 0.3-6 L/min. It consists of a Hall-effect sensor and a fluid rotor enclosed in a plastic valve casing. Fluid flowing through the rotor causes a magnetic rotor to spin. The resulting rotating magnetic field cuts across a solenoid wire, causing a current flow and producing a voltage at the terminals of the Hall-effect sensor. The resulting voltage is proportional to the rate of flow of fluid across the rotor and hence serves as a suitable measure of flowrate. The output pulse width signal of the sensor is connected to the microcontroller. The signal output pin is connected to the digital pin D_3 and is programmed to trigger the interrupt 1 on the Arduino Uno to calculate the flowrate.

5.4.11 Temperature Sensor

The Grove temperature sensor V1.2 is used in this research. It has an operating voltage range from 3.3 to 5V and detects from -40 to 125ºC. The ambient temperature is detected by the chip. The resistance of a thermistor will decrease when the ambient temperature increases. This relationship is useful for predicting the ambient temperature with an accuracy of ± 1.5ºC and is suitable for the application. V_{out} signal is read by the analog pin A_0 of the Arduino Uno.

5.4.12 Liquid Crystal Display (LCD)

The LCD is used as a local display to show the temperature value. It is connected to the Arduino Uno via the I2C bus. The LCD is useful for reading and displaying temperature value on-site. Also, the flowrate and the water level can be displayed here.

5.4.13 Microcontroller 1 (Arduino mega)

The first terminal unit (TU1) is essentially Arduino Mega with Firmata through serial port connection to the Node-RED installed on the local server computer. The voltage, current, rotary encoder, accelerometer, and distance sensors are read by the microcontroller making five (5) field instrumented devices connected to TU1, as shown in Figure 5.2. Besides, the two motors, A and B, are connected to the Arduino Mega via a motor shield and are controlled through Node-RED.

5.4.14 Microcontroller 2 (Arduino Uno)

The second terminal unit, TU2, is an Arduino Uno with serial port connection to the Node-RED running on the local server. Four field instrumented devices are connected to TU1, including three sensors (temperature, flow, level) and a liquid crystal display (LCD). The advantage of using the serial connection in TU2 is that it permits the creation and execution of functions in the Arduino IDE, allowing for complex computations to be executed within the code and only the desired outputs printed over the serial ports.

5.5 Node-RED IoT Platform on the Local Server

The flow of data between interconnected devices is implemented in Node-RED, a web-based programming tool. By wiring nodes together, JavaScript objects and functions are created, flows are built and instantly deployed in Node-RED which consists of a node.js- based runtime. The graphic user interface (GUI) is also available in Node-RED and contains a dashboard with logs and charts for visualization of sensor data in real-time [14, 15]. The design methodology is to provision the web server on the local computer and make it accessible from the Internet, hence client requests to the Node-RED application running on the webserver are transferred from the external IP address, and port of the router to the internal IP address and port of the local server (port forwarding) and server responses are in turn transferred from the webserver to the router (network address translation, NAT) and on to the respective client. Hence port forwarding is implemented by mapping the internal IP address/port of the server to that of the router. This option exposes the Node-RED server on the Internet for remote access. After that, a basic access authentication is implemented using Nginx. Nginx requires the internet client to provide a username and password before access to the Node-RED on the server is granted hence improving the security, as shown in Figure 5.3 [17, 18]. The process flows for position, current, voltage, accelerometer, fluid level, flowrate, temperature, as well as electric motor controls and distance sensors are shown in Figures 5.4 to 5.9, respectively.

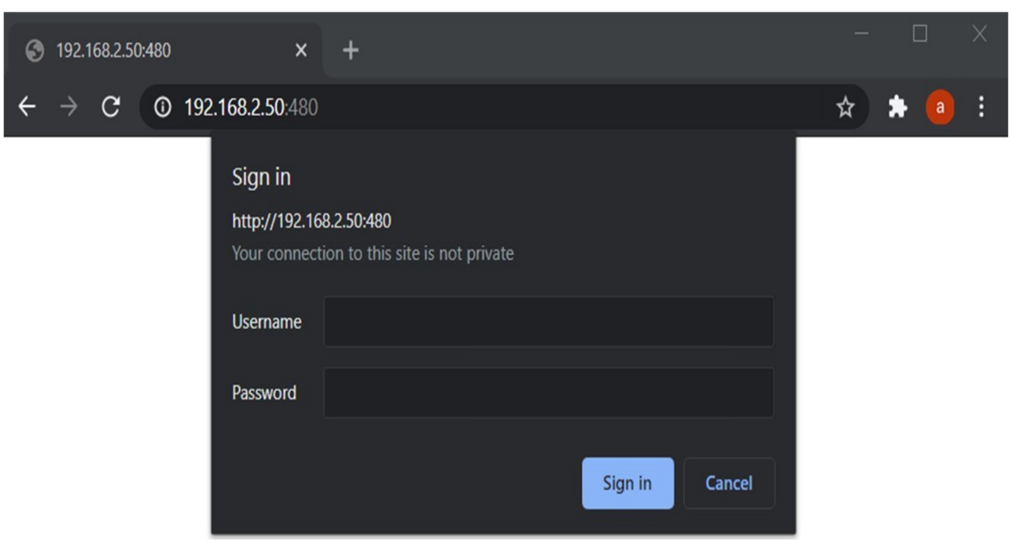

Figure 5.3. NGINX client access authentication page when logging in to the server.

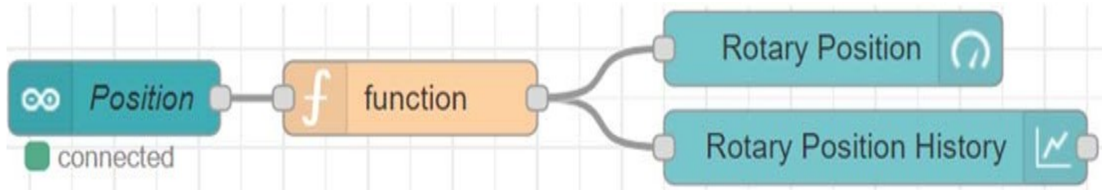

Figure 5.4. Process flow for the Position sensor.

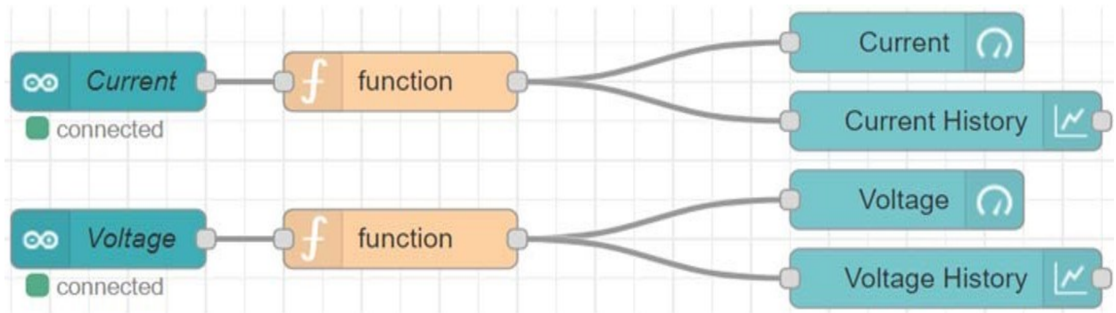

Figure 5.5. Process flow for the current and voltage sensor.

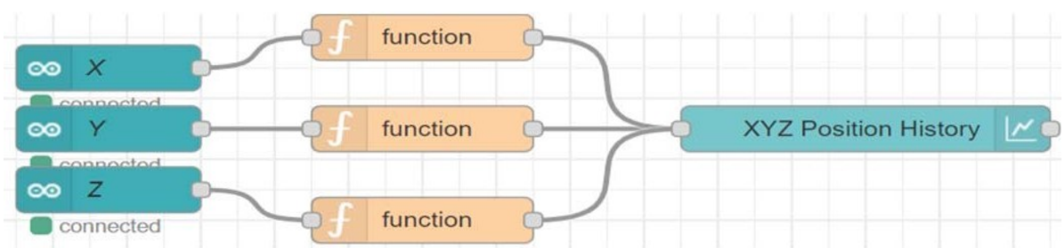

Figure 5.6. Process flow for the accelerometer.

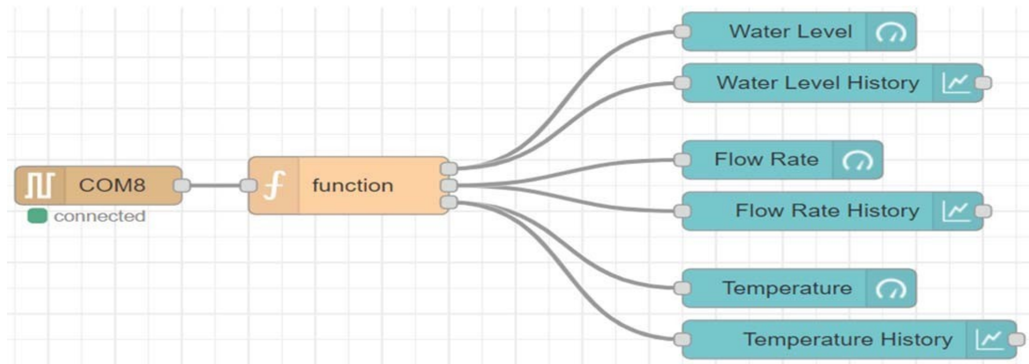

Figure 5.7. Process flow for the fluid level, flowrate and temperature sensor.

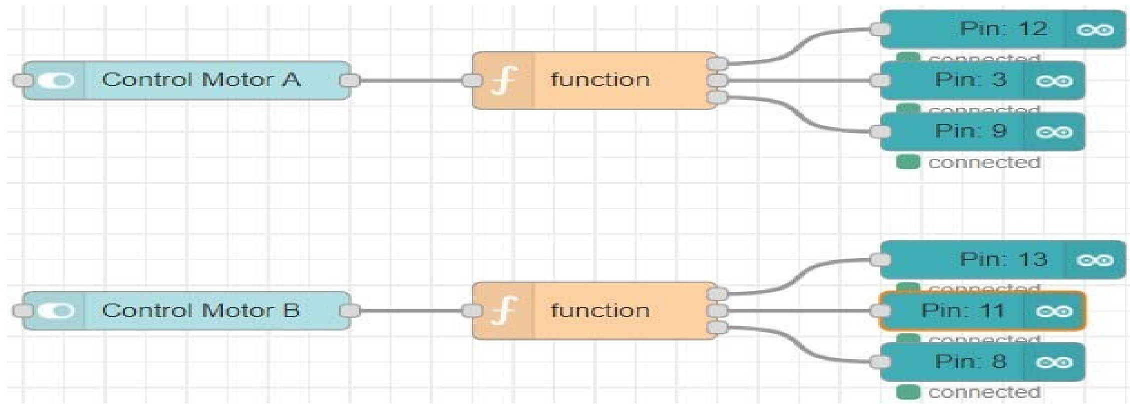

Figure 5.8. Process flow to control motors A and B.

Figure 5.9. Process flow for the distance sensor

5.6 Experimental Setup /Results

The experimental setup of the IoT-based SCADA hardware circuit is shown in Figure 5.10. The Arduino Mega and Uno are connected to the computer via USB ports. In this experimental setup, all the sensors, motors, and display are laid out according to Figure 5.2.

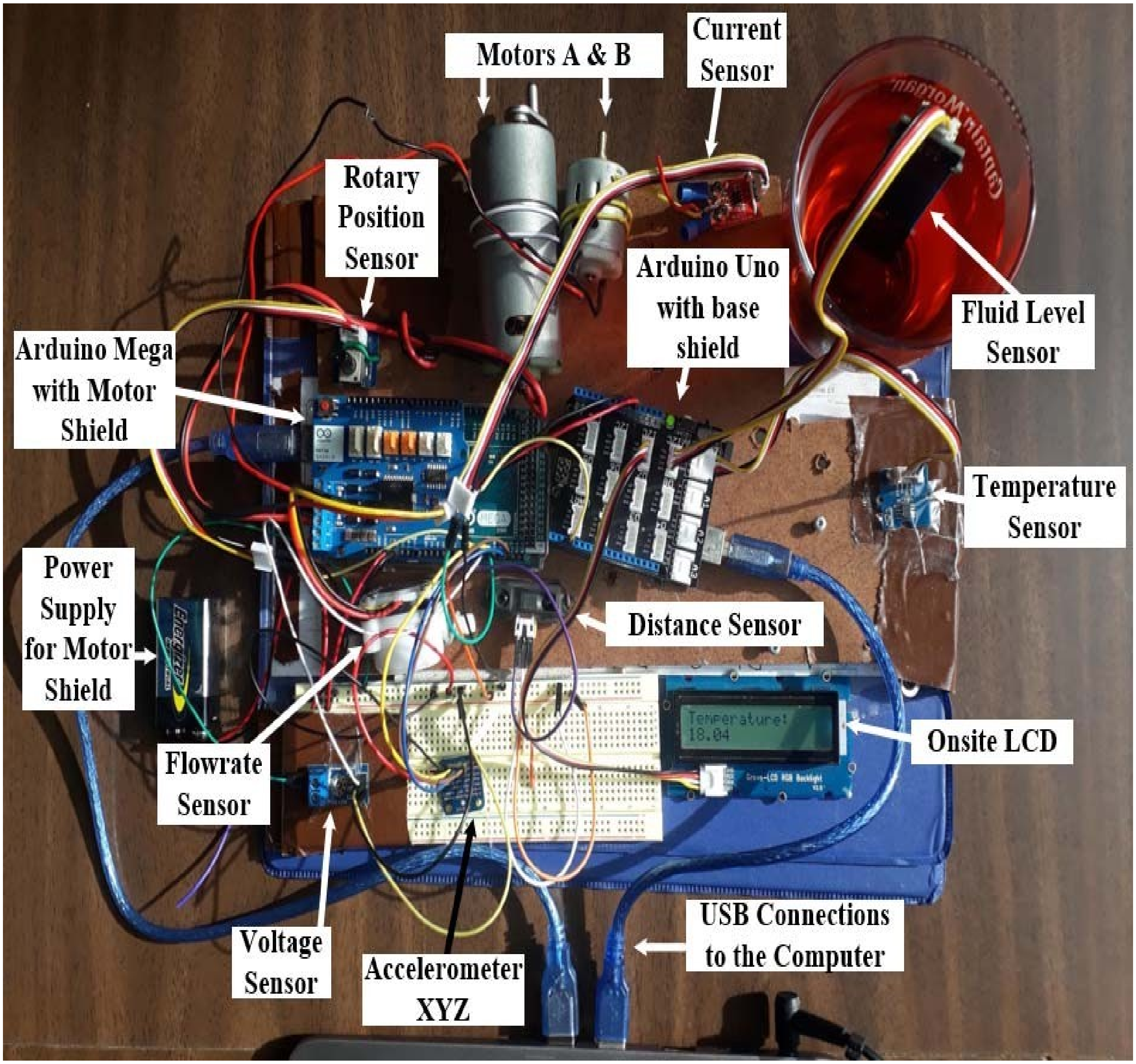

Figure 5.10. Experimental setup of the proposed IoT-based SCADA system

The results are shown by subsystems as follows:

5.6.1 Subsystem 1

The dashboard for sensors connected to Arduino Mega is shown in Figures 5.11 and 5.12. The dashboard for this subsystem includes gauge and chart outputs for current, voltage, distance, accelerometer and rotary position sensors. In this work, the user interface shows the received sensor data, both as a gauge and a chart.

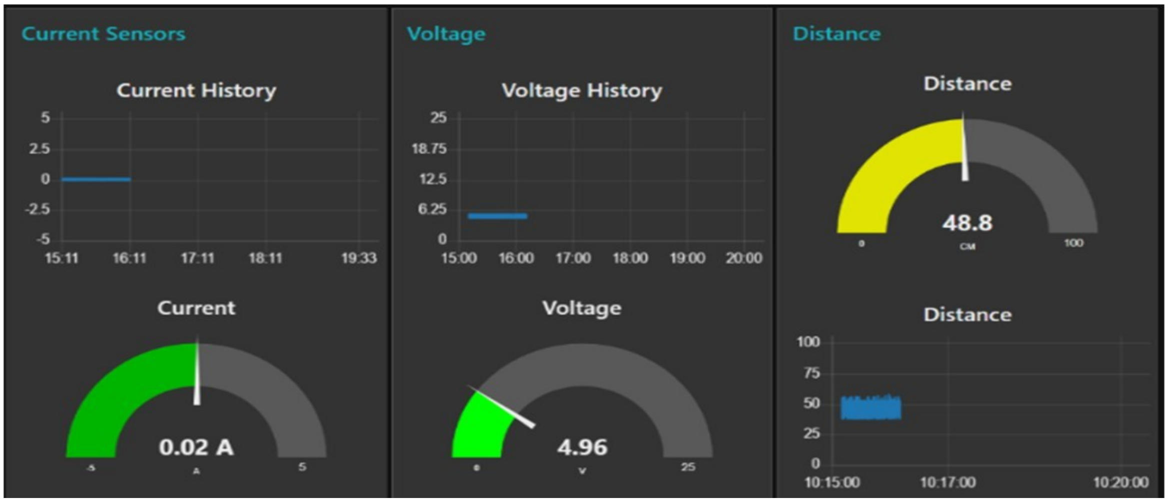

Figure 5.11. Charts and gauges for current, voltage, and distance sensors.

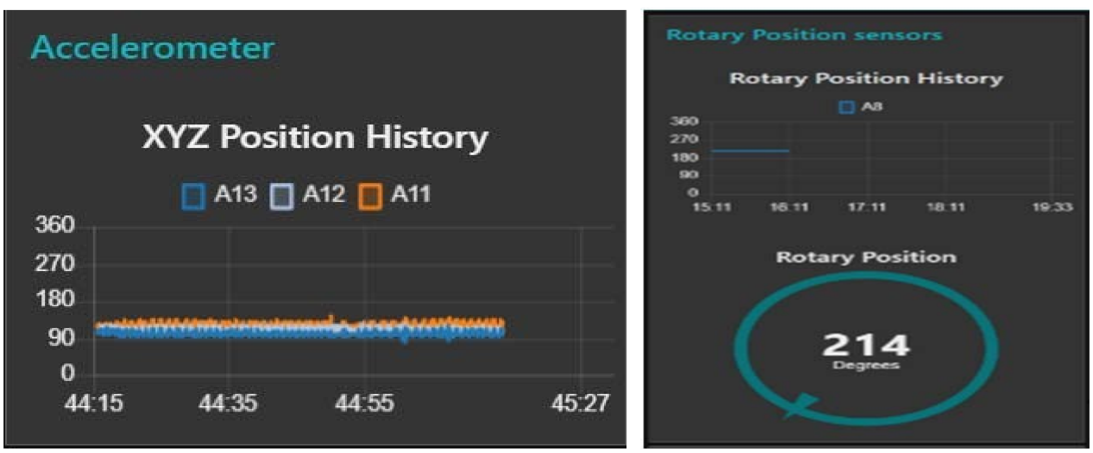

Figure 5.12. Charts for accelerometer, charts, and gauges for the rotary position sensor.

5.6.2 Subsystem 2

The dashboard for the sensors on Arduino Uno is shown in Figure 5.13. It is available in Node-RED as a web GUI that updates or responds in real-time. The user interface shows the sensor data both as a gauge and a chart. It shows the water level, flow rate, and temperature readings.

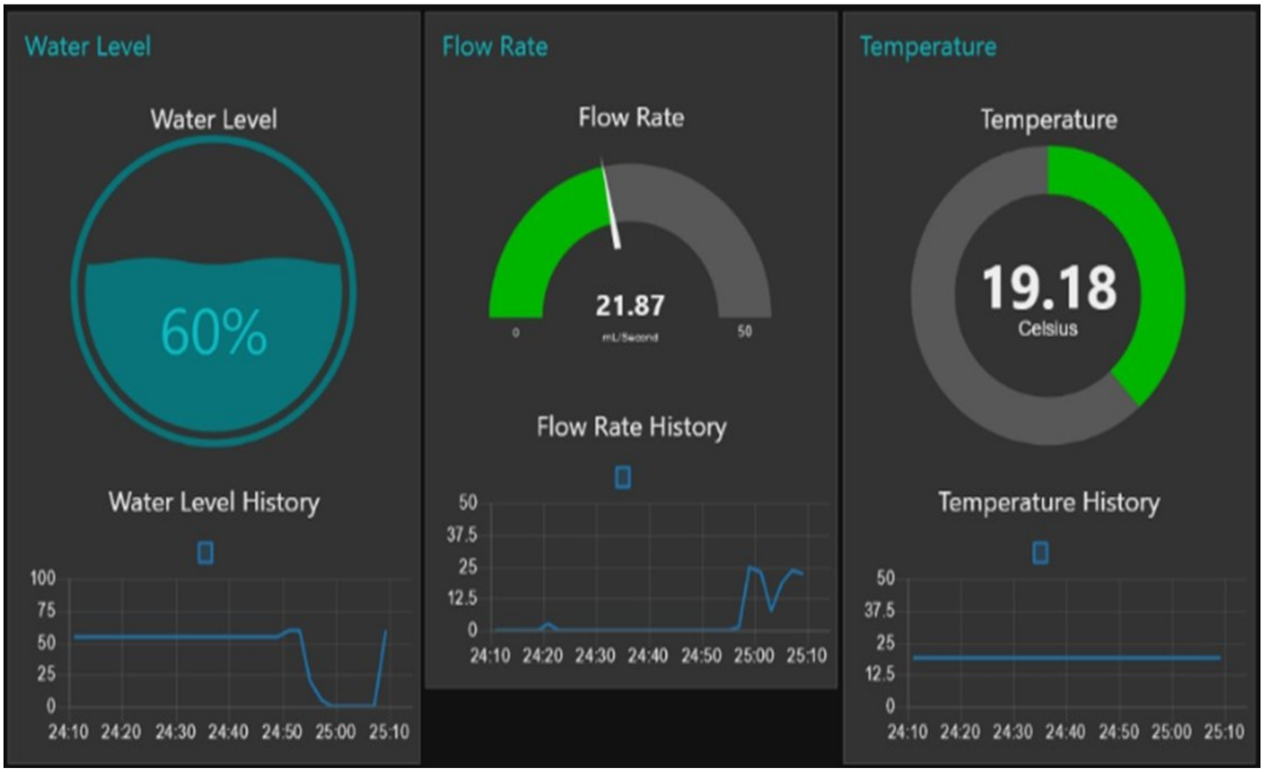

Figure 5.13. Charts and Gauges for water level, flowrate, and temperature sensor.

5.6.3 Subsystem 3

Figure 5.14. shows the dashboard panel to control motors A and B connected to Arduino Mega's motor shield. This dashboard uses Arduino nodes in Node-RED and Firmata on the microcontroller to start and stop the motors.

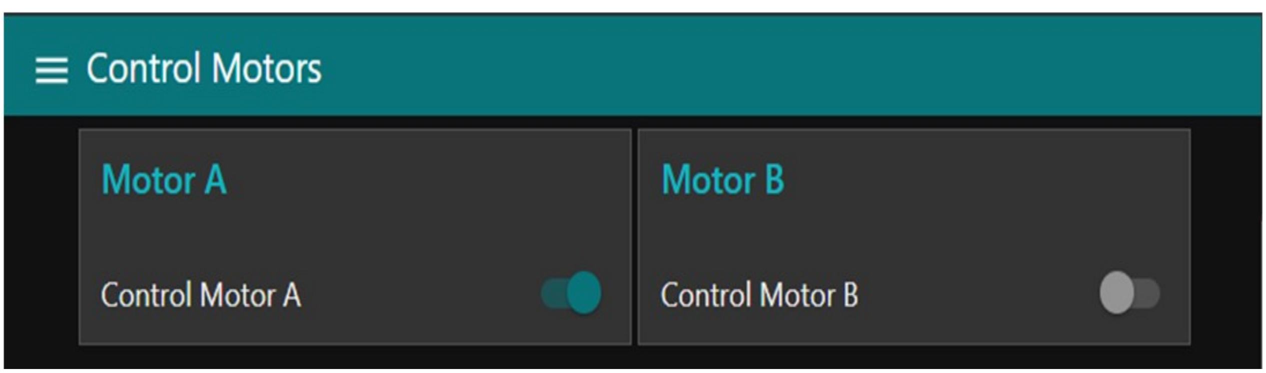

Figure 5.14. Dashboard panel to control motors A and B

5.7 Discussion

Monitoring of the oil well site parameters such as flowrate from the producing well and comparing it with the speed of the electrical motor is imperative to diagnose problems in an actual producing well. When the speed of the electric motor is high, and the flow rate of the produced fluid is declining, based on the thresholds set, it could be an indicator of fluid pound, gas lock, rod failure or wear and tear in the subsurface rod pump. It could also point to sand production at the producing interval or issues in reservoir production. Early-onset of flow assurance problems such as wax and paraffin formation could also be detected by tracking and monitoring the behavior of the voltage and current drawn by the electric motor and mapping trends, which could be further corroborated with flow rate and cross- referenced with downhole temperature and pressure gauges. When the IoT devices are mounted on an actual 3D model and the data acquired is logged and integrated appropriately, these sensor trends could be aggregated into historical data and analyzed for prediction of failure or monitoring production performance.

5.8 Conclusion

A low-cost IoT-based SCADA system is presented in this work; the Arduino Mega and Uno microcontrollers are deployed as terminal units to communicate with and aggregate data from a total of eight (8) sensors, namely the water level, flowrate, temperature, current, voltage, distance, rotary position, and accelerometer sensors. The electric motor and the LCD on-site display are also transducers whose operation and outputs are controlled by the MTU through the terminal units. Designing and securely architecting networks that interconnect these field instrumented devices in the industrial Internet of Things framework is required for remote sensing, instrumentation, and control of critical field parameters.

5.9 Future Work

This research provisioned a server instance on a local computer which hosts both the Node-RED application and graphic user interface on its web browser. In the future, the authors intend to build the Node- RED application as a cloud-native application in IBM Watson. The role of the rotary encoder will also be expanded beyond simple monitoring to automated speed control of the electric motor for direct regulation of motor speed and indirect control of fluid production rate. Email alerts and notification will also be adopted. In terms of security; port forwarding and basic authentication were used in this research, secure sockets layer (SSL) will be further adopted in to encrypt HTTP connection to HTTPS, ensuring that responses to client requests are redirected to a secure version of the Node-RED application running on the provisioned server. The intent is to ultimately mount the sensors on a 3D model of a sucker-rod pump and use the sensor readings in combination with artificial intelligence and machine learning to calibrate a digital twin.

5.10 References

[1] Cuayo, L.D., Culla, J.K., Gualvez, J., Padua, S.E. and Gallano, R.J., 2018, October. Development of a Wireless Microcontroller-based SCADA RTU. In TENCON 2018-2018 IEEE Region 10 Conference (pp. 2566-2570). IEEE.

[2] Aghenta, L.O. and Iqbal, M.T., 2019. Low-cost, open source IoT-based SCADA system design using thinger. IO and ESP32 thing. Electronics, 8(8), p.822.

[3] Zamanlou, M. and Iqbal, M.T., 2020, September. Development of an economical SCADA system for solar water pumping in Iran. In 2020 IEEE International IOT, Electronics and Mechatronics Conference (IEMTRONICS) (pp. 1-4). IEEE.

[4] Purohit, N.L., 2015. Anshika, Data Acquisition of Solar Power Plant Using SCADA System. Int. J. Eng. Trends Technol, 23(4), pp.189-194.

[5] Lu, X., 2014. Supervisory control and data acquisition system design for CO2 enhanced oil recovery. Master of Engineering Thesis, Technical Report No. UCB/EECS-2014-123. EECS Department, University of California at Berkeley.

[6] SEI Insights (2018) '12 Risks, Threats, & Vulnerabilities in Moving to the Cloud', Software Engineering Institute, Carnegie Mellon University, 19 March. Available at: https://insights.sei.cmu.edu/blog/12-risks-threats-vulnerabilities-in-moving-to-the-cloud/ (Accessed: 19 October 2024).

[7] Sierra Wireless (2024) Oil and Gas IoT Solutions | Sierra Wireless. Available at: https://www.sierrawireless.com/industries/energy/oil-and-gas/ (Accessed: 12 October 2024).

[8] SCADALink (2024) Single Well Oil & Battery Monitoring System | SCADALink. Available at: https://www.SCADAlink.com/products/satSCADA/single-well-oil-battery-monitoring-system/ (Accessed: 11 October 2024).

[9] Cardoso, C.B., Alves, I.N. and Ribeiro, G.S., 2003, May. Management of flow assurance constraints. In Offshore Technology Conference (pp. OTC-15222). OTC.

[10] Adeyinka, A., Tsakporhore, A., Oduwole, A., Jumbo, S., Odusote, F., Aliyev, S., Adegoke, O., Lapham, J. and Eme, T., 2020, August. Re-positioning mature fields for sustainability: Deriving additional value by applying the Internet of Things via remote well monitoring. In SPE Nigeria Annual International Conference and Exhibition (p. D013S003R002). SPE.

[11] Elmer, W.G. and Elmer, J.B., 2018. Pump-stroke optimization: case study of twenty-well pilot. SPE production & operations, 33(03), pp.419-436.

[12] Vijay, A. and Unni, V.S., 2012, March. Protection of Petroleum Industry from Hackers by Monitoring and Controlling SCADA System. In SPE Intelligent Energy International Conference and Exhibition (pp. SPE-149015). SPE.

[13] Electrical Engineering Portal (2024) Three Generations of SCADA System Architectures. Available at: https://electrical-engineering-portal.com/three-generations-of-SCADA-system-architectures (Accessed: 10 October 2024).

[14] Node-RED (n.d.) Node-RED. Available at: https://nodered.org/ (Accessed: 5 October 2024).

[15] Lekić, M. and Gardašević, G., 2018, March. IoT sensor integration to Node-RED platform. In 2018 17th International Symposium Infoteh-Jahorina (Infoteh) (pp. 1-5). IEEE.

[16] Chanthakit, S. and Rattanapoka, C., 2018, July. Mqtt based air quality monitoring system using node MCU and node-red. In 2018 Seventh ICT International Student Project Conference (ICT-ISPC) (pp. 1-5). IEEE.

[17] SitePoint (n.d.) Configuring Nginx SSL for Node.js. Available at: https://www.sitepoint.com/configuring-Nginx-ssl-node-js/ (Accessed: 05 October 2024).

[18] NGINX (2024) What is NGINX?. Available at: https://www.nginx.com/resources/glossary/nginx/ (Accessed: 07 October 2024).

Chapter 6

DESIGN, DYNAMIC MODELLING, SIMULATION, AND CONTROL OF A SOLAR-POWERED SUCKER ROD OIL PUMP

Co-authorship statement

This chapter achieves research objective 5 of this thesis as stated in Section 1.3. It presents the design, modelling, simulation, and control of a solar-powered sucker rod oil pump for a remote oil well in Canada, with a focus on demonstrating the stability and robustness of the 100% solar-powered microgrid in delivering the active and reactive power required for oil production. The resilience of the model to varying environmental and operational conditions is demonstrated by integrating actual historical weather data to account for the variation in ambient temperature and solar irradiance in the dynamic modelling and simulation. The results demonstrate stable, reliable, and optimal operation as key performance indicators including solar PV power, bus voltage, battery power, step-up transformer rating, and real and reactive power requirements of the sucker rod pump system are visualized in the model.

I (Charles Aimiuwu Osaretin) am the principal author and contributed to the Conceptualization, Methodology, Software Investigation, Writing of Original Drafts, and Editing of the research manuscript. The research in this chapter was supervised by Dr. M. Tariq Iqbal, and Dr. Stephen Butt. The supervisors contributed to the conceptualization and methodology. They also supervised the entire chapter, reviewed and corrected the research manuscript. The work in this Chapter has been submitted for publication in the Journal of Electronics and Electrical Engineering(JEEE), Volume 4, Issue 1, January 2025, Pages 105–137, Article ID 275877094, 33 pages,

https://doi.org/10.37256/jeee.4120256168.

Abstract

The sucker rod pump is a crucial artificial lift system widely deployed in the oil industry to extract crude oil from producing wells. Accurate modelling of the sucker rod pump has become essential as a viable strategy for optimizing performance, and ensuring both efficient and economic operation. This paper presents a comprehensive methodology for the design, dynamic modelling, simulation, and control of a solar-powered sucker rod oil pump. It combines load modelling of the sucker rod pump using SolidWorks with design, dynamic modelling, simulation, and control of the solar microgrid in Matlab's Simscape and Simulink. The model seamlessly integrates the mechanical and electrical systems with 100% renewable energy to power the sucker rod pump system. This approach combines the solar photovoltaic system, battery charge control system, battery energy storage system, step-up transformer, and the squirrel cage induction motor, which serves as the electric motor prime mover. The surface pump model is first developed in SolidWorks and then converted to Simscape. The rating of the pump is then implemented as a load in the solar-powered electrical microgrid. Environmental conditions such as solar irradiance and ambient temperature for summer and winter are obtained from data repositories and included in the modelling and analysis of the overall system performance; demonstrating stable operation, robustness, and resilience to changing environmental and operational conditions.

6.1 Introduction

As global energy demand continues to increase, the oil and gas industry ironically continues to suspend, orphan, and abandon oil wells at an alarming rate due to technical, policy, and environmental reasons [1]. The increasing demand to reduce the energy footprint of producing wells is compounded by the leakage of methane and other potent greenhouse gases from idle and inactive wells [2]. Electricity cost constitutes a significant part of the overheads incurred in producing wells and with these wells sufficiently remote from the electric grid, onsite generation of 100% renewable energy presents a promising opportunity to invest in solar and wind energy microgrids, providing the energy required to restore these inactive oil wells to production while investing in distributed generation from 100% renewable energy powered microgrids [3]. This ensures that the landowners continue to earn lease revenue, and well operators remain in business, sustaining the income for site operators, tax revenue for the government, and employment for engineers; when production from these legacy wells is sustainably restored. It also reduces the carbon footprint of these idle wells, as restoring them to production curtails the unintended emissions from the well [4]. Over 50% of all oil wells worldwide have an artificial lift system installed. Approximately 40% use the sucker rod pump as shown in Figure 6.1. It accounts for approximately 500,000 beam pumps worldwide [5], hence the selection of sucker rod pump (SRP) artificial lift technology for this study given its widespread use in the oil industry

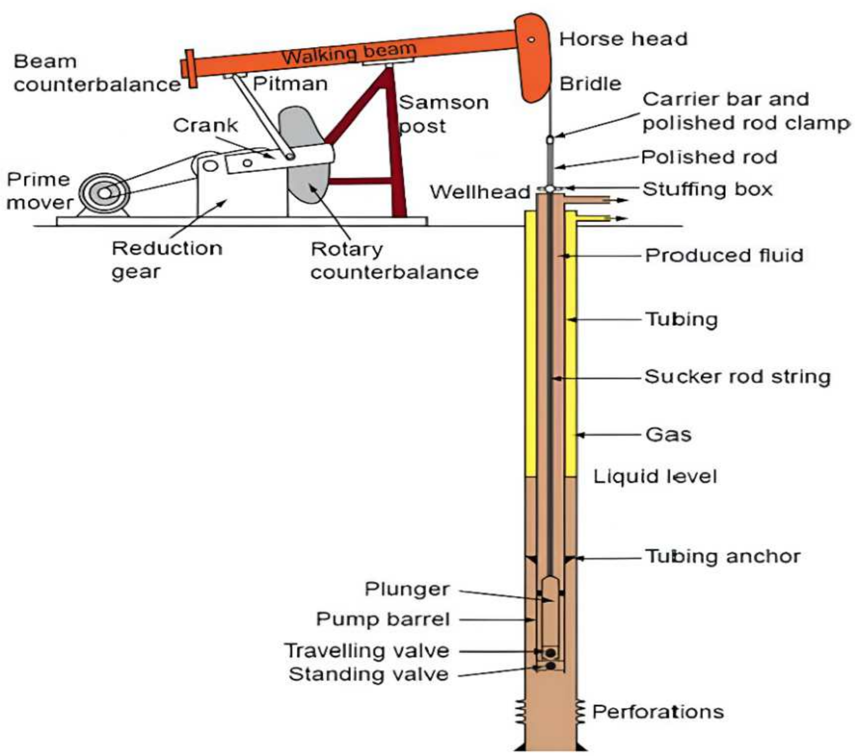

Figure 6.1. The sucker rod pumping system [6].

The Canadian province of Alberta has historically been one of the largest oil producers in Canada. Still, the province's upstream oil and gas sector reportedly contributed substantial methane emissions, accounting for approximately 70% of Alberta's emissions in 2014 [7]. The scale of Alberta's petroleum industry is evident in its vast number of registered wells, which exceeds 470,000 in 2024 [8]. Among these, a considerable number—around 155,000—are currently inactive, awaiting either reactivation or permanent decommissioning and land reclamation. More specifically, the Petrinex Alberta Public Data database indicates that about 81,000 wells in the province are classified as suspended [9]. The surface location of inactive petroleum wells in Alberta, Canada is given in Figure 6.2.

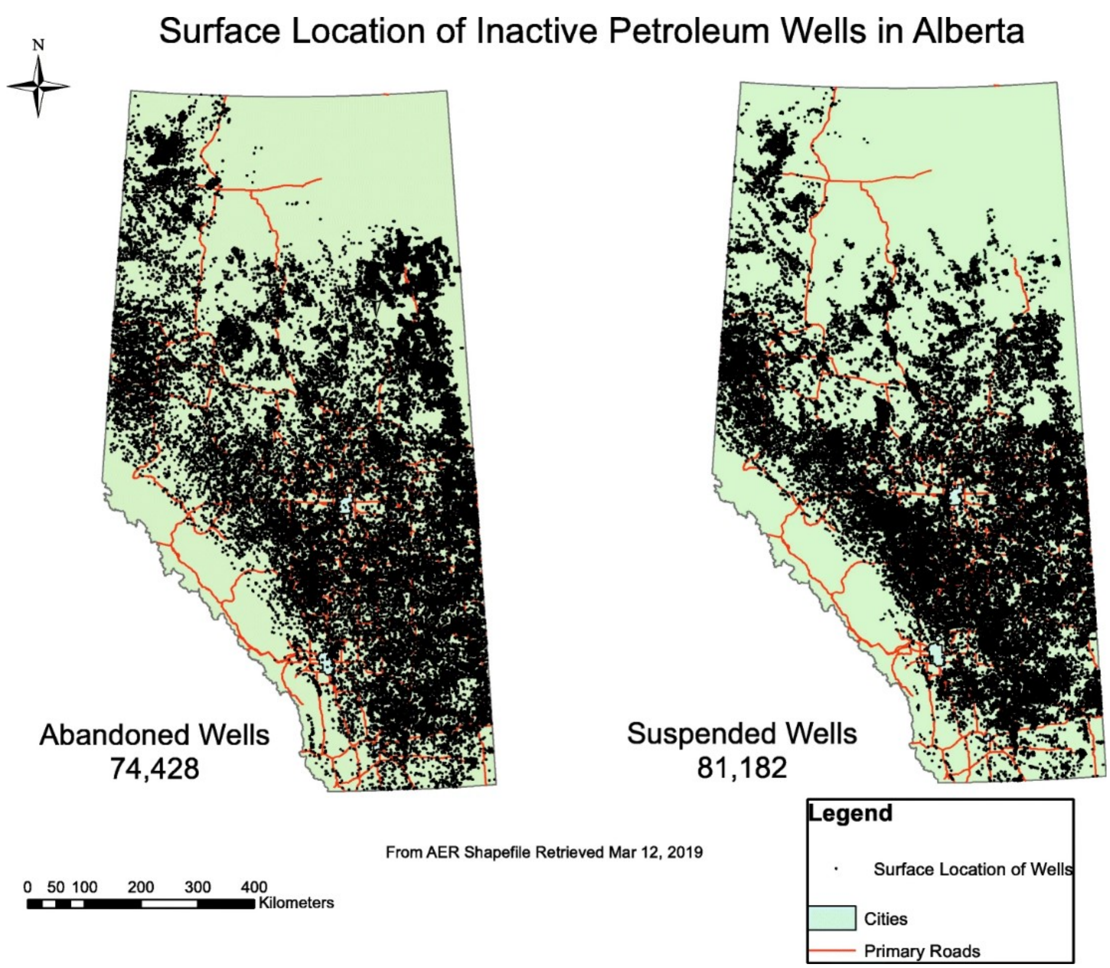

Figure 6.2. Surface location of inactive petroleum wells in Alberta, Canada [9].

The cost of orphaned well clean-up in Canada is estimated to reach $1.1 billion by 2025 [10], hence with the growing energy demand and the regulatory requirement to reduce the carbon intensity of the Canadian upstream oil and gas sector, the adoption of renewable energy is gaining attention to reduce the impact of oil production on the electrical grid and mitigate the associated cost of electricity required to pump the aging wells [11, 12]. The feasibility of combining PV with diesel for powering oil wells is considered in [13]. In previous research by the author, the technical and economic feasibility of using 100% renewable energy in powering inactive wells was examined [14]. The goal of this study is to model a sucker rod pump as a load and incorporate its rating in designing, modelling, and controlling a 100% solar-powered microgrid. The electric motor prime mover in Simscape is driven by a 100% solar-powered microgrid consisting of solar PV arrays, a charge controller, battery storage, a 3-phase inverter, a transformer, and a 3-phase squirrel cage induction motor.

6.2 Objectives

The objective of this paper is to develop a model-based simulation of the solar-powered sucker rod pump's behavior, allowing for the identification of opportunities for efficiency optimization at each subsystem. The study decouples the microgrid into subsystems, supporting efficiency enhancements and performance improvement across the entire system from solar PV source to electric motor load. The work supports adaptation to various environmental and operating conditions, so the system behavior can be analyzed and potential issues identified and addressed before prototyping and real-world implementation. The study incorporates load modelling from SolidWorks and Simscape into the Simulink model, providing a realistic representation of the actual system, and leading to more representative simulation results. The robust approach combines mechanical (SolidWorks) and electrical (Simscape) models which are crucial for designing effective controls for the sucker rod pump. The study begins with load modelling of the sucker rod pump system, utilizing SolidWorks for geometry development and translating to a Simscape model in capturing the functional mechanical and electrical characteristics of the pump. This is followed by the Solar PV array source design and modelling, including panel configurations, charge controller, power inverter, and step-up transformer for conditioning the inverter output to the load requirements. Energy storage system modelling incorporates a battery storage model to address the intermittent nature of solar power and ensure consistent and reliable operation of the oil pump. The control system for the microgrid is designed and implemented to optimize power flow, manage battery state of charge (SOC), and ensure efficient pump operation. Extensive simulations under various environmental conditions are performed to evaluate system behavior and stability. The design is iterated to improve overall system performance and reliability.

6.3 System Description

A process flow diagram of a typical sucker rod pump-driven artificial lift system is shown in Figure 6.3. It typically consists of a prime mover; a hydrocarbon-powered internal combustion engine (chemical to mechanical energy) or an electricity-powered, balanced, 3-phase, squirrel cage induction motor. The rotational energy from the prime mover is converted by the crank mechanism of the sucker rod into vertical rectilinear reciprocating motion, providing a push motion in the down stroke and a pull motion in the upstroke, effectively pumping produced fluids to the surface, where it is collected, stored, separated or piped downstream. A typical sucker rod pumping system consists of several key components, each playing a critical role in the overall operation. The surface unit includes the prime mover, gearbox, walking beam, pitman arms, and horsehead; which interact to convert rotational motion into the reciprocating motion needed to drive the rod string. The rod string itself is a series of connected steel or fiberglass rods that transmits this motion to the downhole pump, which includes the pump barrel, plunger, and valves responsible for lifting the fluid to the surface [5] where it is collected, separated, piped and stored accordingly as shown in Figure 6.3.

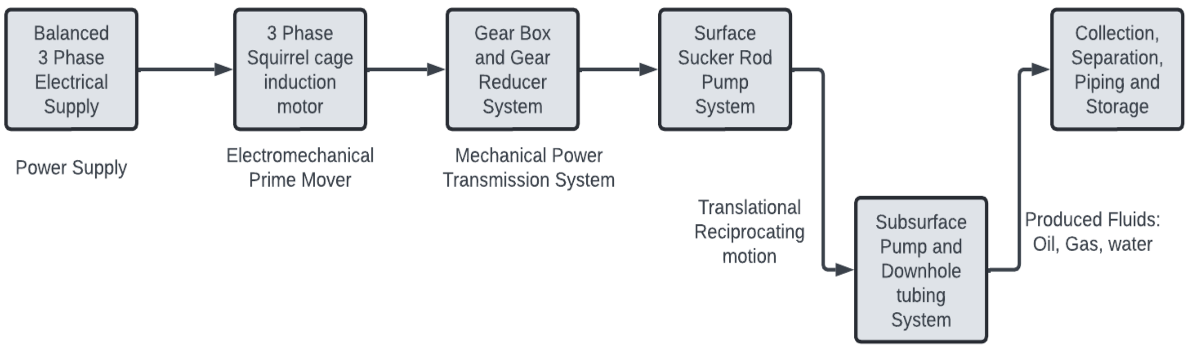

Figure 6.3. Beam pump system operation and process workflow.

6.4 Methodology

The integration of electrical power supply, power electronics, and mechanical system models within a single simulation environment enables a comprehensive analysis of the system's behavior as shown in Figure 6.3 . This approach allows for the simulation of various operating scenarios and the deployment of optimal control strategies for different conditions. This paper builds on the foundation of previous SolidWorks and Simscape computer-aided design modelling of sucker rod pumps, by developing a detailed model of a sucker rod pump using these advanced simulation tools. The modelling approach encodes the kinematic equations of the walking beam, rod string stress analysis and dynamic load calculations into the surface pumping unit model in Simscape multibody. The gear ratio equations, transmission efficiency and mechanical loss behavior are integrated into the gearbox and gear reducer subsystem, while the rod string subsystem, pump displacement equations, fluid dynamics models, pressure and flow calculations are integrated into the subsurface pump and downhole tubing subsystem. The voltage equations, frequency specifications, and power ratings of the 3-phase electrical supply source subsystem are defined by the equivalent circuits of the 3-phase, 100% solar power source which drives the squirrel cage induction machine model. The rotor and stator equations, electromagnetic torque equations, speed-torque characteristics, and machine parameters (resistance, inductance etc) are integrated into the Simscape model of the squirrel cage induction motor. The oil well powered by a sucker rod pump is modeled as a mechanical load to the squirrel cage induction motor prime mover. Overall, the integrated model in Simscape uses appropriate blocks from the Simscape library: Simscape foundation library, Simscape electrical, and Simscape multibody.

6.4.1 Methodology for Modelling Sucker Rod Pump in Solidworks and Simscape

The geometric model of the sucker rod pump developed and adapted from SolidWorks model is converted to Simscape multibody model using the Simscape multibody link plugin. This process enabled the authors to integrate the CAD assembly with other systems for simulation and analysis in the MATLAB/Simulink environment [15]. The conversion process begins with installing the Simscape multibody link plugin for SolidWorks, the SolidWorks assembly is developed and then exported to an XML file and the corresponding geometry files using the plugin [16]. The XML file is then imported into MATLAB/Simulink to create a Simscape multibody model [17]. The exported model preserves important properties from the SolidWorks assembly: Mass, inertia, and center of gravity of parts are automatically transferred [17]. Assembly topology and constraints are converted to appropriate joints and constraints in Simscape. The 3D geometry of parts is preserved in the simulation model [17]. This workflow allows for system-level simulation and optimization, integrating mechanical components with electrical, hydraulic, and control systems. It reduces the need for physical prototypes by enabling virtual testing and validation. The authors refined component designs based on accurate system-level requirements [15]. When creating SolidWorks models intended for export, the authors followed certain best practices to ensure clean conversion to Simscape, as they map to specific joint types in Simscape multibody [18]. CAD models from Solidworks are converted in Simulink to Simscape multibody flowcharts using the smimport function, which utilizes XML files to recreate and approximate the original model. The conversion process occurs in two stages: export, where the CAD assembly is converted to XML and geometry files, and import, where these files are transformed into a Simscape multibody model and M-data file [19]. The resulting model obtains all input parameters from the data file, enabling an accurate representation of the original CAD model in Simulink as shown in Figure 6.4.

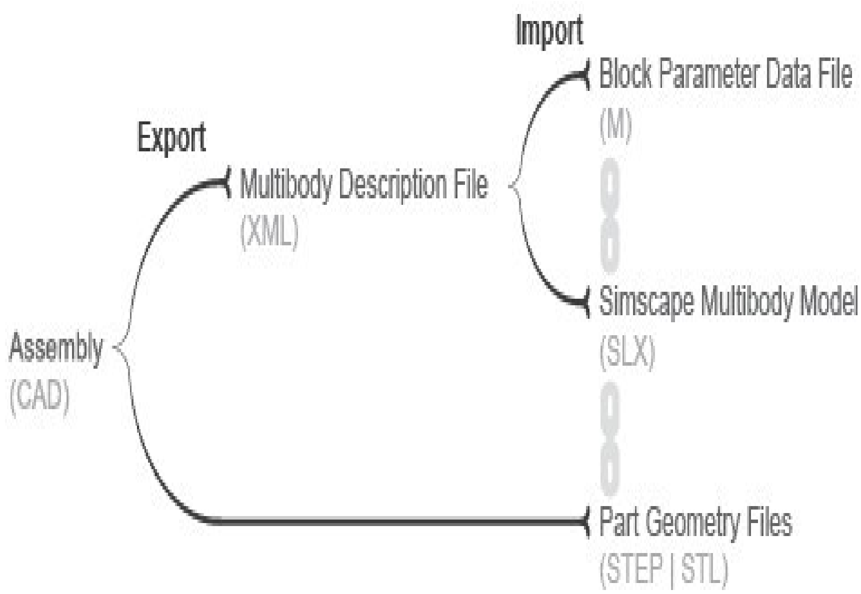

Figure 6.4 Converting CAD to Simscape Model [20].

In SolidWorks, the process of creating assemblies relies heavily on the use of mates and constraints to define relationships between components [21]. These elements are crucial in determining how parts interact within the assembly, influencing their relative positions and movements [22]. By accurately defining these relationships, the author ensured that components fit together properly and behave realistically, which is essential when transferring the assembly to simulation environments like Simscape multibody [23]. The precise definition of these connections is vital for maintaining design intent and ensuring the assembly functions as intended in both virtual and physical contexts [22]. The transition from SolidWorks to Simscape multibody involves converting mates and constraints into equivalent joints and constraints within the simulation environment [24]. This conversion process is critical, as different types of SolidWorks mates correspond to specific joint types in Simscape. For example, a concentric mate in SolidWorks might be translated into a revolute joint in Simscape.

The accuracy of the conversions directly impacts the fidelity of the simulation results, influencing the model's behavior under various conditions [25]. Well-constrained models not only facilitate more efficient system-level simulations but also enhance the overall reliability of the analyses performed in Simscape [22]. Smooth transition of models from SolidWorks to Simscape multibody is ensured by carefully considering and applying appropriate mates and constraints. This thoughtful approach preserves the intended mechanical relationships and behaviors, leading to more accurate simulations and analyses. The quality of the original SolidWorks model, including well-defined mates and constraints, directly correlates with the functionality and accuracy of the resulting Simscape multibody model. This attention to detail in the initial design stages significantly enhanced the overall effectiveness of subsequent simulations and analyses. The foundational SolidWorks model for this research was adapted from earlier work by [26], which presents a SolidWorks model designated as a crank balance, clockwise, “conventional” beam pump (“C”), with “double-gear” reduction (“D”), maximum torque capacity of 228,000 inch-pounds (in-lbs.), maximum polished rod load of 17,300 pounds (lb), and maximum stroke length of 74 inches.

6.4.2 SolidWorks Model of Sucker Rod Pump

Pumping Unit Mechanism: The SolidWorks model includes detailed representations of the surface unit components as shown in Figure 6.5. Figure 6.6 shows the Mechanics Explorer view of a Simscape multibody model.

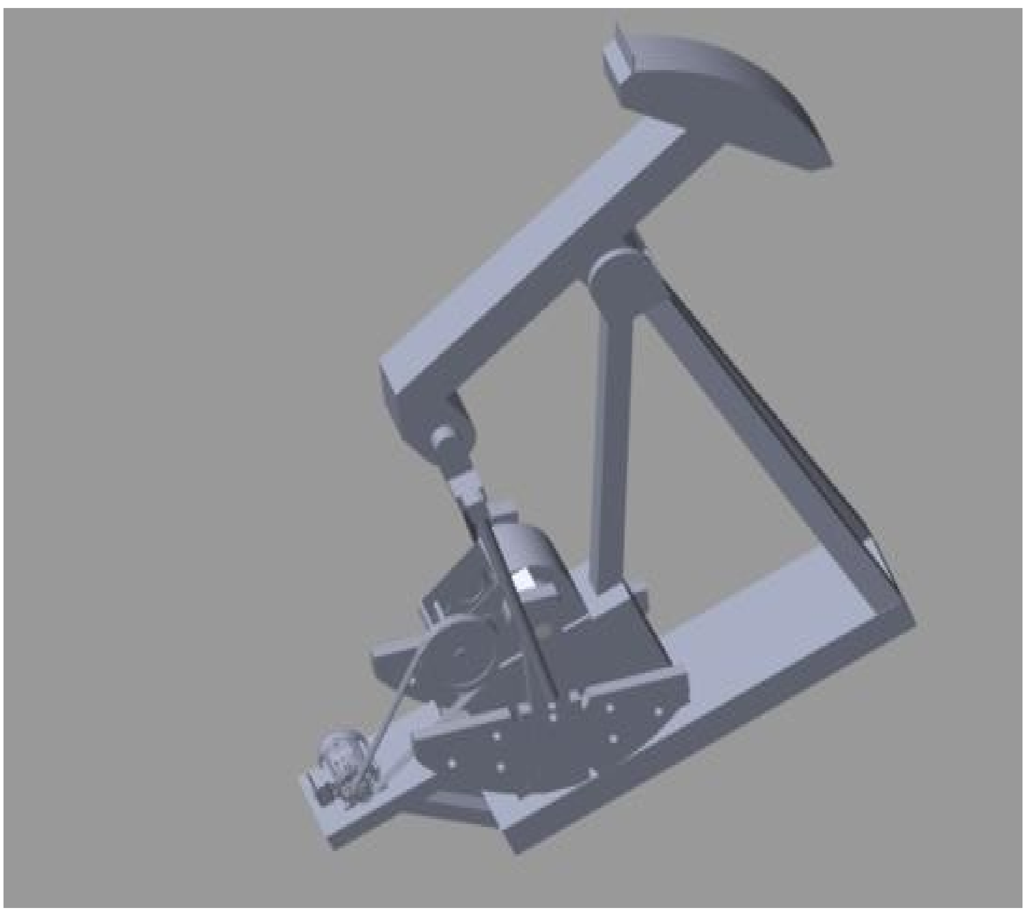

Figure 6.5 CAD Simulation of Surface Unit.

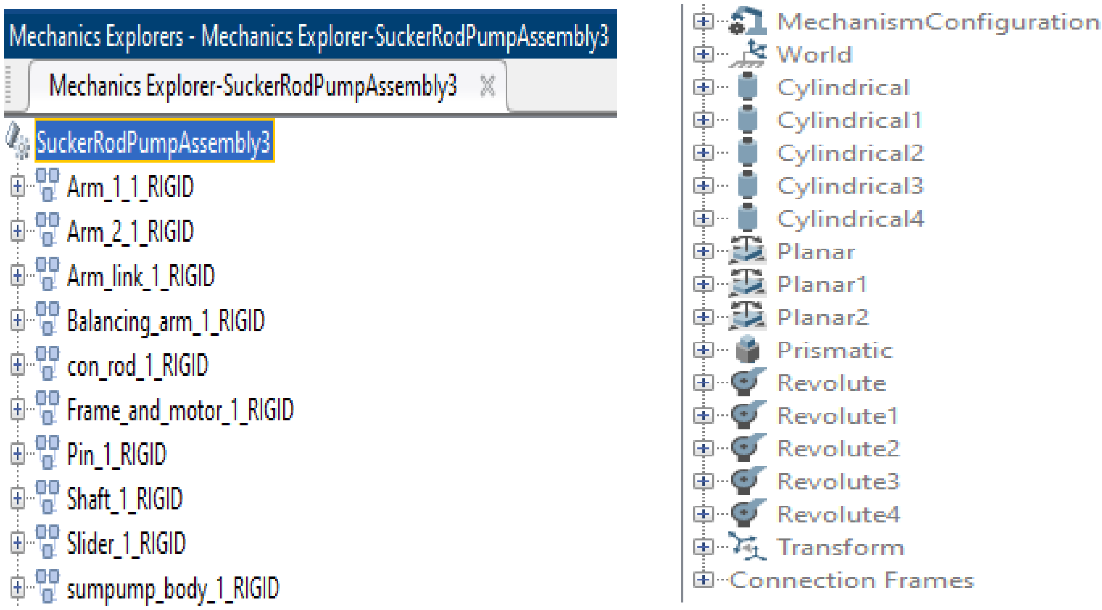

(a) (b)

Figure 6.6. Resolved Simscape model showing joints and interactions.

(a) Rigid bodies. (b) Degree of freedom

Figure 6.6a shows the rigid body elements exported from SolidWorks. The model elements are SuckerRodPumpAssembly3 which is the main assembly of the sucker rod pump. Balancing_arm_1_RIGID is a counterbalanced arm, consisting of the horse head and walking beam as shown in Figure 6.7. Frame_and_motor_1_RIGID is the pump's frame, saddle bearing, Samson post, and motor assembly as shown in Figure 6.8. Shaft_1_RIGID is a shaft component connecting the counterbalanced arms as shown in Figure 6.9. Arm_1_RIGID, and Arm_2_RIGID are the left and right crank and counterweight, rigid bodies representing pump arms as shown in Figures 6.10 and 6.11. Arm_link_1_RIGID is made of rigid link connecting arms consisting of the equalizer, equalizer bearing, and pitman as shown in Figure 6.12. Pin_1_RIGID is a pin which provides a fulcrum for the Con_rod_1_RIGID which is a connecting rod to the sucker rod string as shown in Figure 6.13. Slider_1_RIGID is the Sucker rod string mechanism.

Sumpump_body_1_RIGID is the main body of the downhole submersible pump, consisting mainly of the pump barrel, and standing and travelling valves as shown in Figure 6.14.

Figure 6.6b shows the degree of freedom and the mechanical dependency of the rigid bodies from the SolidWorks CAD to the Simscape software environment. The "Mechanism Configuration" defines how the part behaves in a mechanism or assembly. The "World" is the global coordinate system reference. "Cylindrical" (1–5) are cylindrical geometric features or constraints. "Planar" (1–2) are planar surfaces or constraints. "Prismatic" represents a linear motion constraint or feature. "Revolute" (1–4) are rotational motion constraints or features. "Transform" defines the part's position and orientation while "Connection Frames" are points for connecting to other parts in an assembly. This model represents a structured approach for sucker rod pump simulation, allowing for detailed analysis of surface equipment and downhole pump. Its comprehensive nature makes it a valuable tool for oil production engineers and operators in designing, analyzing, and troubleshooting sucker rod pumping systems.

The representation of the subsystem components is defined in (a), (b) and (c) as follows:

(a) Three Dimensional Computer Aided Design (3D CAD) representation of Sucker rod component from Solidworks visualized in the Mechanics Explorer tool in Matlab.
(b) Simscape block equivalent of Solidworks component showing the force inputs "F".
(c) Sub-component resolution to fundamental blocks showing coordinate transformations and force relationships in the system.

6.4.3 Subsystem Level Modelling for Surface Unit

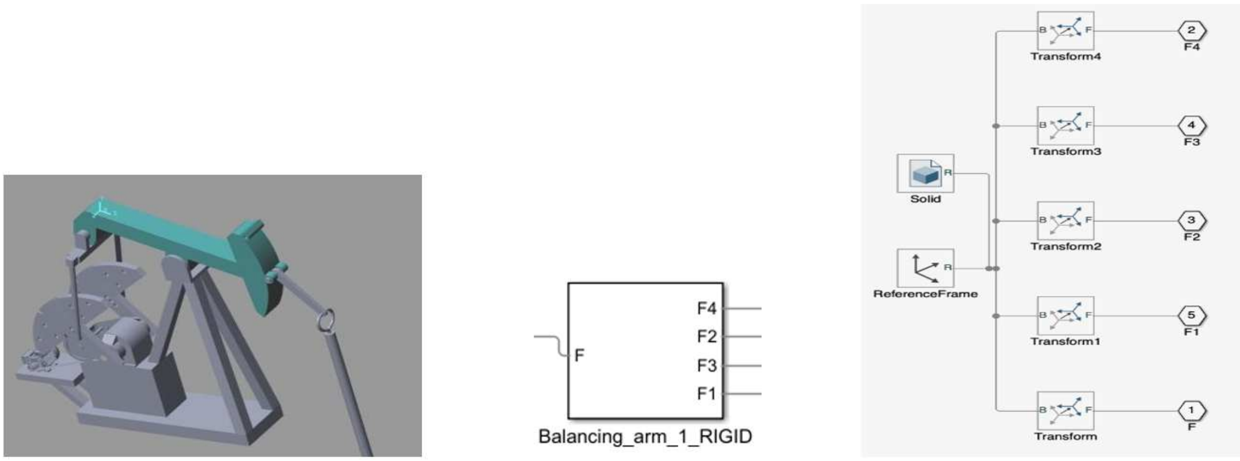

(a) (b) (c)

Figure 6.7. Balancing arm (Balancing_arm_1_RIGID): A counterbalanced arm, consisting of the horse head and walking beam. (a) 3D model of Balancing Arm (b) Simscape block equivalent of Balancing Arm showing the force input and outputs (c) Sub-component resolution of Balancing Arm with fundamental blocks showing coordinate transformations and force relationships in the system.

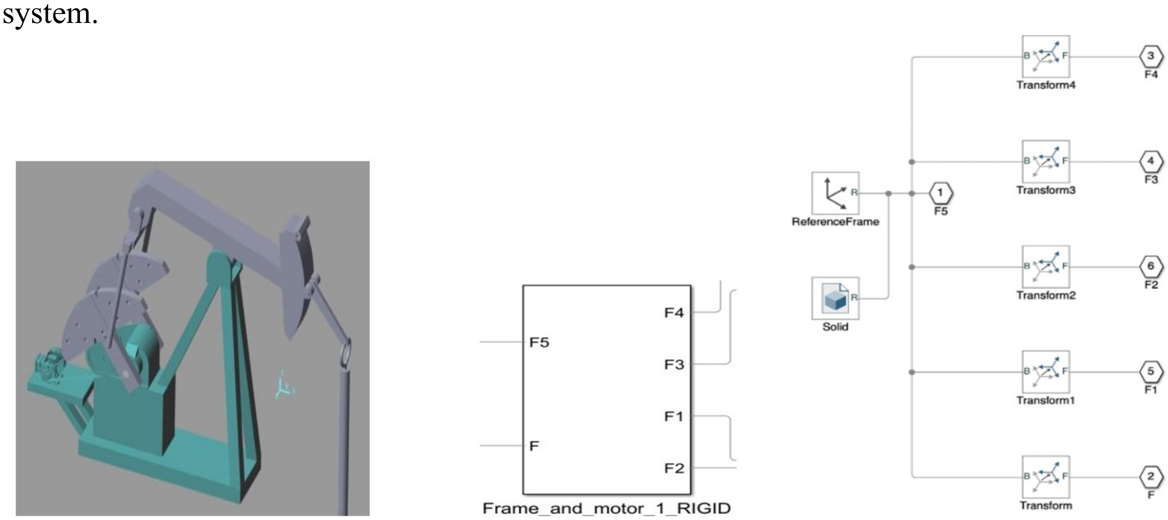

(a) (b) (c)

Figure 6.8. Frame and motor (Frame_and_motor_1_RIGID): The Samson post, pump's frame, and motor assembly. (a) 3D model of Samson post, pump's frame, and motor assembly (b) Simscape block equivalent of Samson post, pump's frame, and motor assembly showing the force input and outputs (c) Sub-component resolution of Samson post, pump's frame, and motor assembly with fundamental blocks showing coordinate transformations and force relationships in the system.

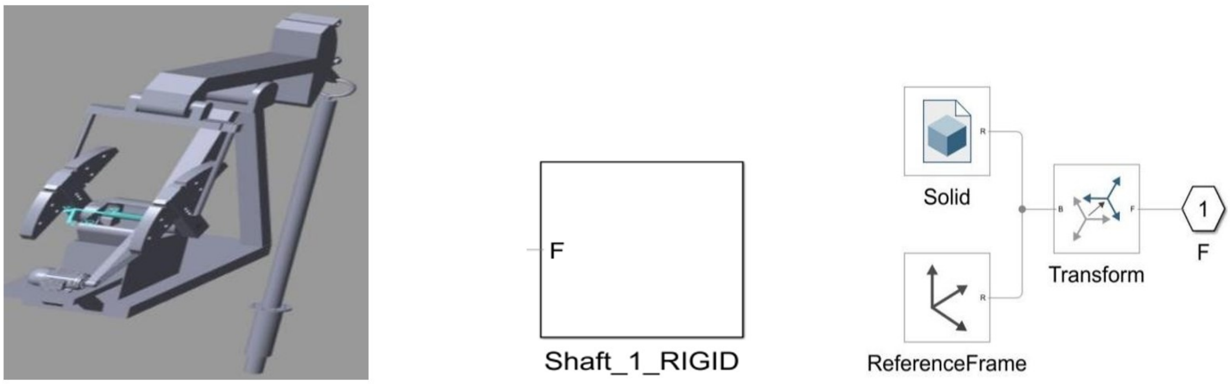

(a) (b) (c)

Figure 6.9. Shaft 1 rod (Shaft_1_RIGID): A shaft component. (a) 3D model of shaft Rod (b) Simscape block equivalent of shaft rod showing the force input and outputs (c) Sub-component resolution of Shaft Rod with fundamental blocks showing coordinate transformations and force relationships in the system.

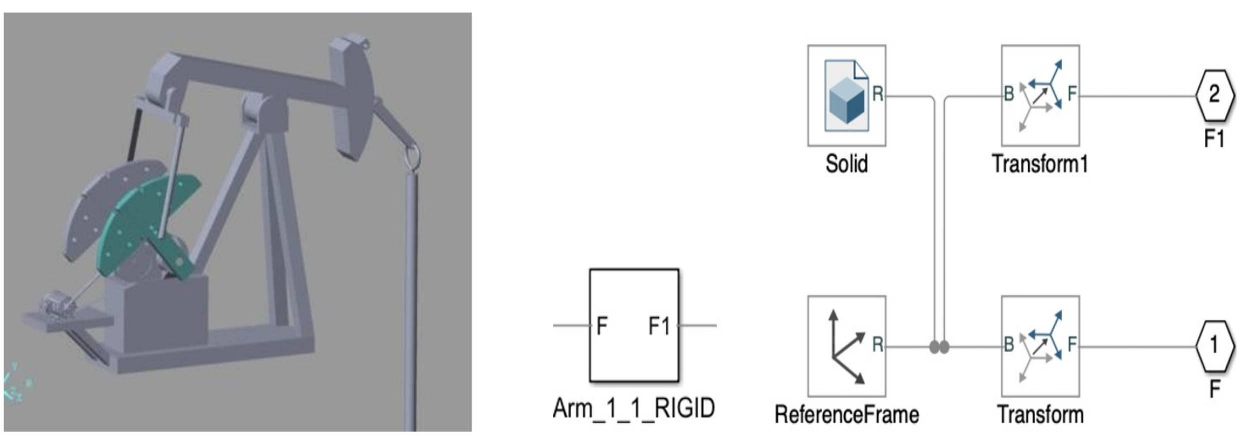

(a) (b) (c)

Figure 6.10. Arm 1. Arm_1_RIGID (Arm 1): A Crank and Rotary counterbalance Arm (first). (a) 3D model of a crank and rotary counterbalanced arm (b) Simscape block equivalent of crank and rotary counterbalanced arm showing the force input and outputs (c) Sub-component resolution of crank and rotary counterbalanced arm with fundamental blocks showing coordinate transformations and force relationships in the system.

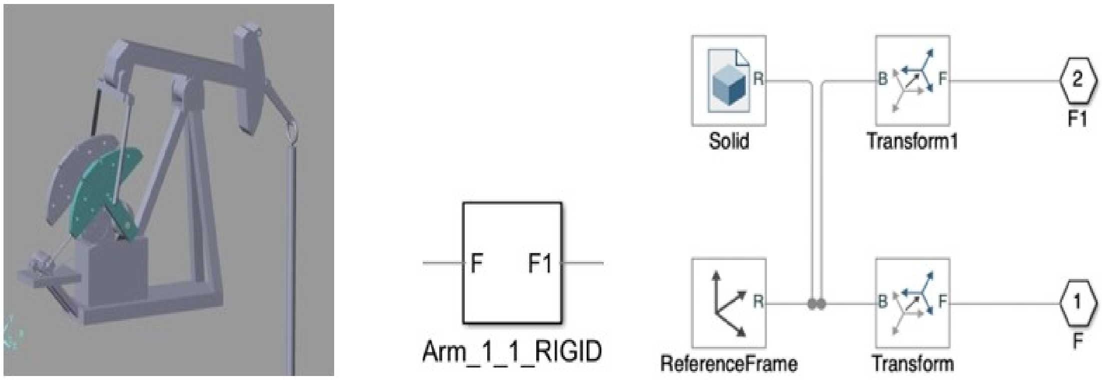

(a) (b) (c)

Figure 6.11. Arm 2 (Arm_1_RIGID, Arm_2_RIGID): Rigid bodies representing pump arms: Crank and counterweight. Arm_2_RIGID (Arm 2): A Crank and Rotary counterbalance Arm (second). (a) 3D model of the crank and rotary counterbalanced arm (b) Simscape block equivalent of the crank and rotary counterbalanced arm showing the force input and outputs (c) Sub-component resolution of the crank and rotary counterbalanced arm with fundamental blocks showing coordinate transformations and force relationships in the system.

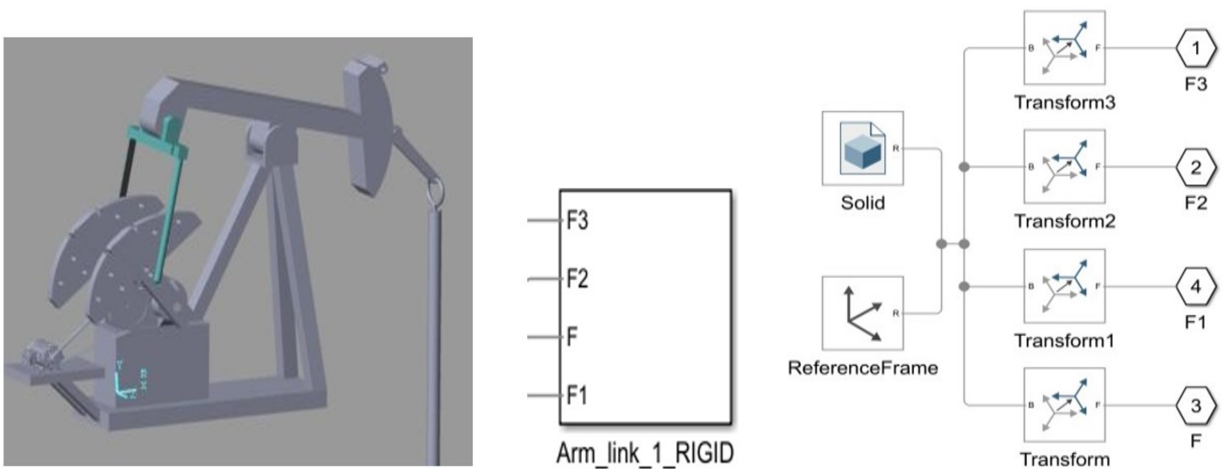

(a) (b) (c)

Figure 6.12. Arm link 1 RIGID (Arm_link_1_RIGID):A rigid link connecting arms consisting of the equalizer, equalizer bearing, and pitman. (a) 3D model of an arm link (b) Simscape block equivalent of arm link showing the force input and outputs (c) Sub-component resolution of arm link with fundamental blocks showing coordinate transformations and force relationships in the system

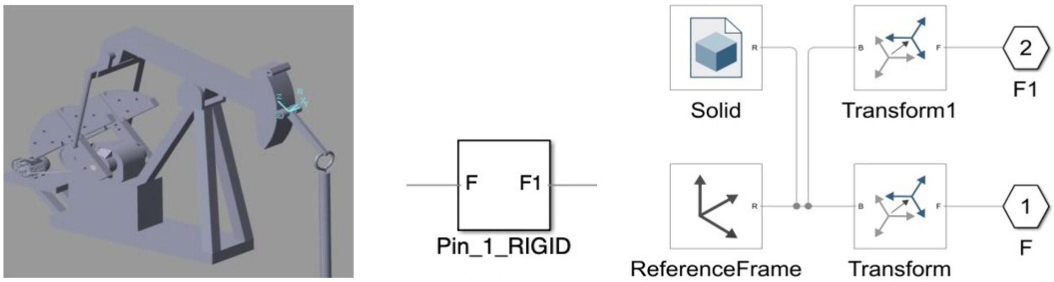

(a) (b) (c)

Figure 6.13. Pin 1 rod (Pin_1_RIGID): A pin joint. Pin 1 rod (Pin_1_RIGID): A pin fulcrum for the connecting rod. (a) 3D model of a pin fulcrum (b) Simscape block equivalent of pin fulcrum showing the force input and outputs (c) Sub-component resolution of pin fulcrum with fundamental blocks showing coordinate.

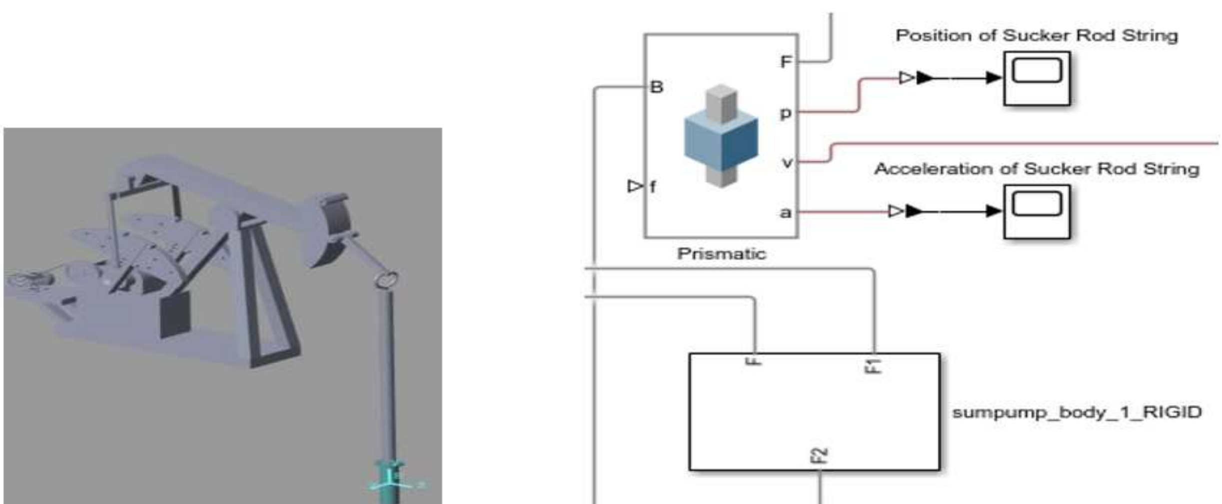

Figure 6.14. Down hole pump rigid (sumpump_body_1_RIGID): The main body of the sump pump. (a) 3D model of the main body of the subsurface pump (b) Simscape block equivalent of the subsurface pump showing the force input and outputs (c) Sub-component resolution of the subsurface pump with fundamental blocks showing coordinate transformations and force relationships in the system.

6.4.4 Detailed Analysis of Model-based Subsystems

(i) Prime Mover: A balanced 3-phase induction motor is modeled in Simscape electrical machines. The Squirrel cage induction motor model uses an asynchronous machine squirrel cage (fundamental) block from the Simscape electrical library to represent the balanced 3-phase induction motor. The induction motor was modeled first in Simscape electrical and then modeled again to simulate integration with the overall circuit in Simscape Power systems, the initial parametrization of the induction motor has been included in Figure 6.15a based on a previous work by the authors in [27], while the full motor parameters and nameplate data are presented in Table 6.8. The equivalent circuit parameters for the squirrel cage induction motor are presented in Figure 6.15a and the squirrel cage induction motor model and its integration into the sucker rod pump system is presented in Figure 6.15b.

The Squirrel cage induction motor is a common choice for most sucker rod pumps due to its robustness, efficiency, and ability to handle the cyclic loading characteristic of these systems [5]. The three-phase supply (ports a1, b1, c1) represents the three-phase power input to the motor, which is standard for industrial applications due to its efficiency and smooth power delivery [5]. The wye configuration (ports a2, b2, c2) connected to electrical reference (ground), is common in oil field applications as it provides a good balance of voltage and current characteristics [27]. Mechanical output (port R) is connected to the gearbox, providing the rotational mechanical power to drive the pumping unit. Case connection (port C) connected to the mechanical rotational reference, represents the motor's fixed mounting, which is crucial for proper torque transfer

(ii) Gearbox and Gear Reducer System

This system is modeled in Simscape multibody. It receives input angular velocity from the prime mover and outputs torque to the sucker rod pump. If the angular velocity of the mating gear is constant, then n, d and T are the gear speed, diameter, and the number of teeth, while 1 and 2 are the driver and driven gears respectively [29].

$$\text{Gear ratio} = \frac{\omega_1}{\omega_2} = \frac{n_1}{n_2} = \frac{d_2}{d_1} = \frac{T_2}{T_1} \quad \text{(i) [39]}$$

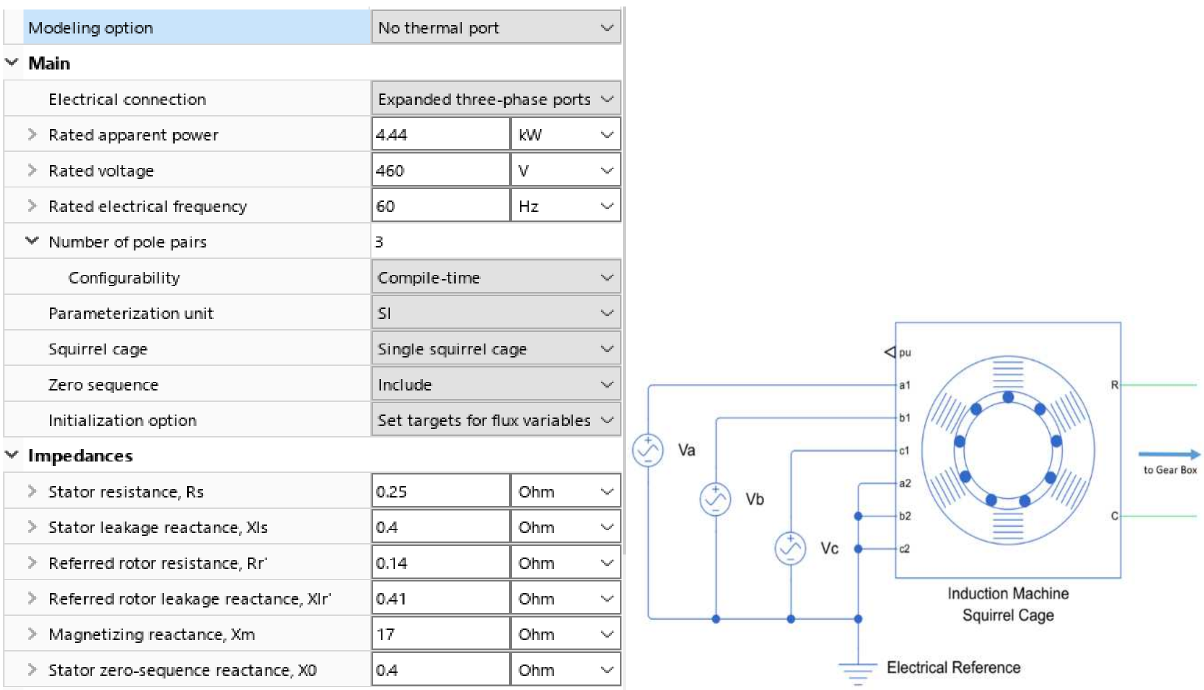

(a) (b)

Figure 6.15. (a) Equivalent circuit parameters, (b) Three-phase electric motor in Simscape

An equivalent representation of the Simscape model of the gearbox subsystem for a sucker rod pump is shown in Figure 6.16a. Gearbox block represents the physical gearbox in a sucker rod pumping unit. In actual systems shown in Figure 6.16b, the gearbox (also called speed reducer) is crucial for converting the high-speed, low-torque output of the prime mover (electric motor) into the low-speed, high-torque input required by the crank [5]. The gearbox uses a worm gear arrangement for its high reduction ratio, enabling it to handle the cyclic loading characteristic of sucker rod pumps. Port S represents the input shaft connection from the prime mover, while Port

O stands for the Output shaft connection to the crank. The rotational multibody interface serves as an interface between the 1D rotational domain (gearbox) and the 3D multibody domain (pumping unit mechanism). It is essential for accurately translating the rotational motion and torque from the gearbox to the rest of the pumping unit model. Port W is the angular velocity input, while T is the torque input, R is the rotational frame connection, and C is the connection to the 3D multibody system (which represents the Crank). The spring-damper icon models some compliance and damping in the connection, which is important for capturing the dynamic behavior of the system. Mechanical rotational reference provides a fixed reference frame for the rotational components, essential for defining the absolute motion of the system [30, 31].

Key aspects of this model are power transmission, speed reduction, the interface between domains, and power transmission for dynamic behavior. The model accurately represents the power flow from the prime mover through the gearbox to the pumping unit mechanism. This is crucial for analyzing the efficiency of power transmission and the loads on various components for speed reduction. At the same time, the gearbox model allows for the simulation of speed reduction, which is vital in sucker rod pump operations [5]. As an interface between domains, the rotational multibody interface is a sophisticated element that bridges the gap between simplified one-dimensional rotational dynamics and complex three-dimensional multibody dynamics. This is crucial for accurately simulating of the entire system and for studying the dynamic behavior. The inclusion of compliance and damping (represented by the spring-damper icon) allows for the modelling of dynamic effects such as torsional vibrations, which can be significant in sucker rod pumping systems [32].

The gearbox output directly influences the motion of the sucker rods and downhole pump. Accurate modelling here is essential for predicting downhole pump behavior. The gear ratio affects pumping speed, which directly impacts fluid dynamics in the downhole pump and wellbore. The gearbox's performance influences load distribution along the entire rod string, affecting stress on downhole components and proper gearbox modelling is crucial for optimizing overall system efficiency, including downhole pump performance.

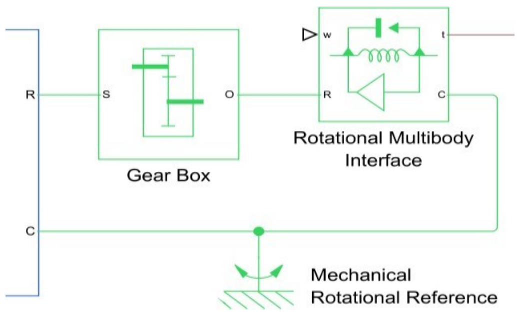

(a)

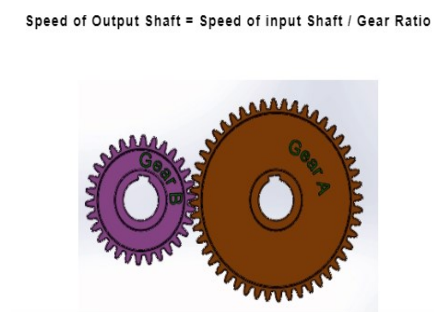

(b)

Figure 6.16. (a) Gearbox and gear reducer system, (b) Gear reduction [29]

(iii) **Sucker rod surface pumping unit**: Correlating each element to its physical counterpart, a detailed analysis of the Simscape model of the sucker rod pump and rod string system is shown in Figure 6.17. Correlating each element to its physical counterpart, "World" and "Transform" blocks establish the global reference frame and coordinate transformations, essential for accurately positioning components in 3D space. Frame_and_motor_1_RIGID represents the pump's structural frame and prime mover (a 3-phase electric motor). This is the foundation of the surface equipment. Revolute joints (Revolute, Revolute1, Revolute2, Revolute3) simulates the rotational connections in the pumping unit, such as Crank-Frame connection, Crank-Pitman connection, Pitman-Walking beam connection, Walking beam-Stand connection, Arm_2_1_RIGID, Arm_1_1_RIGID, Arm_link_1_RIGID represent the pump arms: crank and counterweight, and rigid link connecting arms consisting of equalizer, equalizer bearing, and pitman.

Balancing_arm_1_RIGID simulates the counterweight system, a counterbalance arm, consisting of the horse head and walking beam, which balances the sucker rod string load and reduces peak torque requirements. Cylindrical joints (Cylindrical, Cylindrical1, Cylindrical2, Cylindrical3, and Cylindrical4) represent connections that allow both rotational and translational motion, such as where the pitman connects to the crank and walking beam. Planar and Planar1, Planar2 constrain motion to a plane, used to ensure components move in the correct 2D plane of the pumping unit.

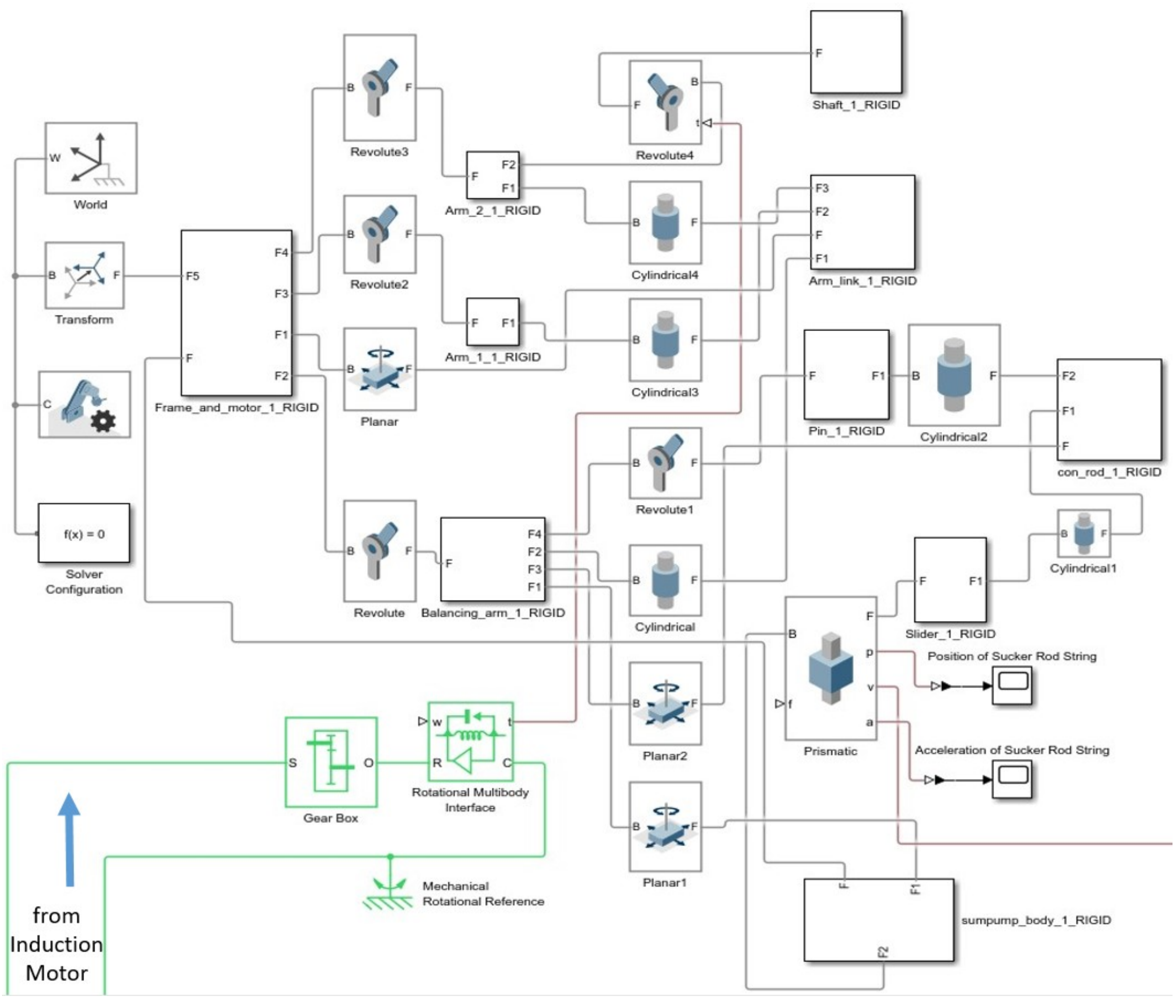

Figure 6.17. Model of Surface pumping unit (connected to Gearbox and Gear reducer system).

The prismatic joint represents a sliding connection, simulating the motion of the sucker rod string within the tubing. Shaft_1_RIGID represents the polished rod, which connects the surface equipment to the sucker rod string. Pin_1_RIGID represents a connection point, where the horse head connects to the walking beam. Con_rod_1_RIGID represents the bridle (wireline hanger), bridle block, and carrier bar, which connect the horse head to the polished rod. Slider_1_RIGID represents the polished rod that translates translational reciprocating motion from the surface to the downhole pump. Sumpump_body_1_RIGID represents the main body of the pumping unit, providing structural support [30, 33].

(iv) Subsurface pump and downhole tubing

In analyzing the Simscape model of the downhole pump of the sucker rod pump system, each element is correlated to its physical counterpart in a downhole pump setup as shown in Figure 6.18.

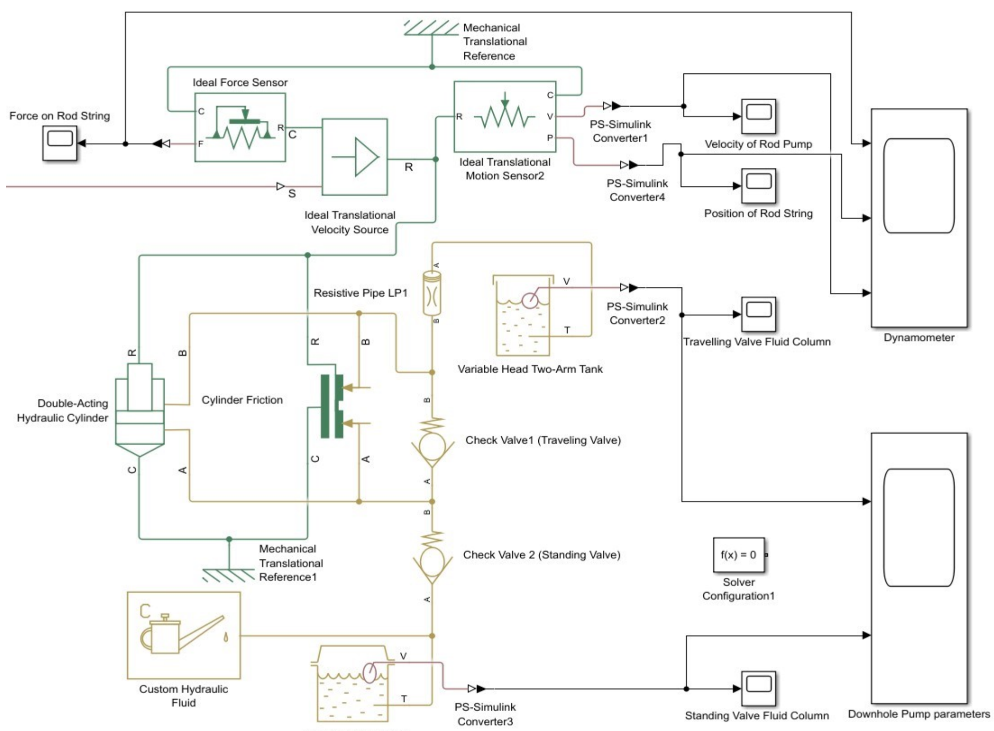

Figure 6.18. Model of Submerged Pump Barrel Assembly [27].

During the upstroke, the standing valve opens as the plunger moves up, creating a pressure differential that allows fluid to enter the pump barrel from the reservoir. Simultaneously, the travelling valve closes, allowing the fluid above it to be lifted towards the surface. On the down stroke, the standing valve closes to prevent fluid from flowing back into the reservoir. The travelling valve opens, allowing fluid to pass through the plunger, positioning it for the next upstroke. This operation closely mirrors the actual functioning of sucker rod pumps as described in the literature [5].

This Simscape model provides a comprehensive representation of the sucker rod pump's operation, allowing simulation of various operating conditions, ensuring robust analysis of pump performance, and optimizing production parameters. The model effectively considers the key dynamics of a sucker rod pumping system. However, it is important to note that while this model captures many essential aspects of beam pump operation, real-world complexities such as gas interference, sand production, or complex fluid behaviors in the wellbore are beyond the scope of this model.

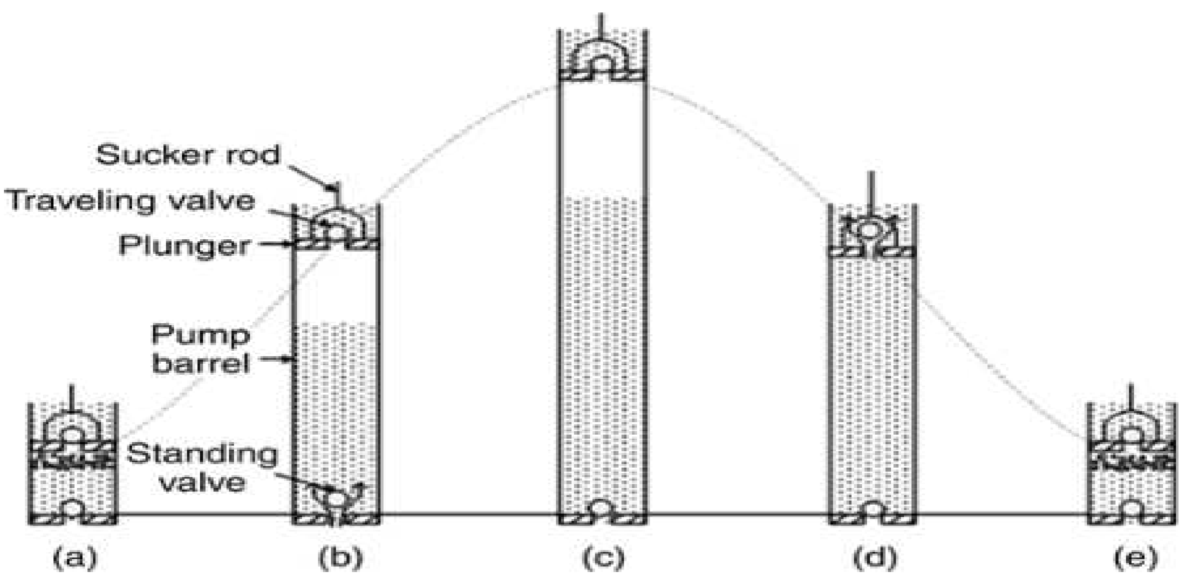

(a)

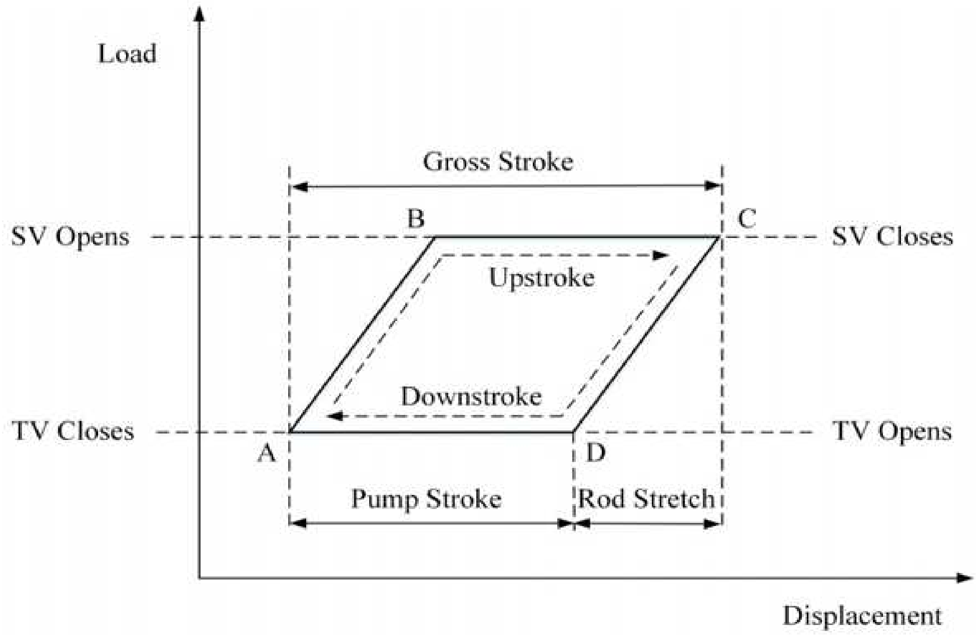

Figure 6.19. Visual representation of the operating principles of a sucker rod pump.

(a)The pump stroke cycle of the downhole pump. (b)Load/displacement dynamics

6.4.5 Methodology for Modelling Solar-powered sucker rod oil pump

The methodology for modelling a solar-powered sucker rod pump combines the estimated load rating of the sucker rod pump from previous work by the author in [14], with the subsequent feasibility study on optimal sizing, technical and economic analysis of a renewable power system for a remote oil well [27]. A renewable energy microgrid consisting of a solar-powered sucker rod oil pump is designed, modeled, simulated, and controlled in Simulink/Simscape. The selected site is near Medicine Hat, a city in Southeast Alberta, Canada. Latitude $50^{0}2'32''$ N and longitude $110^{0}48'49''$ W. Like most of the Prairies, there is an abundance of idle and inactive wells that have been suspended, orphaned, and abandoned in this area, most of which are significantly remote and do not have access to the power grid. Typical solar irradiation for the area is 3.61 kWh/m2/day, the average estimated daily electrical demand is 2.59 kW, with a peak demand of 4.44 kW [27].

6.5 PV System Design

The schematic of the proposed system is presented in Figure 6.20. It consists of the Solar PV array, DC/AC inverter, battery storage, and the induction motor, with an associated step-up transformer for voltage transformation. In the previous research by the author [27], the technical and economic feasibility of sizing a 100% solar-powered system with battery storage was extensively studied in hybrid optimization of multiple energy resources (HOMER Pro) software.

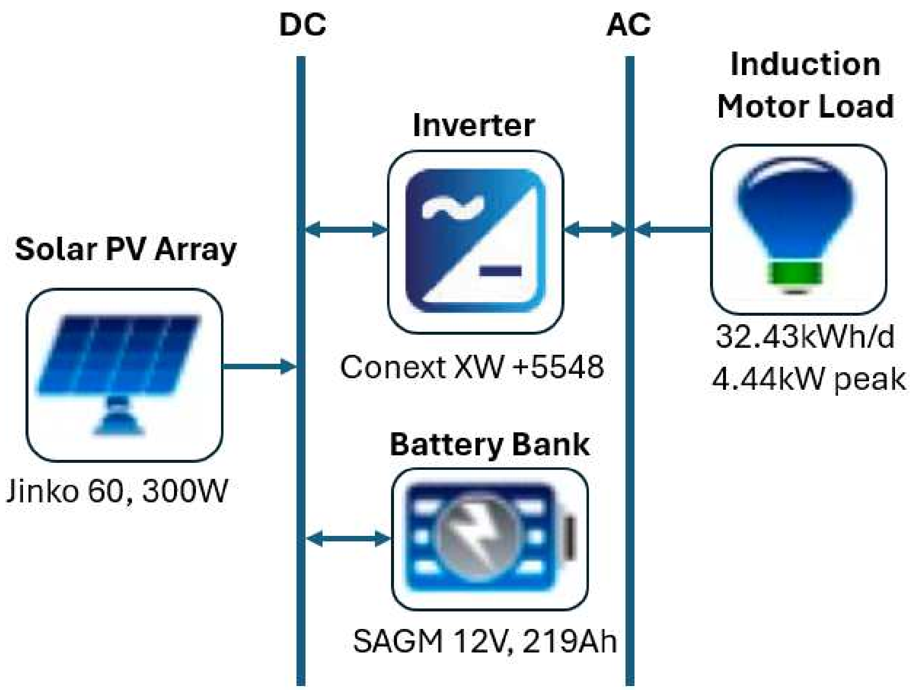

Figure 6.20. Schematic diagram of the proposed system

The conclusion from comparing various scenarios with continuous and intermittent pumping configurations using several criteria including net present cost, levelized cost of energy, total production, consumption, and excess electricity, is that continuous pumping with hybrid generation (solar PV, wind and battery storage) has the least unmet load and capacity storage with 0 kWh/yr of unmet load, capacity storage of 0.56 kWh/yr, a net present cost of $145,150.50, a levelized cost of energy of $0.51/kWh and an operating cost of $3056.04/yr; while intermittent pumping configuration with solar PV and battery system with 4.55 kWh/yr of unmet load, capacity storage of 11.70 kWh/yr, a net present cost of $64,969, a levelized cost of energy of $0.425/kWh and an operating cost of $1318/yr. Intermittent pumping with solar PV and battery system will be the chosen configuration for further design in this research because considering production from inactive oil wells (suspended and idle), the unmet load for the solar PV and battery system can be suitably accommodated in the pumping schedule as a trade-off to the significantly reduced cost in comparison to the solar PV, wind and battery storage system. Hence the solar PV and battery system would be adopted for powering the remote oil well. The system proposed by the author in [27] comprises a 27.3kW Solar PV array, and battery bank, comprising 64 units of deep cycle batteries, of 16 strings and 4 batteries per string. A system converter rated 4.49 kW and a load dispatch of cycle charging is implemented, implying that the primary load (electric motor) receives supply first and the excess generation goes to charge the battery bank. The elements and parameters of the solar PV supply are defined in Table 6.1, as defined in the previous design and feasibility study by the authors [27].

Table 6.1 Solar microgrid source.

Component	**Name**	**Size**
PV	Jinko eagle PERC60	27.3 kW
Storage	Deep cycle batteries, SAGM (12 V, 219Ah)	64 units (16 strings)
System converter	Schneider (Conext XW + 548)	4.49 kW
Dispatch	Cycle charging	

To analyze the system performance, robustness, and resilience under different environmental conditions, the average solar irradiance data obtained in January for winter and June for summer are extracted from the open-source Canadian Weather Energy and Engineering Climate (CWEC) data at [34] from the official website, and the average hourly daily temperatures are also available from [35, 36]. This research makes a novel contribution in considering the response of the system to varying environmental factors and changes in operational conditions, by performing parallel simulations of the key performance indicators for a "representative" or sample winter and summer months, January for winter and June for summer. The average solar irradiance and temperature data for summer and winter are respectively given in Tables 6.2 and 6.3. The plot of the hourly solar irradiance data is presented in Figure 6.21a,b.

Table 6.2. Average solar irradiance and temperature data for winter at Medicine Hat [34, 35]

Time (Hrs)	**Irr (W/m^2)**	**Temp (Deg. C)**
1	0	−7
2	0	−8
3	162	−8
4	752	−8
5	1239	−7
6	1548	−6
7	1657	−6
8	1558	−5
9	1260	−6
10	781	−7
11	198	−8
12	0	−9

Table 6.3. Average solar irradiance and temperature data for summer at Medicine Hat [34, 36]

Time (Hrs)	Irr (W/m^2)	Temp (Deg. C)
1	0	10
2	138	10
3	785	10
4	1513	12
5	2236	15
6	2904	19
7	3472	22
8	3900	23
9	4160	25
10	4234	25
11	4117	25
12	3817	27
13	3354	27
14	2760	27
15	2075	27
16	1347	27
17	624	26
18	60	24
19	0	21

Considering the data available from Tables 6.2 and 6.3 and the plots in Figure 6.21a,b, and scaling the data accordingly for 1 h ≡ 1 s for simulation, we can infer that there is significantly higher average hourly irradiance and correspondingly higher temperatures for the chosen location in the summer months than in winter.

Figure 6.22 shows the equivalent circuit diagram for the design, dynamic modelling, simulation, and control of a solar-powered sucker rod oil pump. The same system equivalent circuit design and model are adopted for summer and winter, with the output power wholly dependent on the daily solar irradiance and ambient temperature as shown in Tables 6.2 and 6.3, and Figure 6.21. The block diagram of the proposed system is shown in Figure 6.23.

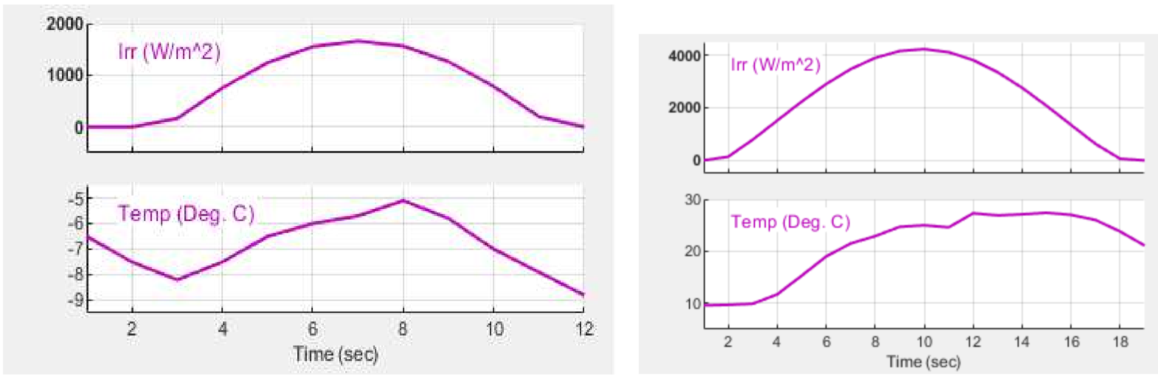

(a) (b)

Figure 6.21. Sample average daily solar irradiance and temperature data for Medicine Hat for winter and summer respectively. (a) Sample winter data (January). (b) Sample summer data (June)

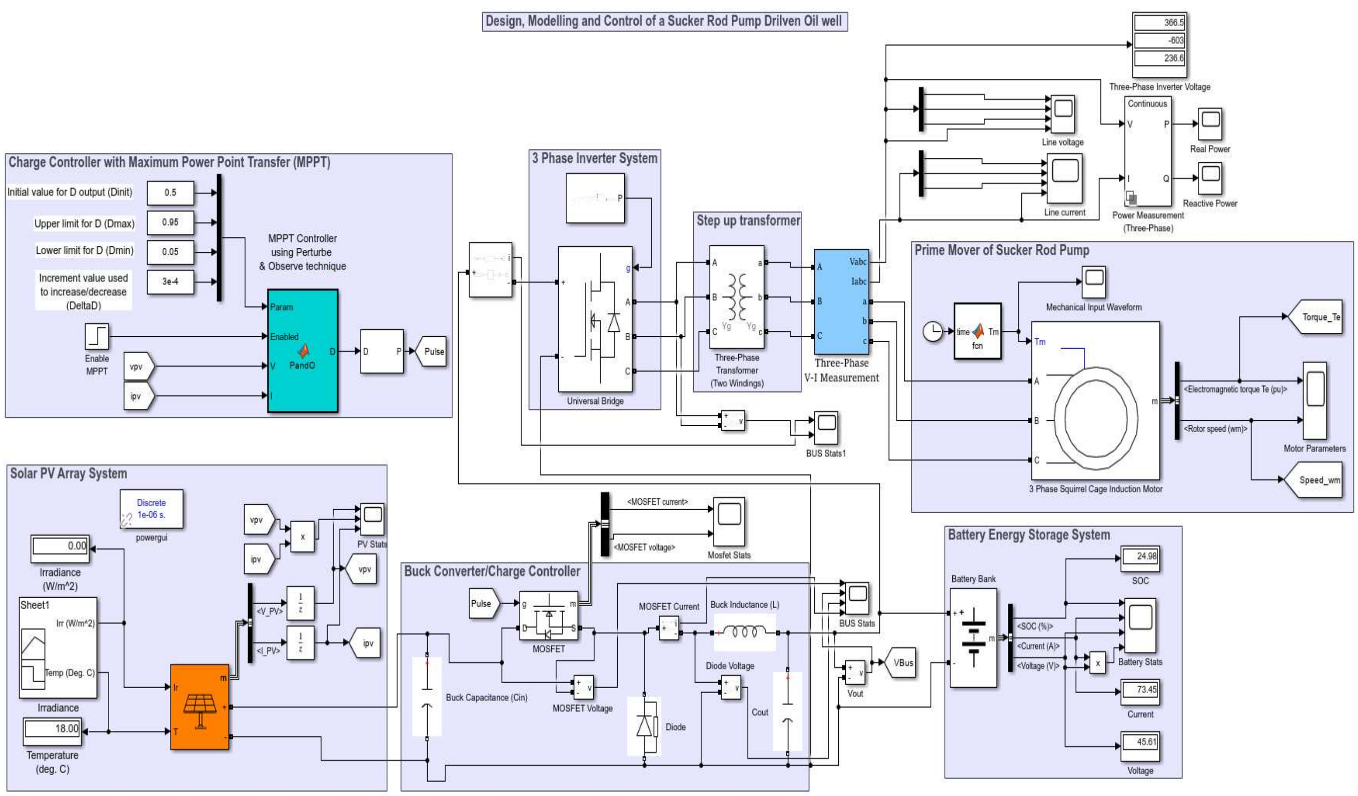

Figure 6.22. Circuit diagram showing subsystems modeled to achieve 100% microgrid

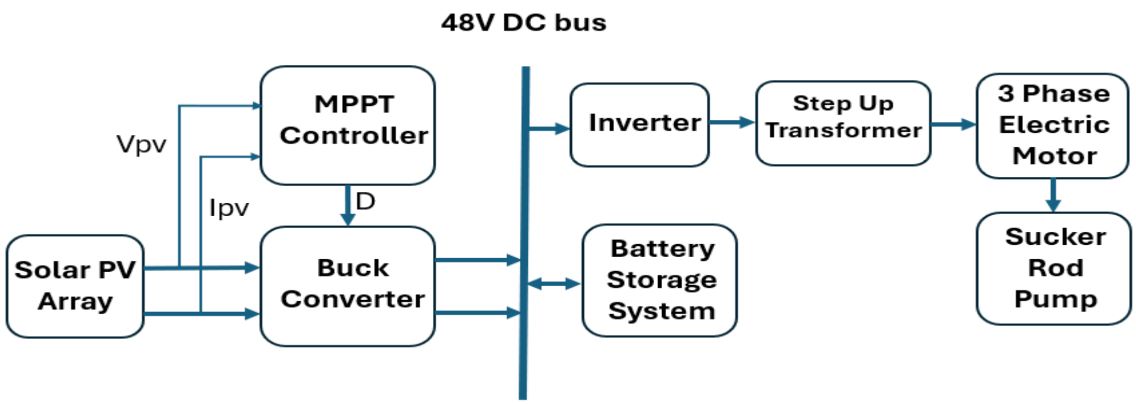

Figure 6.23. Block diagram of proposed solar PV microgrid

6.5.1 Solar PV System

The solar photovoltaic system consists of several modules combined in required numbers and configurations to generate sufficient direct current power from the solar irradiance received. To attain the required power configuration, the PV modules could be connected in series to form strings, this leads to an increase in the resulting voltage, while the current remains the same. Multiple strings could also be connected together to form solar PV arrays, leading to an increase in current while the voltage remains the same. There are several types of solar cells for PV systems, and this affects the behavior, performance, and efficiency of the resulting PV array. Environmental factors such as the ambient temperature and solar irradiance also affect the performance of selected modules as shown by the Current-Voltage (I–V) and Power-Voltage (P-V) curve of the 60-cell, 300W PV module in Figure 6.24.

The PV cells selected for this study are Passive Emitter and Rear Contact (PERC), a new technology designed to achieve a (1–2)% higher energy conversion efficiency, due to the added dielectric passivation layer on the cell's rear. To determine the I-V and P-V characteristics curve, the PV cell's output current I_{PV} is given by Kirchhoff's current law as Equation (2).

$$I_{PV} = I_{ph} - I_D - I_{sh} = I_{ph} - I_O\left[\exp\left\{\frac{q(V_{PV}+R_S I_{PV})}{nkT}\right\} - 1\right] - \frac{(V_{PV}+R_S I_{PV})}{R_{sh}} \quad (2)$$

Where I_{ph}, I_D and I_{sh} represent photogenerated current which increases with light intensity, diode current that accounts for internal recombination losses and leakage current across shunt resistance of parallel paths respectively. I_O is the reverse saturation current, n is the diode ideality factor, q is the elemental charge, k, Boltzmann constant, T, absolute temperature (K), where, R_s and R_{sh} are series resistance (preferably very small) and shunt resistance (preferably very large) as shown on the equivalent circuit of the solar PV cell in Figure 6.25.

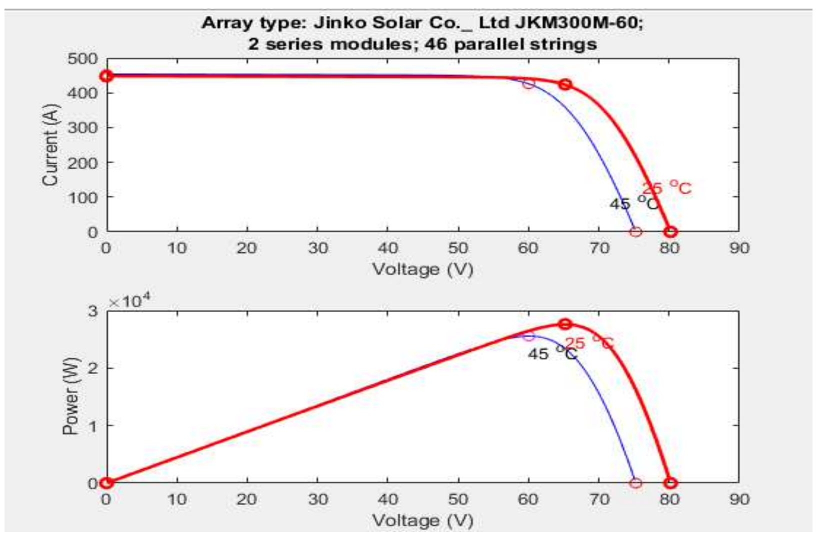

Figure 6.24. Output power and current of the PV versus voltage

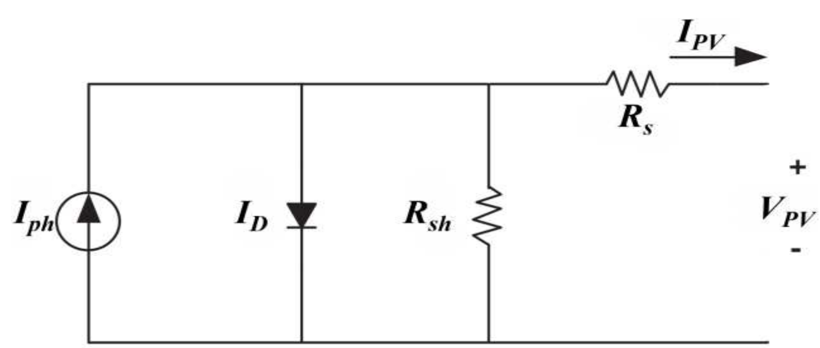

Figure 6.25. Equivalent circuit model of single PV cell

To obtain the required DC bus voltage (48V) and the target power of the array (27.3kW), we consider the number of parallel strings and the number of series-connected modules per string. Each 60-cell solar panel has a voltage at a maximum point V_{mpp} of 32.6V, sufficient for reliably charging a 24V battery system, which needs over 30V to charge. The system uses two 60-cell solar panels connected in series. Given a PV rating of 27.3kW, and a maximum power per module of 300W. The total number of solar PV panels required is theoretically 27.3kW divided by 300W which equals 91. Using an average of 24V per panel and series-connected modules per string N_s of 2 (panels in series), we have a minimum series voltage (V_{in-min}) of 48 volts, and given V_{mpp} of 32.6, we get a maximum series voltage (V_{in-max}) of ~66V. The range of output voltage for the PV system is thus (48-66) V. Given 2 series-connected modules per string and 91 panels, the number of parallel string pairs N_p will be 91 divided by 2, which is ~ 46. Given a PV rating of 27.3kW, and a minimum series voltage (V_{in-min}) of 48.

From the Array specifications in Figure 6.26, we can infer that the theoretical maximum power that can be reliably extracted from the solar PV array is given by Equation (3) [37]:

$$\begin{aligned} P_{mpp} &= (N_p \times I_{mpp}) \times (N_s \times V_{mpp}) \qquad [37] \qquad (3) \\ &= (46 \times 9.21) \times (2 \times 32.6) \approx 27.6\,kW \\ &= Total\ Number\ of\ modules \times Maximum\ Power\ per\ module \\ &= (46 \times 9.21) \times (2 \times 32.6) \\ &\approx 27.6\,kW \end{aligned}$$

The Solar PV array design specifications for modelling are given in Figure 6.26. The parameters for the design and sizing of the Solar PV source are presented in Table 6.4.

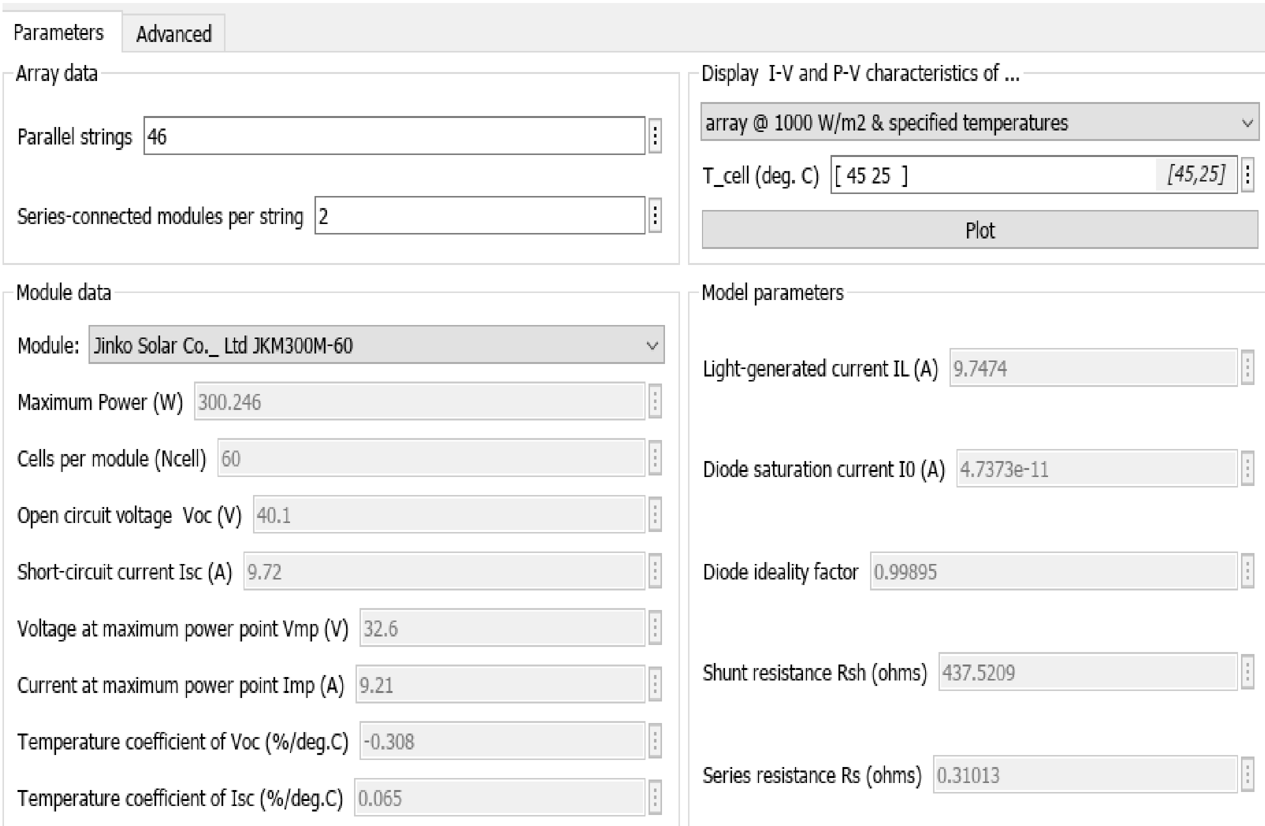

Figure 6.26. Solar PV array design specifications for modelling

Table 6.4 Solar PV System Parameters

System Parameters	**Ratings**	**Unit**
Module Peak Power of a Single Module (P_{mp})	300.25	W
Module Open Circuit Voltage (V_{oc})	40.1	V
Module Short Circuit Current (I_{sc})	9.72	A
Module Voltage at MPP (V_{mp})	32.6	V
Module Current at MPP (I_{mp})	9.21	A
Array Peak Power (P_{mp})	27.6	kW
Array Open Circuit Voltage (V_{oc})	80.2	V
Array Short Circuit Current (I_{sc})	447.12	A
Array Voltage at MPP (V_{mp})	65.2	V
Array Current at MPP (I_{mp})	423.66	A

6.5.2 DC-DC Buck Converter

DC-DC converters are essential components in photovoltaic systems, acting as intermediaries that optimize power transfer through impedance matching. These devices enable maximum power point tracking by dynamically adjusting their duty cycles, allowing the system to operate at its most efficient point on the current-voltage characteristic curve. The buck converter stands out as a particularly effective topology when DC voltage reduction is needed between source and load. This makes it especially suitable for systems where PV module output voltage exceeds battery charging requirements as in this design. From Figure 6.27, when the switch activates, the output capacitor begins charging, the inductor regulates the current flow, creating a controlled charging process, and the capacitor voltage rises gradually throughout each switching cycle. This configuration enables efficient voltage step-down while maintaining stable output characteristics, making it ideal for renewable energy applications where precise voltage control is crucial for system performance. The bus voltage is 48V, and the range of output voltage for the PV system is (48-66) V hence a buck converter is required. Where V_{in-min} and V_{in-max} are minimum and maximum input voltages, V_{out} and I_{out} are output voltage and currents, f is the switching frequency, and V_{in} is the sample input voltage. Given the transfer function of a Buck converter from [38] where $V_{out} = 48V, V_{in} = 66V$, minimum input capacitance used $C_{in} = 4740\mu F$, minimum inductor value is $L_{Buck} = 17.319\mu H,$ while the output capacitance $C_{Out} = 5924.48\mu F.$ The output voltage is held constant at 48V, while the input voltage from the PV array at MPPT ~ 66V. The equivalent circuit diagram of the buck converter design is shown in Figure 6.27. The parameters for the design and sizing of the charge controller implemented as a DC-DC buck converter are presented in Table 6.5.

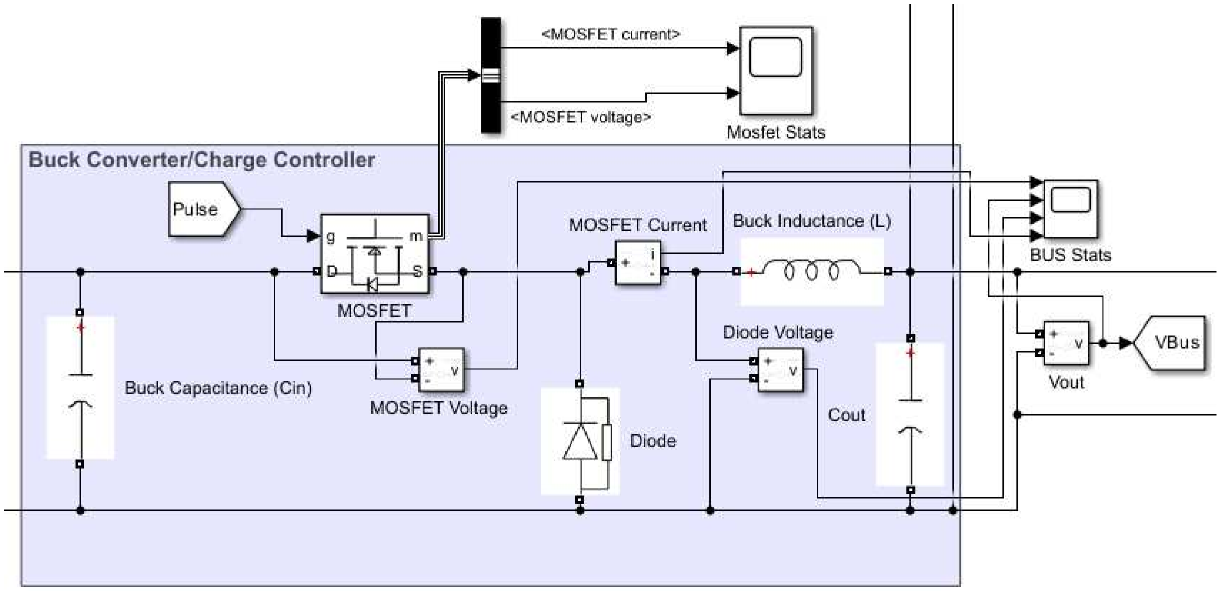

Figure 6.27. Equivalent circuit of Buck Converter for charge control and MPPT implementation.

Table 6.5 Buck Converter System Parameters

System Parameters	Ratings	Unit
Input Voltage at MPPT (V_{in})	66	V
Frequency (f)	5	kHz
Buck Inductance (L_{Buck})	17.32	µH
Buck Capacitance (C_{Buck})	4740	µF
Output Capacitance (C_{out})	5924.48	µF
Output Voltage for bus (V_{out})	48	V

6.5.3 MPPT Charge Control

Environmental factors such as shading, cloudiness, dust, snow accumulation, solar irradiance, ambient temperature, and operational conditions such as varying load impedance, battery charging conditions, and PV system configuration (string vs array) directly influence the power that can be extracted from the solar PV array relative to the voltage across its output. A maximum power point charge controller is deployed to dynamically adjust the system's operating point on the P-V curve in order to extract maximum power from the solar PV source, required to drive the sucker rod pump and charge the battery. The MPPT algorithm varies the duty cycle of the DC-DC buck converter, hence changing the effective impedance of the load across the buck converter. This adjusts the voltage of the solar PV source and ultimately controls the output power the array delivers. The Perturb and Observe (P&O) method operates by making small, deliberate adjustments to the PV array's operating voltage and monitoring the resulting power output changes. The controller systematically modifies the voltage in discrete steps, analyzing how each change affects the array's power production as seen in Figure 6.28.

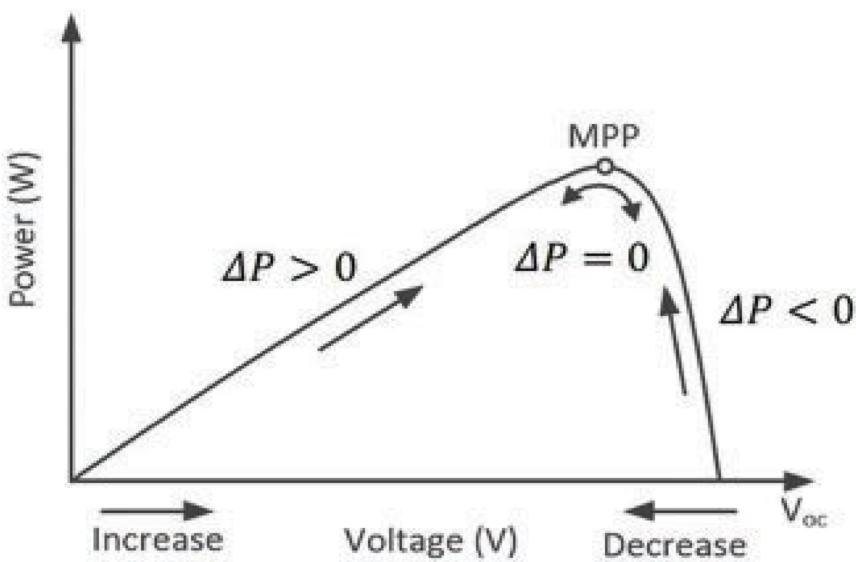

Figure 6.28. MPPT controller using perturb and observe (P&O) algorithm

This iterative process is shown in Figure 6.29 and continues, with the system adjusting the voltage either upward or downward, until it identifies the optimal operating point where maximum power extraction occurs.

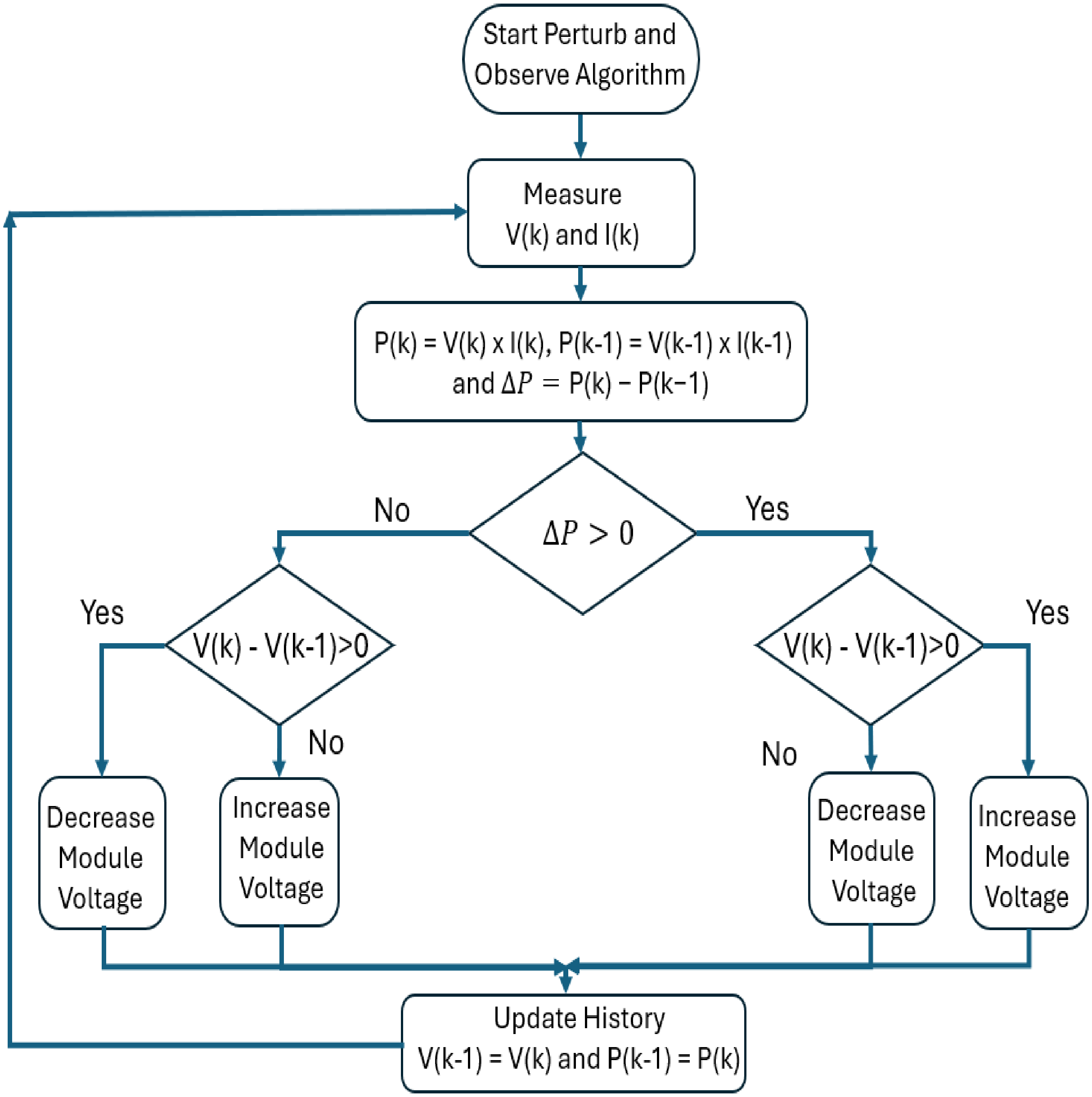

Figure 6.29. Flow chart and representation of perturb and observe (P&O) algorithm for MPPT

The algorithm deployed in Simscape maintains this exploration pattern, constantly fine-tuning the operating point to ensure the PV array delivers its peak performance despite varying environmental conditions. The representation of the P&O algorithm for MPPT in Simscape is shown in Figure 6.30.

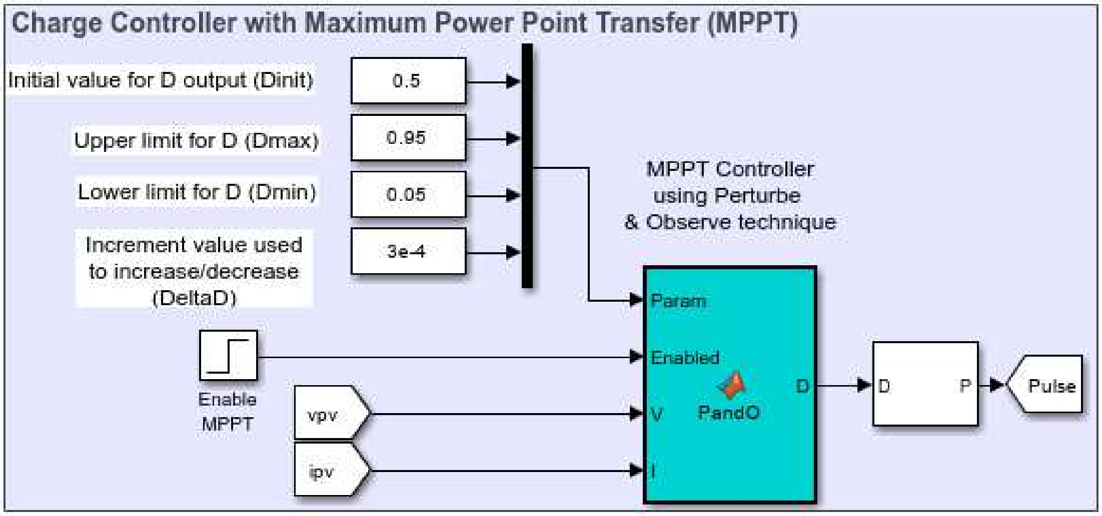

Figure 6.30. Perturb and observe algorithm with MPPT strategy in Simscape

6.5.4 Battery Energy Storage System (BESS)

The battery energy storage system consists of a total of 64 lead-acid batteries, made up of 4 batteries per string, grouped as 16 strings of lead-acid batteries, and the DC-DC buck converter serves as the battery charge controller. The battery stores excess electricity during periods of high PV power output and augments the system when there is a shortfall in generated power due to adverse environmental and operating conditions. Given the capacity per battery is 219 Ah, the rated capacity for 16 strings is 219 *16 = 3504 Ah.

The total amount of energy that the battery bank can store and release under optimal conditions is given by the nominal capacity, and for 64, 12 V batteries of 219 Ah current capacity, the nominal capacity is 64*12*219 = 168,192 VAh or 16.192 kWh. The rated current capacity is nominal capacity divided by bus voltage (16.192 kWh/48 V) = 3504 Ah. The parameters for the design and sizing of the battery energy storage system (BESS) are given in Table 6.6 and Figure 6.31. The equivalent circuit for modelling the BESS is presented in Figure 6.32.

Table 6.6 BESS parameters.

Battery bank data	Ratings	Unit
Number	64	(4 bt/string)
Strings in parallel	16	Strings
Bus voltage	48	V
Nominal capacity	168	kWh
Usable nominal capacity	118	kWh
Energy in	3860	kWh/yr
Energy Out	3294	kWh/yr

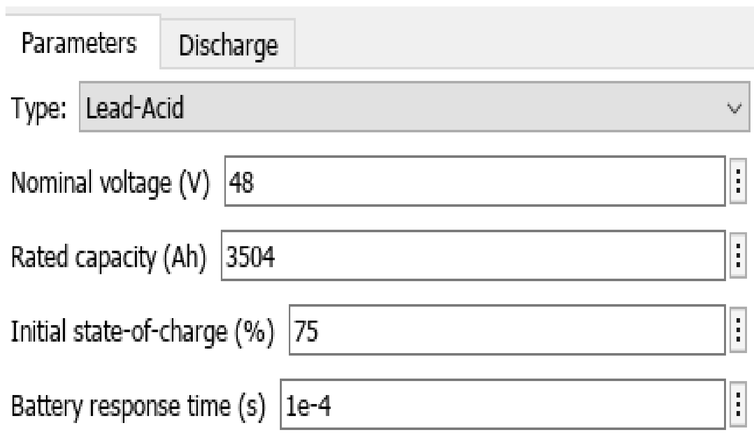

Figure 6.31. Design specifications of BESS

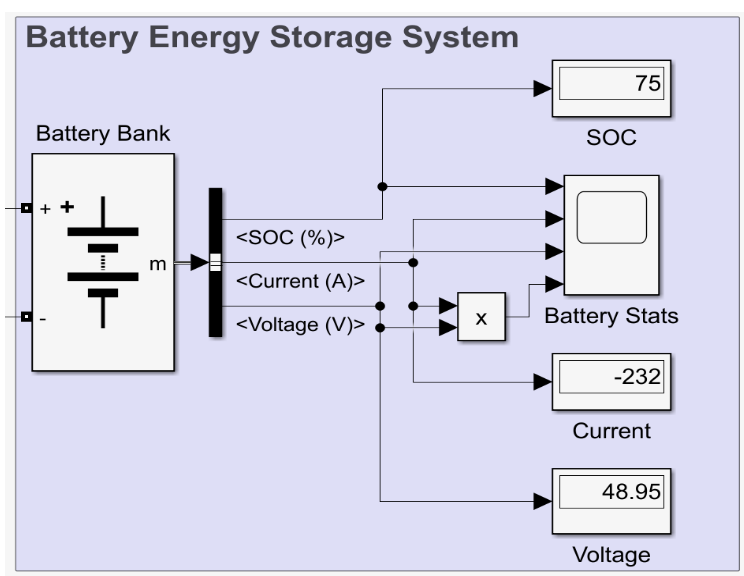

Figure 6.32. Equivalent circuit of battery energy storage system

6.5.5 Power Conditioning System

The power conditioning system consists of a 3-phase inverter for converting the DC from the solar PV source to alternating current in the charging cycle during the day, and for converting stored DC battery power into AC during the discharging cycle at low irradiance. A three-phase two-winding transformer also transforms the low voltage, high current inverter output, into a high voltage, low current output, suitable for the three-phase squirrel cage induction motor. To relate the DC bus voltage to the AC line-to-line voltage output, we use the formula:

$$m \times \frac{V_{DC}}{\sqrt{2}} = \mathrm{V}_{L-L(rms)} \tag{4}$$

The step-up transformer has a voltage transformation ratio ($\frac{V_1}{V_2}$) of 30/460 and the line-to-line rms voltage, hence the RMS inverter output voltage $\mathrm{V}_{L-L(rms)} = m \times 0.7071 \times V_{DC}$, assuming modulation index is m = 1.0. The inverter system has a bus input voltage of ~48V,

$$\mathrm{V}_{L-L(rms)} = 0.7071*48 = 33.84\mathrm{V}.$$

To supply the power required by the electric motor, a step-up transformer of 7 kVA, and a primary to secondary voltage ratio of 30/460 at 60 Hz are selected and deployed. The equivalent circuit for modelling the power conditioning system is presented in Figure 6.33a. The parameters for the design and sizing of the power conditioning system are given in Table 6.7 and Figure 6.33b.

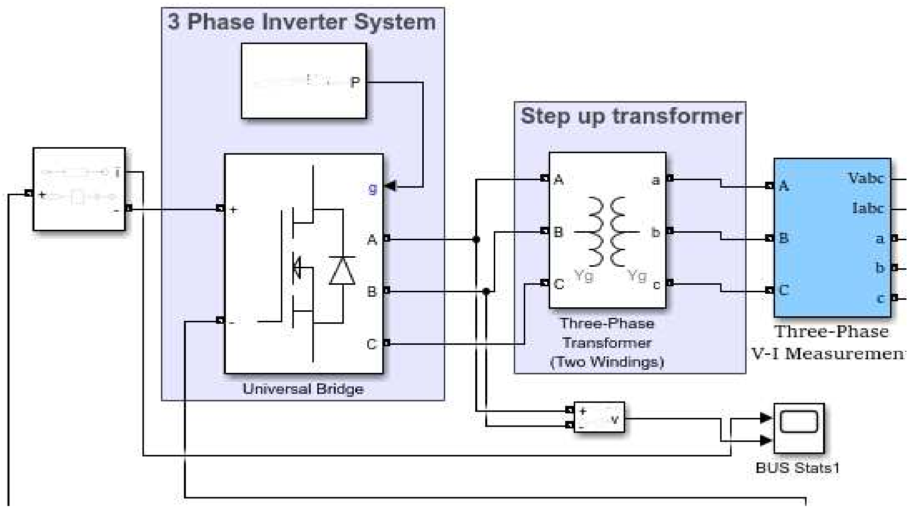

(a)

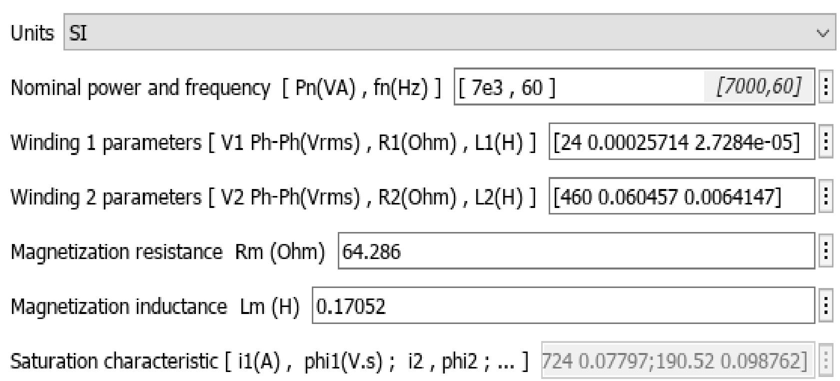

(b)

Figure 6.33. An equivalent circuit of a power conditioning system for the induction motor load. (a) Equivalent circuit of a power conditioning system. (b) Design parameters

Table 6.7. Power conditioning system parameters.

Power Conditioning System Parameters	**Ratings**	**Unit**
Primary Voltage (V_1)	30	V
Secondary Voltage (V_2)	460	V
Frequency (f)	60	Hz
RMS Line-to-Line Voltage $V_{L-L(rms)}$	33.84	V
Nominal Power	7	kVA
Modulation index, m (assumed)	1	

6.5.6 Mechanical Waveform Input

The mechanical torque profile of the induction motor is defined by the sinusoidal waveform shown in Figure 6.34. It defines the parameters for the pump torque profile as per unit. The pump operates in a cyclic motion to lift oil from the subsurface. The torque requirement of the motor fundamentally varies throughout each stroke cycle due to the higher torque needed to lift the fluid column in the upstroke and the lower torque required in the down stroke as gravity assists the motion. The mechanical torque function block T_m simulates the mechanical input torque for the balanced operation of the motor, accounting for the impact of the counterbalance weights in the up-stroke, hence the waveform is symmetrical.

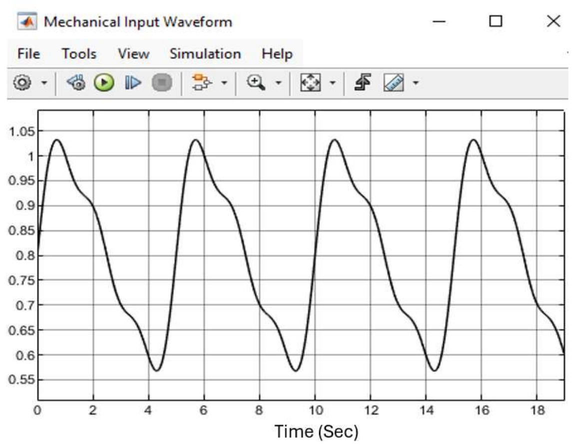

Figure 6.34. The waveform of mechanical torque requirement of Squirrel cage induction motor

6.5.7 Load System.

The electrical motor system is a three-phase, squirrel cage, induction motor that operates at a line-to-line voltage of 460 volts receiving power from the solar PV system and driving the mechanical load of the sucker rod pump. The theoretical peak load is 4.44 kW. Considering the output mechanical power of the squirrel cage induction motor type AEEAFP (067R50) from [39] rated 7.5 hp, 1110 full load rpm, at a frequency of 60 Hz, with power factor of 0.83 and full load current and efficiency of 10 A and 83.5% respectively. The full load torque is 35.4 lb-ft at nominal power P_n (kVA) rating is (7.5*0.7457)/(0.83) = 6.74 kVA, with a safety factor (SF) of 1.15. Number of poles p = 120*f/N_s = (120*60)/1200 = 6 poles (3 pole pairs). The parameters for the sizing of the 3-phase squirrel cage induction motor are given in Table 6.8.

Table 6.8 Nameplate of 3-phase induction motor parameters

Motor Parameters	**Ratings**	**Unit**
Line-to-line Voltage	460	V
Full Load Current	10	A
Peak Load	4.44	kW
Rated Power	7.5	hp
Full load speed	1110	rpm
Full load torque	35.4	lb-ft
Efficiency	83.5	%
Power factor	0.835	
Safety factor	1.15	

The peak power available to the squirrel cage induction motor load = 0.835 (7.5*0.7457) = 4.67kW, which is sufficient to drive the sucker rod pump load of peak load 4.44kW. The equivalent circuit of the electric motor load system is presented in Figure 6.35.

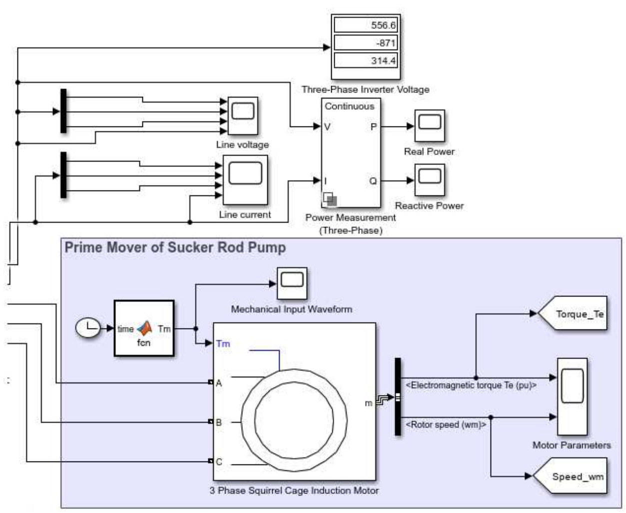

Figure 6.35. Equivalent circuit of the squirrel cage Induction motor prime mover.

6.6 Analysis of Results

The simulation examines system performance under changing environmental conditions. The impact of solar irradiance in W/m^2 and the ambient temperature in degrees Celsius are simulated. The location of interest is an idle well in the town of Medicine Hat in Alberta, Canada as presented in a previous work by the authors [27]. As expected in the northern hemisphere, the average hourly solar irradiance, average hourly temperature and the length of daytime solar exposure is generally higher in summer than in winter. Using June as a sample summer month in Medicine Hat, it is shown to have longer daytime hours and higher levels of solar irradiance, with warmer temperatures. In comparison with January taken as a sample winter month which is observed to have shorter hours and lower levels of solar irradiance, at lower temperatures. The impact of weather and environmental fluctuations on the system's effectiveness is carefully studied and presented in Figures 6.36 – 6.40. Key measured parameters reveal that overall system performance remains robust and satisfactory during steady-state operation, with momentary deviations staying within design parameters.

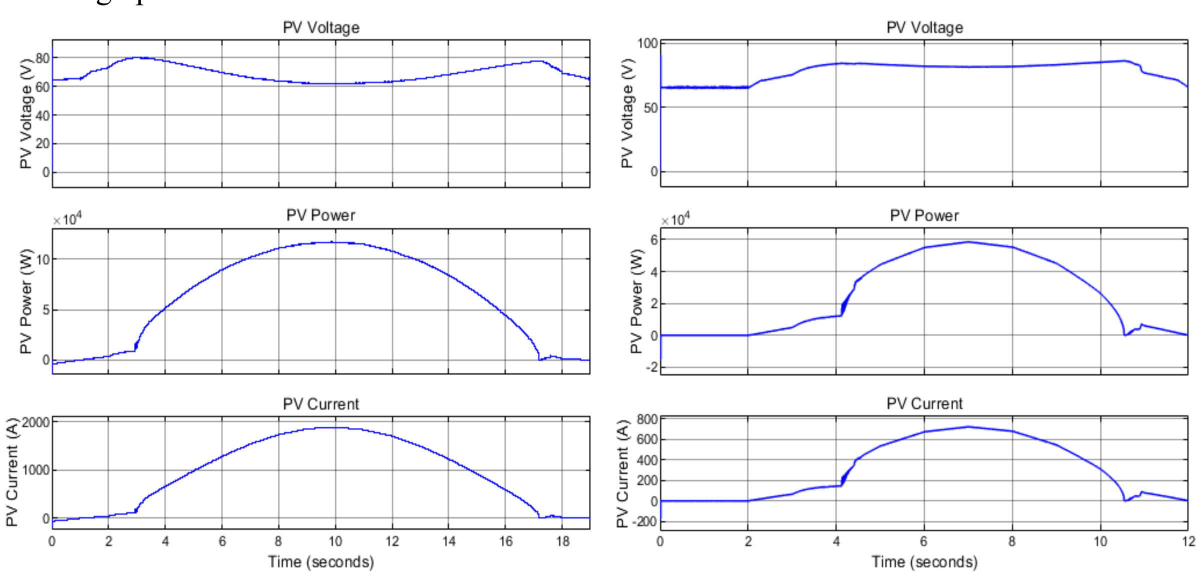

(a) (b)

Figure 6.36. Solar PV voltage, current, and power. (a) Summer. (b) Winter

The maximum power point tracking system implemented with the solar PV source continuously monitors the incremental changes in the power generated and compares with the incremental voltage changes, ensuring that the maximum power is being received by the electric motor and the excess power generated is provided to charge the battery energy storage system. This is achieved by effectively matching of the source to load impedance and facilitating maximum transfer of power from the solar PV source to the load. As environmental parameters shift, the tracker identifies new optimal operating points, supplying the power needed to provide the needed motor torque and maintain optimal performance despite the fluctuating power availability from the solar PV array. This ensures that sufficient charging current is delivered to the energy storage system to maintain the bus voltage. As shown in the state of charge from Figure 6.37, at low solar irradiance, the battery supplies the energy required to sustain production and drains, while during the day, it charges, while the load receives the energy required to sustain production.

From Figure 6.37, the current, voltage and power of the battery energy storage system are steady, predictable and consistent with the expected behavior for steady state operation. Considering state of charge, in summer it increases gradually from ~75% to ~90% over 19 s, while winter shows similar upward trend from ~75% to ~85% over 12 s. Considering current and voltage stability, both seasons show relatively stable current oscillating around $\pm 2 \times 10^5$ A, voltage

remains consistent around 60–80 V in both cases. Winter profile shows slightly less fluctuation in both parameters. The power fluctuates between approximately -2×10^7 to 2×10^7 W. The plot shows similar power profiles between seasons though winter shows marginally less variation, both maintain consistent power delivery despite seasonal differences. Although summer profile runs longer (19 s vs 12 s), winter shows slightly more stable parameters with less fluctuation, winter also achieves lower maximum SOC (~85% vs ~90%) and demonstrates marginally better parameter stability overall. This comparison suggests the battery system maintains reliable performance across seasonal variations, with winter operation showing slightly more stable characteristics despite shorter operating duration.

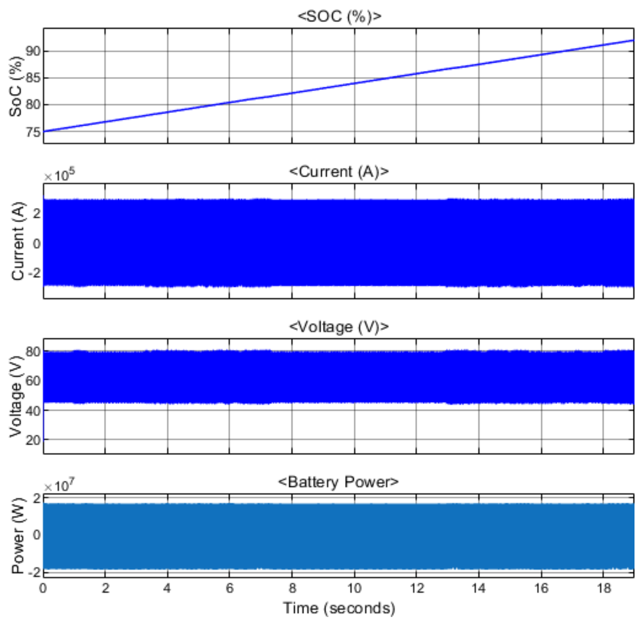

(a)

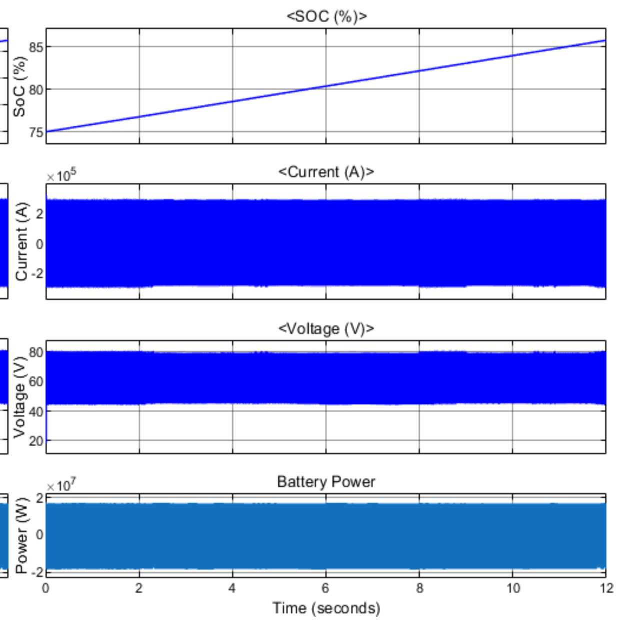

(b)

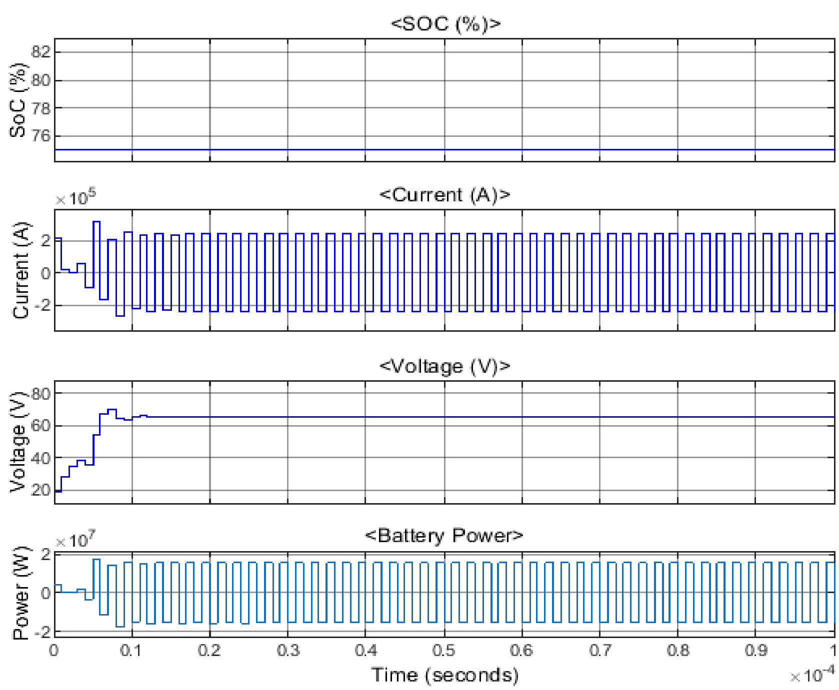

(c)

Figure 6.37. Battery state of charge (SOC%), current, voltage, and power for battery energy storage system. (a) Summer. (b) Winter. (c) Battery parameters (higher resolution)

The pulsating direct current (DC) power supply (from the solar PV system and the battery backup) is converted to alternating current (AC) by the three-phase inverter system and the sinusoidal line voltages and line currents received by the three-phase squirrel cage induction motor are given in Figure 6.38a,b, respectively.

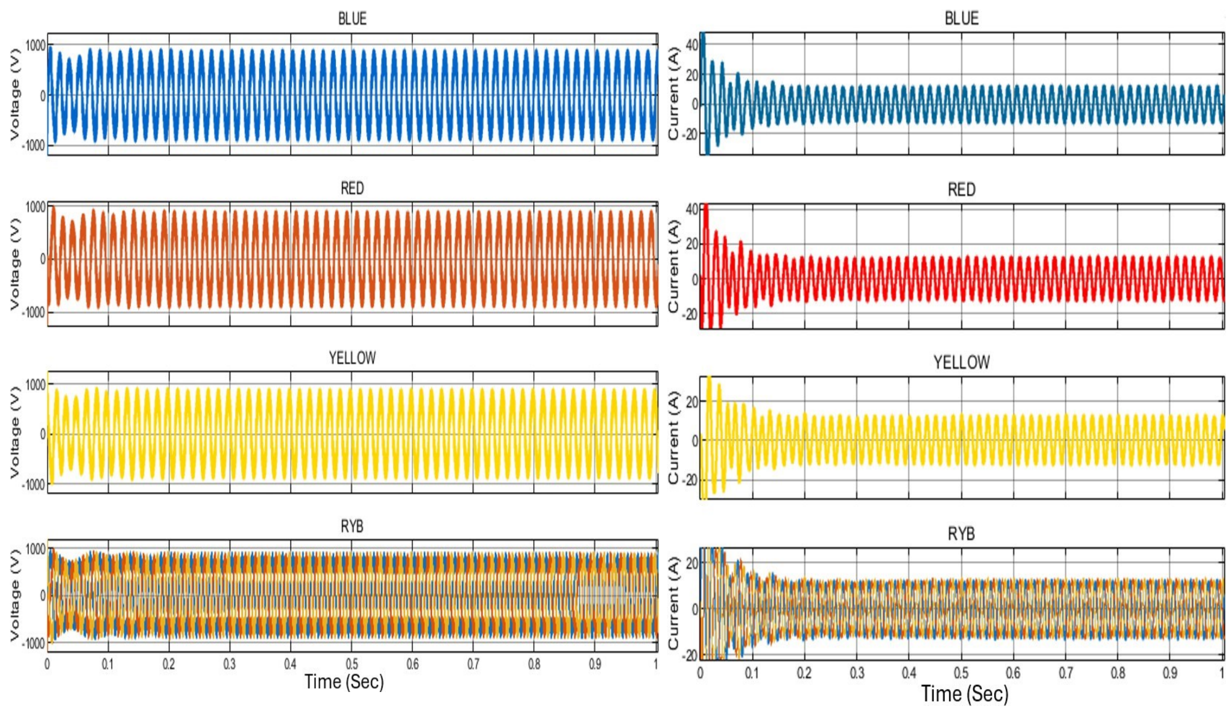

(a) (b)

Figure 6.38. Similar sinusoidal load current and voltage I_{RYB}, V_{RYB} for summer and winter.
(a) Sinusoidal load voltage V_{RYB}. (b) Sinusoidal load current I_{RYB}.

The active and reactive power of the induction motor in summer and winter is presented in Figures 6.39 and 6.40. The load is observed to have significant reactive power demand. Comparing Figures 6.39a and 6.40a, summer is observed to have more pronounced variations in its real power demand compared to winter and comparing Figures 6.39b and 6.40b, summer also shows periodic sharp transitions in the reactive power demand.

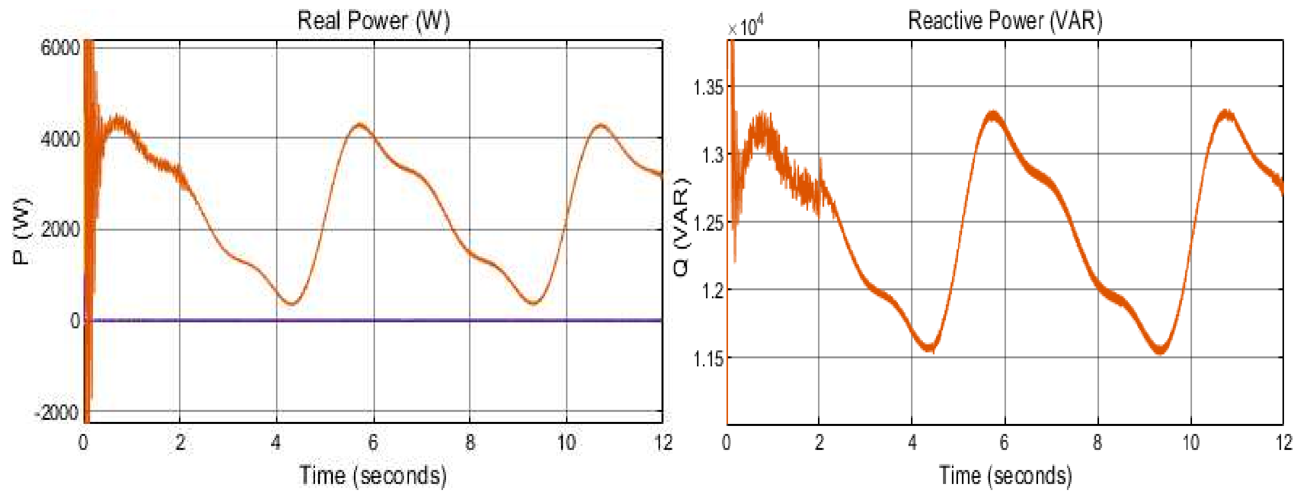

(a) (b)

Figure 6.39. Similar real and reactive power demand for winter.

(a) Real power demand. (b) Reactive power demand

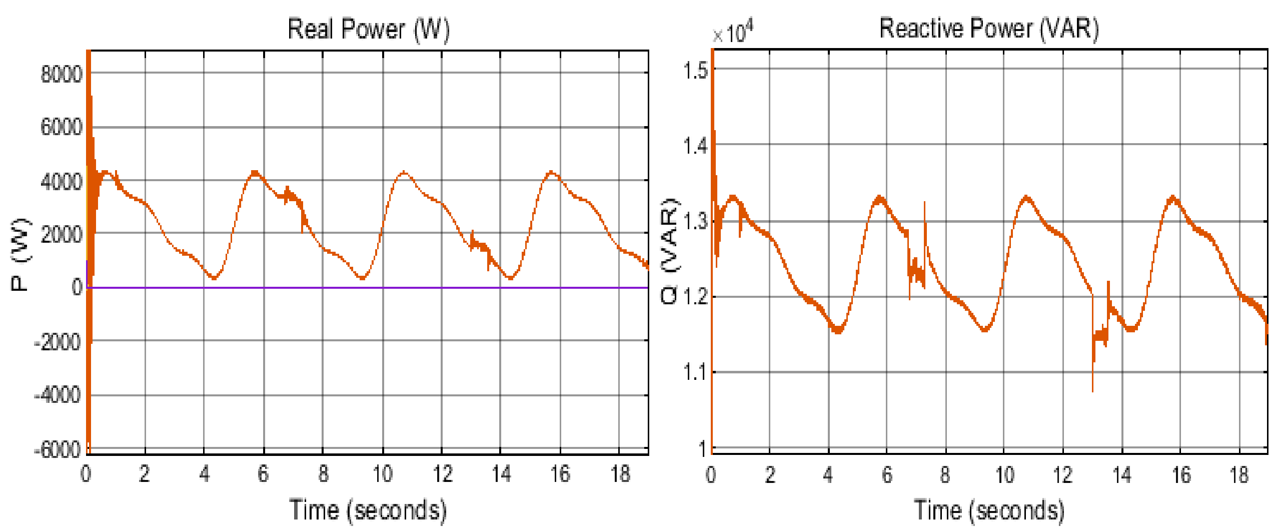

(a) (b)

Figure 6.40. Similar real and reactive power demand for summer.

(a) Real power demand. (b) Reactive power demand

Per unit torque and speed characteristics of the 3-phase squirrel cage induction motor are given in Figure 6.41. The system reaches a relatively stable operating point after the initial transient period.

The persistent torque oscillations indicate mechanical system dynamics due to the sucker rod load fluctuations.

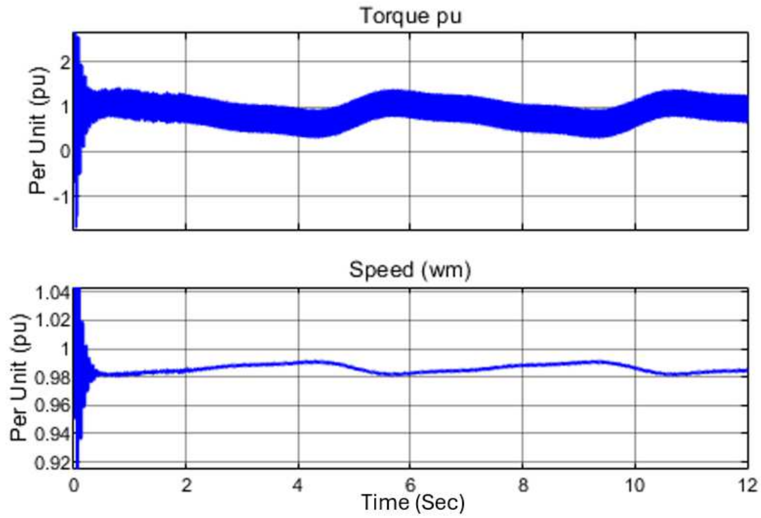

Figure 6.41. Similar torque and speed characteristics for summer and winter

From the analysis of incorporating the representative solar irradiance and temperature data for the location, the design ensures that the required load current and voltage are sustained, irrespective of environmental fluctuations, and the real power from the solar PV array and battery storage is demonstrated to be sufficient to drive the load and charge the battery. It can be inferred that the lower power output anticipated due to reduced irradiance levels for winter is compensated for by the improved semiconductor efficiency at cold temperatures. Correspondingly, higher energy generation due to increased irradiance and longer days in summer are counterbalanced by temperature-induced efficiency losses during peak heat periods.

The results of the simulations indicate that the Simscape/Simulink model provides a detailed representation of sucker rod pump dynamics. Simulating mechanical and electrical microgrids within a single framework, this offers significant advantages for understanding and optimizing pump performance. The integration of summer and winter irradiance and temperature data in the analysis provides a clear indication of the system's performance under various environmental and operational conditions. The MPPT battery charge control strategies further enhances the model's capability to optimize performance under varying load conditions, while the energy storage system ensures the load demands can still be met at lower irradiance levels and durations. The integrated model of the solar powered sucker rod pump is presented in Figure 6.42, showing the various subsystems modeled in this research work. The comprehensive system model for an oil well pumping system, integrates electrical, mechanical, and hydraulic components in a single unified design. The schematic diagram emphasizes the power transmission path from electrical input through mechanical systems to the final pumping action. Although the subsurface pump and downhole tubing subsystem are included in the schematic, analysis and visualization of the metrics in this subsystem is beyond the scope of this research.

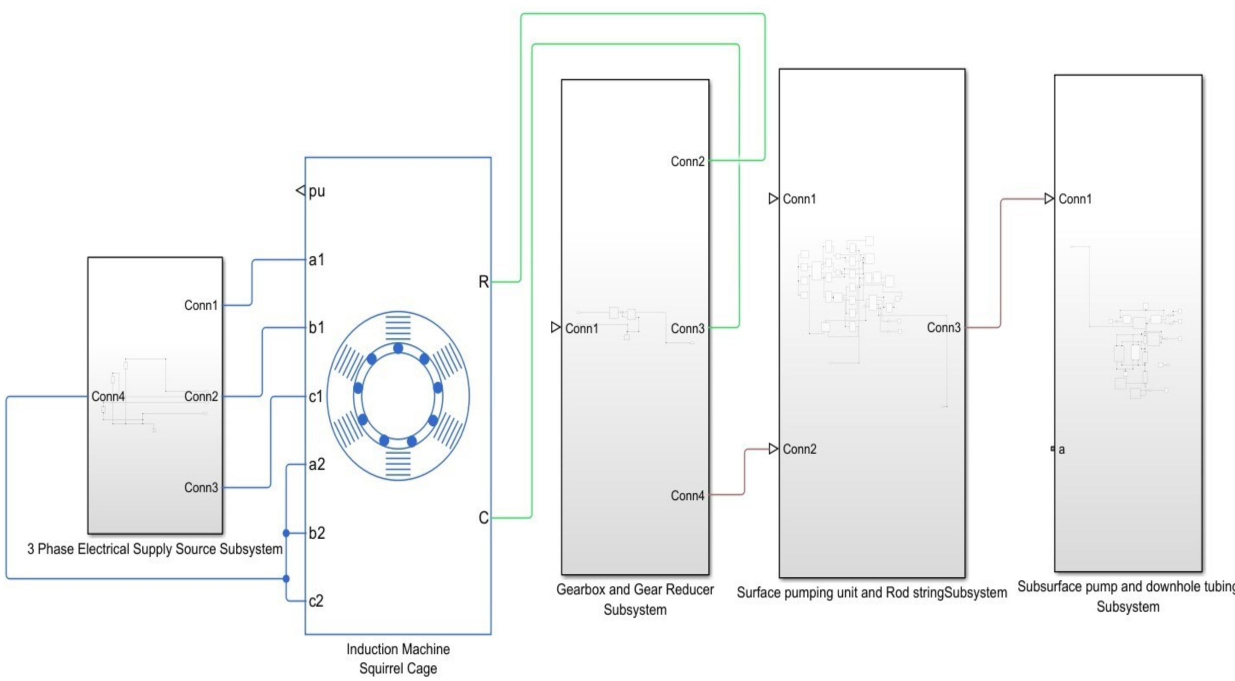

Figure 6.42. Schematic diagram of integrated sub-systems in model-based simulation

6.7 Conclusion

The integrated design, modelling, simulation, and control of a solar-powered sucker rod oil well within a single simulation environment offers significant advantages for understanding and optimizing sucker rod pump systems. This comprehensive study focuses on developing an integrated model for solar-powered sucker rod pumps, integrating both mechanical and electrical subsystems to optimize overall performance. The research employs a systematic approach by decoupling the microgrid into distinct subsystems, enabling detailed analysis and efficiency improvements from the solar PV source through to the electric motor load. The methodology combines modelling tools including SolidWorks for mechanical design and Simscape for electrical characteristics, creating a digitally representative model that facilitates system optimization before physical implementation. The integration of energy storage solutions and control systems, coupled with extensive simulation testing under various scenarios, demonstrated reliable operation despite ambient temperature variation and solar intermittency, while providing a robust framework for performance evaluation and system refinement. Key performance indicators such as solar PV power, battery power, bus voltage, step-up transformer rating, and real and reactive power requirements of the sucker rod pump system are visualized in the model. The files and intellectual property created in executing this research are shared by the author and available from [40].

6.8 Organization of The work

This work is a comprehensive study of the design, dynamic modelling, simulation and control of a sucker rod oil pump and its integration with a solar power system. The content is organized into several main sections and subsections. The chapter begins with an introduction and objectives, followed by a system description. The methodology forms the core of the work, divided into four main parts: modelling the sucker rod pump in SolidWorks and Simscape, detailed analysis of model-based subsystems, methodology for modelling a solar-powered sucker rod oil pump, and PV system design. Each of these sections is further broken down into specific components and processes, such as the prime mover, gearbox, surface pumping unit, and subsurface pump for the sucker rod system, and various elements of the solar power system including the PV array, DC-DC converter, MPPT charge control, and battery storage. The research concludes with an analysis of the simulation outcome, providing a logical flow from conceptualization and modelling to results analysis.

6.9 Conflict of interest

The authors declare no conflict of interest.

6.10 References

[1] Kang, M., Brandt, A.R., Zheng, Z., Boutot, J., Yung, C., Peltz, A.S. and Jackson, R.B., 2021. Orphaned oil and gas well stimulus—Maximizing economic and environmental benefits. Elem Sci Anth, 9(1), p.00161.

[2] El Hachem, K. and Kang, M., 2023. Reducing oil and gas well leakage: a review of leakage drivers, methane detection and repair options. Environmental Research: Infrastructure and Sustainability, 3(1), p.012002.

[3] Anglani, N., Di Salvo, S.R., Oriti, G. and Julian, A.L., 2020, June. Renewable energy sources and storage integration in offshore microgrids. In 2020 IEEE International Conference on Environment and Electrical Engineering and 2020 IEEE Industrial and Commercial Power Systems Europe (EEEIC/I&CPS Europe) (pp. 1-6). IEEE.

[4] Raimi, D., Krupnick, A.J., Shah, J.S. and Thompson, A., 2021. Decommissioning orphaned and abandoned oil and gas wells: New estimates and cost drivers. Environmental science & technology, 55(15), pp.10224-10230.

[5] Takacs, G., 2015. Sucker-rod pumping handbook: production engineering fundamentals and long- stroke rod pumping. Gulf Professional Publishing.

[6] Fakher, S., Khlaifat, A., Hossain, M.E. and Nameer, H., 2021. A comprehensive review of sucker rod pumps' components, diagnostics, mathematical models, and common failures and mitigations. Journal of Petroleum Exploration and Production Technology, 11(10), pp.3815-3839

[7]Alberta Energy Regulator (AER) n.d., 'Methane Reduction', viewed 27 November 2024, https://www.aer.ca/protecting-what-matters/protecting-the-environment/methane-reduction.

[8] Alberta Energy Regulator (AER) n.d., 'Well Status', viewed 27 November 2024, https://www.aer.ca/providing-information/data-and-reports/data-hub/well-status.

[9] Schiffner, D., Kecinski, M. and Mohapatra, S., 2021. An updated look at petroleum well leaks, ineffective policies and the social cost of methane in Canada's largest oil-producing province. Climatic Change, 164(3), p.60.

[10] Office of the Parliamentary Budget Officer 2022, 'Estimated Cost of Cleaning Canada's Orphan Oil and Gas Wells', viewed 27 November 2024, https://www.pbo-dpb.ca/en/publications/RP-2122-026-S--estimated-cost-cleaning-canada-orphan-oil-gas-

wells--cout-estimatif-nettoyage-puits-petrole-gaz-orphelins-canada.

[11] Temizel, C., Aydin, H., Hosgor, F.B., Yegin, C. and Kabir, C.S., 2023. Green Energy Sources Reduce Carbon Footprint of Oil & Gas Industry Processes: A Review. Journal of Energy and Power Technology, 5(1), pp.1-25.

[12] Yashin, A., Konev, A. and Khakimyanov, M., 2021, November. Power Supply of The Sucker Rod Pump Unit Electric Drive Using Renewable Energy Sources. In 2021 International Conference on Electrotechnical Complexes and Systems (ICOECS) (pp. 43-46). IEEE.

[13] Elyamany, M., Abdellatif, S.O. and Ghali, H., 2022, February. Online sucker-rod pumping with photovoltaic driven system sizing tool for oil and gas industrial sector. In International Conference on Remote Engineering and Virtual Instrumentation (pp. 174-185). Cham: Springer International Publishing.

[14] Osaretin, C.A., Butt, S.D., & Iqbal, M.T. (2020). Sizing, Parametric Investigation and Analysis of Automated Sucker Rod Pump using Beam Pump Simulators. Journal of Chemical and Petroleum Engineering.

[15] SolidWorks, "Simscape Multibody Link," Accessed: Aug. 15, 2024. [Online]. Available: https://www.solidworks.com/partnerproduct/simscape-multibody-link.

[16] MathWorks, "Export a SolidWorks Robot Assembly Model—MATLAB & Simulink," Accessed: Aug. 15, 2024. [Online]. Available: https://www.mathworks.com/help/smlink/ug/export-robot-assembly-from-solidworks-software.html.

[17] MathWorks, "Import SolidWorks Assemblies into Simscape Multibody," Accessed: Aug. 15, 2024. [Online]. Available: https://www.mathworks.com/videos/import-solidworks-assemblies-into-simscape-multibody-1701670328083.html.

[18] MathWorks, "SolidWorks—MATLAB & Simulink," Accessed: Aug. 15, 2024. [Online]. Available: https://www.mathworks.com/help/smlink/solidworks.html.

[19] MathWorks, "CAD Translation [Online]," Accessed: Aug. 14, 2024. [Online]. Available: https://www.mathworks.com/help/physmod/sm/ug/cad-translation.html.

[20] Mishchenko, E. and Mishchenko, V., 2021. Exploring the cad model of the manipulator using cad translation and simscape multibody. In E3S Web of Conferences (Vol. 279, p. 03014). EDP Sciences.

[21] Boschetti, G. and Sinico, T., 2024. Designing Digital Twins of Robots Using Simscape

Multibody.Robotics, 13(4), p.62.

[22] Tickoo, S., 2019. Learning SOLIDWORKS 2019: A Project Based Approach. CADCIM Technologies.

[23] MathWorks, n.d. Modeling Joint Connections - MATLAB & Simulink. [online] Available at https://www.mathworks.com/help/physmod/sm/ug/modeling-joint-connections.html [Accessed 14 August 2024].

[24] MathWorks, n.d. Mates and Joints - MATLAB & Simulink. [online] Available at: https://www.mathworks.com/help/smlink/ref/mates-and-joints.html [Accessed 14 August 2024]

[25] MathWorks, n.d. Constraints and Joints - MATLAB & Simulink. [online] Available at: https://www.mathworks.com/help/sm/ug/constraints-and-joints.html [Accessed 14 August 2024]

[26] Corrales, U. (2018) A simple example of beam pump mechanism in SolidWorks. Available at: https://grabcad.com/library/beam-pump-3 (Accessed: 14 April 2024).

[27] Osaretin, C.A., Iqbal, T., and Butt, S., 2020. Optimal sizing and techno-economic analysis of a renewable power system for a remote oil well. AIMS Electronics and Electrical Engineering, 4(2), pp.132-153.

[28] Semenov, A.V., Tecle, S.I. and Ziuzev, A., 2020, September. Modeling induction motor driven sucker rod pump in MATLAB Simscape. In 2020 Russian Workshop on Power Engineering and Automation of Metallurgy Industry: Research & Practice (PEAMI) (pp. 67-71). IEEE

[29] SMLease Design (2024) 'Gear Train: Gear Ratio, Torque and Speed Calculations', SMLease Design. Available at: https://smlease.com/entries/mechanism/gear-train-gear-ratio-torque-and-speed-calculation/

[30] The MathWorks Inc. 2024, Rotational Multibody Interface Documentation, viewed 27 November, 2024, https://www.mathworks.com/help/simscape/ref/rotationalmultibodyinterface.html.

[31] The MathWorks Inc. 2024, Gear Box Documentation, viewed 27 November 2024, https://www.mathworks.com/help/simscape/ref/gearbox.html.

[32] Lao, L., & Leuterman, A. (2012). Torsional Vibration of Sucker Rod Strings. SPE Annual Technical Conference and Exhibition. Society of Petroleum Engineers. SPE-159703-MS.

[33] The MathWorks Inc. 2024, Translational Multibody Interface Documentation, viewed 27

November 2024,
https://www.mathworks.com/help/simscape/ref/translationalmultibodyinterface.html.

[34] Environment and Climate Change Canada (2024) 'Engineering Climate Datasets', Available at: http://climate.weather.gc.ca/prods_servs/engineering_e.html (Accessed: 28 November 2024).

[35] Government of Canada (2017) 'Historical Climate Data', Available at: Hourly Data Report for January 31, 2017 - Climate - Environment and Climate Change Canada (Accessed: 28 November 2024).

[36] Government of Canada (2017) 'Historical Climate Data', Available at: Hourly Data Report for June 01, 2017 - Climate - Environment and Climate Change Canada (Accessed: 28 November 2024).

[37] Singh, B., Sharma, U. and Kumar, S., 2018. Standalone photovoltaic water pumping system using induction motor drive with reduced sensors. IEEE transactions on industry applications, 54(4), pp.3645-3655.

[38] Texas Instruments (2024) 'BUCK-CONVCALC: Component Calculator for BUCK Converters', Available at: https://www.ti.com/tool/BUCK-CONVCALC (Accessed: 28 November 2024).

[39] TECO-Westinghouse Motors (Canada) Inc. (2024) 'NEMA Premium Efficiency ODP - Commercial Duty', Available at: https://tecowestinghouse.ca/motors/low-voltage/optim-odp/ (Accessed: 28 November 2024).

[40] Osaretin, C. A. (n.d.). Sucker Rod Pump Modeling. Available at: https://github.com/caosaretin/Sucker-Rod-Pump-Modeling (Accessed: 30 December 2024).

Chapter 7

CONCLUSION

7.1 Summary

Canada is currently confronted with exponentially increasing number of oil wells that are suspended, orphaned or abandoned. As remote oil wells continue to age, the need for deploying innovative solutions that adopt systems thinking to mitigate the environmental and economic impact of these aging infrastructures cannot be over-emphasized. This research provides low-cost, lean framework that well operators, facility managers and policy makers can quickly deploy to estimate the energy requirement and perform insightful feasibility study on the most suitable renewable energy system architecture that can be sustainably deployed to re-purpose aging candidate oil wells in a selected oil field. The framework provides technical and economic criteria that serve as key performance indicators to select the most feasible wells for implementation. The approach laid out in this research selects the sucker rod pump as a common artificial lift system and examines the impact of various parameters on the pumping mode in both intermittent and continuous production profiles, deploying 100% off-grid solar PV renewable energy and/or wind energy and battery storage.

This research designs an open-source, supervisory control and data acquisition system to meet the energy and communications needs of this critical off-grid infrastructure and executes the design, modelling, simulation and control of the system, to ensure sustainable operation based on site-specific historical renewable energy resource data. This framework lays a firm foundation for distributed renewable energy generation and decentralized microgrid adoption at scale , providing clean energy beyond the life of the oil wells for diverse uses such as onsite irrigation for agriculture and strengthens the distributed renewable energy infrastructure for the Prairies in Canada.

The summary of phases accomplished in this research is as follows:

Sizing, Parametric Investigation, and Analysis of Automated Sucker Rod Pump using Beam Pump Simulators is presented in the third chapter. It applies an integrated approach combining Two (2) artificial lift simulators that are integrated for automated sizing of beam-pumped systems. A sucker-rod artificial lift system is optimally sized for a case study oil well, to obtain the minimum API rating of the pumping unit, sustain the target production rate, and determine the corresponding minimum prime mover required to drive the pump sustainably. Compared to using a single simulator for the case study, the integrated approach reduces the damped and polished rod horsepower by 54.9% and 26.5% respectively, for a corresponding decrease in minimum NEMA D motor size by 38.6%. These key performance indicators demonstrate the benefits of simulator integration in automated sizing of beam pumps.

In the fourth chapter of this study, a novel analysis, design, optimal sizing, and techno-economic analysis of a renewable power system for a remote oil well is executed. Intermittent and Continuous production profiles are identified and combined with different renewable energy configurations to identify the optimal scenario. Using the intermittent pumping with solar PV and battery system as the benchmark, the **continuous** pumping system with hybrid generation demonstrates the following percentage changes:

- Unmet Load: Reduced by 100% (from 4.55 kWh/yr to 0 kWh/yr).
- Capacity Storage: Decreased by 95.2% (from 11.70 kWh/yr to 0.56 kWh/yr).
- Net Present Cost (NPC): **Increased** by 123.4% (from $64,969 to $145,150.50).
- Levelized Cost of Energy: **Increased** by 20% (from $0.425/kWh to $0.51/kWh).
- Operating Cost: **Increased** by 132% (from $1,318/yr to $3,056.04/yr).

These metrics highlight the trade-offs between cost efficiency and performance, with the hybrid system achieving zero unmet load and significantly lower capacity storage requirements at higher costs. The research recommends the hybrid architecture with the least unmet load (solar photovoltaic, wind turbine, and battery storage) for continuous pumping scenario, and the architecture with the least system cost but with slightly higher unmet load (solar photovoltaic with battery storage), for intermittent pumping.

In the fifth chapter, the authors demonstrated both the software and hardware implementations of an Open-source, IoT-Based SCADA System for Remote Oil Facilities Using Node-RED and Arduino Microcontrollers. For data monitoring, logging, and visualization. Node-RED server that is hosted on a local machine is adopted. Terminal units are used for transmitting and aggregating sensor data to the master terminal unit on the local server. The system is designed for monitoring, supervision, and remotely controlling motors and sensors deployed for low flow-rate oil and gas facilities.

In the sixth chapter, the authors perform complete load modelling of the sucker rod pump in SolidWorks and combine it with a Solar PV and battery system design, modelling, simulation and control in Simscape. Two parallel scenarios are specified for winter and summer operation. The onsite historical solar irradiance and temperature data for January and June are integrated with the microgrid model simulation. The state of charge under required load conditions in summer is observed to increase gradually from ~75% to ~90% over 19 s, while winter shows similar upward trend from ~75% to ~85% over 12 s. This verifies that the output power from the renewable energy system is sufficient to drive the squirrel cage induction motor prime mover and charge the battery storage system under normal operating conditions.

7.2 Future Study

Significant advancements have been made in optimizing sucker-rod pump systems, integrating renewable energy sources, implementing low-cost SCADA solutions, and developing dynamic models for renewable-powered pumps. These innovations offer promising pathways for enhancing oil well productivity, sustainability, and operational efficiency. Future research should focus on the key aspects identified for each research area as follows :

a. **Sizing, parametric investigation and analysis of automated sucker rod pump using beam pump simulators:**

- Expanding the scope of the integrated sizing approach for sucker rod pumps, beyond beam pumps to other artificial lift methods, to include a wider range of well conditions and production scenarios.
- Incorporating feature engineering and advanced machine learning algorithms to optimize the parametric investigation and parameter selection process to further reduce iteration time and accuracy required for optimal sizing of sucker rod pump-powered oil wells.
- Comparing the energy efficiency and economic benefits of this approach across different oil fields, diverse geological formations, well conditions and geographical contexts.
- Field validation of the energy efficiency and economic analysis of this approach across different oil fields and geological formations to enhance its applicability across diverse well conditions, and facilitate integration with broader smart oilfield concepts.
- Performing a comprehensive study using measured site data of PVT, well deviation survey, geothermal gradient, Inflow Performance relationship, Vertical Lift performance, and equipment data (surface and downhole equipment data).

- Investigating the long-term performance and reliability of systems designed using this integrated method to provide valuable insights for industry practitioners.
- Developing a user-friendly software interface that seamlessly integrates design and sizing using multiple simulators to streamline the design process for engineers.

b. **Optimal sizing and techno-economic analysis of a renewable power system for a remote oil well:**

- Investigating the technical and economic feasibility of a 100 % wind-powered oil well.
- Comparing the use of hydraulic versus electric power from wind turbines to drive oil wells.
- Investigating the design, modelling, simulation and control of a hybrid renewable energy system comprising of 100% solar and wind energy powered oil well, with various types of artificial lift configurations.
- Exploring the technical and economic feasibility of grid-tied solar and wind energy systems in an oil well, accounting for the carbon footprint of renewable energy integration and estimating the scope 1 and scope 2 emissions abated in MtCO2e.
- Investigating the impact of grid-tied, large scale, distributed on-site renewable energy powered oil wells, on demand-side management strategies and smart grid technologies
- Integrating advanced energy storage technologies, such as flow batteries or hydrogen fuel cells, into the renewable microgrid and investigating to improve system reliability, performance and reduce costs.
- Comprehensive life cycle assessment to evaluate the environmental impact of the proposed system compared to conventional power sources.

c. **Open Source IoT-Based SCADA System for Remote Oil Facilities Using Node-RED and Arduino Microcontrollers:**

- Transitioning the Node-RED application to a cloud-native platform, such as IBM Watson, to improve scalability and accessibility.
- Investigation of wireless sensor data transmission, edge computing, cloud analytics, and machine learning to produce insights from sensor data.
- Collecting real-time data from various sensors, including proximity sensors and load cells mounted on the sucker rod pump, so as to generate various dynamometer card plots.
- Implementing email alerts and notifications to enhance real-time monitoring capabilities.
- Mounting the transducers and sensors on a 3D model of a sucker-rod pump and integrating artificial intelligence and machine learning algorithms to develop a calibrated digital twin.
- Expanding the functionality of the rotary encoder to enable automated speed control of the electric motor to optimize fluid production rates.
- Strengthening security measures by adopting Secure Sockets Layer (SSL) encryption for HTTPS connections.

d. **Design, dynamic modelling, simulation, and control of a solar-powered sucker rod oil pump**:

- Adoption of machine learning-powered algorithms for maximum power point tracking to effectively track maximum power from the solar PV arrays, using measured real-time data.
- Investigating the dynamic modelling, simulation and control of other renewable energy sources, such as wind or geothermal
- Developing advanced control systems and closed loop feedback systems to drive the performance of the induction motor under varying load conditions and actively compensate through reactive power supply and load balancing.
- Designing more sophisticated energy storage systems, exploring emerging technologies like flywheels, flow batteries or hydrogen for energy savings in sucker rod pump driven oil wells.
- Scaling up the model to simulate and optimize multiple interconnected induction motor prime movers powering several oil wells in an oilfield, potentially leading to more efficient field-wide resource management and production strategies.

7.3 List of Publications

7.3.1 Journal Articles

a. Osaretin, C., Butt, S., Iqbal, M. T. (2020). Sizing, Parametric Investigation and Analysis of Automated Sucker Rod Pump using Beam Pump Simulators, Journal of Chemical and Petroleum Engineering, 54(2), pp. 235-251. https://doi.org/10.22059/jchpe.2020.295689.1303.

b. Osaretin, C.A., Iqbal, T., and Butt, S., 2020. Optimal sizing and techno-economic analysis of a renewable power system for a remote oil well. AIMS Electronics and Electrical Engineering, 4(2), pp.132-153. https://doi.org/10.3934/electreng.2020.2.132.

c. Osaretin, C.A., Iqbal, M.T. and Butt, S., 2025. Design, Dynamic Modelling, Simulation and Control of a Solar Powered Sucker Rod Oil Pump. Journal of Electronics and Electrical Engineering, 4(1), pp.105-137. https://doi.org/10.37256/jeee.4120256168.

7.3.1 Conference Publications

a. Osaretin, C.A., Zamanlou, M., Iqbal, M.T. and Butt, S., 2020, November. Open source IoT-based SCADA system for remote oil facilities using node-RED and Arduino microcontrollers. In 2020 11th IEEE Annual Information Technology, Electronics and Mobile Communication Conference (IEMCON) (pp. 0571-0575). IEEE. https://doi.org/10.1109/iemcon51383.2020.9284826.